

Reprint Compendium

Bio-protocol Selections 2022

Cancer Research

Foreword

We are pleased to launch the 2022 *Bio-protocol* series of reprint collections, comprising some of the most used protocols published in 2021 in several research areas. This collection focuses on Cancer Research.

Established in 2011 by a group of Stanford scientists, Bio-protocol aims to improve research reproducibility and usability through the publication of high quality step-by-step peer-reviewed life science protocols. *Bio-protocol* invites contributions from authors who have published methods in brief, as part of other research articles, and who might want to provide more detailed versions to facilitate use by others.

A survey carried out in 2018 showed that, of more than 2300 users who had followed a protocol published in *Bio-protocol*, 91% (2166 users) were able to successfully reproduce the method they tried.

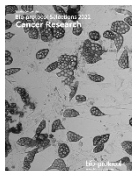
In this reprint collection, we have selected 22 of the most viewed, downloaded, and cited research protocols related to Cancer Research that were published in *Bio-protocol* in 2021.

Hopefully, you will find this collection intriguing and visit <http://www.bio-protocol.org> to check out the entire archive of protocols. Please feel free to email us (eb@bio-protocol.org) with feedback, and please consider contributing a protocol to Bio-protocol in the future.

The Bio-protocol Editorial Team

1. A Rigorous Quantitative Approach to Analyzing Phagocytosis Assays 1
Caponegro, M. D. *et al.* [Original Research Article: Sci Rep 10(1), 19333]
2. Generation of the Compression-induced Dedifferentiated Adipocytes (CiDAs) Using Hypertonic Medium 9
Li, Y. *et al.* [Original Research Article: Sci Adv 6(4):eaax5611]
3. Preparation of an Orthotopic, Syngeneic Model of Lung Adenocarcinoma and the Testing of the Antitumor Efficacy of Poly(2-oxazoline) Formulation of Chemo-and Immunotherapeutic Agents 20
Vinod, N. *et al.* [Original Research Article: Sci Adv 6(25):eaba5542]
4. An Image-based Dynamic High-throughput Analysis of Adherent Cell Migration 26
Sun, M. *et al.* [Original Research Article: Ann Rheum Dis 78(12):1621-1631]
5. Preparation and Characterization of Poly(2-oxazoline) Micelles for the Solubilization and Delivery of Water Insoluble Drugs 35
Vinod, N. *et al.* [Original Research Article: Sci Adv 6(25):eaba5542]
6. Atomic Force Microscopy to Characterize Ginger Lipid-Derived Nanoparticles (GLDNP) 41
Long, D. *et al.* [Original Research Article: J Control Release 323:293-310.]
7. A Robust Mammary Organoid System to Model Lactation and Involution-like Processes 52
Charifou, E. *et al.* [Original Research Article: Front Cell Dev Biol 8:68.]
8. ATAC-Seq-based Identification of Extrachromosomal Circular DNA in Mammalian Cells and Its Validation Using Inverse PCR and FISH 68
Su, Z. *et al.* [Original Research Article: Sci Adv 6(20):eaba2489]
9. Surface Engineering and Multimodal Imaging of Multistage Delivery Vectors in Metastatic Breast Cancer 85
Goel, S. *et al.* [Original Research Article: Sci Adv 6(26):eaba4498]
10. Analysis of the Effects of Hexokinase 2 Detachment From Mitochondria-Associated Membranes with the Highly Selective Peptide HK2pep 96
Ciscato, F. *et al.* [Original Research Article: EMBO Rep 21(7):e49117]
11. Antisense Oligo Pulldown of Circular RNA for Downstream Analysis 111
Das, D. *et al.* [Original Research Article: Nucleic Acids Res 45(7):4021-4035]
12. Modeling the Nonlinear Dynamics of Intracellular Signaling Networks 121
Rukhlenko, O. S. and Kholodenko, B. N. [Original Research Article: Elife 24;9:e58165]
13. Fe-NTA Microcolumn Purification of Phosphopeptides from Immunoprecipitation (IP) Eluates for Mass Spectrometry Analysis 128
Sanford, E. J. and Smolka, M. B. [Original Research Article: Genes Dev 32 (11-12):822-835]
14. A Genetically Engineered Mouse Model of Venous Anomaly and Retinal Angioma-like Vascular Malformation 140

- Cao, X. *et al.* [Original Research Article: *Elife* 5:e21032]
15. Measuring DNA Damage Using the Alkaline Comet Assay in Cultured Cells 149
Clementi, E. *et al.* [Original Research Article: *BMC Biol* 18(1):36]
16. Neutral Comet Assay to Detect and Quantitate DNA Double-Strand Breaks in Hematopoietic Stem Cells 163
Roy, I. *et al.* [Original Research Article: *Stem Cell Reports* 15(2):340-357]
17. Comprehensive Identification of Translatable Circular RNAs Using Polysome Profiling 174
Ye, Y. *et al.* [Original Research Article: *Cell Res* 27(5):626-641]
18. Analysis of Leukemia Cell Metabolism through Stable Isotope Tracing in Mice 183
van Gastel, N. *et al.* [Original Research Article: *Cell Metab* 32(3):391-403.e6]
19. Measuring Real-time DNA/RNA Nuclease Activity through Fluorescence 194
Wyrzykowska, P. *et al.* [Original Research Article: *Sci Rep* 9(1):8853]
20. Measurement of DNA Damage Using the Neutral Comet Assay in Cultured Cells 203
Clementi, E. *et al.* [Original Research Article: *BMC Biol* 18(1):36]
21. Measurement of Bone Metastatic Tumor Growth by a Tibial Tumorigenesis Assay 213
Zhang, B. *et al.* [Original Research Article: *Nat Commun* 12(1):1714]
22. Reconstruction of Human AML Using Functionally and Immunophenotypically Defined Human Haematopoietic Stem and Progenitor Cells as Targeted Populations 223
Zeisig, B. B. *et al.* [Original Research Article: *Sci Transl Med* 13(582):eabc4822]



On the Cover:

Image from protocol "**Generation of the Compression-induced Dedifferentiated Adipocytes (CiDAs) Using Hypertonic Medium**".

A Rigorous Quantitative Approach to Analyzing Phagocytosis Assays

Michael D. Caponegro, Kaitlyn Koenig Thompson, Maryam Tayyab and Stella E. Tsirka*

Molecular and Cellular Pharmacology Program, Department of Pharmacological Sciences, Stony Brook University, Stony Brook, NY 11794-8651, USA

*For correspondence: styliani-anna.tsirka@stonybrook.edu

Abstract

Studying monocytic cells in isolated systems *in vitro* contributes significantly to the understanding of innate immune physiology. Functional assays produce read outs which can be used to measure responses to selected stimuli, such as pathogen exposure, antigen loading, and cytokine stimulation. Integration of these results with high quality *in vivo* models allows for the development of therapeutics which target these cell populations. Current methodologies to quantify phagocytic function of monocytic cells *in vitro* either measure phagocytic activity of individual cells (average number of beads or particles/cell), or a population outcome (% cells that contain phagocytosed material). Here we address technical challenges and shortcomings of these methods and present a protocol for collecting and analyzing data derived from a functional assay which measures phagocytic activity of macrophage and macrophage-like cells. We apply this method to two different experimental conditions, and compare to existing work flows. We also provide an online tool for users to upload and analyze data using this method.

Keywords: Monocyte, Macrophage, Microglia, Phagocytosis, Quantification, Analysis, Microscopy

This protocol was validated in: Sci Rep (2020), DOI: 10.1038/s41598-020-76383-w

Background

Monocytic lineage cells (monocytes, macrophages, and microglia) survey tissue for pathological threats, and act as hubs of the innate immune system. They exercise innate immune functions in numerous ways: by secreting cytokines and chemokines, acting through complement signaling pathways, and phagocytosing pathogens and debris. The extent of macrophage activation can tip the balance of immune response within the body during health and disease. In diseases such as cancer, the activation of monocytic cells can result in either pro- or anti-tumoral responses, which trigger different disease outcomes. Similarly, monocytic cells modulate the progression and remission of auto-immune and inflammatory diseases. It is therefore critical to characterize these cells and their responses, to identify steps which may be exploited therapeutically.

In vitro systems interrogate the functions of these innate immune cells in response to stimuli via specific assays. The phagocytosis assay is an essential tool in characterizing the magnitude of monocytic cell activation. Several variations, such as pulse-chase assay, particle loading, and/or bead loading, exist. Upon stimulation of the monocytic cell population with drugs, cytokines, or preconditioned cell media, the results of the assay report to what extent the cells have increased or decreased their ability to engulf particles from the environment, thus giving insight into how such stimuli may affect monocytic cells during health and disease *in vivo*.

Here we discuss some of the technical challenges associated with deriving high-quality data from standard phagocytosis assays. The variability of phagocytic activity of cells within a single sample makes this a particularly difficult function to assess. Most current studies count phagocytosed particles per cell, however, individual particles can be difficult to discern, and this measure can be misleading in cells that have higher baseline phagocytosis. Other studies simply analyze how many cells are phagocytosing (versus not), which gives a very broad and less quantitative picture of phagocytosis. Here, we have developed and propose the use of a new technical pipeline to collect and more sensitively analyze phagocytosis data. We then apply it to two different experiments for which macrophage phagocytosis is often assayed.

Materials and Reagents

1. Glass coverslips (Fisher Scientific, catalog number: 12-545-100)
2. 40 µm cell strainer (Fisher, catalog number: 22-363-547)
3. Adult C57Bl/6 mice
4. L929 cells [or 100 U/mL recombinant M-CSF (Prospec, catalog number: CYT-439)]
5. GL261 murine glioma cells
6. 2.5% avertin
7. Hank's Buffered Saline Solution (HBSS)
8. Fluorescent latex beads (carboxylate-modified polystyrene, fluorescent red; 0.5-µm mean particle size, Sigma, catalog number: L3280)
9. Fluorescence-conjugated AlexaFluor 488 goat anti-rabbit (Life Technologies, catalog number: A-11008)
10. Hank's Buffered Saline Solution (HBSS) (Corning, catalog number: MT-20-023-CV)
11. DMEM (Corning, catalog number: 10-017-CM)
12. FBS (VWR, catalog number: 10221-866)
13. Antibiotic-Antimycotic (Fisher, catalog number: 10-221-866)
14. Sodium pyruvate (VWR, catalog number: 13-115E)
15. PFA (4% paraformaldehyde) (Acros, catalog number: AC169650010)
16. Triton X-100 (Sigma, catalog number: X100)
17. Normal goat serum (Southern Biotech, catalog number: 0060-01)
18. BSA (VWR, catalog number: RLBSA50)
19. DAPI Fluormount (Southern Biotech, catalog number: 0100-20)
20. Iba1 antibody (Wako USA, catalog number: 19-19741)
21. LPS (Sigma, catalog number: L6511)
22. Mouse IFN γ (Roche, catalog number: 11276905001)

Equipment

1. Leica SP8X confocal imaging system
Beads ($\lambda_{\text{ex}} \sim 575$ nm; $\lambda_{\text{em}} \sim 610$ nm)
AlexaFluor 488 ($\lambda_{\text{ex}} 490$ nm; $\lambda_{\text{em}} \sim 525$ nm)
2. -80 °C freezer

Software

1. Fiji (Schindelin *et al.*, 2012)

Procedure

A. Cell Culture

Note: The cells, unless otherwise noted, are grown in 10% FBS with 1% Antibiotic-Antimycotic at 5% CO₂ and 37°C.

1. Generate glioma conditioned media (GCM) using GL261 murine glioma cells which are grown to 80-90% confluence and serum starved for 24 h. The media are collected and stored at -80°C until use.
2. Generate L cell media by collecting it from L929 cells grown to 90-100% confluence and maintained for 10 days. These media are rich in colony stimulating factor 1 (CSF1), a factor used to drive proliferation and differentiation of monocytic cells into macrophages.
3. Monocytes are cultured from adult C57Bl/6 mice as previously described (Zhang *et al.*, 2008): Briefly, animals are deeply anesthetized with 2.5% avertin and euthanized by cervical dislocation. Femurs and tibiae are dissected, and the internal bone cavity is flushed with 1% serum in Hank's Buffered Saline Solution (HBSS). The collected bone marrow is filtered through a 40-μm cell strainer and plated in complete media containing DMEM, 10% FBS, 1% Antibiotic-Antimycotic, 1% sodium pyruvate, and 20% L cell media (or 100 U/mL recombinant M-CSF).
4. Cells are kept at 5% CO₂ and 37°C. Macrophage differentiation is achieved after 7-9 days of culture.

B. Phagocytosis assay

Experiment 1: Macrophages are plated on glass coverslips and incubated with either complete media, as described above, or complete media plus 50% GCM for 24 h.

Experiment 2: Macrophages, as above, are incubated with saline (control) or both 100 ng/mL LPS (Sigma) and 100 U/mL IFNγ (Roche) for 24 h.

1. Fluorescent latex beads (carboxylate-modified polystyrene, fluorescent red; 0.5-μm mean particle size, Sigma, L3280) are added to a final concentration of 0.1 μg/mL, and incubated for 2 h. After rinsing with HBSS to remove excess beads, cells are fixed in 4% PFA at room temperature for 20 min.
2. Fixed cells are rinsed with PBS and blocked for 1 h in 0.1% Triton X-100 and 5% normal goat serum. They are incubated with anti-Iba1 (1:500, Wako) in 0.01% Triton X-100 and 30 mg/mL BSA overnight at 4°C.
3. The cells are then rinsed with PBS, and incubated with fluorescence-conjugated AlexaFluor 488 goat anti-rabbit for 1 h.
4. Cells are rinsed again with PBS and coverslipped using DAPI Fluormount (Southern Biotech).

C. Confocal Imaging

Images are acquired on a Leica SP8X confocal imaging system. 10 μm z-stacks are taken at 40 \times at a resolution of 512 \times 512 pixels. Confocal images are processed using Fiji (Schindelin *et al.*, 2012). For this procedure, five fields are imaged, and at least 100 cells are quantified in total per treatment. For evaluation of phagocytosis, total number of cells, and number of cells with internalized beads are counted. The images are further analyzed by counting the number of beads per cell, and measuring cell area and the integrated density of sum-projected pixels from the fluorescent bead channel. Integrated density values are analyzed for outliers before downstream analysis. The step-by-step image analysis protocol is provided in [Supplementary document 1](#).

Data analysis

Data analysis is performed in R for Windows. The method and interactive UI can be accessed via GitHub for users to upload and analyze data ([RShinyApp](#); [GitHub Repo](#)).

Results

A high throughput method of data collection

In the first experiment, we quantified macrophage phagocytosis in response to GCM. Tumor associated macrophages are known to be highly activated and pro-tumorigenic. Their phagocytic activity may be related to their tumor supporting behavior by mechanisms that promote wound healing and anti-inflammatory phenotypes. Confocal imaging allows complete 3D capture of macrophages engulfing fluorescent beads (Figure 1A). Standard methods attempt to count the number of beads that each cell has engulfed. However, some cells exhibit low, basal level of phagocytic activity, while others become stimulated and intake more beads. This non-standardized phagocytic activity can be problematic for quantification and analysis. The beads overlap within and across z-stack layers, making distinguishing and counting individual beads difficult. Further, counting the number of beads per cell in a single field of view can take more than 15 min, making data acquisition time-consuming for large numbers of technical replicates. This highlights the technical challenges associated with this method of quantification.

To address this, others have quantified the number of cells positive or negative for bead signal, thereby creating a ratio of cells which are phagocytic in response to treatment (Lian *et al.*, 2016; Roy *et al.*, 2018). While more time-efficient, this method does not capture the changes in *relative amount* of phagocytosis occurring, *i.e.*, phagocytic activity of each cell. As seen in Figure 1A, cells engulf variable amounts of beads. Other methods to access phagocytosis, such as fluorescently-activated cell sorting (FACS), have also been used (Pul *et al.*, 2013), however they require more preparation time, experimental controls (negative fluorescent controls, compensation techniques *etc.*), and several costly reagents and conjugated antibodies.

We developed a technical pipeline which takes advantage of the discrete fluorescent signal produced by the latex beads. By summing the fluorescent pixels across the z-stack of the bead channel, we create a single metric. By using region of interest (ROI) functionality, we can capture this metric for each cell within a field of view. This method of data collection allows the analysis of all cells within a field in under 2 min, appreciably faster than counting individual beads/cell. It allows hundreds of cells to be analyzed in a single experiment.

To validate this fluorescent metric, we compared the signal produced by this method with the counted number of beads per cell, as previously performed (Figure 1B). Simple linear regression analysis was used. The model yielded high significance ($P < 0.001$) with a slope coefficient of 0.53 and an adjusted $r^2 = 0.363$. This relationship was also confirmed with a Spearman's rho value of 0.683. Thus, generating a fluorescent signal by summing the pixels throughout the z-stack is an accurate and sensitive measurement, reflecting the number of beads each cell has engulfed. It provides a high throughput alternative to existing quantification methods.

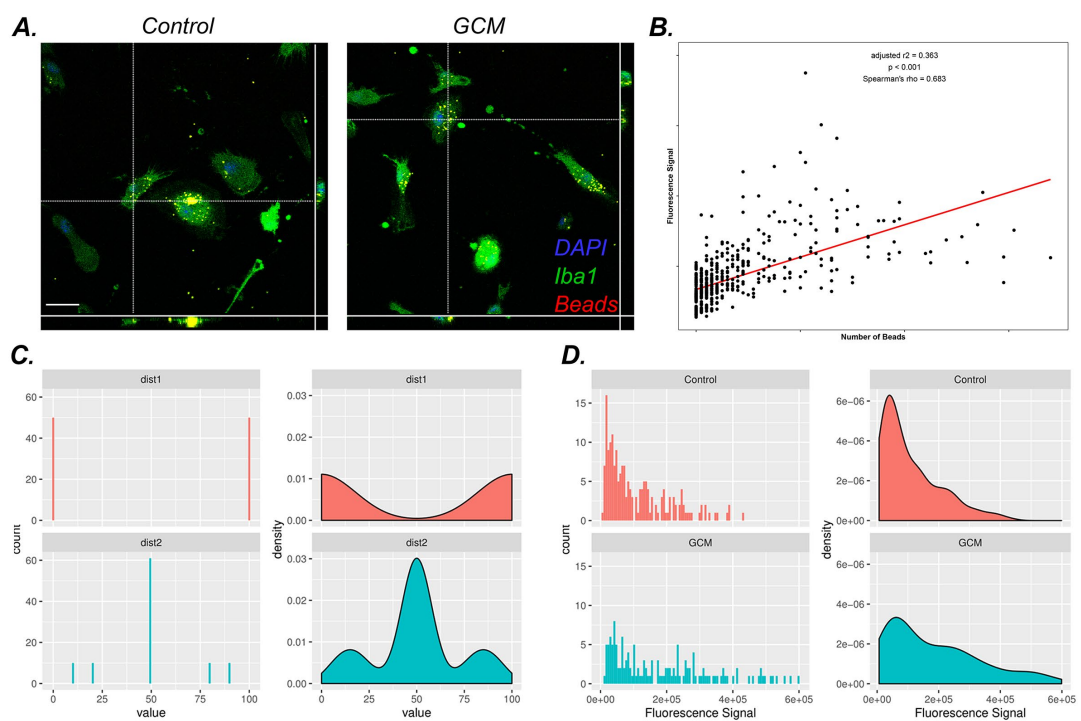


Figure 1. Confocal imaging and analysis of macrophages following incubation with fluorescent latex beads.

A. Macrophages stained for Iba1 (green) can be seen engulfing fluorescent latex beads (red) in both treatment conditions. Orthogonal views are also shown, demonstrating complete uptake of the beads by the cells. Note the varying levels of bead signal among cells. DAPI marks nuclei. B. Scatter plot comparing the fluorescence signal derived from beads versus the actual number of beads counted per cell. $y = -22.40619 + 0.52782x$. $P < 2.2e^{-16}$. Adjusted $r^2 = 0.3634$. Spearman's $\rho = 0.683$. C. Histogram and density plots of hypothetical datasets. For both populations *dist1* and *dist2*, $n = 100$, mean = 50, median = 50. D. Histogram and density plots of experimentally derived data from panel A, Experiment 1. Complete descriptive statistics are in [Table S1](#). Scale bar for panel A is 20 μ m.

Utilizing empirical cumulative distribution functions as a measure of phagocytic activity

The data rendered by this method create a continuous distribution of fluorescent signal across all cells within an experimental group (Figure 1D). Standard statistical methods would use a parametric or non-parametric statistical test to compare the means or medians of each distribution, respectively. However, let us consider two hypothetical distributions, for which the probability distribution functions (PDF) are non-congruent, but the mean and median between them are equal (Figure 1C, [Table S1](#)). Both parametric and non-parametric tests reject the alternative hypothesis and infer no difference between the two distributions, yet it is clear visually that the distribution of events is vastly different between the two samples. This suggests that for non-parametric, multi-modal distributions the standard *t*-test or Mann-Whitney U test is insufficient, and can break down under certain conditions. Interpreted biologically, these tests may lack the ability to detect the ‘shifts’ in phagocytic influx that occur when macrophages are challenged, for example by treatment with GCM.

If we consider the empirical cumulative distribution function (ECDF) of these distributions, it more aptly represents the changes that exist as the PDF expands (Figure 2A). To compare these distributions, we applied principals from the field of optimal mass transport, otherwise known as Earth mover’s theory. These methods seek to compare data based on their underlying ECDFs. To compute differences between the ECDF derived from our hypothetical and experimental data, we next performed the Kolmogorov-Smirnov test (KS test), where the *D* statistic given by:

$$D_{n,m} = \sup |F_{1,n}(x) - F_{2,m}(x)|$$

Where $F_{1,n}$ and $F_{2,m}$ are the ECDF from two 1 dimensional datasets, and \sup is the supremum function, computes the absolute maximum distance between the ECDFs (Figure 2A). To reject the null hypothesis H_0 , which states that both samples come from the same population, at a given significance level α , $D_{n,m} > D_{n,m,\alpha}$, where $D_{n,m,\alpha}$ is the critical value given by:

$$D_{n,m,\alpha} = c(\alpha) \sqrt{\frac{n+m}{nm}}$$

For the hypothetical distributions *dist1* and *dist2* the two sample KS test yields $D = 0.5$ and $P = 2.778e^{-11}$. This clearly indicates the advantage of using this method for multimodal distributions over standard t-test or Mann-Whitney U test. When applied to our experimental data, KS results in $D = 0.24$ and $P = 2.2e^{-4}$ (Figure 2B), indicating that the probability that a macrophage has increased phagocytic activity is more accurately reflected in the collected data by the shift in its PDF, which is captured by analyzing the ECDF. These results also demonstrate that exposure to GCM significantly increases macrophage phagocytic activity.

Comparing KS test to reported methods

To further assess KS test sensitivity, we performed a second experiment exposing macrophages to the canonical pro-inflammatory/M1 activating agents LPS and IFN γ . We calculated the percentage of phagocytosing cells by dividing the number of cells positive for engulfed beads by the total number of cells within the field of view, as reported (Lian *et al.*, 2016; Roy *et al.*, 2018). The results yielded a trend towards increase in phagocytosis in cells exposed to LPS and IFN γ , however the high variability and lack of technical replicates fail to reject the null hypothesis using standard two sample parametric and non-parametric tests (Figure 2C). We then employed the KS test to generate PDF and ECDF of the two treatment groups (Figure 2D). This resulted in $D = 0.15$ and $P = 0.04$, thus detecting a small but significant shift in phagocytic activity, which can be seen by the rightward shift in the histogram, density curve, and ECDF. While not as large of an increase relative to that observed after GCM treatment, this result agrees with published literature (Wu *et al.*, 2009; Scheraga *et al.*, 2016; Caponegro *et al.*, 2019; Thompson *et al.*, 2020) and validates the approach, highlighting its high throughput and sensitivity.

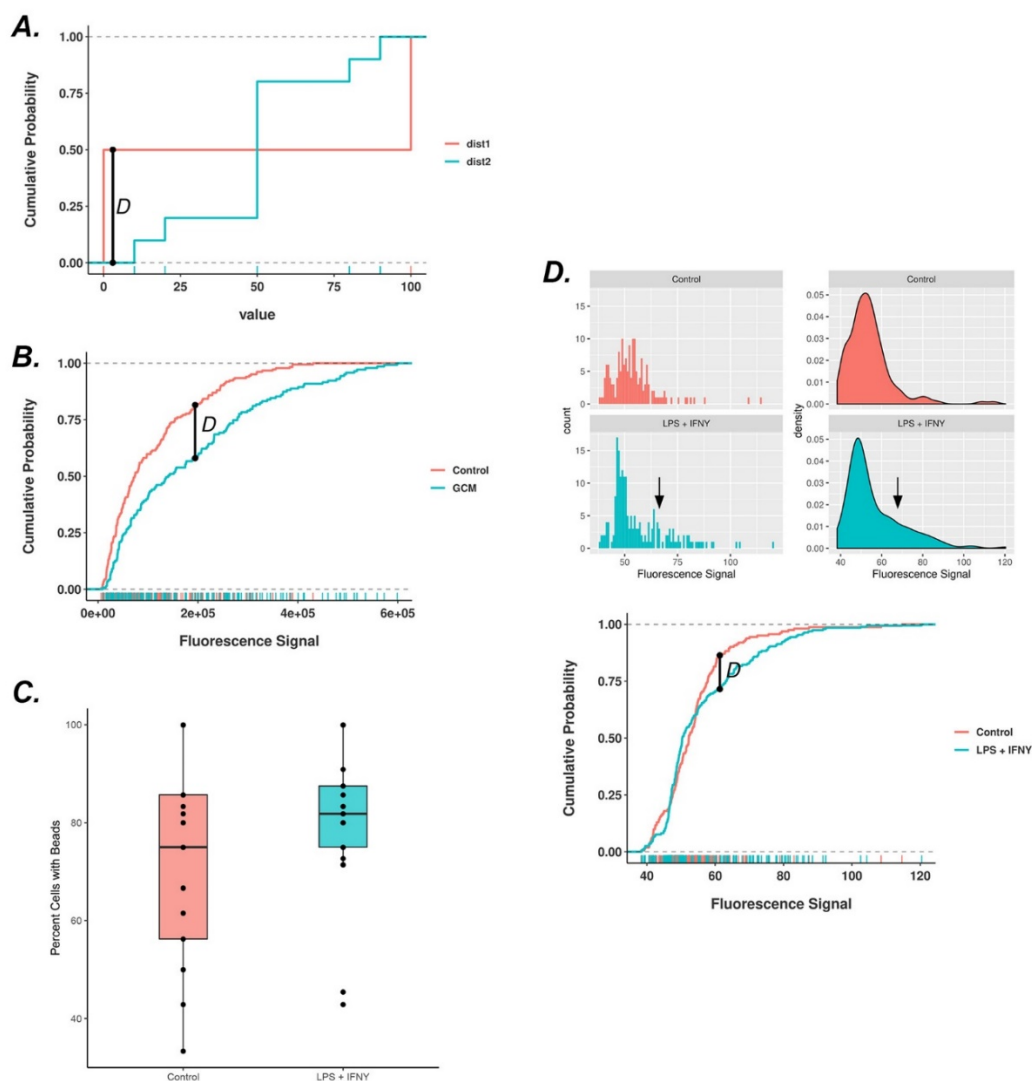


Figure 2. Comparison of quantification of phagocytosis using traditional metrics vs the proposed new method of analysis.

A. Empirical cumulative distribution functions (ECDFs) of non-parametric, multimodal hypothetical datasets *dist1* and *dist2*. The ECDF more accurately portrays the changes that occur in the underlying PDF. B. ECDFs of data experimentally derived from Figure 1A, Experiment 1. The D statistic is plotted, showing the maximal distance between the curves. C. Using traditional metrics to quantify phagocytosis *in vitro*, cells that were positive for bead engulfment were divided by the total number of cells per field of view. Data are derived from Experiment 2. D. *Top panel*: Using the new methodology histogram and density curves of data derived from Experiment 2. A right-shift in the PDF is denoted by an arrow. *Bottom panel*: ECDFs of data derived from Experiment 2. The D statistic is plotted, showing the maximal distance between the curves.

Discussion

There is a lack of standardization in collecting and analyzing phagocytosis assay data. While several techniques offer solutions to quantification of actively phagocytosing cells, the increase of phagocytic activity, *i.e.*, the relative amount or magnitude of phagocytic increases/decreases, is not investigated. Here we propose using the KS test following transformation of the continuous data into an ECDF. The KS test is supported by the theory of optimal mass transport, which ultimately describes two distributions, and seeks to calculate the distances between them.

Many principles of optimal mass transport theory, such as those that utilize the Wasserstein distance metric or Earth Mover's distance, have been used in various areas of research from engineering, to machine learning, to cell biology (Kolouri *et al.*, 2018; Schiebinger *et al.*, 2019). Such analyses of CDFs thus deeply describe the higher order PDF and real-world data from which it is derived. This is a sensitive and accurate technical pipeline to collect and analyze data from monocytic cell phagocytosis assays. The finer detail of data derived reflects the magnitude of changes these innate immune cells undergo. While we show that the signal captured by our method correlates directly with number of beads per cell, investigators should be aware of experimental caveats, such as background from non-engulfed beads, cell-cell engulfment, as well as incomplete capture of the axial plane.

Acknowledgments

We would like to thank members of the Tsirka lab and Dr Rome Sandhu for helpful discussions and edits. This work was partially supported by K12GM102778 (KKT), R25CA214272 (MT) and SBU seed funding (SET).

Competing interests

The authors declare no conflicts of interest or competing interests.

References

- Caponegro, M. D., Torres, L. F., Rastegar, C., Rath, N., Anderson, M. E., Robinson, J. K. and Tsirka, S. E. (2019). [Pifithrin-mu modulates microglial activation and promotes histological recovery following spinal cord injury](#). *CNS Neurosci Ther* 25(2): 200-214.
- Kolouri, S., Pope, P. E., Martin, C. E. and Rohde, G. K. (2018) [Sliced-wasserstein autoencoder: an embarrassingly simple generative model](#). *arXiv e-prints*.
- Lian, H., Roy, E. and Zheng, H. (2016). [Microglial phagocytosis assay](#). *Bio-protocol* 6(21): e1988.
- Pul, R., Chittappan, K. P. and Stangel, M. (2013). [Quantification of microglial phagocytosis by a flow cytometer-based assay](#). *Methods Mol Biol* 1041: 121-127.
- Roy, S., Bag, A. K., Dutta, S., Polavaram, N. S., Islam, R., Schellenburg, S., Banwait, J., Guda, C., Ran, S., Hollingsworth, M. A., Singh, R. K., Talmadge, J. E., Muders, M. H., Batra, S. K. and Datta, K. (2018). [Macrophage-derived neuropilin-2 exhibits novel tumor-promoting functions](#). *Cancer Res* 78(19): 5600-5617.
- Scheraga, R. G., Abraham, S., Niese, K. A., Southern, B. D., Grove, L. M., Hite, R. D., McDonald, C., Hamilton, T. A. and Olman, M. A. (2016). [TRPV4 mechanosensitive ion channel regulates lipopolysaccharide-stimulated macrophage phagocytosis](#). *J Immunol* 196(1): 428-436.
- Schiebinger, G., Shu, J., Tabaka, M., Cleary, B., Subramanian, V., Solomon, A., Gould, J., Liu, S., Lin, S., Berube, P., Lee, L., Chen, J., Brumbaugh, J., Rigollet, P., Hochedlinger, K., Jaenisch, R., Regev, A. and Lander, E. S. (2019). [Optimal-transport analysis of single-cell gene expression identifies developmental trajectories in reprogramming](#). *Cell* 176(4): 928-943 e922.
- Schindelin, J., Arganda-Carreras, I., Frise, E., Kaynig, V., Longair, M., Pietzsch, T., Preibisch, S., Rueden, C., Saalfeld, S., Schmid, B., Tinevez, J. Y., White, D. J., Hartenstein, V., Eliceiri, K., Tomancak, P. and Cardona, A. (2012). [Fiji: an open-source platform for biological-image analysis](#). *Nat Methods* 9(7): 676-682.
- Thompson, K. K. and Tsirka, S. E. (2020). [Guanabenz modulates microglia and macrophages during demyelination](#). *Sci Rep* 10(1): 19333.
- Wu, T. T., Chen, T. L. and Chen, R. M. (2009). [Lipopolysaccharide triggers macrophage activation of inflammatory cytokine expression, chemotaxis, phagocytosis, and oxidative ability via a toll-like receptor 4-dependent pathway: validated by RNA interference](#). *Toxicol Lett* 191(2-3): 195-202.
- Zhang, X., Goncalves, R. and Mosser, D. M. (2008). [The isolation and characterization of murine macrophages](#). *Curr Protoc Immunol* Chapter 14: Unit 14 11.

Generation of the Compression-induced Dedifferentiated Adipocytes (CiDAs) Using Hypertonic Medium

Yiwei Li¹, Angelo S. Mao^{2,3}, Bo Ri Seo^{2,3}, Xing Zhao¹, Satish Kumar Gupta¹, Maorong Chen⁴, Yu Long Han¹, Ting-Yu Shih^{2,3}, David J. Mooney^{2,3} and Ming Guo^{1,*}

¹Department of Mechanical Engineering, Massachusetts Institute of Technology, Cambridge, MA 02139, USA

²John A. Paulson School of Engineering and Applied Sciences, Harvard University, Cambridge, MA 02138, USA

³Wyss Institute for Biologically Inspired Engineering, Harvard University, Cambridge, MA 02138, USA

⁴F. M. Kirby Neurobiology Center, Boston Children's Hospital, Department of Neurology, Harvard Medical School, Boston, MA 02115, USA

*For correspondence: guom@mit.edu

Abstract

Current methods to obtain mesenchymal stem cells (MSCs) involve sampling, culturing, and expanding of primary MSCs from adipose, bone marrow, and umbilical cord tissues. However, the drawbacks are the limited numbers of total cells in MSC pools, and their decaying stemness during *in vitro* expansion. As an alternative resource, recent ceiling culture methods allow the generation of dedifferentiated fat cells (DFATs) from mature adipocytes. Nevertheless, this process of spontaneous dedifferentiation of mature adipocytes is laborious and time-consuming. This paper describes a modified protocol for *in vitro* dedifferentiation of adipocytes by employing an additional physical stimulation, which takes advantage of augmenting the stemness-related Wnt/β-catenin signaling. Specifically, this protocol utilizes a polyethylene glycol (PEG)-containing hypertonic medium to introduce extracellular physical stimulation to obtain higher efficiency and introduce a simpler procedure for adipocyte dedifferentiation.

Keywords: Mesenchymal stem cells, Dedifferentiation, Adipocytes, Compression, Wnt/β-catenin signaling

This protocol was validated in: Sci Adv (2020), DOI: 10.1126/sciadv.aax5611

Background

Adipose tissue currently is one of the most appealing sources of mesenchymal stem cells (MSCs), due to its large abundance and relatively less-invasive harvest methods (Shen *et al.*, 2011; González-Cruz *et al.*, 2012; Konno *et al.*, 2013). Adipose-derived MSCs, that isolated from the stromal-vascular fraction of subcutaneous adipose tissue, have been demonstrated to display multilineage potentials both *in vitro* and *in vivo* (Anghileri *et al.*, 2008; González *et al.*, 2009; Gonzalez-Rey *et al.*, 2010; Jumabay *et al.*, 2010; Mao *et al.*, 2017 and 2019; Darnell *et al.*, 2018). To isolate adipose-derived MSCs, the widely-used method is to dissect the stromal-vascular fraction from the adipose tissue, and then sort the MSCs by either fluorescence-activated cell sorting (FACS) or culture selection (Aronowitz *et al.*, 2015; Raposio *et al.*, 2017; Gentile *et al.*, 2019). However, heterogeneous groups of cells are contained in a stromal-vascular fraction of adipose tissue, and limited cell markers are available for MSCs selection; these make it difficult to purify adipose-derived MSCs (Gimble *et al.*, 2011; González-Cruz *et al.*, 2012; Konno *et al.*, 2013).

Alternatively, the adipocytes, rather than the other types of cells in adipose tissue, can spontaneously dedifferentiate into multipotent mesenchymal cells named the dedifferentiated fat (DFAT) cells during *in vitro* culturing (Sugihara *et al.*, 1986; Shen *et al.*, 2011; Taniguchi *et al.*, 2016). Because of the multipotency of the DFAT cells and the large abundance of the mature adipocytes, the DFAT cells have been regarded as an ideal source for human postnatal mesenchymal multipotent stem cells (Matsumoto *et al.*, 2008; Shen *et al.*, 2011; Côté *et al.*, 2019). However, the current ceiling culturing for adipocyte dedifferentiation requires a long duration (typically 4 weeks) to enable the adipocytes to spontaneously lose all obvious lipid droplets (Lessard *et al.*, 2015; Taniguchi *et al.*, 2016). Thus, further increasing the efficiency of adipocyte dedifferentiation and shortening its processing time is attractive for its wider applications.

Adipocytes and adipose progenitor cells are also important components in tumor microenvironments (Chandler *et al.*, 2012; Seo *et al.*, 2015; Ling *et al.*, 2020). Recent studies revealed that the dedifferentiation of adipocytes occurred during tumor development, which might be attributed to the activated Wnt signaling (Gustafson and Smith, 2010; Bochet *et al.*, 2013) and Notch signaling (Bi *et al.*, 2016). Recent studies also revealed that the dedifferentiation of adipocytes could occur *in vivo* in mice models (Bochet *et al.*, 2013; Liao *et al.*, 2015; Wang *et al.*, 2018). Tumor progression also largely alters the local physical microenvironments, including elevated osmotic pressure, increased compressive force, and matrix stiffening (Nia *et al.*, 2020). These physical cues largely influence the cell fates of both adipose stromal cells and cancer cells (Guo *et al.*, 2017; Li *et al.*, 2019 and 2020a; Han *et al.*, 2020). Indeed, our recent study reported that the generation of osmotic stress *in vitro* to mimic the elevated osmolarity in *in vivo* tumors could also induce the dedifferentiation of adipocytes (Li *et al.*, 2020b). Consistently, another study also reported that a tough implant *in vivo* drove the dedifferentiation of the local surrounding adipocytes (Ma *et al.*, 2019). Thus, these studies inspired us to develop an alternative protocol to generate multipotent mesenchymal cells by mechanically dedifferentiating adipocytes.

The protocol described here includes the experimental set-ups to induce and verify the reprogramming of adipocytes into multipotent mesenchymal cells using our hypertonic dedifferentiation medium. We also include the procedures to generate adipocytes from preadipocytes or mesenchymal stem cells, and the differentiation assays to confirm the multilineage potentials of the CiDAs.

Materials and Reagents

Reagents

1. Minimum Essential Medium Eagle Alpha Modification media (Sigma-Aldrich, catalog number: M8042)
2. Fetal bovine serum (Gibco, catalog number: 10-082-147)
3. Penicillin/streptomycin (Gibco, catalog number: 15140148)
4. Polyethylene glycol 300 (Sigma-Aldrich, catalog number: 8.07484)
5. KnockOut Serum Replacement (Gibco, catalog number: 10828-028)
6. Preadipocyte Growth Medium-2 (Lonza, catalog number: PT-8202)
7. SingleQuots (Lonza, catalog number: PT-9502)

8. Paraformaldehyde (VWR, catalog number: IC0219998380)
9. PBS (Sigma-Aldrich, catalog number: P5119)
10. Triton-X-100 (Sigma-Aldric, catalog number: X100)
11. Oil Red O (Sigma-Aldrich, catalog number: O0625)
12. DMEM (Sigma-Aldrich, Brand, catalog number: D5546)
13. Horse serum (Gibco, catalog number: 26050070)
14. Dexamethasone (Sigma-Aldrich, catalog number: D4902)
15. Hydrocortisone (Sigma-Aldrich, catalog number: H0888)
16. Hydrogen peroxide (Sigma-Aldrich, catalog number: H1009)
17. Anti-MyoD1 (Abcam, catalog number: ab16148)
18. Donkey anti-Rabbit Alexa 488 (Invitrogen, catalog number: R37118)
19. β -glycerophosphate (Sigma-Aldrich, catalog number: G9422)
20. L-ascorbic acid (Sigma-Aldrich, Brand, catalog number: A4403)
21. ELF-97 (Invitrogen, catalog number: E6588)
22. TGF- β (R&D Systems, catalog number: 240-B)
23. Anti-aSMA (Abcam, catalog number: ab5694)
24. DAPI (Thermo Scientific, Brand, catalog number: 62248)
25. Trypsin (2.5%) (Thermo Fisher Scientific, GibcoTM, catalog number: 15090046)

Cell culture plasticware

1. T75 and/or T25 flasks (Corning, catalog numbers: 430641U for T75 and 3056 for T25)
2. Centrifuge tubes (15 ml; 50 ml, Corning, catalog numbers: 430790; 430828)
3. Cryovials (STARLAB, catalog number: E3110-6122)
4. Pipette tips (TipOne, STARLAB, catalog numbers: S1111-3700; S1111-1706; S1111-6701)
5. 35-mm cell culture dish (Thermo Fisher Scientific, catalog number: 153066)
6. 6-well plates (Corning, Falcon[®], catalog number: 353934)
7. 100 mm cell culture dish (Thermo Fisher Scientific, Thermo ScientificTM, catalog number: 150464)

Equipment

1. Centrifuge (Eppendorf, model: 5810)
2. Bright-LineTM Hemacytometer (Sigma-Aldric, catalog number: Z359629)
3. Water bath (Thermo Scientific, catalog number: TSCIR19)
4. Humidified incubator at 37 °C, 5% CO₂ (Thermo Fisher Scientific, Heraeus, model: HeracellTM 150)
5. Leica TCS SP8 Confocal Microscope (Leica)
6. ZEISS Axio Zoom V16 microscope (ZEISS)
7. Xenon Arc Lamp (ZEISS)
8. Hamamatsu Orca Flash 4.0 V3 (Scientifica)
9. Aspirator (Dry vacuum pump/compressor, Welch Vacuum - Gardner Denver, model: 2511)

Software

1. ImageJ (<https://imagej.nih.gov/ij/>)
2. LAS X (Leica Microsystems, Mannheim, Germany)
3. HCImage (<http://www.hamamatsu.com/>)

Procedure

A. Cell culture (Figure 1, step 1)

1. Purchase clonally derived mouse MSCs (OP9) from the American Type Cell Culture (ATCC).
2. Expand MSCs (OP9) subconfluently in Minimum Essential Medium Eagle Alpha Modification media supplemented with 20% fetal bovine serum and 1% penicillin/streptomycin (complete α MEM) in the condition of 5% CO₂, 37°C, and 95% humidity.
3. Assess cell viability using calcein acetoxymethyl and ethidium homodimer-1 (Invitrogen, Eugene, OR) or trypan blue exclusion (Beckman Coulter).
4. Purchase subcutaneous primary human preadipocytes from Lonza.
5. Culture primary human preadipocytes at subconfluence in Preadipocyte Growth Medium-2 (Lonza) in the condition of 5% CO₂, 37°C, and 95% humidity, following the manufacturer's instructions.

B. Generation of adipocytes from preadipocytes or mesenchymal stem cells (Figure 1, step 2)

1. Induce adipogenesis of OP9 mMSCs by supplementing cells with MEM (Gibco) containing 15% KnockOut Serum Replacement (Gibco).
2. Induce adipogenesis of human preadipocytes by culturing cells in Preadipocyte Growth Medium-2 (Lonza) supplemented with SingleQuots (Lonza) consisting of insulin, dexamethasone, indomethacin, and isobutyl-methylxanthine, as per the manufacturer's instructions.

C. Sort adipocytes from the mixed cell population

1. Trypsinize the mixed cell population after adipogenesis induction.
2. Transfer the cell suspension into a 15 mL centrifuge tube, and centrifuge at a low speed (150 × g, 5 min). The differentiated adipocytes are then floating on the top layer of the medium in the centrifuge tube due to their lower density as compared to the culture medium (Figure 1, step 3).
3. Take up only the differentiated adipocytes from the top layer in the centrifuge tube, and seed 10⁵ cells per culture flask (Falcon 3012; 25 cm²). Incubate cells at 37°C in a medium consisting of Minimum Essential Medium Eagle Alpha Modification media supplemented with 20% fetal bovine serum.
4. Completely fulfill the flask with medium to provide the mixed cells with an air-free environment (Figure 1, step 4).
5. Turn the flask upside down on the first day during culturing, allowing the adipocytes to float up in the medium and adhere to the top inner surface (ceiling surface) of the flasks (Figure 1, step 5).
6. Turn the flask back after cells are fully attached (in most cases 1 day is enough, not exceeding 2 days) so that cells are back on the bottom of the flask again (Figure 1, step 6).
7. To obtain purified and monodispersed adipocyte population, sufficiently digest and pipet the cells.
8. Gently wash away the medium and the residual unattached cells.
9. Culture adipocytes with 5 mL medium contained in one Flask in the condition of 5% CO₂, 37°C, and 95% humidity. There are also some numbers of undifferentiated mesenchymal stem cells or preadipocytes attached to the ceiling surface of the flask. Without the supplement of a medium, these cells are then exposed directly to the air and die shortly (Figure 1, step 7).

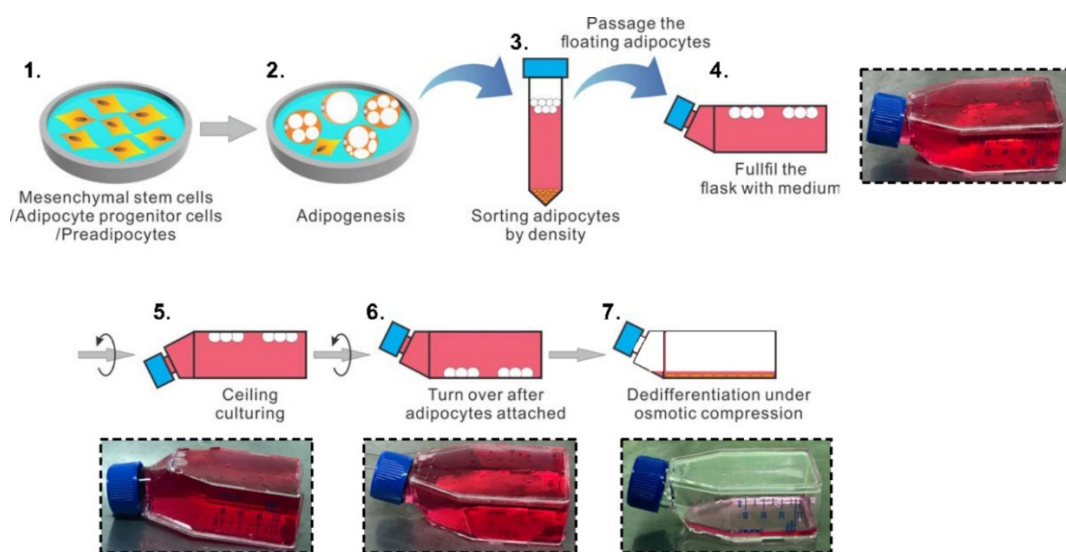


Figure 1. Schematic illustration of the procedure to generate compression-induced dedifferentiation of adipocytes.

1. Mesenchymal stem cells or adipocyte progenitors are homogeneously seeded in tissue culture plate (Step A). 2. Induction of adipogenesis of MSCs or adipocyte progenitors using adipogenesis medium (Step B). 3. Trypsinize the cells and sort generated adipocytes by density (Steps C1-C2). 4. Fulfill the cell culture flask using cell medium and the floating adipocytes (Steps C3-C4). 5. Turn the cell culture flask upside to allow adipocytes attaching to the bottom of the flask by ceiling culturing (Step C5). 6. Turn over the cell culture flask after the adipocytes fully attached to the bottom of flask (Step C6). 7. Induction of dedifferentiation of adipocyte using osmotic compression (Step D).

D. Induction of compression-induced dedifferentiation of adipocytes

1. Aspire and remove half of the culture medium (2.5 mL) from the flask.
2. Add 2.5 mL hypertonic dedifferentiation medium into the flask [Minimum Essential Medium Eagle Alpha Modification media supplemented with 20% fetal bovine serum, 1% penicillin/streptomycin, and 4% PEG-300 (MW: 300, v/v ratio)]. Avoid shaking the flask, and allow the hypertonic medium to slowly diffuse and mix with a residual culturing medium in the flask. Culture the cells in the condition of 5% CO₂, 37°C, and 95% humidity.
3. Exchange the hypertonic dedifferentiation medium every 3 days. Aspire and remove 4 mL of the medium from the flask, and refill with 4 mL hypertonic dedifferentiation medium [Minimum Essential Medium Eagle Alpha Modification media supplemented with 20% fetal bovine serum, 1% penicillin/streptomycin, and 2% PEG-300 (MW: 300, v/v ratio)].
4. Avoid complete removal of the medium and avoid any shear that could be applied to adipocytes. Because of the fragile property of the adipocytes and their contained lipid droplets, any shear or rapid osmotic stress changes may damage the cells.
5. Image the cultured adipocytes during culturing. In 10 days, we likely observe half of the population of the adipocytes transiting and dedifferentiating to mesenchymal stromal cell-like cells (Figure 2). Other adipocytes remain large lipid droplets, many of which would not undergo dedifferentiation.

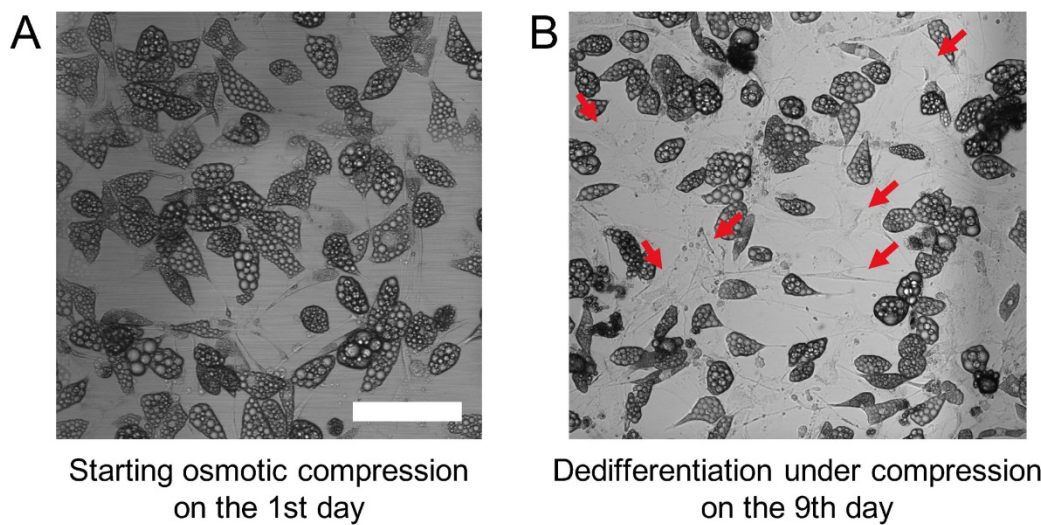


Figure 2. Dedifferentiation of adipocytes before and after 9 days of compression treatment.

A. Adipocytes with cellular lipid droplets before osmotic compression-induced dedifferentiation. B. Anticipated results of CiDAs. The red arrows indicate the regions CiDAs are located, while some other adipocytes are remaining their lipid droplets. Scale bar, 100 μ m. (Step D)

6. Trypsinize all the cells and transfer them to a 15 mL centrifuge tube. Centrifuge the cells at a speed of 150 $\times g$ for 5 min.
7. Remove the top layer residual adipocytes and the supernatant. Resuspend the CiDAs in MSCs expansion medium (Minimum Essential Medium Eagle Alpha Modification media supplemented with 20% fetal bovine serum, 1% penicillin/streptomycin) and seed the cells back to a flask with a density of 10^5 cells per culture flask. Culture the cells in the condition of 5% CO₂, 37 °C, and 95% humidity.
8. Exchange the expansion medium every other day, and keep doing this up to 2 weeks until the CiDAs reaching 80% confluence of the flask surface.

E. Inducing osteogenesis of CiDAs to test the multilineage potential of CiDAs

1. Seed the harvested CiDAs in the wells of 6-well plates with a density of 3×10^5 cells per well, and culture them with MSCs expansion medium (5% CO₂, 37°C, and 95% humidity) until CiDAs reaching more than 90% confluence in the well.
2. Exchange the expansion medium with osteogenic medium (complete DMEM supplemented with 10 mM β -glycerophosphate and 250 μ M L-ascorbic acid). Cycle the osteogenic medium every 2 days.
3. To test ALP activity, fix CiDAs after 6 days of culturing in an osteogenic medium. Permeabilize CiDAs with Triton X-100. Stain the fixed CiDAs with ELF-97 (Thermo Fisher Scientific), following the manufacturer's instructions.
4. Image the stained CiDAs using epifluorescence microscopy, consisting of a Xenon lamp, an Axio Zoom V16 microscope, and Hamamatsu Flash 4.0 v3. Anticipate observing over 50% of the cells are positive with the blue color of ALP staining (Figure 3A). The positive ratio of calcium deposition can be accessed using ImageJ, which is defined by the number of pixels positive with red color divided by the total numbers of pixels of the image.
5. To test mineral deposition of osteogenesis of CiDAs, firstly aspirate the medium from the well. Then, fix the cells in ice-cold 70% ethanol for 5 min at room temperature. Aspirate alcohol and rinse cells twice with DI water (5 min each time). Aspirate the water and add 1 ml 2% Alizarin Red S solution, which is adjusted to a pH value of 4.1-4.3 with ammonium hydroxide. Incubate the well plate at room temperature for 3 min. Aspirate Alizarin Red S solution and wash the wells five times with 2 mL water.

6. Image the stained CiDAs using epifluorescence microscopy, consisting of a Xenon lamp, an Axio Zoom V16 microscope, and Hamamatsu Flash 4.0 v3. Anticipate to observe over 50% of the surface is positive with the red color of calcium deposition staining (Figure 3B).

F. Inducing adipogenesis of CiDAs to test the multilineage potential of CiDAs

1. Seed the harvested CiDAs in the wells of 6-well plates with a density of 3×10^5 cells per well, and culture them with MSCs expansion medium (5% CO₂, 37°C, and 95% humidity) until CiDAs reaching more than 90% confluence in the well.
2. If the CiDAs is originating from mouse MSCs (OP9), exchange the expansion medium with an adipogenic medium (MEM (Gibco) containing 15% KnockOut Serum Replacement (Gibco)). Cycle the osteogenic medium every 2 days.
3. If the CiDAs is originating from human primary preadipocytes, exchange the expansion medium with an adipogenic medium (Preadipocyte Growth Medium-2 (Lonza) supplemented with SingleQuots (Lonza) consisting of insulin, dexamethasone, indomethacin, and isobutyl-methylxanthine). Cycle the osteogenic medium every 2 days.
4. To test lipid droplet accumulation after 10 days of incubation, fix CiDAs with 4% paraformaldehyde (Thermo Fisher Scientific) in phosphate-buffered saline (PBS) (Gibco) with 0.1% Triton X-100 (Sigma-Aldrich) for 30 min at 25°C. Wash CiDAs with PBS 3 times. Neutral lipid accumulation was visualized by Oil Red O (Abcam) staining as a functional marker for adipogenesis. Rinse cells with PBS 3 times for 10 min each.
5. Image the stained CiDAs using epifluorescence microscopy, consisting of a Xenon lamp, an Axio Zoom V16 microscope, and Hamamatsu Flash 4.0 v3. Anticipate to observe over 50% of the cells is positive with the red color of Oil Red O staining (Figure 3C). The positive ratio of Oil Red O staining can be accessed using Image J, which is defined by the number of cells positive with red color divided by the total number of the cells.

G. Inducing myogenic of CiDAs to test the multilineage potential of CiDAs

1. Seed the harvested CiDAs in the wells of 6-well plates with a density of 3×10^5 cells per well, and culture them with MSCs expansion medium (CO₂, 37°C, and 95% humidity) until CiDAs reaching more than 90% confluence in the well.
2. Exchange the expansion medium with myogenic medium (complete DMEM supplemented with 5% horse serum (HS) (Gibco), 0.1 µM dexamethasone (Sigma-Aldrich), and 50 µM hydrocortisone (Sigma-Aldrich)) for 10 days. Cycle the myogenic medium every 2 days.
3. To test myogenesis efficiency after 10 days of incubation, fix CiDAs with 4% paraformaldehyde (Thermo Fisher Scientific) in PBS (Gibco). Wash the fixed sample three times with PBS. Incubate the fixed sample with PBS (Gibco) with 0.1% Triton X-100 (Sigma-Aldrich) for 30 min at 25°C. Block nonspecific sites in the fixed sample using blocking buffer (PBS, 10% HS, and 0.1% Triton X-100) for an additional 60 min. Wash three times for 5 min each. Incubate the fixed cells with primary antibody anti-MyoD1 (Abcam) in blocking buffer. Rinse cells extensively in blocking buffer and incubate secondary antibody donkey anti-rabbit Alexa 488 (Thermo Fisher Scientific) for 1 h. Rinse cells by PBS 3 times for 10 min each. Incubate cells with DRAQ5 solution for 10 min before imaging.
4. Image the stained CiDAs using confocal microscopy, with LAS X. Anticipate to observe over 50% of the cells are positive with the anti-MyoD1 staining (Figure 3D). The positive ratio of MyoD1 staining can be accessed using ImageJ, which is defined by the number of cells positive with anti-MyoD1 divided by the total number of the cells.

H. Inducing myofibrogenesis of CiDAs to test the multilineage potential of CiDAs

1. Seed the harvested CiDAs in the wells of 6-well plates with a density of 3×10^5 cells per well, and culture

- them with MSCs expansion medium (5% CO₂, 37°C, and 95% humidity) until CiDAs reach more than 70% confluence in the well.
2. Exchange the expansion medium with myofibrogenic medium (complete DMEM supplemented with 2 ng/mL TGF-β (Abcam)) for 7 days. Cycle the myogenic medium every 2 days.
 3. To test myofibrogenesis efficiency after incubation, fix CiDAs with 4% paraformaldehyde (Thermo Fisher Scientific) in PBS (Gibco). Wash the fixed sample three times with PBS. Incubate the fixed sample with PBS (Gibco) with 0.1% Triton X-100 (Sigma-Aldrich) for 30 min at 25°C. Block nonspecific sites in the fixed sample using blocking buffer (PBS, 10% HS, and 0.1% Triton X-100) for an additional 60 min. Wash three times for 5 min each. Incubate the fixed cells with primary antibody anti-α-SMA1 (Abcam) in blocking buffer. Rinse cells extensively in blocking buffer and incubate secondary antibody donkey anti-rabbit Alexa 488 (Thermo Fisher Scientific) for 1 h. Rinse cells by PBS 3 times for 10 min each. Incubate cells with DRAQ5 solution for 10 min before imaging.
 4. Image the stained CiDAs using confocal microscopy, with LAS X. Anticipate to observe over 50% of the cells are positive with the anti-α-SMA1 staining (Figure 3E). The positive ratio of α-SMA1 staining can be accessed using ImageJ, which is defined by the number of cells positive with anti-α-SMA1 divided by the total number of the cells.

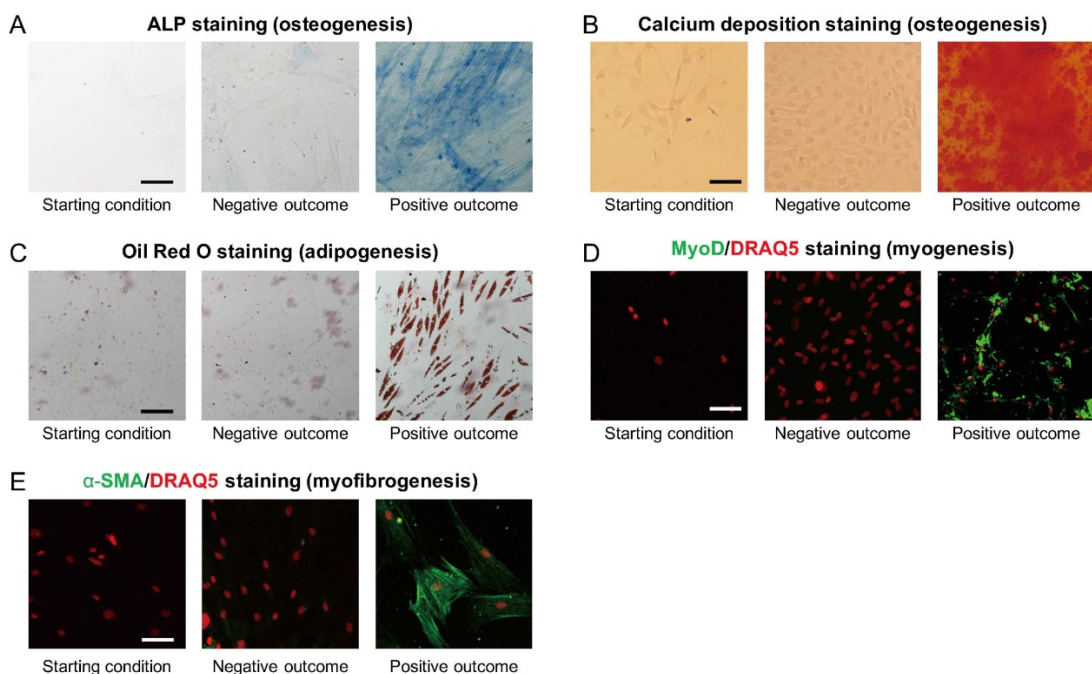


Figure 3. Expected results of multilineage induction from CiDAs.

A. Expected ALP staining to test osteogenesis of CiDAs, at starting points, negative outcome, and positive outcome. Scale bar, 100 μm. (Step E). B. Expected calcium deposition staining to test osteogenesis of CiDAs, at starting points, negative outcome, and positive outcome. Scale bar, 50 μm. (Step E). C. Expected Oil Red O staining to test adipogenesis of CiDAs, at starting points, negative outcome, and positive outcome. Scale bar, 100 μm. (Step F). D. Expected MyoD staining to test myogenesis of CiDAs, at starting points, negative outcome, and positive outcome. Scale bar, 50 μm. (Step G). E. Expected α-SMA staining to test myofibrogenesis of CiDAs, at starting points, negative outcome, and positive outcome. Scale bar, 50 μm. (Step H)

Trouble-shooting

1. Low efficiency of adipogenesis of mesenchymal stem cells or adipose progenitors

- Possible cause: Low cell density before induction of adipogenesis.
- Possible repair: Increasing expansion time of MSCs/adipocyte progenitors culturing before exchanging to adipogenesis induction medium. MSCs/adipocyte progenitors should reach 90% confluence before exchanging to the adipogenesis induction medium.
2. Contamination with non-adipocytes after ceiling culturing

Possible cause: Insufficient digestion of adipocytes before density sorting.

Possible repair: Increasing digestion time to trypsin the cells, and gently pipette the cells to sufficiently break down cell-to-cell contact and generate monodispersed cells.
 3. A limited number of adherent adipocytes after ceiling culturing

Possible cause: Flow shear or harsh pipetting damages adipocytes during preparation.

Possible repair: Be gentle when digest and pipette the cells; keep the cells at 4°C during density sorting; avoiding flow shearing during fulfilling the culture flask, and be sure to remove all the air bubbles before turning the flask upside down.
 4. Adipocytes dying and detaching during culturing under high osmotic compression

Possible cause: Quick exchange of hypertonic medium and quick osmotic shock.

Possible repair: Exchange only half of the medium when changing medium, let the hypertonic medium slowly diffuse into the remaining culture medium, and reach the final concentration.

Future direction

There is significant heterogeneity in primary adipose tissue, which makes adipocytes isolated from different original sites behave much differently from each other. Thus, future works could involve optimizing the protocol to generate CiDAs from adipocytes of different origins. Secondly, mesenchymal stem cells or progenitor cells from different tissue usually exhibit different lineage potentials. Thus, for CiDAs generated from different origins of adipocytes, we also need to test their lineage potentials, which will help to define their practical applications in stem cell therapy, tissue engineering, and regenerative medicine. Another direction is further improving the efficiency of generating CiDAs and shortening the time required for the dedifferentiation of adipocytes. This could be done by combining mechanical stimulations and biochemical treatment. Current work from our group revealed that Wnt/β-catenin signaling plays an important role in adipocytes differentiation (Li *et al.*, 2020b), which is also supported by another work (Gustafson and Smith, 2010). Another study from Kuang's group revealed that Notch activation drove adipocyte dedifferentiation (Bi *et al.*, 2016). Based on these understandings, a dedifferentiation cocktail medium, that not only mimics native physical stresses but also contains growth factors regulating Wnt/β-catenin signaling or Notch signaling, could more efficiently induce dedifferentiation of adipocytes and generate CiDAs. Overall, we hope that further development of this method may make CiDAs more accessible for many groups, and more stable for applications in regenerative medicine.

Acknowledgments

The authors would like to acknowledge the support from National Cancer Institute grant no. 1U01CA202123, National institute of general medical sciences grant no. 1R01GM140108, and the Jeptha H. and Emily V. Wade Award at MIT. A.S.M., B.R.S., T.-Y.S., and D.J.M. are supported by the NIH 5R01 DE013033 and 2R01 DE013349.

Competing interests

The authors declare no conflict of interests.

References

- Anghileri, E., Marconi, S., Pignatelli, A., Cifelli, P., Galie, M., Sbarbati, A., Krampera, M., Belluzzi, O. and Bonetti, B. (2008). [Neuronal differentiation potential of human adipose-derived mesenchymal stem cells](#). *Stem Cells Dev* 17(5): 909-916.
- Aronowitz, J. A., Lockhart, R. A. and Hakakian, C. S. (2015). [Mechanical versus enzymatic isolation of stromal vascular fraction cells from adipose tissue](#). *Springerplus* 4: 713.
- Bi, P., Yue, F., Karki, A., Castro, B., Wirbisky, S. E., Wang, C., Durkes, A., Elzey, B. D., Andrisani, O. M., Bidwell, C. A., Freeman, J. L., Konieczny, S. F. and Kuang, S. (2016). [Notch activation drives adipocyte dedifferentiation and tumorigenic transformation in mice](#). *J Exp Med* 213(10): 2019-2037.
- Bochet, L., Lehuede, C., Dauvillier, S., Wang, Y. Y., Dirat, B., Laurent, V., Dray, C., Guiet, R., Maridonneau-Parini, I., Le Gonidec, S., Couderc, B., Escourrou, G., Valet, P. and Muller, C. (2013). [Adipocyte-derived fibroblasts promote tumor progression and contribute to the desmoplastic reaction in breast cancer](#). *Cancer Res* 73(18): 5657-5668.
- Côté, J. A., Ostinelli, G., Gauthier, M. F., Lacasse, A. and Tchernof, A. (2019). [Focus on dedifferentiated adipocytes: characteristics, mechanisms, and possible applications](#). *Cell Tissue Res* 378(3): 385-398.
- Chandler, E. M., Seo, B. R., Califano, J. P., Andresen Egiluz, R. C., Lee, J. S., Yoon, C. J., Tims, D. T., Wang, J. X., Cheng, L., Mohanan, S., Buckley, M. R., Cohen, I., Nikitin, A. Y., Williams, R. M., Gourdon, D., Reinhart-King, C. A. and Fischbach, C. (2012). [Implanted adipose progenitor cells as physicochemical regulators of breast cancer](#). *Proc Natl Acad Sci U S A* 109(25): 9786-9791.
- Darnell, M., O'Neil, A., Mao, A., Gu, L., Rubin, L. L. and Mooney, D. J. (2018). [Material microenvironmental properties couple to induce distinct transcriptional programs in mammalian stem cells](#). *Proc Natl Acad Sci U S A* 115(36): E8368-E8377.
- Gentile, P., Calabrese, C., De Angelis, B., Pizzicannella, J., Kothari, A. and Garcovich, S. (2019). [Impact of the Different Preparation Methods to Obtain Human Adipose-Derived Stromal Vascular Fraction Cells \(AD-SVFs\) and Human Adipose-Derived Mesenchymal Stem Cells \(AD-MSCs\): Enzymatic Digestion Versus Mechanical Centrifugation](#). *Int J Mol Sci* 20(21): 5471.
- Gimble, J. M., Bunnell, B. A., Chiu, E. S. and Guilak, F. (2011). [Concise review: Adipose-derived stromal vascular fraction cells and stem cells: let's not get lost in translation](#). *Stem Cells* 29(5): 749-754.
- González-Cruz, R. D., Fonseca, V. C. and Darling, E. M. (2012). [Cellular mechanical properties reflect the differentiation potential of adipose-derived mesenchymal stem cells](#). *Proc Natl Acad Sci U S A* 109(24): E1523-1529.
- González, M. A., Gonzalez-Rey, E., Rico, L., Buscher, D. and Delgado, M. (2009). [Adipose-derived mesenchymal stem cells alleviate experimental colitis by inhibiting inflammatory and autoimmune responses](#). *Gastroenterology* 136(3): 978-989.
- Gonzalez-Rey, E., Gonzalez, M. A., Varela, N., O'Valle, F., Hernandez-Cortes, P., Rico, L., Buscher, D. and Delgado, M. (2010). [Human adipose-derived mesenchymal stem cells reduce inflammatory and T cell responses and induce regulatory T cells in vitro in rheumatoid arthritis](#). *Ann Rheum Dis* 69(1): 241-248.
- Guo, M., Pegoraro, A. F., Mao, A., Zhou, E. H., Arany, P. R., Han, Y., Burnette, D. T., Jensen, M. H., Kasza, K. E., Moore, J. R., Mackintosh, F. C., Fredberg, J. J., Mooney, D. J., Lippincott-Schwartz, J. and Weitz, D. A. (2017). [Cell volume change through water efflux impacts cell stiffness and stem cell fate](#). *Proc Natl Acad Sci U S A* 114(41): E8618-E8627.
- Gustafson, B. and Smith, U. (2010). [Activation of canonical wingless-type MMTV integration site family \(Wnt\) signaling in mature adipocytes increases beta-catenin levels and leads to cell dedifferentiation and insulin resistance](#). *J Biol Chem* 285(18): 14031-14041.
- Han, Y. L., Pegoraro, A. F., Li, H., Li, K., Yuan, Y., Xu, G., Gu, Z., Sun, J., Hao, Y., Gupta, S. K., Li, Y., Tang, W., Tang, X., Teng, L., Fredberg, J. J. and Guo, M. (2020). [Cell swelling, softening and invasion in a three-dimensional breast cancer model](#). *Nat Phys* 16(1): 101-108.
- Jumabay, M., Zhang, R., Yao, Y., Goldhaber, J. I. and Bostrom, K. I. (2010). [Spontaneously beating cardiomyocytes derived from white mature adipocytes](#). *Cardiovasc Res* 85(1): 17-27.
- Konno, M., Hamabe, A., Hasegawa, S., Ogawa, H., Fukusumi, T., Nishikawa, S., Ohta, K., Kano, Y., Ozaki, M., Noguchi, Y., Sakai, D., Kudoh, T., Kawamoto, K., Eguchi, H., Satoh, T., Tanemura, M., Nagano, H., Doki, Y.,

- Mori, M. and Ishii, H. (2013). [Adipose-derived mesenchymal stem cells and regenerative medicine](#). *Dev Growth Differ* 55(3): 309-318.
- Lessard, J., Cote, J. A., Lapointe, M., Pelletier, M., Nadeau, M., Marceau, S., Biertho, L. and Tchernof, A. (2015). [Generation of human adipose stem cells through dedifferentiation of mature adipocytes in ceiling cultures](#). *J Vis Exp*(97): e52485.
- Li, Y., Chen, M., Hu, J., Sheng, R., Lin, Q., He, X. and Guo, M. (2020a). [Volumetric Compression Induces Intracellular Crowding to Control Intestinal Organoid Growth via Wnt/β-Catenin Signaling](#). *Cell Stem Cell*. S1934-5909(20)30458-6. doi: 10.1016/j.stem.2020.09.012.
- Li, Y., Guo, F., Hao, Y., Gupta, S. K., Hu, J., Wang, Y., Wang, N., Zhao, Y. and Guo, M. (2019). [Helical nanofiber yarn enabling highly stretchable engineered microtissue](#). *Proc Natl Acad Sci U S A* 116(19): 9245-9250.
- Li, Y., Mao, A. S., Seo, B. R., Zhao, X., Gupta, S. K., Chen, M., Han, Y. L., Shih, T. Y., Mooney, D. J. and Guo, M. (2020b). [Compression-induced dedifferentiation of adipocytes promotes tumor progression](#). *Sci Adv* 6(4): eaax5611.
- Liao, Y., Zeng, Z., Lu, F., Dong, Z., Chang, Q. and Gao, J. (2015). [In vivo dedifferentiation of adult adipose cells](#). *PLoS One* 10(4): e0125254.
- Ling, L., Mulligan, J.A., Ouyang, Y., Shimpi, A.A., Williams, R.M., Beeghly, G.F., Hopkins, B.D., Spector, J.A., Adie, S.G., and Fischbach, C. (2020). [Obesity-Associated Adipose Stromal Cells Promote Breast Cancer Invasion through Direct Cell Contact and ECM Remodeling](#). *Adv Funct Mater* 1910650.
- Ma, J., Xia, J., Gao, J., Lu, F. and Liao, Y. (2019). [Mechanical Signals Induce Dedifferentiation of Mature Adipocytes and Increase the Retention Rate of Fat Grafts](#). *Plast Reconstr Surg* 144(6): 1323-1333.
- Mao, A. S., Ozkale, B., Shah, N. J., Vining, K. H., Descombes, T., Zhang, L., Tringides, C. M., Wong, S. W., Shin, J. W., Scadden, D. T., Weitz, D. A. and Mooney, D. J. (2019). [Programmable microencapsulation for enhanced mesenchymal stem cell persistence and immunomodulation](#). *Proc Natl Acad Sci U S A* 116(31): 15392-15397.
- Mao, A. S., Shin, J. W., Utech, S., Wang, H., Uzun, O., Li, W., Cooper, M., Hu, Y., Zhang, L., Weitz, D. A. and Mooney, D. J. (2017). [Deterministic encapsulation of single cells in thin tunable microgels for niche modelling and therapeutic delivery](#). *Nat Mater* 16(2): 236-243.
- Matsumoto, T., Kano, K., Kondo, D., Fukuda, N., Iribe, Y., Tanaka, N., Matsubara, Y., Sakuma, T., Satomi, A., Otaki, M., Ryu, J. and Mugishima, H. (2008). [Mature adipocyte-derived dedifferentiated fat cells exhibit multilineage potential](#). *J Cell Physiol* 215(1): 210-222.
- Nia, H. T., Munn, L. L. and Jain, R. K. (2020). [Physical traits of cancer](#). *Science* 370(6516): eaaz0868.
- Raposo, E., Simonacci, F. and Perrotta, R. E. (2017). [Adipose-derived stem cells: Comparison between two methods of isolation for clinical applications](#). *Ann Med Surg (Lond)* 20: 87-91.
- Seo, B. R., Bhardwaj, P., Choi, S., Gonzalez, J., Andresen Eguiluz, R. C., Wang, K., Mohanan, S., Morris, P. G., Du, B., Zhou, X. K., Vahdat, L. T., Verma, A., Elemento, O., Hudis, C. A., Williams, R. M., Gourdon, D., Dannenberg, A. J. and Fischbach, C. (2015). [Obesity-dependent changes in interstitial ECM mechanics promote breast tumorigenesis](#). *Sci Transl Med* 7(301): 301ra130.
- Shen, J. F., Sugawara, A., Yamashita, J., Ogura, H. and Sato, S. (2011). [Dedifferentiated fat cells: an alternative source of adult multipotent cells from the adipose tissues](#). *Int J Oral Sci* 3(3): 117-124.
- Sugihara, H., Yonemitsu, N., Miyabara, S. and Yun, K. (1986). [Primary cultures of unilocular fat cells: characteristics of growth *in vitro* and changes in differentiation properties](#). *Differentiation* 31(1): 42-49.
- Taniguchi, H., Kazama, T., Hagikura, K., Yamamoto, C., Kazama, M., Nagaoka, Y. and Matsumoto, T. (2016). [An Efficient Method to Obtain Dedifferentiated Fat Cells](#). *J Vis Exp*(113): e54177.
- Wang, Q. A., Song, A., Chen, W., Schwalie, P. C., Zhang, F., Vishvanath, L., Jiang, L., Ye, R., Shao, M., Tao, C., Gupta, R. K., Deplancke, B. and Scherer, P. E. (2018). [Reversible De-differentiation of Mature White Adipocytes into Preadipocyte-like Precursors during Lactation](#). *Cell Metab* 28(2): 282-288 e283.

Preparation of an Orthotopic, Syngeneic Model of Lung Adenocarcinoma and the Testing of the Antitumor Efficacy of Poly(2-oxazoline) Formulation of Chemo-and Immunotherapeutic Agents

Natasha Vinod^{1,2}, Duhyeong Hwang¹, Salma H. Azam³, Amanda E. D. Van Swearingen³, Elizabeth Wayne¹, Sloane Christian Fussell⁴, Marina Sokolsky-Papkov¹, Chad V. Pecot^{3, 5, 6, *} and Alexander V. Kabanov^{1, 7, *}

¹Center for Nanotechnology in Drug Delivery and Division of Pharmacoeengineering and Molecular Pharmaceutics, Eshelman School of Pharmacy, University of North Carolina at Chapel Hill, NC, U.S.A.

²Joint UNC/NC State Department of Biomedical Engineering, University of North Carolina, Chapel Hill, NC, U.S.A.

³Lineberger Comprehensive Cancer Center, University of North Carolina at Chapel Hill, Chapel Hill, NC, U.S.A.

⁴Department of Biology, Department of Chemistry, University of North Carolina at Chapel Hill, Chapel Hill, NC, U.S.A.

⁵Division of Hematology & Oncology, University of North Carolina at Chapel Hill, Chapel Hill, NC, U.S.A.

⁶Department of Medicine, University of North Carolina at Chapel Hill, Chapel Hill, NC, U.S.A.

⁷Laboratory of Chemical Design of Bionanomaterials, Faculty of Chemistry, M.V. Lomonosov Moscow State University, Moscow, Russia

*For correspondence: pecot@email.unc.edu; kabanov@email.unc.edu

Abstract

Tumor xenograft models developed by transplanting human tissues or cells into immune-deficient mice are widely used to study human cancer response to drug candidates. However, immune-deficient mice are unfit for investigating the effect of immunotherapeutic agents on the host immune response to cancer (Morgan, 2012). Here, we describe the preparation of an orthotopic, syngeneic model of lung adenocarcinoma (LUAD), a subtype of non-small cell lung cancer (NSCLC), to study the antitumor effect of chemo and immunotherapeutic agents in an immune-competent animal. The tumor model is developed by implanting 344SQ LUAD cells derived from the metastases of *Kras*^{G12D}; *p53*^{R172HAG} genetically engineered mouse model into the left lung of a syngeneic host (Sv/129). The 344SQ LUAD model offers several advantages over other models: 1) The immune-competent host allows for the assessment of the biologic effects of immune-modulating agents; 2) The pathophysiological features of the human disease are preserved due to the orthotopic approach; 3) Predisposition of the tumor to metastasize facilitates the study of therapeutic effects on primary tumor as well as the metastases (Chen *et al.*, 2014). Furthermore, we also describe a treatment strategy based on Poly(2-oxazoline) micelles that has been shown to be effective in this difficult-to-treat tumor model (Vinod *et al.*, 2020b).

Keywords: Xenograft, Immune-competent, Immune-deficient, Orthotopic, Syngeneic

This protocol was validated in: Sci Adv (2020), DOI: 10.1126/sciadv.aba5542

Background

NSCLC has a poor prognosis because most patients have advanced stage of cancer at the time of diagnosis, and patients with early-stage tumors are very likely to encounter post-surgical metastasis and recurrence (Zappa and Mousa, 2016; Renaud *et al.*, 2016). Transplanted tumors grown subcutaneously in immune-deficient nude mice do not faithfully recapitulate the metastatic disease, and therefore, better models are needed (Manzotti *et al.*, 1993). The 344SQ LUAD cell line forms spontaneous metastasis due to the suppression of the microRNA-200 (miR-200) expression, resulting in an epithelial-mesenchymal transition (EMT) phenotype having increased motility (Chen *et al.*, 2014). Moreover, with a considerably low number of tumor-infiltrating cytotoxic T lymphocytes, the Kras/p53 mutant LUAD model exhibits an 'immunologically cold' phenotype. The low number of anticancer lymphocytes renders it less receptive to treatments like anti-PD1 that depends on pre-existing T cells, making it an ideal model to test alternative strategies for the treatment of "immunologically cold tumors" (Pfirschke *et al.*, 2016; Espinosa *et al.*, 2017).

Platinum-based chemotherapy is a standard of care in NSCLC. However, acquired resistance to platinum drugs presents a serious challenge in NSCLC management (Galluzzi *et al.*, 2012). Here, we describe a procedure to adopt the Poly(2-oxazoline) (POx)-based nanomicelle formulation strategy for the coadministration of agents that reverse drug resistance (a.k.a. chemosensitizers) with platinum drugs and assess their efficacy in the LUAD model of NSCLC. Further, we describe an immunotherapeutic approach for treating LUAD by using POx micelle formulation of a small molecule biologic response modifier, Resiquimod (administered alone or in combination with checkpoint blockade therapy). POx micelle formulation of poorly soluble drugs has been previously demonstrated to be safe and effective in various tumor models (He *et al.*, 2016). POx micelles are easy to prepare (Vinod *et al.*, 2020a) and can be used to solubilize a broad range of poorly soluble compounds for drug delivery applications.

Materials and Reagents

1. Alcohol swab (B.D. Biosciences)
2. Nair hair removal cream
3. Cotton swab
4. Sterile gauze pads
5. Tuberculin syringe (B.D. Biosciences)
6. 344SQ-green fluorescent protein/Firefly luciferase (GFP/fLuc) cells (source: J. Kurie, MD Anderson Cancer Center)
7. Hanks' Balanced Salt solution (Gibco)
8. Matrigel (Corning)
9. D-luciferin (PerkinElmer)
10. 1× DPBS (Gibco)
11. Isofluorane (VetOne)
12. Ketamine (Vedco)
13. Xylazine (Acorn animal health)
14. Acepromazine (Vedco)
15. Anesthetic cocktail (see Recipes)

Note: Refer to Vinod *et al.* (2020a) (protocol based exclusively on Poly(2-oxazoline) preparation for reagents for Sections C and D).

Equipment

1. Surgical instruments
 - a. Autoclip Wound Closing System – Staples + Applier (Braintree Scientific, Inc)
 - b. Iris Surgical Scissors, 4½ inch, curved (Fisher Scientific)
 - c. Delicate Specialty Dissection Forceps, Serrated, 5" (Fisher Scientific)
2. IVIS-Lumina II optical imaging system (PerkinElmer Inc., Hopkinton, MA)
3. Small Animal induction chamber

Software

1. Living Image® software

Procedure

A. Preparation of animal tumor model of NSCLC

1. Prepare a suspension of 344SQ-green fluorescent protein (GFP)/fLuc cells in 50% Hanks' Balanced Salt Solution and 50% Matrigel (v/v).
2. Anesthetize the mice by injecting the anesthetizing cocktail intraperitoneally and lay it in the right lateral decubitus position.
3. Apply hair removal cream using cotton swab in the chest area and leave for 1 min (be sure not to exceed 1 min to avoid giving the mice a chemical burn). Wipe away with dry sterile gauze pad. Use damp sterile gauze pad to remove any residual cream.
4. Clean the skin surface with an alcohol swab and make an incision between ribs 10 and 11 by placing the blade parallel to the rib cage (see **Figure 1A**).
5. Transfer the cell suspension to a 1-ml tuberculin syringe and inject 50 µL of 2.5×10^3 - 5×10^3 cells into the left lung parenchyma in the lateral dorsal axillary line (see **Figure 1B**).
6. Close the incision using wound closure clips and place the animal in the left lateral decubitus position until recovery.

Note: Day 1 is defined as the day of tumor inoculation.

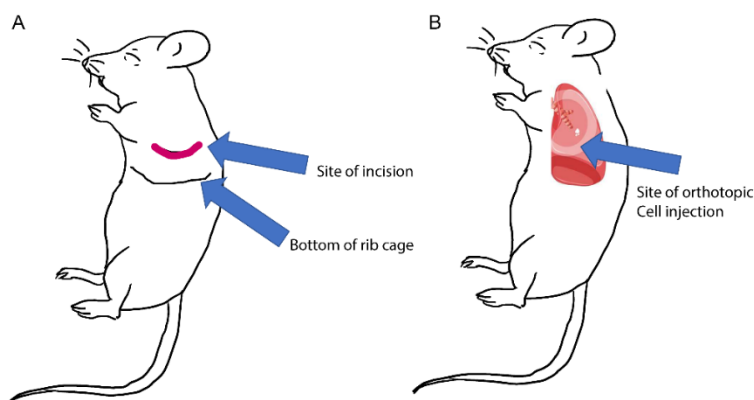


Figure 1. Schematic showing the site of incision (A) and the site of orthotopic injection (B)

B. Bioluminescence imaging

1. Inject 150 mg/kg of 15 mg/mL (in 1× DPBS) D-luciferin solution intraperitoneally and start imaging after 15 min.
2. Anesthetize the mice by placing them in an inhalation induction chamber (for ~5 min) comprising 2-3% isoflurane in oxygen.
3. Place the anesthetized animals in the sample stage of the imaging chamber of the IVIS lumina optical imaging system in the supine position.
4. Acquire luminescent images using the following acquisition settings in the Living Image® software:
 - a. Pixel Width: 1
 - b. Pixel Height: 1
 - c. Image units: counts
 - d. Luminescent exposure (seconds): 60
 - e. Field of view: 24
 - f. Emission filter: open
 - g. Subject size: 1.5

Note: Bioluminescence imaging (B.L.I.) is done once prior to the commencement of the treatments to obtain baseline bioluminescence to confirm the presence of the tumor. Following the start of treatments (Day 8), B.L.I. is performed once every week to monitor tumor growth.

C. Chemotherapy in conjunction with chemosensitizers

1. Randomize mice into four groups of 10 mice each
2. Administer a total of 4 doses (on days 8, 12, 15, and 19) of either of the formulations intravenously (unless indicated otherwise):
 - a. Normal saline (volume: 100-200 µL).
 - b. C₆CP/AZD7762 PM (POx micelles; coloaded with C₆CP and AZD7762 at a weight ratio of 10/20, yielding a final dose of 10 mg/kg of C₆CP and 20 mg/kg of AZD7762).
 - c. C₆CP/VE-822 PM (POx micelles; coloaded with C₆CP and VE-822 at a weight ratio of 10/10, yielding a final dose of 10 mg/kg of C₆CP and 10 mg/kg of VE-822).
 - d. Anti-PD-1 antibody (250 µg per mouse; administered intraperitoneally).

D. Immunotherapy alone and in combination with immune checkpoint blockade

1. Randomize mice into four groups of 13 mice each.
2. Administer a total of 4 doses (on days 8, 12, 15, and 19) of either of the formulations intravenously (unless indicated otherwise):
 - a. Normal saline (volume: 100-200 µL).
 - b. Resiquimod PM (5 mg/kg).
 - c. Anti-PD-1 antibody (250 µg per mouse; administered intraperitoneally and continued after day 17 for four more times – days 22, 26, 29, and 33).

Note: Since the mice in this group reached the study endpoint before day 33, they did not receive the fourth dose.

- d. Resiquimod PM (5 mg/kg) + anti-PD-1 (250 µg per mouse; administered intraperitoneally and continued after day 17 for four more times – days 22, 26, 29, and 33).

Data analysis

Analyze the B.L.I. data by specifying a region of interest outlining the tumor and quantify the total radiance using Living Image Software to measure the luciferase activity, which is representative of the tumor burden. Refer to Vinod *et al.* (2020b) for representative BLI images.

Recipes

1. Anesthetic cocktail

To prepare the anesthetic cocktail, dilute stock solutions of Ketamine, Xylazine and Acepromazine in 1× DPBS and administer 100 µL of the cocktail per 10 g of mouse body weight. Use the following doses of each anesthetic:

Ketamine: 80 mg/kg (stock conc. 100 mg/mL)

Xylazine: 8 mg/kg (stock conc. 100 mg/ml)

Acepromazine: 1 mg/kg (stock conc. 10 mg/mL)

Acknowledgments

The original work (Vinod *et al.*, 2020b) was funded by the National Cancer Institute (NCI) Alliance for Nanotechnology in Cancer (U54CA198999, Carolina Center of Cancer Nanotechnology Excellence).

Competing interests

A.V.K. is co-inventor on patents pertinent to the subject matter of the present contribution and A.V.K. and M.S.P. have co-founders' interest in DelAqua Pharmaceuticals Inc. having intent of commercial development of POx based drug formulations. The other authors have no competing interests to report.

Ethics

The protocol (IACUC# 18-174) was approved by The University of North Carolina at Chapel Hill Institutional Animal Care and Use Committee. The validity period of IACUC# 18-174 is of 3 years.

References

- Chen, L., Gibbons, D. L., Goswami, S., Cortez, M. A., Ahn Y. H., Byers, L. A., Zhang, X., Yi, X., Dwyer, D., Lin, W., Diao, L., Wang, J., Roybal, J. D., Patel, M., Ungewiss, C., Peng, D., Antonia, S., Mediavilla-Varela, M., Robertson, G., Jones, S., Suraokar, M., Welsh, J. W., Erez, B., Wistuba, I. I., Chen, L., Peng, D., Wang, S., Ullrich, S. E., Heymach, J. V., Kurie, J. M., Qin, F. X.-F. (2014). [Metastasis is regulated via microRNA-200/ZEB1 axis control of tumour cell PD-L1 expression and intratumoral immunosuppression](#). *Nat Commun* 5: 5241.
- Espinosa, E., Marquez-Rodas, I., Soria, A., Berrocal, A., Manzano, J. L., Gonzalez-Cao, M., Martin-Algarra, S. and Spanish Melanoma, G. (2017). [Predictive factors of response to immunotherapy-a review from the Spanish Melanoma Group \(GEM\)](#). *Ann Transl Med* 5(19): 389.
- Galluzzi, L., Senovilla, L., Vitale, I., Michels, J., Martins, I., Kepp, O., Castedo, M. and Kroemer, G. (2012). [Molecular mechanisms of cisplatin resistance](#). *Oncogene* 31(15): 1869-1883.

- He, Z., Wan, X., Schulz, A., Bludau, H., Dobrovolskaia, M. A., Stern, S. T., Montgomery, S. A., Yuan, H., Li, Z., Alakhova, D., Sokolsky, M., Darr, D. B., Perou, C. M., Jordan, R., Luxenhofer, R. and Kabanov, A. V. (2016). [A high capacity polymeric micelle of paclitaxel: Implication of high dose drug therapy to safety and in vivo anticancer activity.](#) *Biomaterials* 101: 296-309.
- Manzotti, C., Audisio, R. A. and Pratesi, G. (1993). [Importance of orthotopic implantation for human tumors as model systems: relevance to metastasis and invasion.](#) *Clin Exp Metastasis* 11(1): 5-14.
- Morgan, R. A. (2012). [Human tumor xenografts: the good, the bad, and the ugly.](#) *Mol Ther* 20(5): 882-884.
- Pfirschke, C., Engblom, C., Rickelt, S., Cortez-Retamozo, V., Garris, C., Pucci, F., Yamazaki, T., Poirier-Colame, V., Newton, A., Redouane, Y., Lin, Y. J., Wojtkiewicz, G., Iwamoto, Y., Mino-Kenudson, M., Huynh, T. G., Hynes, R. O., Freeman, G. J., Kroemer, G., Zitvogel, L., Weissleder, R. and Pittet, M. J. (2016). [Immunogenic Chemotherapy Sensitizes Tumors to Checkpoint Blockade Therapy.](#) *Immunity* 44(2): 343-354.
- Renaud, S., Seitlinger, J., Falcoz, P. E., Schaeffer, M., Voegeli, A. C., Legrain, M., Beau-Faller, M. and Massard, G. (2016). [Specific KRAS amino acid substitutions and EGFR mutations predict site-specific recurrence and metastasis following non-small-cell lung cancer surgery.](#) *Br J Cancer* 115(3): 346-353.
- Vinod, N., Hwang, D., Azam, S. H., Van Swearingen, A. E. D., Wayne, E., Fussell, S. C., Sokolsky-Papkov, M., Pecot, C. V. and Kabanov, A. V. (2020a). Preparation and characterization of Poly(2-oxazoline) micelles for the solubilization and delivery of sparingly water-soluble drugs. *Bio-protocol* (unpublished).
- Vinod, N., Hwang, D., Azam, S. H., Van Swearingen, A. E. D., Wayne, E., Fussell, S. C., Sokolsky-Papkov, M., Pecot, C. V. and Kabanov, A. V. (2020b). [High-capacity poly\(2-oxazoline\) formulation of TLR 7/8 agonist extends survival in a chemo-insensitive, metastatic model of lung adenocarcinoma.](#) *Sci Adv* 6(25): eaba5542.
- Zappa, C. and Mousa, S. A. (2016). [Non-small cell lung cancer: current treatment and future advances.](#) *Transl Lung Cancer Res* 5(3): 288-300.

An Image-based Dynamic High-throughput Analysis of Adherent Cell Migration

Meng Sun^{1,*}, Bence Rethi¹, Akilan Krishnamurthy¹, Vijay Joshua¹, Heidi Wähämaa¹, Sergiu-Bogdan Catrina² and Anca Catrina^{3,*}

¹Rheumatology Unit, Department of Medicine, Karolinska Institutet, Stockholm, Sweden

²Department of Molecular Medicine and Surgery, Karolinska Institutet, Stockholm, Sweden

³Rheumatology Unit, Department of Medicine, Karolinska University Hospital Center for Rheumatology, Academic Specialist Centre, Stockholm, Sweden

*For correspondence: anca.catrina@ki.se; meng.sun@ki.se

Abstract

In this protocol, we describe a method to monitor cell migration by live-cell imaging of adherent cells. Scratching assay is a common method to investigate cell migration or wound healing capacity. However, achieving homogenous scratching, finding the optimal time window for end-point analysis and performing an objective image analysis imply, even for practiced and adept experimenters, a high chance for variability and limited reproducibility. Therefore, our protocol implemented the assessment for cell mobility by using homogenous wound making, sequential imaging and automated image analysis. Cells were cultured in 96-well plates, and after attachment, homogeneous linear scratches were made using the IncuCyte® WoundMaker. The treatments were added directly to wells and images were captured every 2 hours automatically. Thereafter, the images were processed by defining a scratching mask and a cell confluence mask using a software algorithm. Data analysis was performed using the IncuCyte® Cell Migration Analysis Software. Thus, our protocol allows a time-lapse analysis of treatment effects on cell migration in a highly reliable, reproducible and re-analyzable manner.

Keywords: Cell migration, Scratching assay, Live cell image, Time-lapse imaging, High-throughput

This protocol was validated in: Ann Rheum Dis (2019), DOI: 10.1136/annrheumdis-2018-214967

Background

Scratching assays are a widely used method for investigating cell migration or wound healing capacity. However, the conventional method (manual scratching) requires skill to perform linear scratches and is an end-point assay (Liang *et al.*, 2007; Krishnamurthy *et al.*, 2016). Data are usually manually analyzed with ImageJ or other software. Recently, we employed a high-throughput automatic imaging system, IncuCyte ZOOM from Essen Bioscience, in a cell migration assay (Sun *et al.*, 2019). By using IncuCyte® WoundMaker, linear scratches can be created homogeneously in up to 96-wells at the same time. With the appropriately defined algorithm, by analysis of phase-contrast, cell confluence masks and scratching masks, cell migration can be simultaneously evaluated. In brief, the conventional method is more laborious and time-consuming than the method we present here. This protocol provides a method with minimized time and effort for processing high-throughput samples and analyzing data in an unbiased way over time.

Materials and Reagents

1. IncuCyte® ImageLock 96-well Plates (Essen Bioscience, catalog number: 4379)
2. Synovial fibroblast (Isolated from RA patients undergoing joint replacement, Sun *et al.*, 2019)
3. Normal human dermal fibroblasts (PromoCell, catalog number: C-12300)
4. Primary Human Osteoarthritis Synovial Fibroblasts (Bioivit, catalog number: HPCSFOA-03)
5. Dulbecco's Modified Eagle Medium (DMEM) (Sigma-Aldrich, catalog number: D5796-500ml)
6. Fetal bovine serum (FBS) (Sigma-Aldrich, catalog number: F7524)
7. Trypsin-EDTA (Sigma-Aldrich, catalog number: T3924-100ml)
8. Phosphate buffered saline (PBS) (Sigma-Aldrich, catalog number: D8537-500ml)
9. Penicillin-streptomycin (PEST) (Sigma-Aldrich, catalog number: P4333-100ml)
10. Anti-citrullinated protein antibody (Purified from peripheral blood of RA patients, Ossipova *et al.*, 2014)
11. Recombinant Human TNF- α (Peprotech, catalog number: 300-01A)
12. Recombinant Human IL-8/CXCL8 Protein (R&D Systems, catalog number: 208-IL-010)
13. Alconox powder (VWR, catalog number: 21835-123)
14. Sachets, Rely+On™ Virkon® powder (VWR, catalog number: 148-0200)
15. Sterile distilled water (produced in house)
16. 70% ethanol (Sigma-Aldrich, catalog number: 470198-1L)
17. Synovial fibroblasts culture medium (10% FBS) (see Recipes)
18. Starvation medium (serum free) (see Recipes)
19. Low-serum cell culture medium (2% FBS) (see Recipes)

Equipment

1. IncuCyte® WoundMaker with two wash boats (Essen Bioscience, catalog number: 4493)
2. IncuCyte ZOOM live-cell analysis system (Essen Bioscience, model: IncuCyte® ZOOM)
3. Multi-Channel pipette, 8-channel, 20-200 μ L (VWR, Ergonomic High Performance Multichannel Pipettor, catalog number: 89079-948)

Software

1. Cell Migration Analysis Software Module (Essen Bioscience, catalog number: 4400)
2. Prism 6 (GraphPad Software)
3. IncuCyte® Zoom software (2018A)

Procedure

A. Prepare Cells

1. Seed Cells in 150 µL complete growth medium in a 96-well imagerlock plate using a multi-channel pipette at a cell density that will reach up to 95% confluence overnight. In 96-well plates, it is advisable to exclude the outer wells from the experiment due to evaporation effects.

Note: We seed 20,000 synovial fibroblasts or human dermal fibroblasts per well to reach full confluence within 24 h.

2. Fill the outer wells with 300 µL PBS to counteract evaporation-effects in rest of the wells.
3. Grow cells at 37°C in a humidified incubator with 5% CO₂ overnight or until cells reach 95% confluence.
4. Wash cells with 100 µL PBS twice using a multi-channel pipette.
5. Starve cells with 100 µL FBS free culture medium in a humidified incubator with 5% CO₂ for 2 h to deplete growth factors.

Note: In our setting, we starve cells for 2 h. Overnight starvation is commonly used for growth factor depletion. Starvation time may differ; depending on the experimental setting.

B. Make scratch

1. Clean the wound maker in the wash boat for 5 minutes each in a series of four wash solutions (45 ml of each)
 - a. 0.5% Alconox
 - b. 1% Virkon
 - c. sterile distilled water
 - d. 70% ethanol
2. Use the IncuCyte® Wound Maker to create homogenous scratches (<https://www.youtube.com/watch?v=x7pMzJ1ViA&feature=youtu.be>)
 - a. Remove top of the wound maker and place it in an empty wash boat.
 - b. Insert plate into base plate holder and remove plate cover.
 - c. Replace pin block by guiding the rear dowels of pin block into the rear holes of the base plate.
 - d. Push and hold the black lever.
 - e. Lift pin block while continuing to hold the black lever down.
3. Discard the medium using multi-channel pipette without disturbing the scratch.
4. Add 200 µL of Low-serum culture medium (2% FBS) containing the experimental treatments.

Note: We treat our synovial fibroblasts or human dermal fibroblasts with anti-citrullinated protein antibodies (ACPA) (Ossipova et al., 2014), control IgG, Tumor necrosis factor (TNF) and medium only.

C. IncuCyte Zoom Scan setup (Figure 1A and [Figure S1](#))

To avoid interrupting an ongoing scan, it is very important to check device status. Place a new plate only between scheduled scans. Do not eject door during scanning ([Figure S2](#)).

1. Place 96-well Imagerlock plate and click ‘Schedule Scans’.
2. Select the tray position of interest.
3. Click ‘add vessel’ and select ‘96-well Essen Imagerlock’ in Zoom software.
4. Set scan type to ‘Scratch Wound’ with ‘Wide Mode’ and ‘Scan pattern’.
5. Select ‘Phase contrast’ channels in Zoom software and Set plate layout as desired.
6. Select the desired scan frequency and timing by, right clicking on the time base and selecting ‘Set Interval’.

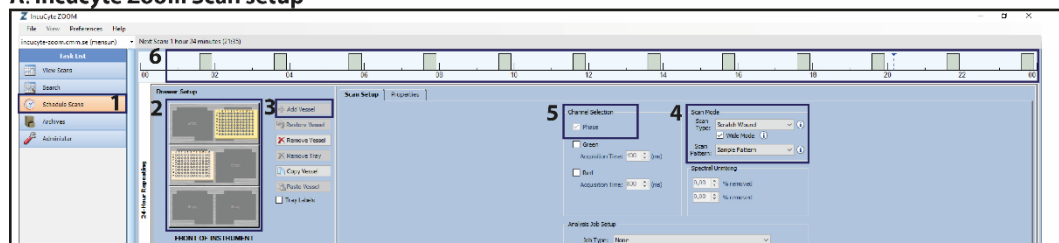
Scan interval depends on how many wells need to be scanned. We recommend a 1-2 h interval for a migration assay.

7. Click ‘Apply’ button to finish setting. Any unapplied changes will not be performed.

D. Plate Setup (optional) (Figure 1B)

- i. Under ‘properties’ panel, enter ‘label’, ‘cell type’, ‘passage’ and ‘notes’. In a high throughput assay, it is advisable to keep detailed information about experiments for further reference.
- ii. Click ‘plate map’ and select ‘add’ in dropdown list to create assay layout. It is highly recommended to use plate map for further analysis.
- iii. In plate map editor, click ‘NEW’ to create treatment.
- iv. Select wells in the plate layout, enter concentration or dilution of treatment and add to selected wells.
- v. Apply step 4 to all treatments and complete plate map.
- vi. Click ‘OK’ button to save plate map.

A. Incucyte Zoom Scan setup



B. Plate Setup

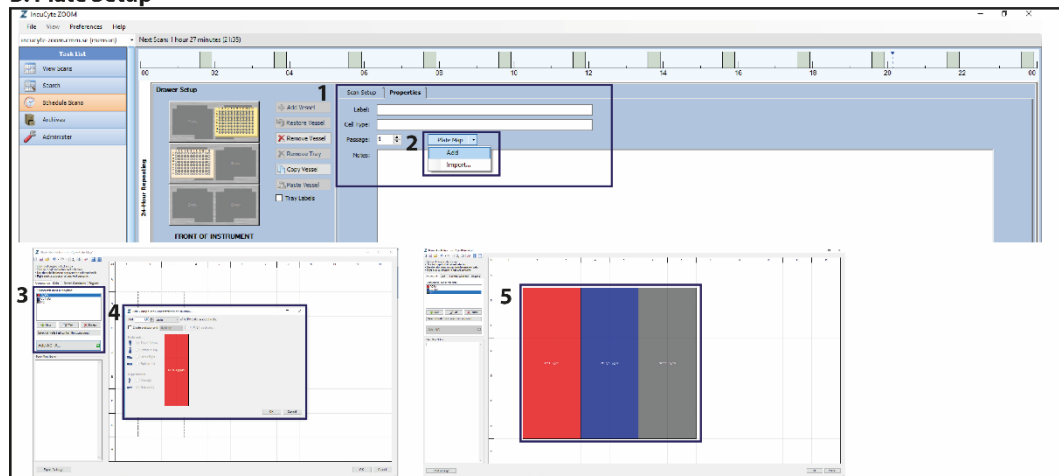


Figure 1. An illustration of scan and plate setup for using IncuCyte ZOOM system.

Screenshots of the IncuCyte ZOOM software for Scan setup and Plate setup. A. Steps 1 to 6 show the procedure to setup plate position, scan mode, channel and intervals for scan setup. B. Steps 1 to 5 show the procedure to setup experiment properties, plate layout and treatment information.

E. Data Collection and Processing

1. In side menu, select the experiment that needs to be analyzed.
2. Create or Add image collection (Figure 2A).
 - a. In ‘analysis job utilities’, click ‘Create or Add image collection’.
 - b. Select several images to create image collection for algorithm definition. It is recommended to select from different locations from plate layout and different time points from scan time to represent whole

- experiment.
- c. Save the image collection with appropriate title.
 3. New processing definition (Figure 2B).
 - a. In ‘analysis job utilities’, click ‘New processing definition’.
 - b. Select the newly created image collection and continue to define the scratching mask.
 - c. In left side menu, drag slide bar towards either ‘background’ or ‘cell’ to adjust segmentation.
 - d. In clean up panel section, enter a certain number to fill up the holes between cells (optional).
 - e. In filter section, select ‘min’ in ‘Area’ and enter a number to exclude cell debris in the image.
 - f. Select ‘phase contrast’ in Image Channel, ‘scratching wound mask’ and ‘confluence mask’ in Analysis Mask.
 - g. Click ‘preview’ to check the current processing definition and click ‘preview all’ to apply current definition to all images in collection.
 - h. Adjust the definition until it fits most of images in collection and save it with a proper name.
 - i. The processing definition can be applied for batch experiments.
 4. Launch Analysis Job (Figure 2C).
 - a. In ‘analysis job utilities’, click ‘Launch Analysis Job’.
 - b. In pop-up window, enter the name of the analysis.
 - c. Select start and finish time point to define time range.
 - d. Select wells in plate layout and click ‘Launch’ to start analysis job.
 - e. Check analysis result in main menu in ‘search’ and under ‘analysis job’ tab.

F. Data Export (Figure 2D)

1. In side menu, select the experiment that needs to be exported.
2. Select ‘Metrics’ panel, choose appropriate ‘phase metrics’ and click ‘Graph/Export’ button.
3. In pop-up window, select ‘wells’ and ‘time points/time range’ and click ‘Data Export’ button.
4. In ‘Export Metrics’ window, select ‘Layout’, ‘Destination’, ‘Other option’ and Click ‘Export’ button to export data for further analysis.

G. Lens Changing (Figure S3)

IncuCyte Zoom offers three different optical (4×, 10×, and 20× lens). To perform migration assay, it is essential to have 10× lens. To minimize the risk of conflict, changing lens is only available via administer account.

1. In main menu, go to ‘Task list’, click ‘administer’ and select tab ‘optical configuration’.
2. Follow the steps of ‘optics configuration’ to install new lens.
3. Accept the change and create new schedule.

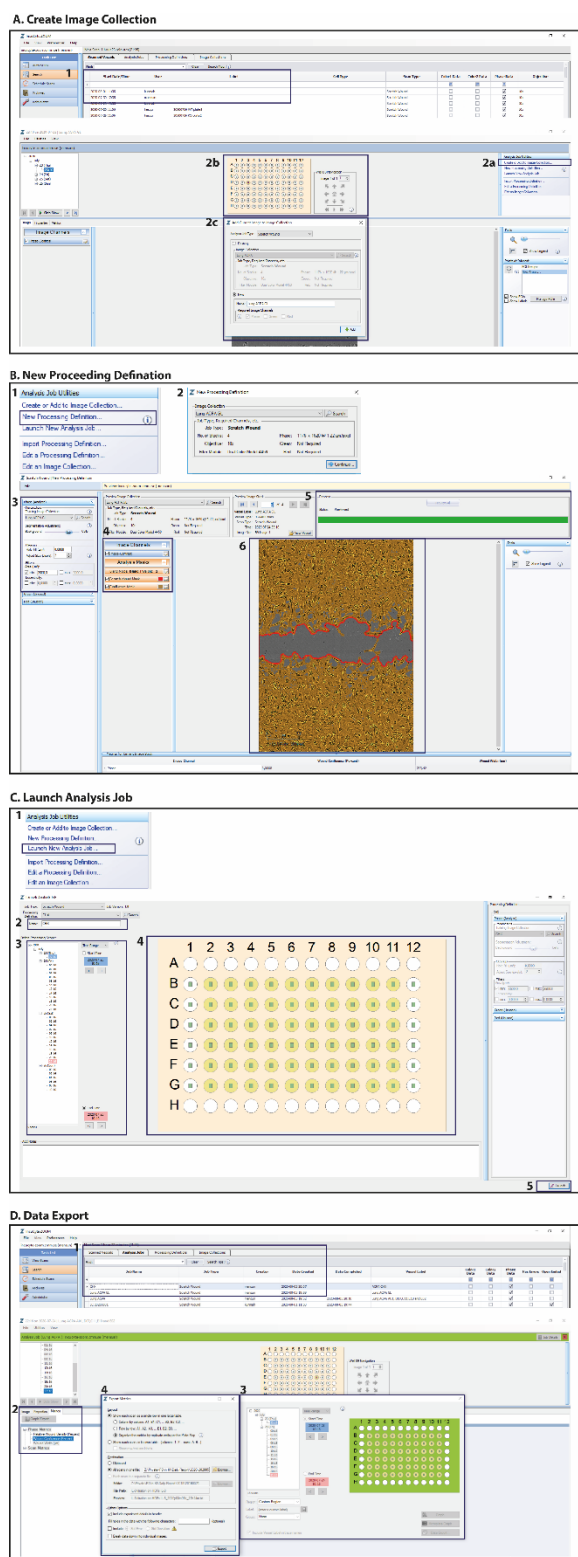


Figure 2. An illustration of data processing for using Cell Migration Analysis Software Module.

Screenshots of the cell migration analysis software for data processing. A. Steps to select re-presentive images from all timepoints to create image collection. B. Steps to define confluence mask and wound mask for images from collection. C. Steps to launch analysis for selected plate and desired time range. D. Steps to export raw data.

Data analysis

1. Representative example of data and confluence mask segmentation

When the analysis job is done, scratch wound mask, confluence mask and initial scratch wound mask are obtained at all timepoints. The wound confluence is simultaneously calculated by IncuCyte® Cell Migration Analysis Software. An example is shown in Figure 3: the confluence mask segmentation at the initial time point, end time point (Figure 3A) and wound confluence curve in time lapse, where cells were treated with antibodies: A, B and control antibody (Figure 3B).

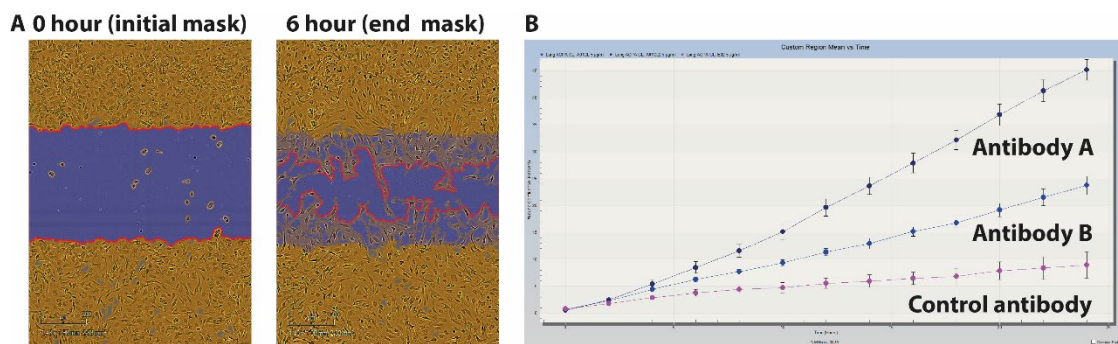


Figure 3. Example of confluence mask, scratch mask and analysis of wound confluence using IncuCyte Cell migration analysis software.

Exported images from IncuCyte analysis software. A. A segmentation example of cell confluence mask (yellow) and scratch mask (red outline) at 0 h (initial time point) and 6 h (end point). B. An example of migration rate curve (wound confluence) between 0 to 24 h, where antibody A and B but not control antibody have effect on cell migration.

2. Data analysis

IncuCyte Zoom software allows data export. The default figure of migration rate (percentage of wound confluence) is good enough for overview results. However, for statistical analysis, it is recommended to export raw data to Prism. Moreover, it is very useful to extract data and compare migration rates at specific time points. In Figure 4, we show migration rate, where fibroblasts were treated with ACPA, Ctrl IgG or medium only [The figure was originally published in Sun *et al.* (2019), Figure 1, as an open access article distributed in accordance with the Creative Commons Attribution 4.0 Unported (CC BY 4.0) license (<https://creativecommons.org/licenses/by/4.0/>)]. Data from same wells, with or without serum starvation, were analyzed for migration up to 20 h (Figures 4A and 4B) and images of the wound mask at time point 6 h is shown in Figure 4C. Data were normalized to the medium-treatment group at time point 6 h and presented as migration fold change (Figures 4D and 4E). We also performed cell migration assays on both human dermal fibroblasts (HDFs) and synovial fibroblasts of osteoarthritis patients (OASFs) with or without stimulation of IL-8 or TNF-alpha (Sun *et al.*, 2019, Supplementary Figure 2).

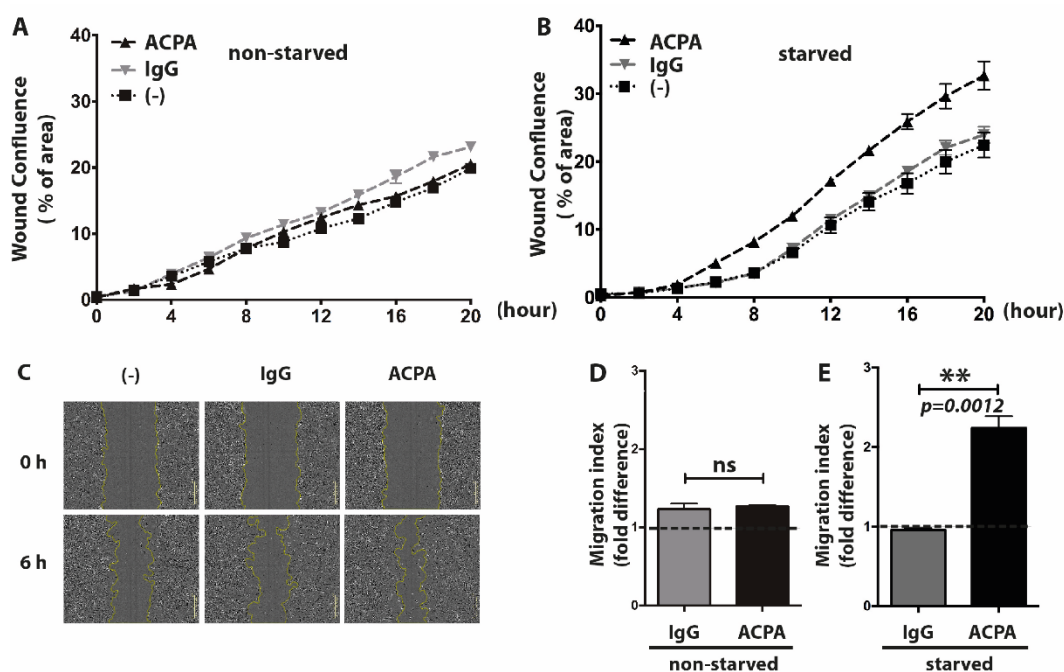


Figure 4. Increased mobility of synovial fibroblasts in the presence of polyclonal ACPAs.

Real-time cell migration was measured in the presence of 1 μ g/ml ACPA, control IgG or without any treatment in non-starved (A) and starved (B) fibroblast cultures using IncuCyte. Image-based evaluation of cell migration in starved fibroblast cultures were performed using Cell Migration Analysis software module with 10 \times magnification (C). Cell mobility was analyzed during a period of 6 h in the presence of 1 μ g/ml polyclonal ACPA IgGs (ACPA) or non-ACPA control IgGs (IgG) or without antibody treatment (-) in both non-starved (D) and starved (E) fibroblast cultures. Dot line indicate migration index of non-treated fibroblasts. The graphs represent mean \pm SD values of 6 replicates for each treatment. *P < 0.05.

Recipes

- Synovial fibroblasts culture medium (10% FBS)**
 - Dulbecco's Modified Eagle Medium (DMEM 500 mL)
 - Add 50 mL heat-inactivated fetal bovine serum (FBS) to reach 10%
 - Add 100 U/mL penicillin
 - Add 100 μ g/mL streptomycin
- Starvation medium (serum free)**
 - Dulbecco's Modified Eagle Medium (DMEM 500 mL)
 - Add 100 U/mL penicillin
 - Add 100 μ g/mL streptomycin
- Low-serum cell culture medium (2% FBS)**
 - Dulbecco's Modified Eagle Medium (DMEM 500 mL)
 - Add 10 mL heat-inactivated fetal bovine serum (FBS) to reach 2%
 - Add 100 U/mL penicillin
 - Add 100 μ g/mL streptomycin

Acknowledgments

This project has received funding from FOREUM, Foundation for Research in Rheumatology, from the European Research Council (ERC) under the European Union's Horizon 2020 research and innovation program (grant agreement CoG 2017 - 7722209_PREVENT RA and grant agreement 777357_RTCure), from the Swedish Research Council and Konung Gustaf V:s och Drottning Victorias Frimurarestiftelse.

Last, we would like to pay our gratitude and our respects to our group leader and colleague, Prof. Anca Catrina who passed away recently. She was a dedicated professor and excellent researcher in the Department of Medicine, Rheumatology Unit, at Karolinska University Hospital. We will continue her work and her style as much as we can.

The protocol was first described in the methods section of Sun *et al.* (2019).

Competing interests

The authors declare that they have no conflicts of interest.

Ethics

This study involves human participants with ethical permit listed below:

1. Kartläggning av prediktiva biomarkörer vid kronisk artrit ID: 2009-358-31-3. (Mapping of predictive biomarkers in chronic arthritis).
2. Kartläggning av inflammatoriska mediatorers betydelse för sjukdomsförlopp vid kroniska ledsjukdomar ID:2009-1262-31-3. (Mapping of inflammatory mediators significance for disease course in chronic joint diseases).

References

- Krishnamurthy, A., Joshua, V., Haj Hensvold, A., Jin, T., Sun, M., Vivar, N., Ytterberg, A. J., Engstrom, M., Fernandes-Cerdeira, C., Amara, K., Magnusson, M., Wigerblad, G., Kato, J., Jimenez-Andrade, J. M., Tyson, K., Rapecki, S., Lundberg, K., Catrina, S. B., Jakobsson, P. J., Svensson, C., Malmstrom, V., Klareskog, L., Wahamaa, H. and Catrina, A. I. (2016). [Identification of a novel chemokine-dependent molecular mechanism underlying rheumatoid arthritis-associated autoantibody-mediated bone loss](#). *Ann Rheum Dis* 75(4): 721-729.
- Liang, C. C., Park, A. Y. and Guan, J. L. (2007). [In vitro scratch assay: a convenient and inexpensive method for analysis of cell migration in vitro](#). *Nat Protoc* 2(2): 329-333.
- Ossipova, E., Cerqueira, C. F., Reed, E., Kharlamova, N., Israelsson, L., Holmdahl, R., Nandakumar, K. S., Engstrom, M., Harre, U., Schett, G., Catrina, A. I., Malmstrom, V., Sommarin, Y., Klareskog, L., Jakobsson, P. J. and Lundberg, K. (2014). [Affinity purified anti-citrullinated protein/peptide antibodies target antigens expressed in the rheumatoid joint](#). *Arthritis Res Ther* 16(4): R167.
- Sun, M., Rethi, B., Krishnamurthy, A., Joshua, V., Circiumaru, A., Hensvold, A. H., Ossipova, E., Gronwall, C., Liu, Y., Engstrom, M., Catrina, S. B., Steen, J., Malmstrom, V., Klareskog, L., Svensson, C., Ospelt, C., Wahamaa, H. and Catrina, A. I. (2019). [Anticitrullinated protein antibodies facilitate migration of synovial tissue-derived fibroblasts](#). *Ann Rheum Dis* 78(12): 1621-1631.

Preparation and Characterization of Poly(2-oxazoline) Micelles for the Solubilization and Delivery of Water Insoluble Drugs

Natasha Vinod^{1,2}, Duhyeong Hwang¹, Salma H. Azam³, Amanda E. D. Van Swearingen³, Elizabeth Wayne¹, Sloane Christian Fussell⁴, Marina Sokolsky-Papkov¹, Chad V. Pecot^{3,5,6} and Alexander V. Kabanov^{1,7,*}

¹Center for Nanotechnology in Drug Delivery and Division of Pharmacoengineering and Molecular Pharmaceutics, Eshelman School of Pharmacy, University of North Carolina at Chapel Hill, NC, USA

²Joint UNC/NC State Department of Biomedical Engineering, University of North Carolina, Chapel Hill, NC, USA

³Lineberger Comprehensive Cancer Center, University of North Carolina at Chapel Hill, Chapel Hill, NC, USA

⁴Department of Biology, Department of Chemistry, University of North Carolina at Chapel Hill, Chapel Hill, NC, USA

⁵Division of Hematology & Oncology, University of North Carolina at Chapel Hill, Chapel Hill, NC, USA

⁶Department of Medicine, University of North Carolina at Chapel Hill, Chapel Hill, NC, USA

⁷Laboratory of Chemical Design of Bionanomaterials, Faculty of Chemistry, M.V. Lomonosov Moscow State University, Moscow, Russia

*For correspondence: kabanov@email.unc.edu

Abstract

Many new drug development candidates are highly lipophilic compounds with low water solubility. This constitutes a formidable challenge for the use of such compounds for cancer therapy, where high doses and intravenous injections are needed (Di *et al.*, 2012). Here, we present a poly(2-oxazoline) polymer (POx)-based nanoformulation strategy to solubilize and deliver hydrophobic drugs. POx micelles are prepared by a simple thin-film hydration method. In this method, the drug and polymer are dissolved in a common solvent and allowed to mix, following which the solvent is evaporated using mild heating conditions to form a thin film. The micelles form spontaneously upon hydration with saline. POx nanoformulation of hydrophobic drugs is unique in that it has a high drug loading capacity, which is superior to micelles of conventional surfactants. Moreover, multiple active pharmaceutical ingredients (APIs) can be included within the same POx micelle, thereby enabling the codelivery of binary as well as ternary drug combinations (Han *et al.*, 2012; He *et al.*, 2016).

Keywords: Lipophilic, Poly(2-oxazoline), Nanoformulation, Surfactants, Active pharmaceutical ingredients, Polymeric micelles

This protocol was validated in: Sci Adv (2020), DOI: 10.1126/sciadv.aba5542

Background

Recent statistics show that only 3.7% of the new drug candidates that enter clinical testing are approved for use in cancer treatment. This has been primarily attributed to the poor pharmacokinetics of poorly water-soluble drug candidates, which results in suboptimal performance (Gala *et al.*, 2020). POx polymeric micelles offer several advantages over traditional drug delivery systems such as liposomes, microparticles, and nanogels, among others. The unparalleled high solubilizing capacity of POx micelles for a large variety of hydrophobic drugs enables the delivery of greater amounts of drugs with a substantially lesser amount of excipient (Luxenhofer *et al.*, 2010, He *et al.*, 2016). POx-based drug formulations are easy to prepare, safe, and stable. Additionally, a quantitative structure-property relationship (QSPR) model has been developed to predict drug loading into POx micelles, which can be utilized to facilitate high throughput screening of sparingly soluble drug development candidates for incorporation in POx micelles (Alves *et al.*, 2019).

Materials and Reagents

1. PVC tubing (Nalgene, ¼" ID)
2. Eppendorf tubes (Fisher Scientific, catalog number: 05-408-129)
3. Pipette tips (Fisher Scientific)
4. 11 mm plastic autosampler vials (Thermo Scientific, catalog number: C4011-13)
5. UV cuvettes (Fisher Scientific, catalog number: NC0628994)
6. 0.2-micron syringe filter, Nylon (Fisherbrand, catalog number: 13100108)
7. Poly(2-oxazoline) triblock copolymer ($P[MeOx_{37}-b-BuOx_{23}-b-MeOx_{37}]$ -piperazine) was synthesized as described previously (Luxenhofer *et al.*, 2010)
8. Drugs were purchased from either Adooq Bioscience, Apex Bio, or LC laboratories and stored at -20 °C
9. Ethanol 200 proof (Fisher Scientific)
10. Normal Saline (Teknova, catalog number: S5815)

Equipment

1. Pipettes (Fisher Scientific)
2. Sonicator (Branson 2510 ultrasonic bath)
3. Eppendorf heating block (Fisher Scientific, catalog number: 11-715-1250)
4. Desiccator (LabCorp)
5. Rotor vacuum evaporator (Buchi)
6. Vortex mixer (Fisher Scientific, catalog number: 02215365)
7. Benchtop microcentrifuge (Thermo Scientific)
8. Eppendorf Centrifuge Minispin (Fisher Scientific, catalog number: 05-090-100)
9. HPLC (Agilent 1200 series)
10. Zetasizer (Malvern)

Procedure

A. Preparation of drug-loaded POx micelles (Figure 1, Small, μL scale; applicable to single and multi-drug loaded POx micelles)

1. Prepare stock solutions of the drug and polymer in a common solvent.

Note: Commonly used solvents for the preparation of POx micelles are ethanol (200 proof), methanol, and acetone. In some cases, a mixture of two solvents is used to dissolve drugs. The concentration of the stock solution is determined by the solubility of the drug/polymer in the solvent. E.g., Prepare Paclitaxel stock solution in ethanol at a concentration of 10 mg/ml and POx stock solution in the same solvent at a concentration of 10 mg/ml (POx is also soluble in acetone and methanol at ≥ 10 mg/ml). You will need to use an ultrasonic bath for the dissolution of PTX in ethanol.

2. Mix the polymer and drug solutions at a predetermined polymer/drug ratio (w/w).

Note: Polymer:drug weight ratio of 10:2 is a good starting point to determine if the polymer can solubilize the drug. If the thin film disperses well in saline (step 4), work your way up to higher ratios (10:4 and 10:8). E.g., for a 10:4 loading ratio of POx:PTX, add a 50 μ L stock solution of POx with a 20 μ L stock solution of PTX and mix using a vortex mixer (setting 10; for ~10 s).

3. Evaporate the solvent by placing the Eppendorf tube containing the drug-polymer mixture in a heating block and blowing a stream of nitrogen gas into the tube.

The appearance of a clear (not cloudy) thin film is indicative of optimal heating conditions (see Figure 2A). The optimum temperature for evaporation is dictated by the physicochemical properties of the solvent (e.g., vaporization temperature) and drug (e.g., Lipophilicity, polarity, etc.) in use. Of note, the optimized temperature of evaporation for Resiquimod and PTX is 50 °C and 45 °C, respectively, and for other drugs varies from 40 °C to 80 °C.

Note: A disposable pipette tip can be inserted into the end of a PVC tubing and lowered into the Eppendorf tube to facilitate a gentle flow of nitrogen. Further, residual traces of solvent can be removed by placing the thin film in the desiccator overnight.

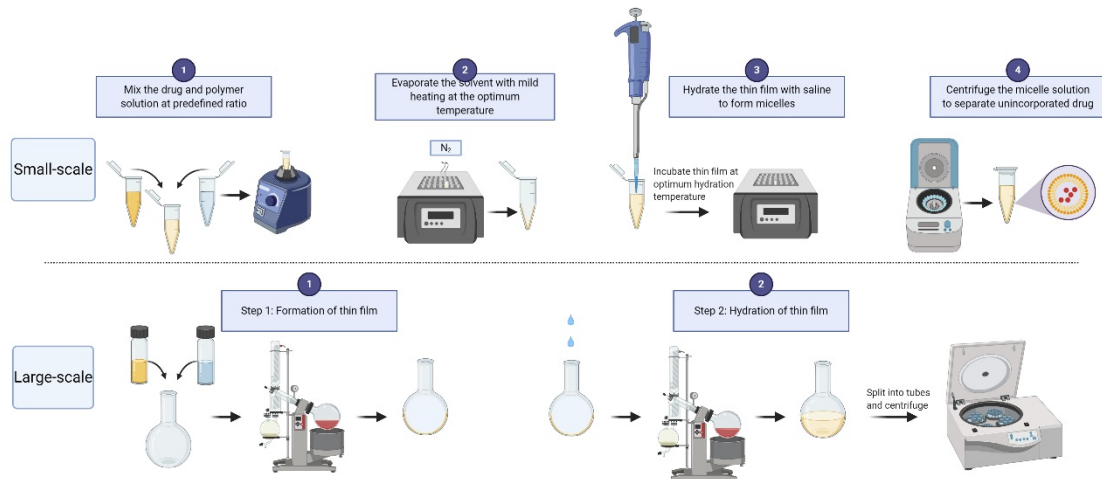


Figure 1. POx micelle preparation workflow (created with BioRender.com)

4. Hydrate the thin film with normal saline.

The volume of saline to be used is determined by the desired final drug(s) concentration. The optimal conditions of hydration vary with each drug. For instance, incubation for 10 min at RT followed by mild agitation by gently flicking the tube is sufficient for solubilizing thin films of Resiquimod. In comparison, Paclitaxel requires incubation at 65 °C for 20 min and gentle agitation every 5 min. The temperature of hydration should be optimized empirically for every single and multi-drug incorporated POx micelles.

Note: Gentle agitation (using a vortex mixer or gently flicking the tube) is necessary to completely disperse

the thin polymer-drug film. Visual inspection is a primary means of telling if the hydration conditions worked. While most drugs solubilize within 10 min, for certain drugs, an additional incubation time can yield better size distribution (Figure 2C) by facilitating specific interactions between the drug and polymer (hydrophobic, hydrogen bonding, etc.)

5. Centrifuge the micelle solution at $10,000 \times g$ for 2-3 min to separate the unencapsulated drug (pellet) and transfer the supernatant containing the drug-loaded micelles to a new tube.
6. Depending on the stability of the POx micelle solution of drugs, these can either be stored at 4°C for up to a couple of weeks or freeze-dried for long-term storage. The lyophilized formulation of POx micelles can be easily re-dispersed in DI water without loss in drug-loading and activity.

B. Preparation of drug-loaded POx micelles (Figure 1, large, mL scale; applicable to single and multi-drug loaded POx micelles)

1. Follow Steps A1 to A2. Use glass vials to accommodate large volumes of stock solutions and a round-bottom (RB) flask for mixing the drug and polymer solutions.
2. Evaporate the solvent using a rotary vacuum evaporator. Adjust the temperature of the water bath as needed.
3. The thin film will form in the bottom half of the RB flask when completed.
4. Hydrate the thin film with saline and immerse it in the water bath at the optimal hydration temperature for the required time – usually 10 to 15 min.
5. The micelle solution can be aliquoted into small volumes and centrifuged as in Step A5.
6. Lyophilize the formulation for long-term storage.

C. Characterization of POx micelles

The primarily used physicochemical characterization techniques for POx micelles include dynamic light scattering (DLS) for the determination of the size distribution and reverse-phase high-performance liquid chromatography for drug loading.

1. Sample Preparation for DLS measurement
 - a. Dilute the micelles 10-fold in saline.

Note: Typical dilutions used for DLS measurements of POx micelles range from 1:2-1:50, which correspond to drug concentrations of 0.1 mg/ml to 2 mg/ml.

 - b. Use nylon syringe filters of 0.2 microns to separate large particles.
 - c. Transfer the filtered solution into a clean cuvette without introducing air bubbles.
 - d. Place the cuvette in the sample holder and, following equilibration for at least 2 min, take 3 separate measurements for every sample.
2. Sample preparation for HPLC measurement
 - a. Dilute the micelle sample 50-fold in a mixture of 50/50 acetonitrile (ACN): water (v/v).
 - b. Filter the diluted sample using a 0.2-micron syringe filter and transfer 100 μl into an HPLC autosampler vial.
 - c. Get rid of any air bubbles from the autosampler vial by gently tapping before placing it in the vial tray.
 - d. Prepare the standards by serially diluting the analyte at concentrations ranging from 6.25 $\mu\text{g}/\text{ml}$ to 200 $\mu\text{g}/\text{ml}$.
 - e. The run settings must be optimized for each drug.

Note: 60/40 ACN: water, 1 mg/ml flow rate, and 10 μl injection volume is usually a good starting point for most drugs. Spiking the mobile phase solvents with 0.1% trifluoroacetic acid helps sharpen the peaks. Make sure the settings used for the sample are identical to the ones used for standards.

Data analysis

1. DLS Analysis

The zeta sizer measures fluctuations in the scattered light intensity with time caused by the Brownian motion of nanoparticles to estimate the hydrodynamic size of nanoparticles. DLS analyzes the raw data using two algorithms, viz., cumulant analysis and distribution analysis. The cumulant analysis reports two values: Z-average, which is the mean value of the particle size distribution, and polydispersity index (PDI), which is analogous to variance. A PDI value lower than 0.2 is indicative of monodisperse particles. The cumulant analysis also provides a correlogram (correlation curve), which reports the decay rate of the signal from the sample. The amplitude of the correlogram is representative of signal to noise ratio. The distribution analysis provides Gaussian distributions of the particle size by number, volume, and intensity. Sample concentration, presence of large aggregates, and impurities or marks on the exterior of the DLS cuvettes can all influence the size distribution. More information about data interpretation can be found at <https://www.malvernpanalytical.com>.

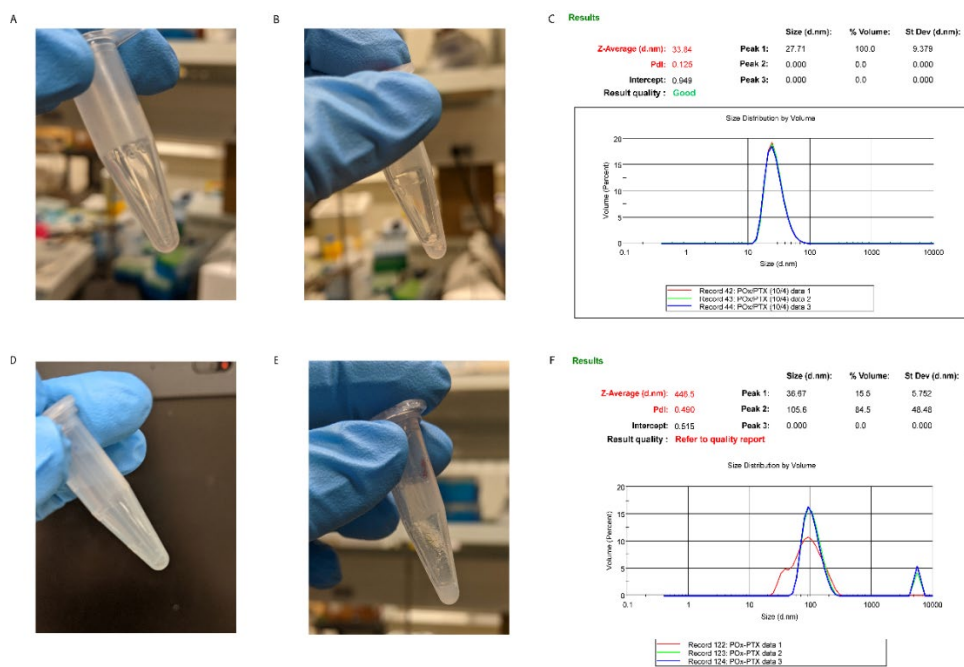


Figure 2. Representative images of the (A, D) thin film, (B, E) hydrated thin film, and (C, F) DLS volume distribution.

The top panel represents drug-incorporated micelles prepared using optimal conditions, as demonstrated by the monodisperse volume distribution with a single peak around 27 nm. The bottom panel is representative of sub-optimal conditions, indicated by the cloudy thin film and the incomplete hydration of the thin film, resulting in polydisperse size distribution with a peak at about 105 nm and a large peak of aggregates in the micrometer range.

Note: The DLS data were obtained from a separate experiment and do not represent the size distribution of the micelles shown in the images and is used here for demonstration purpose only.

2. Drug Loading

Chose the wavelength at which the analyte shows maximum absorbance and then integrate the peak in the

chromatogram to obtain the area, which corresponds to the concentration of the drug in the sample. The retention time of the sample should compare to that of standards. Once the sample concentration is determined from the standard curve, parameters such as loading efficiency and loading capacity can be obtained from the following equations:

$$\text{LC} = \left(\frac{M_{\text{drug}}}{M_{\text{drug}} + M_{\text{excipient}}} \right) \times 100$$
$$\text{LE} = \left(\frac{M_{\text{drug}}}{M_{\text{drug added}}} \right) \times 100$$

M_{drug} : The amount of drug incorporated in the micelle

$M_{\text{excipient}}$: The amount of polymer used in the formulation

$M_{\text{drug added}}$: The amount of drug initially fed

Acknowledgments

The original work (Vinod *et al.*, 2020) was funded by the National Cancer Institute (NCI) Alliance for Nanotechnology in Cancer (U54CA198999, Carolina Center of Cancer Nanotechnology Excellence).

Competing interests

A.V.K. is co-inventor on patents pertinent to the subject matter of the present contribution and A.V.K. and M.S.P. have co-founders' interest in DelAqua Pharmaceuticals Inc. having intent of commercial development of POx based drug formulations. The other authors have no competing interests to report.

References

- Alves, V. M., Hwang, D., Muratov, E., Sokolsky-Papkov, M., Varlamova, E., Vinod, N., Lim, C., Andrade, C. H., Tropsha, A. and Kabanov, A. (2019). [Cheminformatics-driven discovery of polymeric micelle formulations for poorly soluble drugs](#). *Sci Adv* 5(6): eaav9784.
- Di, L., Fish, P. V. and Mano, T. (2012). [Bridging solubility between drug discovery and development](#). *Drug Discov Today* 17(9-10): 486-495.
- Gala, U. H., Miller, D. A. and Williams, R. O., 3rd (2020). [Harnessing the therapeutic potential of anticancer drugs through amorphous solid dispersions](#). *Biochim Biophys Acta Rev Cancer* 1873(1): 188319.
- Han, Y., He, Z., Schulz, A., Bronich, T. K., Jordan, R., Luxenhofer, R. and Kabanov, A. V. (2012). [Synergistic combinations of multiple chemotherapeutic agents in high capacity poly\(2-oxazoline\) micelles](#). *Mol Pharm* 9(8): 2302-2313.
- He, Z., Wan, X., Schulz, A., Bludau, H., Dobrovolskaia, M. A., Stern, S. T., Montgomery, S. A., Yuan, H., Li, Z., Alakhova, D., Sokolsky, M., Darr, D. B., Perou, C. M., Jordan, R., Luxenhofer, R. and Kabanov, A. V. (2016). [A high capacity polymeric micelle of Paclitaxel: Implication of high dose drug therapy to safety and in vivo anti-cancer activity](#). *Biomaterials* 101: 296-309.
- Luxenhofer, R., Schulz, A., Roques, C., Li, S., Bronich, T. K., Batrakova, E. V., Jordan, R. and Kabanov, A. V. (2010). [Doubly amphiphilic poly\(2-oxazoline\)s as high-capacity delivery systems for hydrophobic drugs](#). *Biomaterials* 31(18): 4972-4979.
- Vinod, N., Hwang, D., Azam, S. H., Van Swearingen, A. E. D., Wayne, E., Fussell, S. C., Sokolsky-Papkov, M., Pecot, C. V. and Kabanov, A. V. (2020). [High-capacity poly\(2-oxazoline\) formulation of TLR 7/8 agonist extends survival in a chemo-insensitive, metastatic model of lung adenocarcinoma](#). *Sci Adv* 6(25): eaba5542.

Atomic Force Microscopy to Characterize Ginger Lipid-Derived Nanoparticles (GLDNP)

Dingpei Long^{1,*}, Chunhua Yang^{1,2}, Junsik Sung¹ and Didier Merlin^{1, 2}

¹Institute for Biomedical Sciences, Center for Diagnostics and Therapeutics, Digestive Disease Research Group, Georgia State University, Atlanta, GA, USA

²Atlanta Veterans Affairs Medical Center, Decatur, GA, USA

*For correspondence: dlong26@gsu.edu

Abstract

We have demonstrated that a specific population of ginger-derived nanoparticles (GDNP-2) could effectively target the colon, reduce colitis, and alleviate colitis-associated colon cancer. Naturally occurring GDNP-2 contains complex bioactive components, including lipids, proteins, miRNAs, and ginger secondary metabolites (gingerols and shogaols). To construct a nanocarrier that is more clearly defined than GDNP-2, we isolated lipids from GDNP-2 and demonstrated that they could self-assemble into ginger lipid-derived nanoparticles (GLDNP) in an aqueous solution. GLDNP can be used as a nanocarrier to deliver drug candidates such as 6-shogaol or its metabolites (M2 and M13) to the colon. To characterize the nanostructure of GLDNP, our lab extensively used atomic force microscopy (AFM) technique as a tool for visualizing the morphology of the drug-loaded GLDNP. Herein, we provide a detailed protocol for demonstrating such a process.

Keywords: Atomic force microscopy, Ginger lipid-derived nanoparticles, Colon-targeted drug delivery, 6-shogaol, Metabolites of 6-shogaol

This protocol was validated in: J Control Release (2020), DOI: 10.1016/j.jconrel.2020.04.032

Background

Developing new drug-based therapeutic approaches against Intestinal Bowel Disease (IBD) must overcome numerous challenges, including potential off-target effects, large-scale production costs, and the need to ensure tissue-specific delivery, systemic safety, and low toxicity. Our group and others have recently demonstrated that artificially synthesized nanoparticles could target low doses of drugs (*e.g.*, siRNAs, proteins, or peptides) to colonic tissues or colonic immune cells, such as macrophages (Ulrich and Lamprecht, 2010; Chen *et al.*, 2017). However, these synthetic NPs to date have two major limitations: i) each constituent of the synthesized nanoparticle must be examined for potential *in vivo* toxicity before clinical application; and ii) the production scale is limited. The use of nanoparticles derived from natural sources may overcome these limitations. In this context, we reported that a special population of ginger-derived nanoparticles (GDNP-2) could reduce colitis and colitis-associated colon cancer (Zhang *et al.*, 2016). Naturally occurring GDNP-2 is also safer and cheaper than synthetic NPs. We further identified 6-shogaol as a major candidate that may account for the anti-inflammatory and anti-cancer activities of GDNP-2 (Yang *et al.*, 2020). To construct a nanocarrier that is more clearly defined than GDNP-2, we characterized ginger lipid-derived nanoparticles (GLDNP) and demonstrated that they could be used as a natural carrier to deliver natural anti-inflammatory drug candidates such as 6-shogaol, M2, or M13 to the colon and reduced colitis in mice (Yang *et al.*, 2020).

Atomic force microscopy (AFM) is a versatile and powerful technique to characterize the morphology of nanoscale and submicron structured materials. It has been widely used to visualize different types of NPs, including metal-, inorganic- (non-metallic), and organic-NPs. AFM has the advantages of simplicity in sample preparation and no need for electric conducting treatment (Morris *et al.*, 2010). In previous studies, our group and others have extensively used AFM to analyze the morphology and structure of GLDNP (Zhang *et al.*, 2017; Wang *et al.*, 2019; Sung *et al.*, 2020; Yang *et al.*, 2020). However, no attempt has been taken to document the procedure of sample preparation and AFM parameter setting. In the following protocol, we will use the GLDNP as the specimen to demonstrate the process of obtaining AFM pictures for nanostructure characterization.

Materials and Reagents

1. Pipette tips 0.1-10 µL, 1-200 µL and 100-1,000 µL (Sorenson Bioscience, catalog numbers: 70600, 70520, 70540)
2. Powder-free gloves (Denville Scientific, catalog number: G4162)
3. 50 mL conical tubes (Denville Scientific, catalog number: C1062-P)
4. Phosphate-buffered Saline (PBS) (Corning, catalog number: 21-040-CV)
5. Methanol (Sigma-Aldrich, catalog number: 34860-1L-R)
6. Potassium chloride (KCl, Millipore, catalog number: 7447-40-7)
7. Dichloromethane (Sigma-Aldrich, catalog number: 650463-1L)
8. Deionized-distilled water (ddH₂O)
9. Mica sheet (Electron Microscopy Sciences, catalog number: 71855-15)
10. 1 M KCl solution (see Recipes)

Equipment

1. Pipettes 0.5-10 µL, 10-100 µL and 100-1,000 µL (Eppendorf, model: Research® Plus, Variable Adjustable Volume Pipettes)
2. Milli-Q advantage A10 water purification system (Millipore-Sigma, catalog number: C10117)
3. Glass separatory funnel (Southern Labware, model: 3964-3)
4. Centrifuge (Thermo Fisher Scientific, model: Sorvalis ST16R)
5. Vortexer (Scientific Industries, model: 200-SI0236)
6. Rotary evaporator (Buchi, model: R-210)

7. Vacuum pump (Buchi, model: V-700)
8. Vacuum controller (Buchi, model: V-800)
9. Heating bath (Buchi, model: B-491)
10. Evaporating flask (Buchi, catalog number: Z402982)
11. Notebook computer (ThinkPad, model: T570)
12. CoreAFM controller (Nanosurf, model: CoreAFM controller)
13. CoreAFM system (Nanosurf, model: CoreAFM system)
14. Isostage 300 controller (Nanosurf, model: Isostage 300 controller)
15. CoreAFM tool set (Nanosurf, model: CoreAFM tool set)

Software

1. CoreAFM control software (Version 3.10.0, <https://www.nanosurf.net/en/software/coreafm>)

Procedure

A. Preparation of GLDNP

Please refer to our published bio-protocols Sung *et al.* (2019 and 2020).

Note: Stored GLDNP (in 1× PBS) can be enriched after ultracentrifugation (30,000 × g, 4 °C, and 45 min) and remove the supernatant.

B. Setting up the AFM (see Note 1)

1. Assemble the Nanosurf CoreAFM system according to the steps in the operating instructions of CoreAFM. The AFM equipment after assembly is shown in Figure 1.

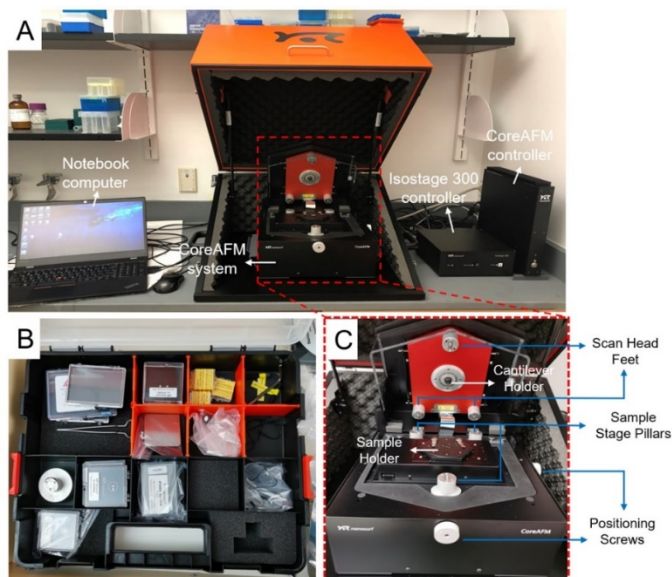


Figure 1. Assembly of the Nanosurf CoreAFM system.

A. The assembled Nanosurf CoreAFM system, which contains CoreAFM system, Isostage 300 controller,

CoreAFM controller, and a laptop, according to the instructions. B. The CoreAFM toolset (see Note 2). C. Enlarged photo of CoreAFM in its opened configuration.

2. Switch on the Nanosurf CoreAFM system (see Note 3).
3. Insert a Nanosurf Dyn190AI dynamic mode cantilever in the cantilever holder, ensuring that the tip is not damaged and attaching the cantilever holder to the magnets at the bottom of the CoreAFM scan head (see Note 3).

C. Loading GLDNP samples for AFM imaging

1. Dilute GLDNP solution in ddH₂O to 1 mg/mL.
2. Deposit 2 μL of nanoparticle sample to mica sheet (Figure 2A).

Note: As a drug delivery vehicle, the precise dose-response is one of the factors that must be considered. For different samples, the solution is usually diluted from high concentration to low concentration, while the volume of the solution is continuously reduced. According to the imaging effect of AFM, the most suitable solution concentration and volume are finally selected. The concentration of GLDNP samples used for imaging in this procedure should be > 0.01 μg/mL.

3. Dry the sample at room temperature (RT) for 2 h.
4. Gently rinse the mica sheet with 5 μL of distilled water three times (Figure 2B).

Note: First, drop distilled water gently into the middle of the mica sheet using the pipette, and then use filter paper to absorb water from the edge of the mica sheet. Since GLDNP samples are stored in PBS, the salt particles from PBS will affect the imaging effect of AFM, so the purpose of gently rinsing the mica sheet is to remove the salt in GLDNP samples.

5. Dry the sample at RT for 2 h again.
6. Leave the mica sheet for 30 min at RT until the sample becomes flat.

Note: To judge whether a sample is dried and becomes flat, we can place the mica sheet in a vertical position, and if we observe no sign of flow from the sample spot, it generally means that the sample is flat and dried. The drying and flatness of the sample on the mica sheet will affect the imaging effect of AFM.

7. Fix the mica sheet on the sample magnet in the center of the standard sample holder (Figure 2C).
8. Close the CoreAFM scan head lid, and the three scan head feet will align with the corresponding sample stage pillars.

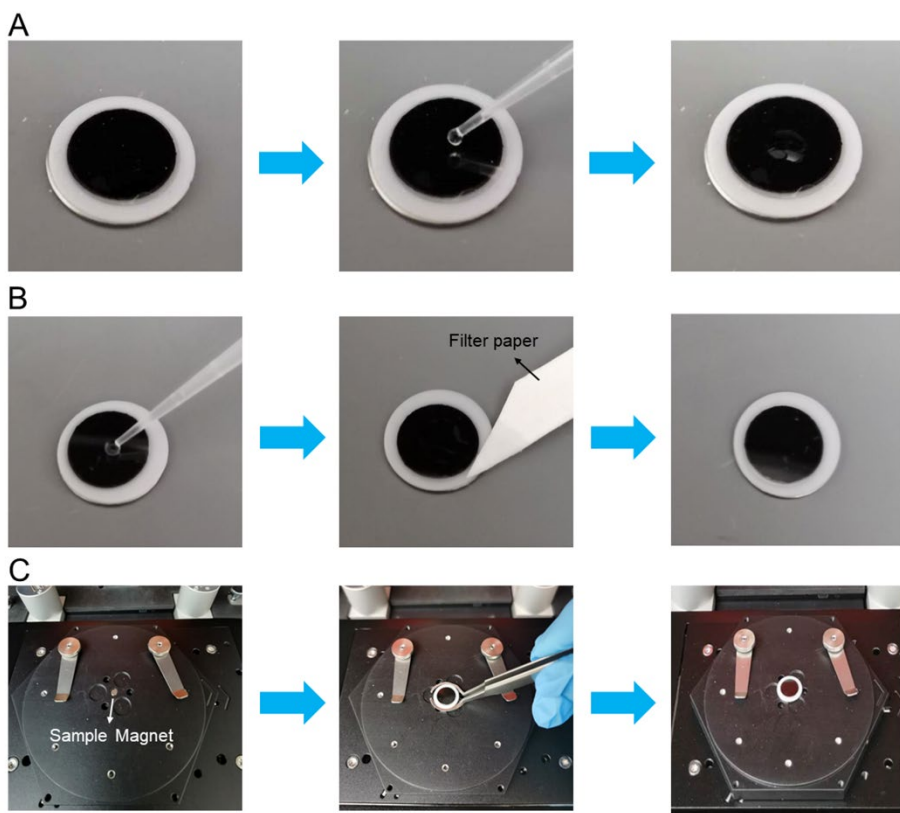


Figure 2. Loading the GNDLN sample to the mica sheet and fixing it on the sample magnet.

A. The process of depositing 2 μL of nanoparticle sample to a mica sheet. B. The process of gently rinsing the mica sheet with distilled water and adsorbing water from the edge of the mica sheet with filter paper. C. The process of fixing the mica sheet on the sample magnet of the standard sample holder (see Note 3).

D. AFM imaging of the GLDNP samples

1. Checking the laser position and quality (see Note 3).
 - a. Attach the CoreAFM system to the CoreAFM controller, and start the equipment and software.
 - b. In the CoreAFM control software, open the *Laser Alignment dialog* (Figure 3A) and switch the CoreAFM to the top view camera (Figure 3B) using the *Camera selector* (Figure 3C).

Note: The Laser Alignment dialog displays the current position of the AFM laser spot on the detector and the used laser power. The dialog is opened by clicking the “Laser Align” button in the Preparation group of the Acquisition tab.

- c. Use the laser alignment tool that came with the CoreAFM system to turn the screws in a clockwise or counterclockwise direction (Figure 3C). An optimally aligned laser would result in Figure 3A.

Note: CoreAFM system comes with 4 holes in the scan head’s top cover that provide access to the laser and detector alignment screws that change different aspects of the laser beam’s optical pathway (Figure 3C). Open the scan head lid to an angle of approximately 30°, and you should now see a red laser spot somewhere on the sample holder or sample holder platform (Figure 3C).

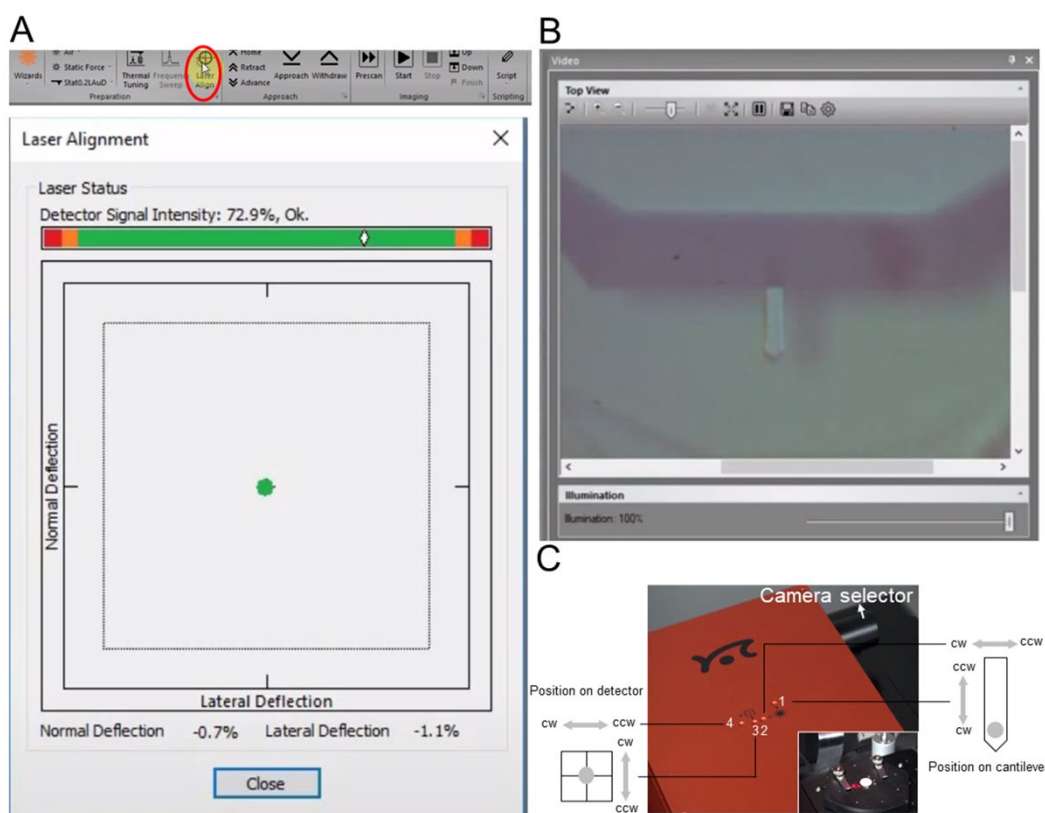


Figure 3. Checking the laser position and quality.

A. The menu of CoreAFM control software application and the proofread completed *Laser Alignment dialog*. This graphical area shows where the deflected laser beam hits the photodiode detector. A green spot anywhere within the area enclosed by the dotted square means that the cantilever deflection detection system (consisting of laser, cantilever, and detector) is properly aligned. If the laser spot falls outside this area, it will become red, meaning that the alignment does not allow proper measurements to take place. B. Top view image of a cantilever and its chip structure. C. Physical photos of the CoreAFM scan head and the sample holder.

2. Configuring measurement parameters of the CoreAFM (see Note 3).
 - a. In the menu of CoreAFM control software, click the “Air” to select the measurement environment from the *Measurement environment* drop-down menu (Figure 4A).
 - b. Click the “Static Force” to select the desired operating mode from the *Operating mode* drop-down menu (Figure 4B).
 - c. Click the “ACL-A” to select the desired cantilever type from the *Cantilever selector* drop-down menu (Figure 4C).
 - d. Click the “Frequency Sweep” button that opens the *Vibration frequency search dialog*. Click the “Find Vibration Frequency” button in this dialog (Figure 4D). Leave the dialog by clicking “OK”.

Note: After the automatic frequency search is finished, you should see a clean resonance curve and a marker showing the vibration frequency.

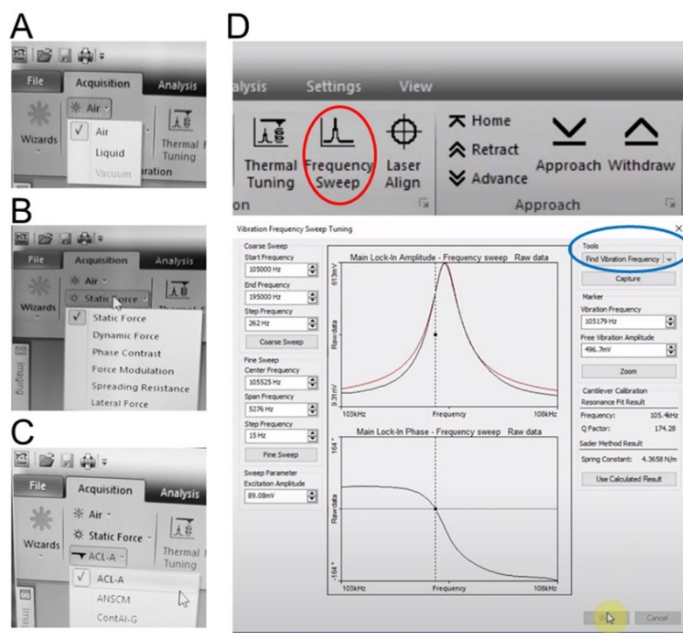


Figure 4. Configuring measurement parameters of the CoreAFM.

A-C. Set the *Measurement environment* to “Air” (A), set *Operating mode* to “Static Force” (B) and select “ACL-A” as cantilever in the *Cantilever selector* (C). D. The menu of CoreAFM control software application and the proofread completed *Vibration frequency search dialog*.

3. Approaching the GLDNP samples (see Note 3).
 - a. Observe the distance between tip and sample in the side view (Figure 5A).
 - b. While observing the tip-sample distance, click and hold the “Advance” button in the *Approach group* of the *Acquisition tab* until the tip is close enough to the sample (Figure 5B).
 - c. Click the “Approach” button in the *Approach group* of the *Acquisition tab* (Figure 5B). Click the “OK” button (Figure 5C).

Note: In this last step, this sample automatically approaches the tip until a given setpoint is reached.

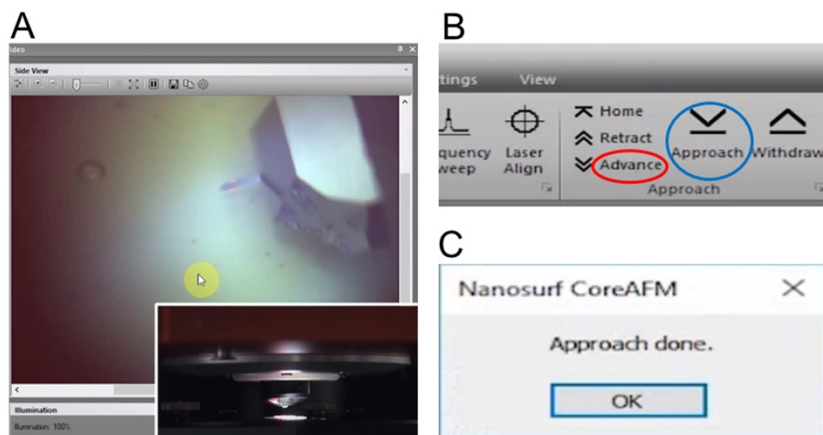


Figure 5. Approaching the GNLDN samples.

A. A side view image of a cantilever. B. The “Advance” and “Approach” buttons in the *Approach group* of the *Acquisition tab*. C. When the Setpoint is reached, the “Approach done” message is displayed.

4. Starting a measurement (see Note 3).

- a. Select the initial scan parameters in the Imaging dialog as follows (Figure 6A):

Image Scan Size = 10.00 μm
 Time/Line = 0.78 s
 Points/Line = 256

Note: The other values on the master panel are the values automatically filled in by the instrument upon the finishing of probe tuning; thus, no changes of these values are needed.

- b. Click the “Start” button in the *Imaging group* of the *Acquisition tab* and start scanning for 1 min to stabilize the cantilever and adjust the instrument to surrounding environmental vibrations (Figure 6B).

Note: Manually lower the “Setpoint” value until surface features start to appear on the height image. Imaging optimization can be achieved by adjusting “Setpoint”, “P-Gain”, and “I-Gain” values (see Note 4). Finally, the “Image Scan Size” can be decreased to 5.00 μm or 4.00 μm for adjusting the scan size of the image, and the “Points/Line” can be increased to 512 or even 1,024 (see Note 5) for more pixels in each image thus enhance the image quality.

- c. Once satisfied with the image quality, click the “Start” button and restart the scan with optimized parameters. After scanning, click the “Stop” button in the *Imaging group* of the *Acquisition tab* (Figure 6B).

*Note: Adjust the positioning screws of the CoreAFM system (see Figure 1C) so that the cantilever can be positioned in different locations of the mica sheet surface for each sample. Then click the “Prescan” button in the *Imaging group* of the *Acquisition tab* (Figure 6B). When the desired position is located by pre-scanning, click the “Start” button for scanning.*

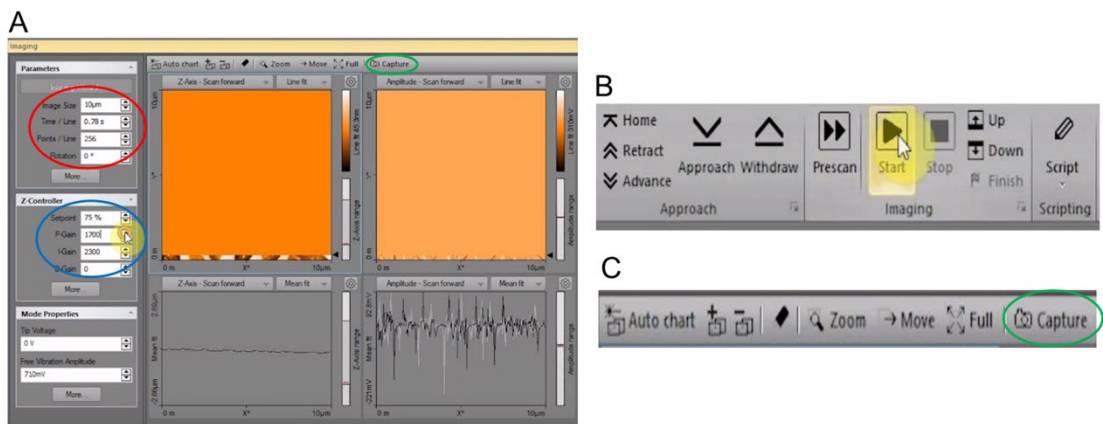


Figure 6. Starting and storing the measurement of the GLDNP samples.

A. Select the initial scan parameters and adjust the “Setpoint”, “P-Gain”, and “I-Gain” values to enhance the image quality in the Imaging dialog. B. The “Prescan”, “Start” and “Stop” buttons in the *Imaging group* of the *Acquisition tab*. C. The “Capture” button in the *Imaging toolbar*.

5. Storing the measurement and working with documents.

- a. By default, each completed measurement is automatically stored (temporarily) on your computer so that it can be used later. You can also take snapshots of measurements still in progress by clicking the “Capture” button (Figure 6C).
- b. The captured document will remain open in the document space of the CoreAFM control software (Figure 7A). Adding or removing a chart, or setting chart parameters is all performed in the Chart Properties dialog (Figure 7B).

- c. Click the “Add Chart” button (“+” in Figure 7B) to create a copy of the currently selected or active chart and add it to the active window in the last position. Click the “Remove Chart” button (“-” in Figure 7B) to remove the currently active chart.
- d. Selects the chart type (Line graph, Color map, 3D view, XY Line Graph, or Force Curve graph) to be used for the display of the measurement data from the “Type” of Chart Parameters (Figure 7B). Figure 7A shows three different chart types of the GLDNP samples.
- e. Use the Chart Properties dialog to set the various parameters of the corresponding chart type of the GLDNP samples.
- f. After setting, click "Close" button (Figure 7B) to close the Chart Properties dialog and click the “Save icon” (Figure 7A) to save the documents.

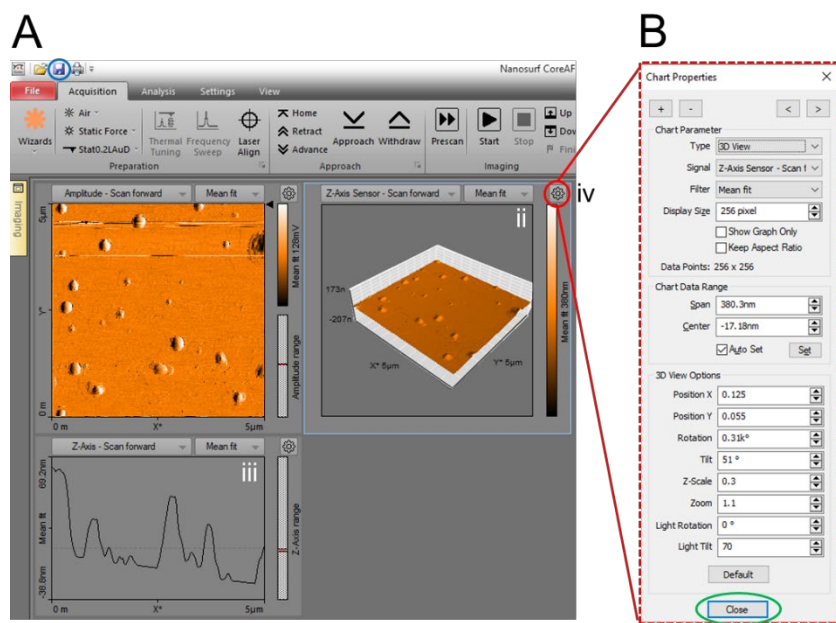


Figure 7. Different chart types of the GLDNP samples and the Chart Properties dialog.

A. (i) Color map, (ii) 3D view and (iii) Line graph of the GLDNP samples, and (iv) the “Chart Properties” button. B. The Charts Properties dialog is used to set all chart properties that influence data display by the respective chart.

Data analysis

1. We used the above process to perform AFM imaging of the GLDNP samples (Figures 8A-8C). Select the final scan parameters in the *Imaging dialog* for the GLDNP as follows:
Image Scan Size = 5.00 μm
Time/Line = 0.78 s
Points/Line = 256
In Figures 8A-8C, AFM images showed that GLDNPs are nano-sized particles and have a spherical shape and presented a size-homogenized appearance.
2. We prepared the synthetic material Poly(lactic-co-glycolic Acid) (PLGA)-based nanoparticles, then used the above process and set the same parameters to obtain the AFM image of PLGA samples (Figures 8D-8F), and compared it with GLDNP. Through the comparison of the images, we can observe that PLGA nanoparticles are also spherical with a size-homogenized appearance, and their particle size is slightly smaller than GLDNP. PLGA nanoparticles show a certain degree of aggregation on mica sheet compared to GLDNP.

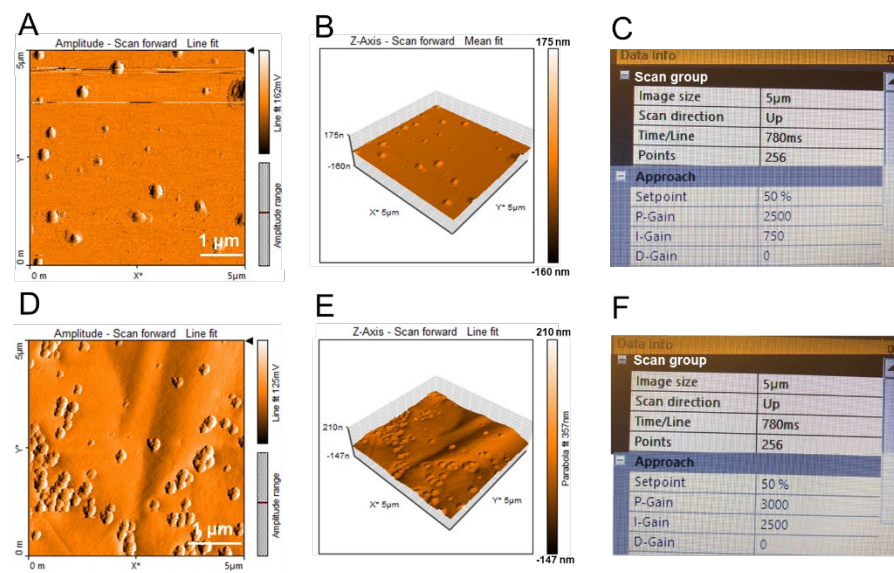


Figure 8. AFM characterization of the GLDNP samples and the poly lactic-co-glycolic acid (PLGA) samples (as control).

A-C. The Color map (A), 3D View (B), and the data information of image scan (C) for AFM characterization of GLDNP. D-F. The Color map (D), 3D View (E), and the data information of image scan (F) for AFM characterization of PLGA.

Notes

1. All procedures here are described for a Nanosurf CoreAFM system. For different models and brands of AFM, the protocol will need to be adapted according to the manufacturer's instructions.
2. The content of the toolset depends on the options included in the user's order. It minimally contains the following items:
Ground cable
Cantilever tweezers: (103A C.A.)
Cantilever exchange tool
Laser alignment tool: Allen key 1.5-mm (ballpoint hex) with a screwdriver handle
Allen key 5-mm: used for the CoreAFM transportation locks
Standard sample holder
Cantilever holder liquid-air flat
3. Prepare and operate the CoreAFM system and use this system to measure the brief program. Video is available at the product official website (<https://www.nanosurf.net/en/products/coreafm-the-essence-of-atomic-force-microscopy>). It will take about 4 h 30 min to prepare nanoparticles-loaded mica sheet for AFM imaging, and 15-20 min for AFM debugging and photography. Therefore, AFM imaging excluding data analysis can be completed within 5 h. In particular, it should be noted that the main limitation of the above procedure is that AFM imaging can only be done on dry samples in an indoor air environment, and AFM imaging of prepared samples (loaded on mica sheet) usually needs to be completed within a limited time (no more than 6 h). In addition, the minimum resolvable particle size of the sample is about 10 nm by the CoreAFM system.
4. Use a low "P-Gain" and "I-Gain" in the beginning to protect the cantilever. These values can be elevated in a later scan for better image quality.
5. "Points/Line" determines the number of pixel points on each line and the number of lines scanned in the image. In most cases, this value should be kept the same.

Recipes

1. 1 M KCl solution

Dissolve 0.745 g potassium chloride (KCl) in 10 mL of ddH₂O and mix well

Acknowledgments

This work is supported by the National Institute of Diabetes and Digestive and Kidney Diseases (RO1-DK-116306 and RO1-DK-107739 to D.M.), the Department of Veterans Affairs (Merit Award BX002526 to D.M.), and the Crohn's and Colitis Foundation of America. D.L. is a recipient of the Research Fellowship Award from the Crohn's and Colitis Foundation of America (Award Number #689659). D.M. is a recipient of the Senior Research Career Scientist Award from the Department of Veterans Affairs (BX004476). This protocol is based on our previously published study (Yang *et al.*, 2020).

Competing interests

The authors declare no conflicts of interest within the work.

References

- Chen, Q., Xiao, B. and Merlin, D. (2017). [Nanotherapeutics for the treatment of inflammatory bowel disease](#). *Expert Rev Gastroenterol Hepatol* 11(6): 495-497.
- Morris, V. J., Kirby, A. R. and Gunning, A. P. (2010). [Atomic Force Microscopy for Biologists](#). 2nd edition. Imperial College Press, ISBN-10: 184816467X.
- Sung, J., Yang, C., Viennois, E., Zhang, M. and Merlin, D. (2019). [Isolation, Purification, and Characterization of Ginger-derived Nanoparticles \(GDNPs\) from Ginger, Rhizome of Zingiber officinale](#). *Bio-protocol* 9(19): e3390.
- Sung, J., Yang, C., Collins, J. F. and Merlin, D. (2020). [Preparation and Characterization of Ginger Lipid-derived Nanoparticles for Colon-targeted siRNA Delivery](#). *Bio-protocol* 10(14): e3685.
- Ulbrich, W. and Lamprecht, A. (2010). [Targeted drug-delivery approaches by nanoparticulate carriers in the therapy of inflammatory diseases](#). *J R Soc Interface* 7 Suppl 1: S55-66.
- Wang, X., Zhang, M., Flores, S. R., Woloshun, R. R., Yang, C., Yin, L., Xiang, P., Xu, X., Garrick, M. D., Vidyasagar, S., Merlin, D. and Collins, J. F. (2019). [Oral gavage of ginger nanoparticle-derived lipid vectors carrying Dmt1 siRNA blunts iron loading in murine hereditary hemochromatosis](#). *Mol Ther* 27(3): 493-506.
- Yang, C., Zhang, M., Lama, S., Wang, L. and Merlin, D. (2020). [Natural-lipid nanoparticle-based therapeutic approach to deliver 6-shogaol and its metabolites M2 and M13 to the colon to treat ulcerative colitis](#). *J Control Release* 323: 293-310.
- Zhang, M., Viennois, E., Prasad, M., Zhang, Y., Wang, L., Zhang, Z., Han, M. K., Xiao, B., Xu, C., Srinivasan, S. and Merlin, D. (2016). [Edible ginger-derived nanoparticles: A novel therapeutic approach for the prevention and treatment of inflammatory bowel disease and colitis-associated cancer](#). *Biomaterials* 101: 321-340.
- Zhang, M., Wang, X., Han, M. K., Collins, J. F. and Merlin, D. (2017). [Oral administration of ginger-derived nanolipids loaded with siRNA as a novel approach for efficient siRNA drug delivery to treat ulcerative colitis](#). *Nanomedicine (Lond)* 12(16): 1927-1943.

A Robust Mammary Organoid System to Model Lactation and Involution-like Processes

Elsa Charifou¹, Jakub Sumbal^{1,2}, Zuzana Koledova², Han Li¹ and Aurélie Chiche^{1,*}

¹Cellular Plasticity & Disease Modeling - Department of Developmental & Stem Cell Biology, CNRS UMR3738 - Institut Pasteur, 25 rue du Dr Roux, Paris 75015, France

²Department of Histology and Embryology, Faculty of Medicine, Masaryk University, Kamenice 3, Brno 625 00, Czech Republic

*For correspondence: aurelie.chiche@pasteur.fr

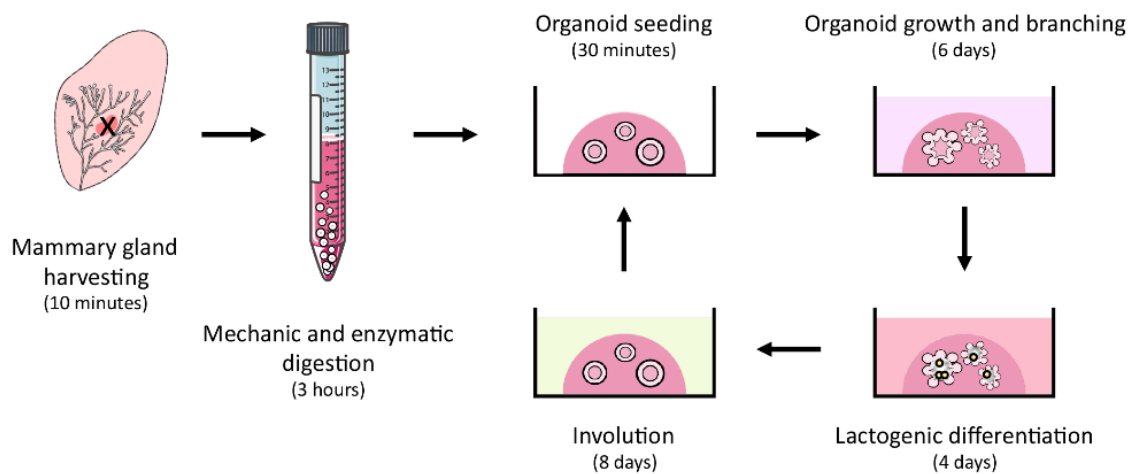
Abstract

The mammary gland is a highly dynamic tissue that changes throughout reproductive life, including growth during puberty and repetitive cycles of pregnancy and involution. Mammary gland tumors represent the most common cancer diagnosed in women worldwide. Studying the regulatory mechanisms of mammary gland development is essential for understanding how dysregulation can lead to breast cancer initiation and progression. Three-dimensional (3D) mammary organoids offer many exciting possibilities for the study of tissue development and breast cancer. In the present protocol derived from Sumbal *et al.*, we describe a straightforward 3D organoid system for the study of lactation and involution *ex vivo*. We use primary and passaged mouse mammary organoids stimulated with fibroblast growth factor 2 (FGF2) and prolactin to model the three cycles of mouse mammary gland lactation and involution processes. This 3D organoid model represents a valuable tool to study late postnatal mammary gland development and breast cancer, in particular postpartum-associated breast cancer.

Keywords: Mouse, Mammary gland, 3D organoid, *Ex vivo*, Lactation, Involution

This protocol was validated in: Front Cell Dev Biol (2020), DOI: 10.3389/fcell.2020.00068

Graphical Abstract:



Mammary gland organoid isolation and culture procedures

Background

The primary function of the mammary gland is to provide nutrition to newborns via milk production. The development of the mammary gland is a highly dynamic process that occurs mainly after birth and is regulated by several factors including hormones and growth factors (Brisken and Rajaram, 2006; Sternlicht, 2006). During puberty, hormones and growth factors regulate ductal morphogenesis from a rudimentary embryonic ductal tree (Brisken and O'Malley, 2010). During each pregnancy, the mammary gland begins a new morphogenetic step initiated by hormonal stimulation, which is characterized by massive proliferation for epithelial expansion and alveolar development accompanied by adipocyte regression (Brisken and O'Malley, 2010). Importantly, prolactin signaling plays a crucial role in the terminal differentiation of luminal cells to enable milk production (Ormandy *et al.*, 1997). At the end of lactation after weaning of the progeny, the mammary gland enters the involution stage characterized by programmed cell death, tissue remodeling, and redifferentiation of adipocytes (Hughes and Watson, 2012; Macias and Hinck, 2012; Zwick *et al.*, 2018; Jena *et al.*, 2019).

Histologically, the mammary gland is composed of a bilayered epithelium consisting of an inner layer of luminal cells (keratin 8+) and an outer layer of contractile basal cells (keratin 5+). Luminal cells are responsible for milk production during lactation, while basal cells aid milk ejection. The epithelium is surrounded by a stromal fat pad that comprises fibroblasts, nerves, vasculature, lymphatics, immune cells, adipocytes, and extracellular matrix (ECM) (Richert *et al.*, 2000).

Over the past decade, organoids of various tissues, such as stomach, colon, lung, and pancreas, have been developed (Huch and Koo, 2015), offering many exciting possibilities for the study of tissue development and disease. The organoid system is a powerful tool that combines the advantages of a 2D culture (easy manipulation, precise control of cell composition and microenvironment, live imaging) with the opportunity to study complex cell–cell and cell–ECM interactions in a more controlled *ex vivo* manner (Huch and Koo, 2015; Shamir and Ewald, 2015; Koledova, 2017; Artigiani and Clevers, 2018).

Several models have been developed to study the mechanisms of mammary branching morphogenesis in primary mammary epithelium using different protocols (Ewald *et al.*, 2008; Huebner *et al.*, 2016; Neumann *et al.*, 2018), cell lines (Xian *et al.*, 2005), sorted cells (Jamieson *et al.*, 2017; Linnemann *et al.*, 2015), or induced pluripotent stem cells (Qu *et al.*, 2017). However, an organoid system modeling key aspects of the late postnatal developmental stages of the mammary gland has remained challenging to establish.

Previously, there have been several attempts to model lactation in 3D culture: spheroids of a breast adenoma cell

line were used to study copper secretion into milk (Freestone *et al.*, 2014); organoids of primary epithelium were shown to produce milk following the administration of a lactogenic stimulus (Mroue *et al.*, 2015; Jamieson *et al.*, 2017); and co-culture of breast epithelium and pre-adipocyte cell lines was shown to initiate an involution-like process (Campbell *et al.*, 2014). However, in-depth characterization of milk production and involution or the proper bilayered architecture of mammary epithelium remained to be carried out.

Recently, we developed a model of lactation and involution of mammary epithelium based on organoids of primary mammary gland tissue cultured in 3D Matrigel® (Sumbal *et al.*, 2020b). Under lactogenic stimuli, primary organoids maintain long-term milk production, retain the contractile myoepithelial layer, and enter involution following hormone withdrawal. Moreover, after involution, the organoids remain hormonally sensitive and are able to enter another round of lactation (Sumbal *et al.*, 2020b). Here, we present a methodological guideline to establish the primary mammary organoid-based *ex vivo* model of lactation and involution, with detailed procedures for obtaining tissue, isolating organoids, establishing and maintaining 3D culture, and preparing organoid samples for subsequent RNA or protein expression analysis or histological examination. This model can be used for studies on lactation biology, mammary stem cell plasticity, regulatory mechanisms of mammary epithelial cell differentiation and death, or other interesting biological phenomena. We believe that this model will initiate the further development of organoid technology, including creative applications in biotechnology and regenerative medicine (Sumbal *et al.*, 2020a).

Materials and Reagents

1. 100-mm tissue culture Petri dish (*e.g.*, Corning, catalog number: 353003)
2. 0.2-μm filters and 50 mL syringes (*e.g.*, GVS, catalog number: FJ25ASCCA002DL01)
3. No. 22 disposable scalpel blades (*e.g.*, Swann-Morton, catalog number: 0508)
4. 50-mL tubes (*e.g.*, Corning, catalog number: 352070)
5. 15-mL tubes (*e.g.*, Corning, catalog number: 352096)
6. 10-mL disposable plastic pipettes (*e.g.*, Corning, catalog number: 357551)
7. 25-mL disposable plastic pipettes (*e.g.*, Corning, catalog number: 357535)
8. 24-well tissue culture plates (*e.g.*, Corning, catalog number: 353047)
9. 30 G insulin syringes (*e.g.*, BD Microfine, catalog number: 324826)
10. Plastic histology molds (*e.g.*, Thermo Scientific, catalog number: 1830)
11. Plastic embedding cassettes (*e.g.*, Simport, catalog number: M492-2)
12. Histology tissue molds (*e.g.*, Simport, catalog number: M474-3)
13. Microscope slides for histology (*e.g.*, Thermo Scientific, catalog number: J1800AMNZ)
14. Mice: virgin females, 7–10 weeks old, inbred strain C57BL/6J (*e.g.*, The Jackson Laboratory, catalog number: 000664)
15. Ethanol (EtOH), 70%, 95%, and 100% (*e.g.*, VWR, catalog number: 83813)
16. Phosphate-buffered saline (PBS) (*e.g.*, Sigma-Aldrich, catalog number: D1408)
17. Dulbecco's modified Eagle medium (DMEM)/F12 (*e.g.*, Gibco, catalog number: 21331-020)
18. Bovine serum albumin (BSA) (*e.g.*, Sigma-Aldrich, catalog number: A3608)
19. Fetal bovine serum (FBS) (*e.g.*, Sigma-Aldrich, catalog number: F0804)
20. Collagenase A (*e.g.*, Roche, catalog number: 11088793001)
21. Trypsin (*e.g.*, Dutcher Dominique, catalog number: P10-022100)
22. Insulin (*e.g.*, Sigma-Aldrich, catalog number: I6634-100MG)
23. Gentamicin (*e.g.*, Sigma-Aldrich, catalog number: G1397)
24. Glutamine (*e.g.*, Gibco, catalog number: 35050-061)
25. DNase I (*e.g.*, Sigma-Aldrich, catalog number: D4527-40KU)
26. Dispase II (*e.g.*, Roche, catalog number: 13 75 2000)
27. Growth factor-reduced Matrigel® (*e.g.*, Corning, catalog number: 354230)
28. Insulin-transferrin-selenium (ITS) (*e.g.*, Gibco, catalog number: 41400-045)
29. Penicillin/Streptomycin (*e.g.*, Gibco, catalog number: 15140-122)
30. FGF2 (*e.g.*, Gibco, catalog number: PM60034)

31. Prolactin (*e.g.*, Sigma-Aldrich, catalog number: SRP4688)
32. Hydrocortisone (*e.g.*, Sigma-Aldrich, catalog number: S H6909)
33. Oxytocin (*e.g.*, Sigma-Aldrich, catalog number: O3251)
34. RNeasy Micro Kit (*e.g.*, Qiagen, catalog number: 74004)
35. β-Mercaptoethanol (*e.g.*, Sigma-Aldrich, catalog number: M6250)
36. Phosphatase inhibitor cocktail II (*e.g.*, Millipore, catalog number: 524625)
37. RIPA buffer (*e.g.*, Sigma-Aldrich, catalog number: R0278)
38. Protease inhibitor cocktail I (*e.g.*, Sigma-Aldrich, catalog number: 539131)
39. Pierce Coomassie (Bradford) Protein Assay Kit (*e.g.*, Thermo Scientific, catalog number: 23200)
40. Paraformaldehyde (PFA), 32% (*e.g.*, Electron Microscopy Sciences, catalog number: 15714)
41. Low gelling temperature agarose (*e.g.*, Sigma-Aldrich, catalog number: A9414)
42. Xylene (*e.g.*, Sigma-Aldrich, catalog number: 534056)
43. Paraffin (*e.g.*, Sigma-Aldrich, catalog number: 1071642504)
44. Dissociation solution (see Recipes)
45. BSA solution (see Recipes)
46. Basal organoid medium (BOM) (see Recipes)
47. Morphogenesis medium (see Recipes)
48. Lactation medium (see Recipes)
49. 4% PFA (see Recipes)
50. RNA lysis buffer (see Recipes)

Equipment

1. Surgical tools
 - Forceps (*e.g.*, Phymep, catalog numbers: 11050-10 and 11051-10)
 - Scissors (*e.g.*, Phymep, catalog number: 14088-10)
2. Dissection board (*e.g.*, Thermo Scientific, catalog number: 36-119)
3. P1000 pipette
4. Laminar flow hood
5. Fridge 4°C (*e.g.*, Liebherr, catalog number: 7083 001-01)
6. Freezer -80°C (*e.g.*, Thermo Scientific, catalog number: 88400V)
7. Liquid nitrogen tank (*e.g.*, Air Liquide Espace 151, catalog number: 2433867)
8. Shaking incubator at 37°C (*e.g.*, Infors HT Multitron)
9. Centrifuge (*e.g.*, Thermo Scientific, model: Sorvall ST40)
10. Incubator for cell culture, 37°C, 5% CO₂ (*e.g.*, Thermo Scientific, model: HERAcell 150i)
11. Heating plate at 37°C (*e.g.*, Techne DRI-Block DB-2A)
12. Microscope and camera (*e.g.*, Olympus model: CKX41)
13. NanoDrop™ (*e.g.*, Implen Nanophotometer NP80)
14. Sonicator (*e.g.*, Diagenode Bioruptor Pico)
15. Incubator at 65°C (*e.g.*, Memmert Incubator I)
16. Embedding workstation (*e.g.*, Leica EG1150C)

Procedure

A. Isolation of mammary primary organoids

1. Dissection of a virgin mouse to harvest mammary glands (see Video 1).

- a. Euthanize the donor mouse using an ethically approved method (e.g., cervical dislocation) and immediately proceed to mammary gland collection.

Notes:

- i. *Cervical dislocation is a common method for animal euthanasia and provides a fast and painless death. With this method, cell/tissue survival in culture is not altered if collected immediately.*
- ii. *In the case of processing multiple mice, euthanize one animal and collect the glands immediately, then proceed to the next animal.*



Video 1. Mammary gland harvesting.

This video was made at Pasteur Institute, according to guidelines from the regulations of Institut Pasteur Animal Care Committees (CETEA), on Animal Care and approved by the French legislation in compliance with European Communities Council Directives (A 75-15-01-3).

- b. Sanitize the ventral side of the animal by spraying 70% EtOH on the skin.

Note: After disinfection, work inside a laminar flow hood to maintain aseptic conditions. Application of aseptic work procedures, together with the presence of antimycotic and antibiotic supplements (gentamicin in digestion solution; penicillin and streptomycin in culture medium) will prevent the occurrence of contamination.

- c. Pin the mouse by its four paws to a dissection board, with the abdomen facing upward (see Figure 1A, pins 1–4).
- d. Using forceps, tightly grasp the skin of the lower part of the abdomen at half the width (see Figure 1A, point A).
- e. Using surgical scissors, make the first incision in the skin at point A.

Note: Be careful to incise only the skin and not rupture the underlying peritoneum.

- f. Continue to incise the skin cranially to the throat of the animal (see Figure 1A, from point A to point B).
- g. From this median line, use forceps to grasp the skin and cut toward each of the four paws (see Figure 1A, incise to join the middle line to points C, D, E or F, respectively).
- h. Using forceps and a cotton swab, gently separate the skin from the peritoneum on one side of the animal. Attach the skin to the dissection board with three pins (see Figure 1B, pins 5–7).
- i. Repeat step 8 on the other side of the animal (see Figure 1B, pins 8–10). The mammary glands are now exposed.

- j. Identify the lymph node of the mammary gland #4 (a small dense structure, round in shape; see Figure 1B, surrounded). Remove the lymph node from both glands using forceps and scissors and discard.
- k. Proceed to the harvest of the mammary glands #3 and #4. Using curved forceps, grasp the mammary glands and gently separate them from the skin and other tissues with scissors.

Note: Carefully separate the mammary glands #3 (whitish and shiny) from the muscles (light brown ribbed structure) since this protocol does not prevent muscle contamination.

- l. Place all the collected glands in the same sterile Petri dish containing cold PBS (approximately 3 mL, previously stored at 4°C) for washing prior to tissue processing.
- m. Properly dispose of the animal corpse and continue with mechanical and enzymatic dissociation of the mammary glands.

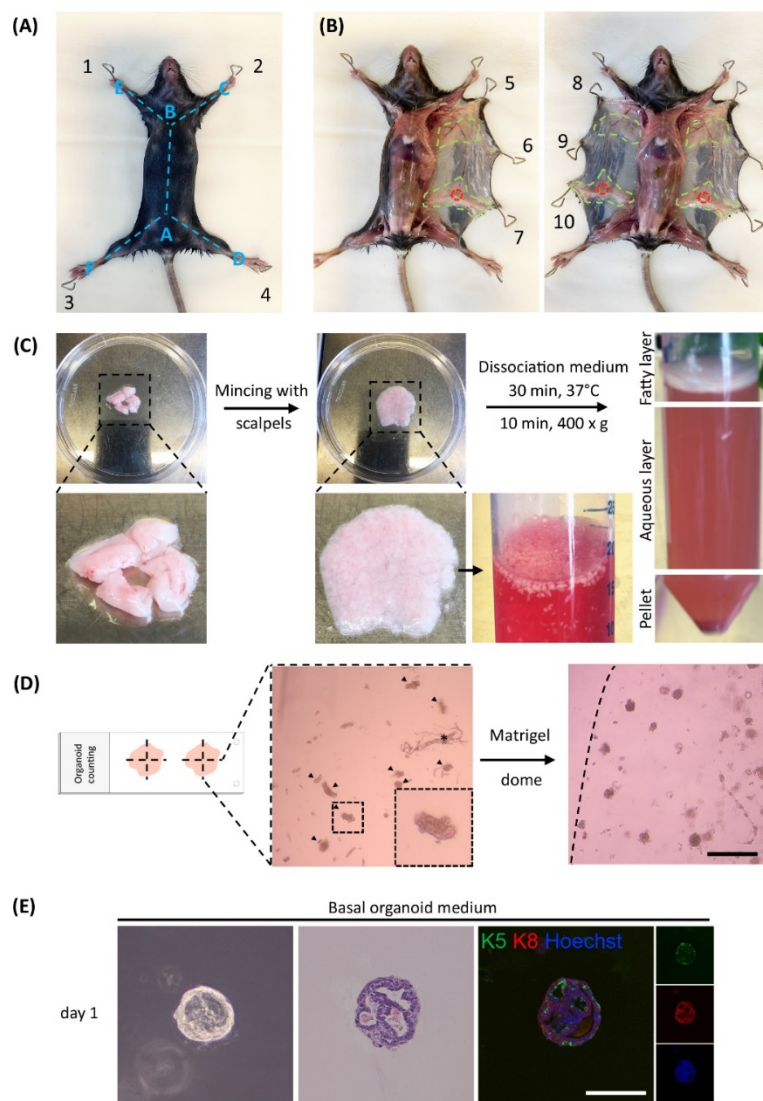


Figure 1. Key steps of mammary gland collection for organoid isolation and 3D culture.

A,B. Images of mouse dissection to access the mammary gland. A. Needles 1–4 represent the points at which to pin the mouse. Needles 5–7 and 8–10 represent the points at which to pin the skin of the mouse. Letters A–F with the blue dotted lines indicate the cuts. B. Green dotted lines denote the mammary gland. The lymph node is denoted in red and must be removed. C. Mammary gland before (left panel) and after

(middle panel) mincing with a scalpel. Mammary organoids after transfer to dissociation medium (right panel). D. Example of mammary organoid counting. Left panel: organoids are surrounded by dotted lines. Star represents nerves. Right panel: organoids after embedding in Matrigel®. Arrow represents the edge of the Matrigel® dome. Scale bar = 500 µm. E. Freshly isolated primary organoid. Left panel: image of a mammary organoid on day 1 post-isolation. Middle panel: Hematoxylin & eosin staining of an organoid on day 1 post-isolation. Right panel: immunofluorescence staining showing the distribution of myoepithelial (keratin 5+, green) and luminal cells (keratin 8+, red) in organoids on day 1 post-isolation. Hoechst, blue (nuclei). Scale bar = 100 µm.

2. Mechanical and enzymatic dissociation

Reminder: Work inside a laminar flow hood to maintain aseptic conditions.

- a. Freshly prepare 10 mL dissociation solution for the four glands collected from one mouse, pass through a 0.2-µm filter, and pre-heat at 37°C.

Note: Do not exceed the maximum 30 mL dissociation solution in a 50-mL tube to ensure correct dissociation.

- b. Transfer the freshly collected mammary glands to a new sterile Petri dish.
- c. Use three scalpels to finely chop the mammary glands and obtain a homogeneous mince of 1-mm³ mammary fragments (see Figure 1C).
- d. Transfer the mince to a 50-mL tube containing the pre-warmed dissociation solution.
- e. Place the tube in a shaking incubator for 30 min at 37°C, 100 rpm.

Notes:

- i. All the following steps are performed at room temperature except incubation with dispase.
- ii. From here on, pre-coat all the pipettes, tips, and tubes with 2.5% BSA solution. Prepare the BSA solution in a 50-mL tube and aspirate/remove from every consumable following coating; this will prevent stickiness and loss of organoids. The BSA solution can then be filtered, stored at 4°C, and re-used.
- f. After incubation, resuspend the dissociated mammary glands by performing ten up-and-down motions with a 10-mL pipette. Centrifuge for 10 min at 400 × g.
- g. After centrifugation, handle the 50-mL tube carefully to prevent disturbance of the three separated layers (see Figure 1C). Keep the epithelial pellet intact and transfer the middle aqueous phase and the top fatty layer into a clean 15-mL tube.
- h. Resuspend the epithelial pellet in 5 mL DMEM/F12 and set it aside.
- i. Focus on the fatty and aqueous solutions in the 15-mL tube: resuspend by performing ten up-and-down motions with a 10-mL pipette. Centrifuge for 10 min at 400 × g.

Note: This step allows recovery of epithelial fragments trapped in the fatty layer.

- j. Again, handle the 15-mL tube carefully to avoid disturbing the three separated layers. Discard the fatty and aqueous layers.
- k. Take the 5 mL resuspended pellet from the 50-mL tube to resuspend the pellet in the 15-mL tube.
- l. Wash the 50-mL tube with 5 mL DMEM/F12, pool with the suspension in the 15-mL tube, and mix.
- m. Centrifuge for 10 min at 400 × g.
- n. Discard the supernatant. Use 4 mL DMEM/F12 to resuspend the pellet. Subsequently, add 80 µL DNase I at 100 µg/mL and agitate for 5 min by hand or on an orbital shaker at 100 rpm.

- o. Add 6 mL DMEM/F12 and resuspend the solution by performing 5 up-and-down motions with a 10-mL pipette.
- p. Centrifuge for 10 min at $400 \times g$.
- q. Discard the supernatant. Use 4 mL DMEM/F12 to resuspend the pellet. Subsequently, add 150 μ L dispase II at 0.5 mg/mL and incubate for 5 min at 37°C.
- r. Add 6 mL DMEM/F12 and resuspend the solution by performing 5 up-and-down motions with a 10-mL pipette.
- s. Centrifuge for 10 min at $400 \times g$.
- t. Discard the supernatant. Resuspend the pellet in 9 mL DMEM/F12.
- u. Perform differential centrifugation to separate the mammary epithelium from the stromal fraction: centrifuge the suspension for 15 s at room temperature, $400 \times g$. Discard the supernatant containing the stromal fraction and resuspend the epithelial pellet in 9 mL DMEM/F12.

Note: Set the time on the centrifuge to 1 min. Once a speed of $400 \times g$ is reached, time 15 s precisely and stop the centrifuge manually.

- v. Repeat the previous step (t) 4 times, for a total of 5 differential centrifugations, to efficiently remove stromal contamination.
- w. Resuspend the final pellet in 1 mL basal organoid medium (BOM) and place on ice. The organoids are now ready to be counted and cultured.

Note: Adjust the volume of resuspension according to pellet size. From a pool of 2–3 mice, the final pellet was resuspended in 1 mL basal organoid medium, for an expected range of 3,000–6,000 organoids. Adjust the volume of BOM for resuspension of the pellet according to the number of mice pooled.

3. Organoid counting

Reminder: Work inside a laminar flow hood to maintain aseptic conditions.

- a. Draw two large crosses with a marker on a microscope slide.
- b. Take the organoid suspension and homogenize by performing five up-and-down motions with a P1000 pipette.
- c. On the reverse side of the slide, spread 10 μ L solution around the center of each cross.

Note: Use a 20- μ L tip or cut the extremity of a 10- μ L tip to avoid large organoids becoming trapped.

- d. Count the organoids under the microscope at 4 \times magnification (see Figure 1D).

Notes:

- i. Take each quarter of the cross as a landmark to avoid double-counting of the same organoid.
 - ii. Organoids appear as rounded structures with a smooth perimeter. Occasionally and unavoidably, nerves and endothelium are also present. The nerves appear as rope-like structures and can be organized in bundles (see Figure 1D). The endothelium has a somewhat ragged look in comparison with the smooth-looking organoids. The minor presence of primary nerves and endothelium does not interfere with organoid lactation or involution.
 - iii. Count only the organoids with a diameter greater than 30–50 μ m since the smaller ones may not develop properly.
- e. Calculate the average of the two counts in 10 μ L solution and multiply according to the volume of BOM used to resuspend the pellet to obtain the total number of organoids.

Note: Freshly isolated organoids can be viably frozen in a solution of FBS containing 10% DMSO for long-term storage in liquid nitrogen and later use.

B. 3D culture of mammary organoids

1. Embedding in Matrigel®

Reminder: Work inside a laminar flow hood to maintain aseptic conditions. Wash the ice bucket and heating plate thoroughly with 70% EtOH prior to placement in the laminar flow hood.

- a. Thaw the Matrigel® on ice or at 4°C.

Notes:

- i. Matrigel® solidifies really fast at room temperature. Always keep it on ice before use and during the plating procedure.
- ii. Keep in mind that Matrigel® thawing takes time; therefore, begin thawing prior to the procedure (2 h for a 1-mL aliquot, 6 h for a 10-mL bottle).

- b. Place a 24-well plate on ice. Calculate the number of wells needed and spread 20-μL Matrigel® in a round patch on the bottom of each well.

Note: Start by placing the tip containing Matrigel® at the center of a well and expand circularly towards the edges of the well, without touching them.

- c. Incubate the 24-well plate in a cell incubator (5% CO₂) for 15 min at 37°C.

- d. In the meantime, pre-heat a heating plate to 37°C.

- e. Prepare the organoid suspension in the Matrigel®: calculate the volume of organoid suspension required to obtain the desired number of organoids. Pipette this volume of suspension into a fresh 1.5-mL tube and centrifuge for 3 min at 400 × g.

Note: Adjust the number of organoids per well depending on the type of experiment: 200 organoids per well for morphology and histology, 400 for gene expression, and 1000 for western blotting analysis.

- f. Carefully remove the supernatant and place the tube on ice. Subsequently, carefully resuspend the pellet in the required volume of cold Matrigel® (50 μL per well), avoiding bubble formation. Keep on ice.

- g. Remove the 24-well plate from the cell incubator and place on the 37°C heating plate.

- h. In each Matrigel®- precoated well, cautiously seed the suspension of organoids (in Matrigel®) as a dome on top of the solidified Matrigel® patch.

- i. Place the 24-well plate back in the cell incubator (5% CO₂) for 30 min at 37°C to solidify the Matrigel® (see Figure 1D).

- j. In the meantime, pre-warm BOM at 37°C.

- k. Following incubation, carefully add 1 mL pre-heated BOM to each well and culture in the cell incubator at 37°C, 5% CO₂.

Notes:

- i. Add medium against the edges of the well to avoid disruption of the dome.
- ii. Characterization of the organoids can be performed using regular histological stains (e.g., hematoxylin & eosin) or immunostaining on day 1 post-recovery in BOM (see Figure 1E and Step B2 of the procedure).

2. Morphogenesis with FGF2

Reminder: Work inside a laminar flow hood to maintain aseptic conditions.

Note: Overnight recovery is optimal for organoid culture; however, FGF2 treatment can be administered immediately after plating the organoids.

- a. Pre-heat the BOM at 37°C.
- b. Add fresh FGF2 at a final concentration of 2.5 nM to pre-heated BOM to obtain the morphogenesis medium.
- c. Aspirate the medium from the wells without touching the Matrigel® dome and replace with 800 µL fresh morphogenesis medium.
- d. Renew all medium with fresh morphogenesis medium every 3 days, for a total of 6 days of treatment.
3. Lactogenic differentiation with prolactin
 - a. Pre-heat the BOM at 37°C.
 - b. Add 1 µg/mL prolactin and 1 µg/mL hydrocortisone to the pre-heated BOM to obtain the lactation medium.
 - c. Aspirate the medium from the wells without touching the Matrigel® dome and replace with 800 µL fresh lactation medium.
 - d. Renew all medium with fresh lactation medium every two days, for a total of 4 days of treatment.
4. Myoepithelial cell contraction with oxytocin
 - a. Prepare fresh lactation medium, filter, and pre-heat at 37°C.
 - b. Add 40 µg/mL recombinant oxytocin to the lactation medium.
 - c. Aspirate the medium from the wells without touching the Matrigel® dome and replace with 800 µL fresh lactation medium supplemented with oxytocin.
 - d. Using live cell imaging, record contraction images every second for 120 s.
5. Mimicking involution by hormonal withdrawal
 - a. Pre-heat the BOM at 37°C.
 - b. Aspirate the medium from the wells without touching the Matrigel® dome and replace with 800 µL fresh BOM.
 - c. Renew all medium with BOM every two days, for a total of 8 days of treatment.
6. Replating

Note: Use tips pre-coated with 2.5% BSA.

- a. Aspirate the supernatant and wash the wells twice with 800 µL cold PBS.
- b. Add 1 mL cold PBS and disrupt the Matrigel® dome using an up-and-down motion with a P1000 pipette.
- c. Check for successful disintegration of the Matrigel® under a microscope.
- d. Transfer the suspension to a 15-mL tube and add cold PBS to a total volume of 10 mL.
- e. Centrifuge for 3 min at 400 × g.
- f. Carefully remove the supernatant, resuspend the organoid pellet in fresh Matrigel® and plate as described in B1.

C. Organoid processing for further analysis

Note: We suggest carefully following organoid development under the microscope before renewing the media. Morphogenesis with FGF2 should induce branching after 3–4 days of treatment, while organoids in culture with BOM only, as the negative control, should remain round. Lactogenic differentiation can be confirmed by analysis of Csn2 mRNA using qPCR, comparing organoids before and after prolactin treatment (d6 versus d10). The involution process can also be confirmed using qPCR by detecting decreased expression of Csn2 mRNA following prolactin withdrawal (d10 versus d18), or at the morphological level by the progressive disappearance of branching (see Figure 2B and Figure 3B).

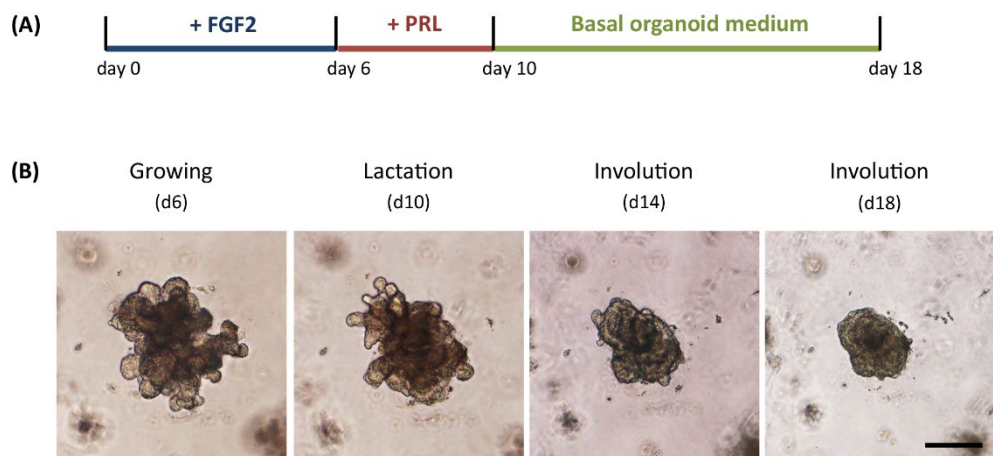


Figure 2. Modeling lactation and involution-like processes in primary mammary organoids.

A. Scheme depicting the experimental design. B. Morphology of primary mammary organoids during lactation and involution-like processes. Bright-field images of organoid morphology following morphogenic and lactogenic stimulation and on days 4 or 8 after hormonal withdrawal. Scale bar = 100 μ m.

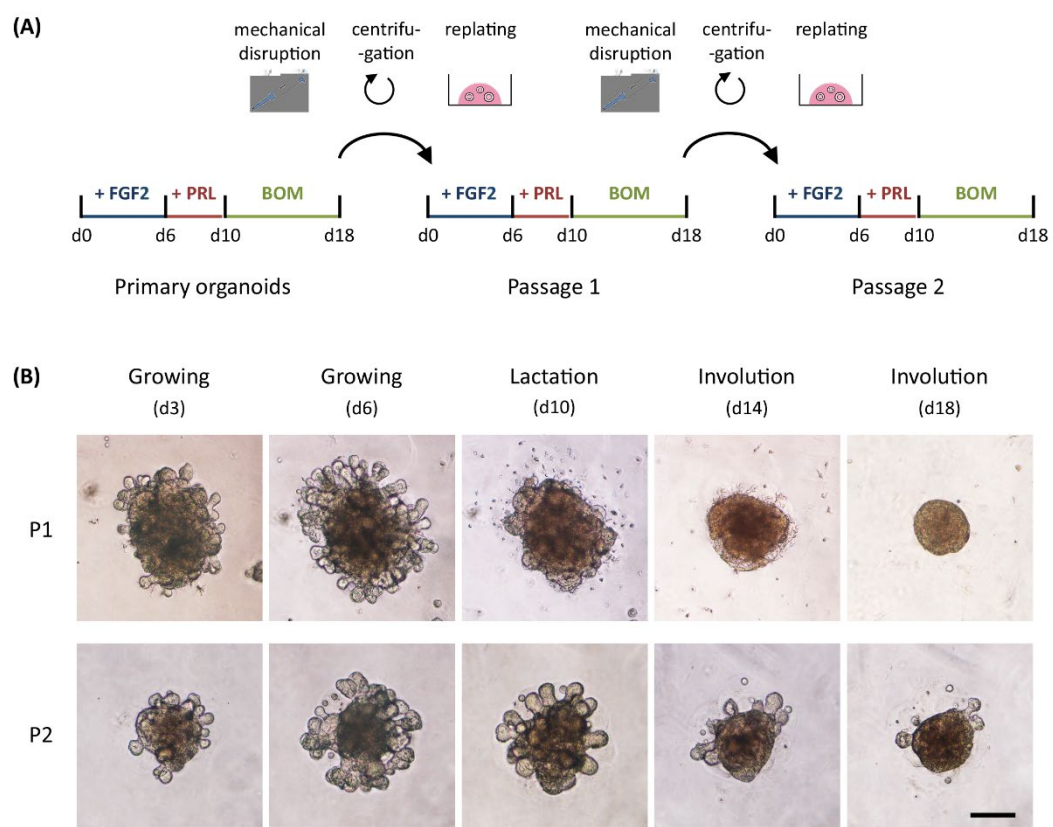


Figure 3. Passage of involution-like organoids.

A. Scheme depicting the experimental design. PRL: Prolactin; BOM: basal organoid medium. B. Morphology of passaged organoids during the lactation and involution-like processes. Brightfield images of passage 1 (upper panel) and passage 2 (lower panel) organoids following morphogenic and lactogenic stimulation and on days 4 or 8 after hormonal withdrawal. Scale bar = 100 μ m.

1. RNA isolation

Note: Embedding in Matrigel® does not interfere with the quality of extracted RNA.

- a. Aspirate the culture medium.
- b. Add 350 µL RLT buffer (RNeasy Micro Kit) containing 3.5 µL β-mercaptoethanol to each well.
- c. Disintegrate the organoid culture in lysis buffer by performing ten up-and-down motions with a P1000 pipette.
- d. Transfer the solution to a fresh 1.5-mL tube and vortex well.
Note: Samples can be stored at -80°C until RNA extraction. To perform RNA extraction, thaw samples on ice and proceed according to the following instructions.
- e. Homogenize RNA lysates by performing ten up-and-down motions with a single-use 30 G insulin syringe.
- f. Process samples as described in the RNeasy Micro Kit booklet, starting from Step C1b.
- g. Measure the RNA concentration using a NanoDrop™.

2. Protein extraction

Note: Embedding in Matrigel® interferes with western blotting analysis. Follow these steps to remove the Matrigel® prior to protein extraction.

- a. Aspirate the culture medium and dissociate the 3D culture with 800 µL cold PBS supplemented with phosphatase inhibitor cocktail II.
- b. Transfer the suspension to a clean 1.5-mL tube and centrifuge for 3 min at 400 × g, 4°C.
- c. Rinse twice with PBS supplemented with phosphatase inhibitor cocktail II.
- d. Discard the supernatant and resuspend the pellet in 100 µL ice-cold ready-to-use RIPA buffer supplemented with protease inhibitor cocktail I and phosphatase inhibitor cocktail II.

Note: Samples can be stored at -80°C until protein extraction. To perform protein extraction, thaw samples on ice and proceed according to the following instructions.

- e. Sonicate the samples twice at 4°C using a 60-kHz ultrasonic wave frequency program (30 s ON/30 s OFF).
 - f. Vortex the samples, cool on ice, and repeat the sonication according to Step C2e.
 - g. Centrifuge for 20 min at >10,000 × g, 4°C.
 - h. Transfer the supernatant to a clean 1.5-mL tube.
 - i. Measure the protein concentration using a Coomassie Protein Assay Kit.
- ## 3. Fixation and embedding for histology
- a. Aspirate the culture medium and rinse the culture twice with 800 µL cold PBS.
 - b. Incubate with 800 µL 4% PFA for 30 min. Following removal of the 4% PFA, wash twice with PBS.

Notes:

- i. Domes should be entirely covered with the solution. Add a greater volume if required.
 - ii. The fixed cultures can be stored in PBS at 4°C until embedding.
- c. Prepare 3% low gelling temperature agarose in PBS and melt slowly in a microwave for 1.5–2 min at 1000 W (homogenize every 30 s by hand rotation).
 - d. Detach the fixed culture using the flat side of a spatula and transfer to a plastic histology mold containing melted agarose. Overlay with more agarose.
 - e. After solidification of the agarose, unmold the block. Use a scalpel to remove the excess agarose surrounding the Matrigel® dome and place in a plastic embedding cassette for histology.

- f. Proceed to sample dehydration: incubate the embedding cassettes in successive 1-h baths of 70% EtOH, 95% EtOH, 100% EtOH (twice), xylene (twice), 50% xylene-50% melted paraffin, and 100% melted paraffin.
- g. Incubate overnight at 65°C in a second bath of 100% melted paraffin.
- h. Embed in a histology tissue mold using an embedding workstation.
- i. Unmold the paraffin blocks after 24 h of solidification.
- j. Cut 5-μm sections and spread on microscope slides. Keep the slides at room temperature until further analysis.
- k. Remove the paraffin prior to any staining by successive 5-min baths of xylene (twice), 100% EtOH (twice), 95% EtOH, 70% EtOH, and H₂O.

Recipes

1. Dissociation solution

Note: This solution is prepared inside a laminar flow hood under aseptic conditions and does not need to be filter-sterilized.

2 mg/mL collagenase
2 mg/mL trypsin
5 μg/mL insulin
50 μg/mL gentamicin
5% FBS
2 mM glutamine
in DMEM/F12

2. BSA solution

Note: This solution can be filter-sterilized and reused several times when stored at 4°C.
2.5% BSA in PBS

3. Basal organoid medium (BOM)

Note: This solution is prepared inside a laminar flow hood under aseptic conditions and does not need to be filter-sterilized.

1× insulin-transferrin-selenium (ITS)
100 U/mL penicillin
100 μg/mL streptomycin
2 mM glutamine
in DMEM/F12

4. Morphogenesis medium

Note: This solution is prepared inside a laminar flow hood under aseptic conditions and does not need to be filter-sterilized.

2.5 nM FGF2 in BOM

5. Lactation medium

Note: This solution is prepared inside a laminar flow hood under aseptic conditions and does not need to be filter-sterilized.

1 μg/mL prolactin
1 μg/mL hydrocortisone
in BOM

6. 4% PFA

Note: This solution is prepared inside a chemical hood and does not need to be filter-sterilized.

4% paraformaldehyde in PBS

7. RNA lysis buffer

Note: This solution is prepared inside a chemical hood and does not need to be filter-sterilized.

10 µL β-mercaptoethanol per 1 mL RLT lysis buffer (from the RNeasy Micro Kit; this solution can be stored for up to one month at room temperature).

8. Phosphatase inhibitor cocktail II

Note: This solution is prepared inside a chemical hood or on a bench and does not need to be filter-sterilized.

2 mM imidazole

1 mM sodium fluoride

1.15 mM sodium molybdate

1 mM sodium orthovanadate

4 mM sodium tartrate dihydrate

in RIPA buffer

9. Protease inhibitor cocktail I

Note: This solution is prepared inside a chemical hood or on a bench and does not need to be filter-sterilized.

500 µM AEBSF hydrochloride

150 nM aprotinin

1 µM protease inhibitor E-64

0.5 mM EDTA

1 µM leupeptin hemisulfate

in RIPA buffer

Acknowledgments

Work in the laboratory of HL is funded by the Pasteur, Centre National pour la Recherche the Agence Nationale de la Recherche (ANR-10-LABX-73 and ANR-16-CE13-0017- 01), Fondation ARC (PJA 20161205028 and 20181208231), Programme Barrande, and AFM-Telethon Foundation. AC was funded by postdoctoral fellowships from the Revive Consortium. EC was funded by a Ph.D. fellowship from Sorbonne Université. ZK was funded by the Grant Agency of Masaryk University (MUNI/G/1446/2018), Mobility grant by Ministry of Education, and Youth and Sports, and by funds from the Faculty of Medicine MU to the junior researcher (ROZV/28/LF/2020). JS was funded by the P-Pool (Faculty of Medicine MU) and the Grant Agency of Masaryk University (MUNI/A/1565/2018). This protocol was derived from the original research paper “Primary Mammary Organoid Model of Lactation and Involution” (Sumbal *et al.*, 2020b).

Competing interests

The authors declare that they have no competing interests.

Ethics

The animal study was reviewed and approved by French legislation in compliance with European Communities Council Directives (A 75-15-01-3) and the regulations of the Institut Pasteur Animal Care Committees (CETEA).

References

- Artegiani, B., and Clevers, H. (2018). [Use and application of 3D-organoid technology](#). *Hum Mol Genet* 27: R99-R107.
- Brisken, C. and O'Malley, B. (2010). [Hormone action in the mammary gland](#). *Cold Spring Harb Perspect Biol* 2(12): a003178.
- Brisken, C. and Rajaram, R. D. (2006). [Alveolar and lactogenic differentiation](#). *J Mammary Gland Biol Neoplasia* 11(3-4): 239-248.
- Campbell, J. J., Botos, L. A., Sargeant, T. J., Davidenko, N., Cameron, R. E. and Watson, C. J. (2014). [A 3-D *in vitro* co-culture model of mammary gland involution](#). *Integr Biol (Camb)* 6(6): 618-626.
- Ewald, A. J., Brenot, A., Duong, M., Chan, B. S. and Werb, Z. (2008). [Collective epithelial migration and cell rearrangements drive mammary branching morphogenesis](#). *Dev Cell* 14(4): 570-581.
- Freestone, D., Cater, M. A., Ackland, M. L., Paterson, D., Howard, D. L., de Jonge, M. D. and Michalczyk, A. (2014). [Copper and lactational hormones influence the CTR1 copper transporter in PMC42-LA mammary epithelial cell culture models](#). *J Nutr Biochem* 25(4): 377-387.
- Huch, M. and Koo, B. K. (2015). [Modeling mouse and human development using organoid cultures](#). *Development* 142(18): 3113-3125.
- Huebner, R. J., Neumann, N. M. and Ewald, A. J. (2016). [Mammary epithelial tubes elongate through MAPK-dependent coordination of cell migration](#). *Development* 143: 983-993.
- Hughes, K. and Watson, C. J. (2012). [The spectrum of STAT functions in mammary gland development](#). *JAKSTAT* 1(3): 151-158.
- Jamieson, P. R., Dekkers, J. F., Rios, A. C., Fu, N. Y., Lindeman, G. J. and Visvader, J. E. (2017). [Derivation of a robust mouse mammary organoid system for studying tissue dynamics](#). *Development* 144(6): 1065-1071.
- Jena, M. K., Jaswal, S., Kumar, S. and Mohanty, A. K. (2019). [Molecular mechanism of mammary gland involution: An update](#). *Dev Biol* 445(2): 145-155.
- Koledova, Z. (2017). [3D Cell Culture: An Introduction](#). *Methods Mol Biol* 1612: 1-11.
- Linnemann, J. R., Miura, H., Meixner, L. K., IrmLer, M., Kloos, U. J., Hirschi, B., Bartsch, H. S., Sass, S., Beckers, J., Theis, F. J., Gabka, C., Sotlar, K. and Scheel, C. H. (2015). [Quantification of regenerative potential in primary human mammary epithelial cells](#). *Development* 142(18): 3239-3251.
- Macias, H. and Hinck, L. (2012). [Mammary gland development](#). *Wiley Interdiscip Rev Dev Biol* 1(4): 533-557.
- Mroue, R., Inman, J., Mott, J., Budunova, I., and Bissell, M.J. (2015). [Asymmetric expression of connexins between luminal epithelial- and myoepithelial- cells is essential for contractile function of the mammary gland](#). *Dev Biol* 399(1): 15-26.
- Neumann, N. M., Perrone, M. C., Veldhuis, J. H., Huebner, R. J., Zhan, H., Devreotes, P. N., Brodland, G. W. and Ewald, A. J. (2018). [Coordination of Receptor Tyrosine Kinase Signaling and Interfacial Tension Dynamics Drives Radial Intercalation and Tube Elongation](#). *Dev Cell* 45(1): 67-82 e66.
- Ormandy, C. J., Camus, A., Barra, J., Damotte, D., Lucas, B., Buteau, H., Edery, M., Brousse, N., Babinet, C., Binart, N. and Kelly, P. A. (1997). [Null mutation of the prolactin receptor gene produces multiple reproductive defects in the mouse](#). *Genes Dev* 11(2): 167-178.
- Qu, Y., Han, B., Gao, B., Bose, S., Gong, Y., Wawrowsky, K., Giuliano, A. E., Sareen, D. and Cui, X. (2017). [Differentiation of Human Induced Pluripotent Stem Cells to Mammary-like Organoids](#). *Stem Cell Reports* 8(2): 205-215.
- Richert, M. M., Schwertfeger, K. L., Ryder, J. W. and Anderson, S. M. (2000). [An atlas of mouse mammary gland development](#). *J Mammary Gland Biol Neoplasia* 5(2): 227-241.
- Shamir, E. R. and Ewald, A. J. (2015). [Adhesion in mammary development: novel roles for E-cadherin in individual and collective cell migration](#). *Curr Top Dev Biol* 112: 353-382.
- Sternlicht, M. D. (2006). [Key stages in mammary gland development: the cues that regulate ductal branching morphogenesis](#). *Breast Cancer Res* 8(1): 201.
- Sumbal, J., Budkova, Z., Traustadottir, G. A. and Koledova, Z. (2020a). [Mammary Organoids and 3D Cell Cultures: Old Dogs with New Tricks](#). *J Mammary Gland Biol Neoplasia*. doi: 10.1007/s10911-020-09468-x.
- Sumbal, J., Chiche, A., Charifou, E., Koledova, Z. and Li, H. (2020b). [Primary Mammary Organoid Model of Lactation and Involution](#). *Front Cell Dev Biol* 8: 68.

- Xian, W., Schwertfeger, K. L., Vargo-Gogola, T. and Rosen, J. M. (2005). [Pleiotropic effects of FGFR1 on cell proliferation, survival, and migration in a 3D mammary epithelial cell model.](#) *J Cell Biol* 171(4): 663-673.
- Zwick, R. K., Rudolph, M. C., Shook, B. A., Holtrup, B., Roth, E., Lei, V., Van Keymeulen, A., Seewaldt, V., Kwei, S., Wysolmerski, J., Rodeheffer, M. S. and Horsley, V. (2018). [Adipocyte hypertrophy and lipid dynamics underlie mammary gland remodeling after lactation.](#) *Nat Commun* 9(1): 3592.

ATAC-Seq-based Identification of Extrachromosomal Circular DNA in Mammalian Cells and Its Validation Using Inverse PCR and FISH

Zhangli Su[#], Shekhar Saha[#], Teressa Paulsen, Pankaj Kumar* and Anindya Dutta*

Department of Biochemistry and Molecular Genetics, University of Virginia School of Medicine, Charlottesville, VA 22908, USA

*For correspondence: ad8q@virginia.edu; pk7z@virginia.edu

[#]Contributed equally to this work

Abstract

Recent studies from multiple labs including ours have demonstrated the importance of extrachromosomal circular DNA (eccDNA) from yeast to humans (Shibata *et al.*, 2012; Dillon *et al.*, 2015; Møller *et al.*, 2016; Kumar *et al.*, 2017; Turner *et al.*, 2017; Kim *et al.*, 2020). More recently, it has been found that cancer cells obtain a selective advantage by amplifying oncogenes on eccDNA, which drives genomic instability (Wu *et al.*, 2019; Kim *et al.*, 2020). Previously, we have purified circular DNA and enriched the population using rolling circle amplification followed by high-throughput sequencing for the identification of eccDNA based on the unique junctional sequence. However, eccDNA identification by rolling circle amplification is biased toward small circles. Here, we report a rolling circle-independent method to detect eccDNA in human cancer cells. We demonstrate a sensitive and robust step-by-step workflow for finding novel eccDNAs using ATAC-seq (Assay for Transposase-Accessible Chromatin using sequencing) combined with a Circle_finder bioinformatics algorithm to predict the eccDNAs, followed by its validation using two independent methods, inverse PCR and metaphase FISH (Fluorescence *in situ* Hybridization).

Keywords: Circular DNA, eccDNA, ATAC-seq, Inverse PCR, FISH

This protocol was validated in: Sci Adv (2020), DOI: 10.1126/sciadv.aba2489

Background

Extrachromosomal circular DNAs (eccDNAs) are unique DNA molecules that carry genetic information in addition to the chromosomal DNAs. These eccDNAs have been found in different organisms from yeast to humans (Shibata *et al.*, 2012; Dillon *et al.*, 2015; Møller *et al.*, 2016; Kumar *et al.*, 2017; Turner *et al.*, 2017; Kim *et al.*, 2020). The length of eccDNAs ranges from small (less than 1kb, also called microDNAs) to large (megabase-long). While the small eccDNAs with micro homology ends may promote genetic heterogeneity (Shibata *et al.*, 2012) or produce short RNAs if transcribed (Paulsen *et al.*, 2019), the long eccDNAs may harbor complete genes and regulatory elements such as enhancers (Morton *et al.*, 2019; Wu *et al.*, 2019; Koche *et al.*, 2020). Emerging evidence suggests that eccDNAs could play underappreciated roles in regulating gene expression and genome instability, which ultimately contributes to the selective advantage of cells (Gresham *et al.* 2010, Koo *et al.*, 2018; Hull *et al.*, 2019). In particular, oncogene-carrying eccDNAs are highly amplified in human cancers and correlate with open chromatin, increased oncogene expression, and chromosome structural rearrangement, in addition to being associated with poor outcomes (Wu *et al.*, 2019; Kim *et al.*, 2020; Koche *et al.*, 2020). Uncovering eccDNAs in the circulation also makes them prospective targets for diagnostic purposes (Kumar *et al.*, 2017; Sin *et al.*, 2020).

The growing research on eccDNAs calls for tool development for eccDNA discovery. Historically, eccDNAs of various sizes were detected by karyotyping, electron microscopy, Southern blotting, and 2-D gel electrophoresis (reviewed in Paulsen *et al.*, 2018). More recently, various high-throughput sequencing (HTS) technologies have been exploited to facilitate the discovery of new eccDNAs (Shibata *et al.*, 2012; Møller *et al.*, 2015; Kim *et al.*, 2020). The basic idea for eccDNA detection via HTS methods is based on their distinctive circular feature – eccDNAs of high confidence can be identified from paired-end reads that (1) could not map as inward pairs on the linear genome, and (2) contain the unique circular junctional sequence that represents the chromosome breakage/ligation point. A unique junctional sequence (shown as “E-A” in Figure 1A) that is not present in the normal reference genome could be formed through ligation of the two ends of a linear DNA, thus creating the circular DNA. However, the majority of eccDNA sequencing pipelines utilize multiple displacement amplification (MDA), an efficient method to amplify small amounts of DNA via rolling circle amplification, which would preferentially amplify short circles. Therefore, we sought to develop an MDA-independent pipeline that incorporates several additional validation assays.

Recently, we demonstrated a robust workflow to detect and validate new eccDNAs from human cancer cell cultures (Kumar *et al.*, 2020). Specifically, ATAC-seq (Assay for Transposase-Accessible Chromatin using sequencing) and a Circle_finder algorithm was employed for new eccDNA prediction. ATAC-seq, first developed in 2013, utilizes engineered Tn5 transposase to cut open chromatin regions (including eccDNAs that are less chromatinized) and insert transposase-associated adapter DNAs (Buenrostro *et al.*, 2013 and 2015). The Circle_finder algorithm (refer to Software for link access) predicts eccDNAs from paired-end sequencing based on: (1) the presence of split reads (one read maps to two sites in the genome); (2) the two fragments on the split read maps on the same chromosome and same strand; and (3) the continuous read maps between the two fragments on the split read and on the opposite strand to the split read. Predicted eccDNAs can be evaluated by two independent validation assays (Figure 1). Inverse PCR (Figure 1B) will specifically amplify eccDNAs with a primer pair that spans the unique junctional sequence (shown as “E-A”); such a primer pair faces outward on genomic DNA and results in no amplification. Alternatively, eccDNA can be visually confirmed by metaphase FISH (Figure 1C), which can detect both genomic DNA signals overlapping with main chromosomes and signals from eccDNAs that do not overlap with chromosomes.

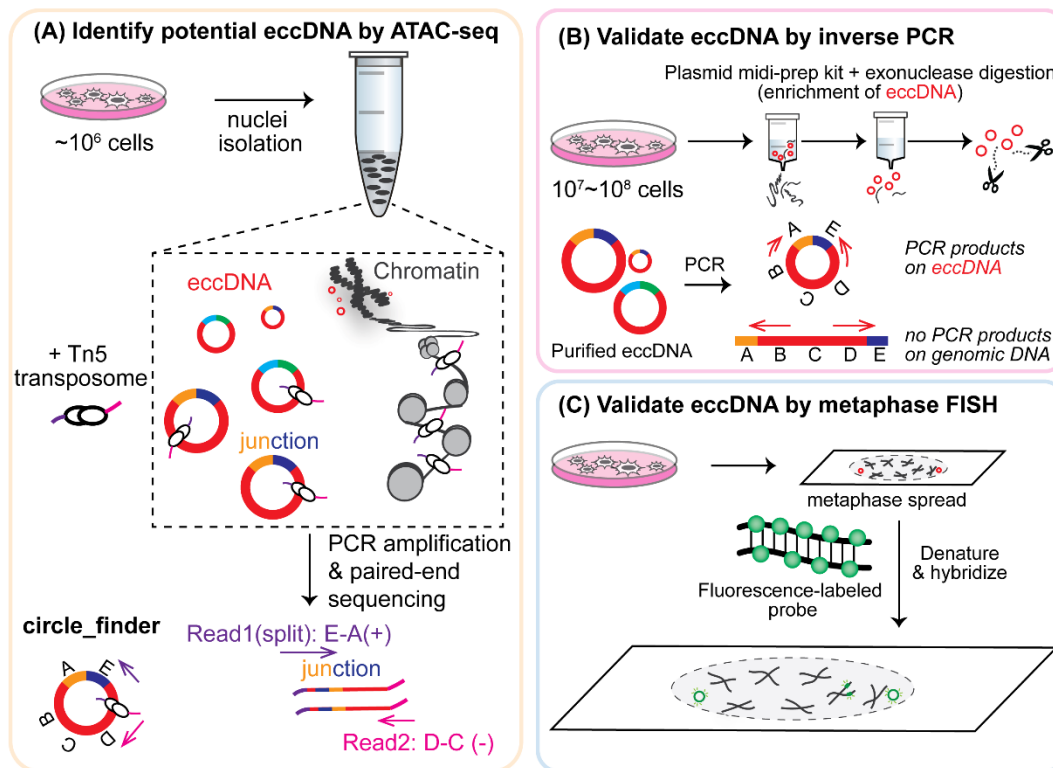


Figure 1. Overview of eccDNA identification and validation by ATAC-seq, inverse PCR, and metaphase FISH

Materials and Reagents

1. 50 mL Falcon conical tubes (Fisher Scientific, catalog number: 1443222)
2. 15 mL Falcon conical tubes (Fisher Scientific, catalog number: 1495949B)
3. 1.5 mL DNA LoBind tubes (Eppendorf, catalog number: 022431021)
4. 1 mL pipette tip
5. 100-200 μ L pipette tip
6. 100 mm Petri dish
7. 0.2 μ m filter
8. Microscope glass slides (Fisher Scientific, catalog number: 4951F-001)
9. 22 mm \times 50 mm cover glass (Fisher Scientific, catalog number: 12-545E)
10. Parafilm (Thermo Fisher Scientific, catalog number: S37440)
11. Aluminum foil (Thermo Fisher Scientific, catalog number: 14-648-236)
12. Mammalian cells in culture. In this protocol, we used the ovarian cancer cell line, OVCAR8, and the prostate cancer cell line, C4-2B, cultured in RPMI medium (Corning, catalog number: 10-040-CV) supplemented with 10% fetal bovine serum (Thermo Fisher Scientific, catalog number: 26140079) and 1% penicillin-streptomycin (Thermo Fisher Scientific, catalog number: 15-140-122)
13. SybrGold dye (Invitrogen, catalog number: S11494)
14. 0.5% trypsin-EDTA (Thermo Fisher Scientific, catalog number: 15400054)
15. UltraPure DNase/RNase-free distilled water (Thermo Fisher Scientific, catalog number: 10977015)
16. 1 M Tris-HCl, pH 7.5 (Thermo Fisher Scientific, catalog number: 15567027, store at 4°C, shelf life: 6 months)
17. 5 M NaCl solution (Thermo Fisher Scientific, catalog number: AM9760G, store at room temperature)

18. 1 M MgCl₂ solution (Thermo Fisher Scientific, catalog number: AM9530G, store at room temperature)
19. Dulbecco's phosphate-buffered saline or DPBS, no calcium, no magnesium (Thermo Fisher/Gibco, catalog number: 14190144, store at 4°C, shelf life: 36 months)
20. 10% Nonidet P40 substitute (Millipore/Sigma-Aldrich, catalog number: 11332473001, store at 4°C, keep protected from light, shelf life: 24 months)
21. 10% (w/v) Tween-20 (Millipore/Sigma-Aldrich, catalog number: 11332465001, store at 4°C under inert gas and keep protected from light, shelf life: 24 months)
22. 20 mg/mL digitonin in DMSO (Promega, catalog number: G9411, store in -20°C)
23. DNA Clean & Concentrator Kit (ZYMO, catalog number: D4033)
24. Nextera DNA Sample Preparation Kit (Illumina, catalog number: FC-121-1030, store at -20°C)

Note: This kit has been discontinued and can be purchased separately: Tagmentation DNA Enzyme/TDE (Illumina, catalog number: 15027865) and Tagmentation DNA Buffer/TDB (Illumina, catalog number: 15027866).

25. Nextera Index Kit, 24 indexes (Illumina, catalog number: 15055289, store at -20°C)
26. NEBNext High-Fidelity 2× PCR Master Mix (New England Biolabs, catalog number: M0541, store at -20°C)
27. Phosphate-buffered saline, pH 7.4 (Thermo Fisher Scientific, catalog number: 10010023)
28. Qiagen HiSpeed Plasmid Midi Kit (Qiagen, catalog number: 12643)
29. Isopropanol (Fisher Chemical, catalog number: A516-500)
30. Ethanol (Thermo Fisher Scientific, catalog number: A4094)
31. Glycogen (Thermo Fisher Scientific, catalog number: AM9510)
32. Plasmid-safe ATP-dependent DNase (Lucigen, catalog number: E3101K)
33. QIAquick PCR Purification Kit (Qiagen, catalog number: 28104)
34. KOD Hot-Start DNA Polymerase (Millipore/Sigma-Aldrich, catalog number: 71086)
35. Thymidine (Millipore/Sigma-Aldrich, catalog number: T1895)
36. 10 mg/mL KaryoMax Colcemid solution in PBS (Thermo Fisher Scientific, catalog number: 15212012)
37. Potassium chloride (Millipore/Sigma-Aldrich, catalog number: P9541)
38. Formamide (Millipore/Sigma-Aldrich, catalog number: 47670)
39. Sodium chloride (Thermo Fisher Scientific, catalog number: BP358)
40. Sodium citrate (Millipore/Sigma-Aldrich, catalog number: W302600)
41. BAC FISH Probe label with 5-fluorescein (Empire Genomics, catalog number: RP11-732I3 and RP11-765O11)
42. Rubber cement (Elmer's Rubber Cement, catalog number: EPIE904)
43. Nonidet P-40 (Sigma, catalog number: I8896)
44. Dextran sulfate (Thermo Fisher Scientific, catalog number: BP1585)
45. VectaShield Mounting Medium with DAPI (Vector Laboratories, catalog number: H-1200-10)
46. Nail polish (OPI Nail Lacquer)
47. Nikon immersion oil for the confocal microscope (Thermo Fisher Scientific, catalog number: 12-624-66A)
48. 1% (10 mg/mL) digitonin (see Recipes, store at -20°C as aliquotes, stable for 6 months)
49. ATAC-Resuspension Buffer (see Recipes)
50. ATAC-Lysis Buffer (see Recipes)
51. ATAC-Wash Buffer (see Recipes)
52. ATAC-Reaction Mastermix (see Recipes)
53. 100 mM thymidine solution (see Recipes)
54. 75 mM KCl Hypotonic Solution (see Recipes)
55. Carnoy's Fixative Solution (see Recipes)
56. 20× Saline-Sodium-Citrate (SSC) buffer (see Recipes)
57. Hybridization Buffer (see Recipes)
58. FISH Denaturation Buffer (see Recipes)
59. FISH Wash Buffer 1 (see Recipes)
60. FISH Wash Buffer 2 (see Recipes)

Equipment

1. Cell culture incubator
2. Tissue culture hood
3. Tabletop microcentrifuge (Eppendorf, model: 5424)
4. Thermomixer (Thermo Scientific, catalog number: 13687711)
5. PCR machine with heated lid (Eppendorf, model: Mastercycler Pro)
6. Tabletop centrifuge (Eppendorf, model: 5804)
7. Water bath (Thermo Fisher Scientific, Isotemp)
8. Coplin jar (Local Company)
9. Hybridization chamber (Thermo Fisher Scientific, Isotemp)
10. Chemical fume hood (Bellco Glass Inc.)
11. Brightfield microscope (Olympus)
12. Confocal microscope (Nikon, model: Ti-E eclipse series)
13. Computer with enough data storage capacity up to TB

Software

1. Circle_finder (github, https://github.com/pk7zuva/Circle_finder/blob/master/circle_finder-pipeline-bwa-mem-samblaster.sh); pre-requisite installation to run Circle_finder: bedtools (<https://github.com/arq5x/bedtools2>), samtools (<http://samtools.sourceforge.net>), parallel (<https://www.gnu.org/software/parallel/>), bwa (<https://github.com/lh3/bwa>), samblaster (<https://github.com/GregoryFaust/samblaster>)
2. Cutadapt (<https://cutadapt.readthedocs.io/en/stable/>)
3. AR Elements Software (Nikon, Japan)
4. ImageJ (NIH, USA)

Procedure

A. ATAC-seq from cultured mammalian cells

1. Nuclei isolation from cultured mammalian cells
 - a. Pellet 50,000 mammalian cells in culture into a 1.5 mL DNA LoBind tube.

Note: Check cell viability prior to the experiment by Trypan Blue staining and ensure cell viability is at least 95%. Please refer to the original ATAC-seq protocol (Corces, 2017) for treatment of cells with DNase to remove extracellular DNAs or to separate cells via ficoll gradient if viability is lower than 95%.

- b. Wash cells in ice-cold DPBS twice at 500 × g.
- c. Add 50 µL ice-cold ATAC-LB to each tube, pipette up and down 3 times with a 100-200 µL pipette tip. Incubate on ice for 3 min.

Note: We have used a 3-min lysis time with several cell lines, including HCT116, OVCAR8, and C4-2B. The lysis time may need to be increased for specific tough-to-lyse cell lines. The efficiency of cell lysis can be checked by Trypan Blue staining under the microscope (blue staining suggests successful lysis).

- d. Immediately dilute the 50 μ L lysate by adding 1 mL ice-cold ATAC-WB into the tube. Invert tube 3 times to mix. Spin at $500 \times g$ for 10 min at 4°C.
- e. Carefully remove the supernatant (containing the cytoplasmic fraction*), first by a 1-mL pipette tip followed by a 100-200- μ L pipette tip. The pellet now contains the nuclei, which should be used for the tagmentation reaction immediately.

*Note: The cytoplasmic fraction can be saved for RNA extraction later.

2. Transposition/tagmentation reaction and clean-up
 - a. Resuspend the nuclei pellet in 50 μ L ATAC-RM by pipetting up and down 6 times. Incubate in a thermomixer at 37°C for 30 min with 1,000 RPM constant mixing.
 - b. Add 250 μ L DNA Binding Buffer (from Zymo DNA Clean and Concentrator Kit) to each 50 μ L ATAC reaction, mix well by pipetting up and down 3 times. Transfer 300 μ L mixture to each column sitting on a collection tube (both from Zymo DNA Clean and Concentrator Kit), spin down at 15,000 $\times g$ for 30 s and discard liquid in the collection tube.
 - c. Wash column with 200 μ L DNA Wash Buffer (from Zymo DNA Clean and Concentrator Kit), spin down at 15,000 $\times g$ for 30 s.

Note: Make sure ethanol is added to the Wash Buffer according to the manufacturer's guidelines.

- d. Repeat the wash with 200 μ L DNA Wash Buffer. Spin down at 15,000 $\times g$ (or maximum speed) for 2 min to ensure efficient removal of all buffers.
- e. Discard the previous collection tube. Carefully displace the column into a new 1.5-mL tube. Add 21 μ L ddH₂O to the center of the column and spin down at 15,000 $\times g$ (or maximum speed) for 30 s to collect eluted DNA. Tagmented DNA can be stored at -20°C (in low DNA-binding tube) at this point if not proceeding to the next step immediately.
3. DNA library PCR amplification and clean-up
 - a. Set up PCR reaction in 0.2-mL PCR tubes on ice:
20 μ L eluted DNA
2.5 μ L 25 μ M Nextera i5 primer (from Nextera index kit)
2.5 μ L 25 μ M Nextera i7 primer (from Nextera index kit)
25 μ L 2 \times NEBNext master mix

Note: If multiple samples will be pooled for sequencing, different combinations of i5 and i7 indexed primers need to be used for each sample. Please refer to specific NGS sequencing platform for recommendation about choice of index combinations. For Illumina sequencing with Nextera index, please refer to [Illumina Index Adapters Pooling Guide](#).

- b. PCR amplification for 10 cycles with the following PCR cycling program (lid set to 105°C):
Step 1. 72°C, 5 min
Step 2. 98°C, 30 s
Step 3. 98°C, 10 s
Step 4. 63°C, 30 s
Step 5. 72°C, 1 min
(Repeat steps 3-5 for a total of 5-10 cycles)
Step 6. 4°C on hold

Note: The optimal number of PCR cycle needs to be optimized for each specific cell line to ensure enough final products while avoiding over-amplification. The cycle number can be optimized by testing a range of different cycle numbers (lowest from 5 cycles to ensure sequencing adaptors attached to DNA fragments) using a small portion of the tagmented DNA. The amplification can be monitored by qPCR or run on an agarose gel (Figure 2).

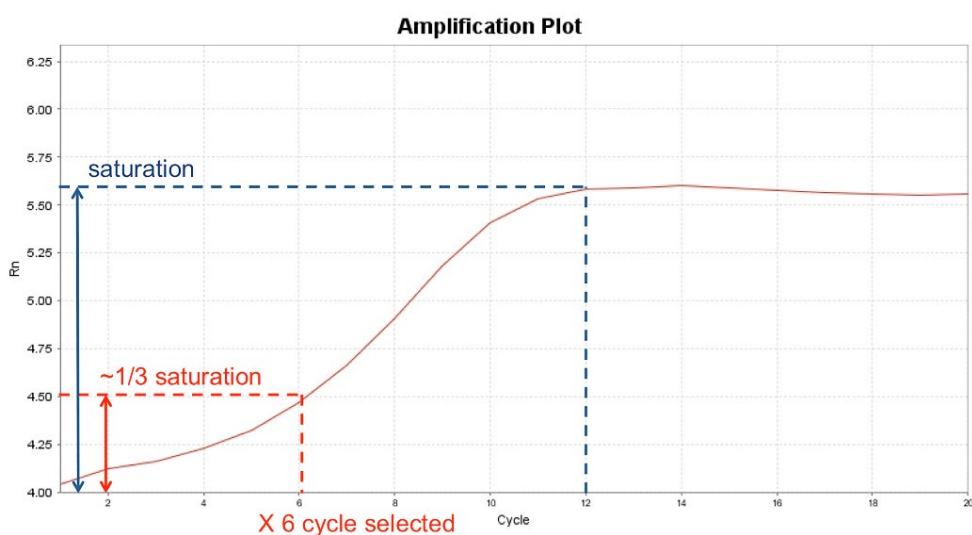


Figure 2. Example of optimizing ATAC-seq PCR cycle number by a qPCR method.

Shown here is an example of using qPCR to determine the optimal number of PCR cycles for ATAC-seq library preparation in C4-2 cells. A separate ATAC reaction with the same number of starting materials was set up in parallel to the actual ATAC-seq reaction, and finished Step A2. The qPCR reaction was set up similar to Step A3a, with the addition of 1:400 dilution of SybrGold Dye (Invitrogen S11494), and set up in a qPCR-compatible plate. The qPCR program was set up the same as Step A3b with real-time fluorescence reading for a total of 20 cycles. Upon finishing qPCR, the Rn (normalized reporter) value is plotted against the cycle number and the saturation point (indicated by the dashed blue line) is determined from the plot. From the Rn-Cycle plot, the cycle number is selected when it reaches 1/3 of the saturation signal (indicated by the red dashed line). In this particular example, a PCR cycle number of 6 was selected. If a separate ATAC reaction is not intended, a small portion (for example, 1/16) of the reaction after Step A2 can be used as input for the qPCR reaction; and the remaining reaction can be used for the final PCR amplification.

- c. Clean up the 50 μ L PCR reaction using a ZYMO DNA Clean and Concentrator Kit (similar to above). Elute in 15 μ L H₂O. Confirm the size distribution of the amplified library using a Bioanalyzer HS DNA Chip (Figure 3).
 - d. Submit ATAC-seq libraries for paired-end Illumina sequencing.
4. Identify potential eccDNA genomic coordinates using the circle_finder algorithm
 - a. Remove the adaptor sequence using the cutadapt program (Martin, 2011) with the following parameters: cutadapt -a ADAPT1 -A ADAPT2 -o out1.fastq -p out2.fastq in1.fastq in2.fastq.

Note: ADAPT1 = CTGTCTTATACACATCTCCGAGCCCACGAGAC, ADAPT2 = CTGTCTTATACACATCTGACGCTGCCGACGA. in1.fastq and in2.fastq are input fastq files before adaptor removal. out1.fastq and out2.fastq are paired-end fastq files after adaptor removal.

- b. The Circle_finder pipeline first maps the paired-end reads (read length should be >75 bases long) onto the genome (in this case hg38 genome build) using bwa aligner (bwa-mem) (Li, 2013). While mapping paired-end reads to the genome, Circle_finder collects those paired-end reads where one read is mapped in a contiguous manner and the partner read is mapped in a non-contiguous (split-read) manner, supposing one end maps on the body of the circular DNA and the other on the circular DNA ligation junction. Returning to the list of paired-end IDs that mapped uniquely to three sites (one contiguously mapped reads and two-position for reads mapped in a split-read manner) in the genome, the pipeline identifies paired-end IDs where the contiguously mapped read is between the two split reads and on the opposite strand (Figure 1A). The start of the first split read and the end of the second

read is annotated as the start and end of the eccDNA. The pipeline (a single script – see next step) to identify eccDNA from paired-end sequencing data of read length >than 75 bases long coming from a specific locus (nonchimeric eccDNA) of any length is available through our GitHub page (refer to software section).

- c. Generate the genome index file: this only needs to be generated once for a specific genome. For example, command to generate an index file for human genome hg38: bwa index hg38.fa.

Note: hg38.fa is the fasta file for the genome of interest (hg38 in this case). This will generate an index under the same name as the genome fasta file name.

- d. Use the bash script with the following logic: #Usage: bash Script_name “Number of processors” “/path-of-whole-genome-file/hg38.fa” “paired-end fastq file 1” “paired-end fastq file 2” “minNonOverlap between two split reads” “Sample name” “genome build”. An example script is shown here (code as a single line):

```
#bash /path-of-script/directory/microDNA-pipeline-bwa-mem-samblaster.sh 16 /path-of-script-directory/hg38.fa S1_R1.fastq S1_R2.fastq 10 S1 hg38
```

Note 1: The pipeline takes seven arguments as below.

Argument 1 = “Number of processors”;

Argument 2 = “Genome fasta file” for example “hg38.fa”;

Argument 3 = “paired-end fastq file 1”;

Argument 4 = “paired-end fastq file 2”;

Argument 5 = “minNonOverlap between two split reads”, for example 10;

Argument 6 = “Sample name”, user may choose any name for their sample;

Argument 7 = “genome build”, user may choose their genome build, such as hg38.

Note 2: The chance of identifying eccDNA depends on sufficient sequencing depth and read length to cover the eccDNA-specific junctional sequence. Here, we used around 100 million read pairs with a 150-bp read length on the Illumina HiSeq platform.

- e. The output file from “circle_finder” will be a file named “microDNA-JT.txt,” which contains four columns including chromosome number, start position of eccDNA coordinate, end position of eccDNA coordinate, and number of junctional tags.

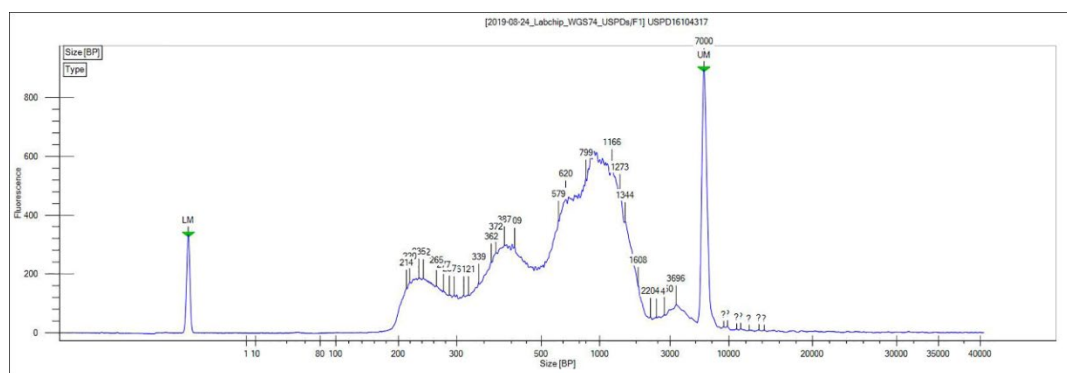


Figure 3. Representative ATAC-seq library size distribution.

ATAC-seq was performed on OVCAR8 nuclei. A characteristic ladder distribution is detected by the bioanalyzer due to the nucleosome arrangement on chromatin.

B. Validation of selective eccDNA by inverse PCR

Note: EccDNA should be treated delicately. EccDNA are prone to shearing and degradation when frozen,

Cite as: Su, Z. et al. (2021). ATAC-Seq-based Identification of Extrachromosomal Circular DNA in Mammalian Cells and Its Validation Using Inverse PCR and FISH. Bio-protocol 11(9): e4003. DOI: 10.21769/BioProtoc.4003.

vortexed, or kept for long-term storage at a low concentration of DNA.

1. Culturing and harvesting cells
 - a. Harvest 10^7 - 10^8 human cancer cells by trypsinization into a 15-mL tube.
 - b. Centrifuge at $300 \times g$, 4°C for 5 min, remove media by aspiration.
 - c. Resuspend cells with 10 mL ice-cold phosphate-buffered saline (PBS).
 - d. Centrifuge at $300 \times g$ for 5 min.
 - e. Remove PBS by careful aspiration.
 - f. Repeat washing steps for a total of two washes, immediately proceed to next step.
2. EccDNA isolation by plasmid columns
 - a. Resuspend cells in 6 mL Buffer P1 from the Qiagen HiSpeed Plasmid Midi Kit.

Note: Add RNase A solution to Buffer P1 prior to experiment and store at 4°C .

- b. Add 6 mL Buffer P2 from the Qiagen HiSpeed Plasmid Midi Kit and mix by gently inverting 4-6 times.
- c. Incubate on the bench at room temperature for 5 min.
- d. Add 6 mL pre-chilled Buffer P3 from the Qiagen HiSpeed Plasmid Midi Kit and mix by gently inverting 4-6 times.
- e. Set up QIAfilter Cartridge from the Qiagen HiSpeed Plasmid Midi Kit by removing the outlet nozzle cap and sitting the cartridge on top of a waste container (such as a 50-mL conical flask). Add the cell lysate (total of 18 mL) into the QIAfilter Cartridge with the cap attached. Incubate at room temperature for 10 min.
- f. While waiting, set up HiSpeed Midi Tip from the Qiagen Plasmid Midi Kit on top of a waste container (such as a 50-mL conical flask) and equilibrate with 4 mL Buffer QBT.
- g. Remove cap from the QIAfilter Cartridge and filter the cell lysate into the HiSpeed Tip by gently inserting the plunger into the cartridge.
- h. After the cell lysate has passed through the HiSpeed Tip, add 10 mL Buffer QC.
- i. After Buffer QC has passed through the HiSpeed Tip, move it to a clean 50-mL conical tube.
- j. Add 5 mL Buffer QF to elute DNA from the HiSpeed Tip.
- k. Add 3.5 mL isopropanol and mix gently by inversion, incubate at room temperature for 5 min.
- l. Attach the QIAprecipitator Module from the Qiagen HiSpeed Plasmid Midi Kit onto a 20-mL syringe after removing the plunger from the syringe.
- m. Add the DNA-isopropanol solution from Step B2k to the syringe and gently push the solution through the QIAprecipitator Module into a waste container.
- n. Remove the 20-mL syringe from the QIAprecipitator Module, pull out the plunger, re-attach the 20-mL syringe to the QIAprecipitator Module, add 20 mL 70% ethanol to the syringe and gently push the plunger to wash the QIAprecipitator Module.
- o. Dry the QIAprecipitator Module by pushing air through the module several times until no more liquid can be pushed out. Dry the QIAprecipitator Module outlet with absorbent paper (such as kimwipes).
- p. Detach the Module from the 20-mL syringe. Attach a new 5-mL syringe (without plunger) to the QIAprecipitator Module.
- q. Add 1 mL Buffer TE from the Qiagen HiSpeed Plasmid Midi Kit to the syringe and push through the QIAprecipitator Module with the plunger into a 1.5-mL Eppendorf tube.
- r. Perform ethanol precipitation: Split the 1,000 μL DNA solution to 500 μL between two 1.5-mL Eppendorf tubes. Add 1,000 μL 100% ethanol and 1 μg glycogen to each of the tubes. Mix by pipetting up and down gently. Centrifuge in a tabletop centrifuge at 13,000 rpm for 30 min.
- s. Remove supernatant as much as possible with 1,000 μL and 100 μL pipette tips without dislodging the DNA pellet. The pellet should be visible at the bottom of the tube. Air dry for 5 min.
- t. Resuspend the DNA in each tube in 20 μL Buffer TE from the Qiagen HiSpeed Plasmid Midi Kit and combine to one tube (40 μL volume).

3. Further enrichment of eccDNAs by DNase digestion to remove linear DNA

- a. To 40 μ L DNA, add 128 μ L ddH₂O, 8 μ L 25 mM ATP, 20 μ L 10 \times Reaction Buffer (from the Plasmid-safe ATP-dependent DNase Kit), and 4 μ L Plasmid-safe ATP-dependent DNase. Incubate at 37°C overnight (10-12 h).
- b. Purify the DNA using the QIAquick PCR Purification Kit by adding 5 volumes of Buffer PB (1,000 μ L) to 1 volume of the digested DNA solution (200 μ L) and mix gently by inversion. Add the mixture to a QIAquick Spin Column, centrifuge for 1 min at 17,900 \times g.
- c. Discard the flowthrough and wash the QIAquick Spin Column with 750 μ L Buffer PE (containing ethanol) by centrifugation for 1 min at 17,900 \times g. Repeat the wash step for a total of two washes.
- d. Elute the DNA with 50 μ L Buffer EB from the QIAquick PCR Purification Kit.
- e. Repeat digestion and purification steps until the DNA concentration no longer decreases. The concentration begins high (>500 ng/ μ L) and should decrease to a low level (<20 ng/ μ L).

Note: For this protocol, we perform a total of 2 rounds of digestion and purification. To optimize the number of digestion/purification rounds needed for each specific cell line, DNA concentration should be measured by Qubit before and after each round of digestion/purification. The concentration will stop decreasing after a certain number of digestion/purification rounds, indicating that the contaminating linear DNA has been successfully removed.

4. Inverse PCR to detect specific eccDNA using an outward-directed primer set
 - a. Perform PCR with primers that target the junction sequence of the eccDNA using the KOD Hot-Start PCR Kit.
 - b. Add 25 μ L Xtreme buffer, 10 μ L dNTPs (2 μ M each), 1.5 μ L each primer (10 pmol/ μ L), 1 μ L KOD Xtreme Hot-Start Polymerase, 200 ng purified DNA, and enough ddH₂O for the final solution to be 50 μ L.
 - c. PCR amplification using a PCR machine with heated lid (lid set to 105°C):
Step 1. 94°C, 2 min
Step 2. 98°C, 10 s
Step 3. 68°C, 1 min/kb
(Repeat Step 2-3 for a total of 30 cycles)
 - d. The PCR product can then be visualized on an agarose gel and sequenced by Sanger sequencing with the primers used for PCR amplification (Figure 4).

C. Metaphase spread and FISH detection of specific circular DNAs

1. Prepare the cells for metaphase spread
 - a. Seed 5×10^5 cells in each of five 100 mm Petri dishes 24 h before thymidine block.

Note: Starting cell number is important to get enough mitotic cells for eccDNA detection.

- b. Add 100 mM thymidine solution to a final concentration of 2 mM to each of the 100 mm plates for 16 h. Release cells for 9 h by replacing regular medium without thymidine solution. Repeat another thymidine block (2 mM final concentration, 16 h) to arrest the cells at the G1-S boundary and release cells for 3 h in regular medium.
 - c. Add 0.1 μ g/mL final concentration Colcemid for 9 h to collect the mitotic cells.

Note: Check cells under a microscope to confirm the round shaped mitotic cells.

- d. Gently shake off the floating mitotic cells from the culture dish and collect into a 15-mL Falcon tube by centrifuging at 300 \times g for 5 min, and wash the pellet twice with cold PBS.

Note: Mitotic cells are fragile, so it is very important to use a low speed during centrifugation.

- e. Gently resuspend the pellet in 5 mL 75 mM KCl Hypotonic Solution and incubate at 37°C in a water bath for 30 min. Invert the tube gently every 10 min to ensure the cells are in suspension. Add 1 mL Carnoy's Fixative Solution to the cell suspension dropwise using a 1,000 µL pipette tip and mix by inverting the tube slowly to keep the metaphase chromosome intact.

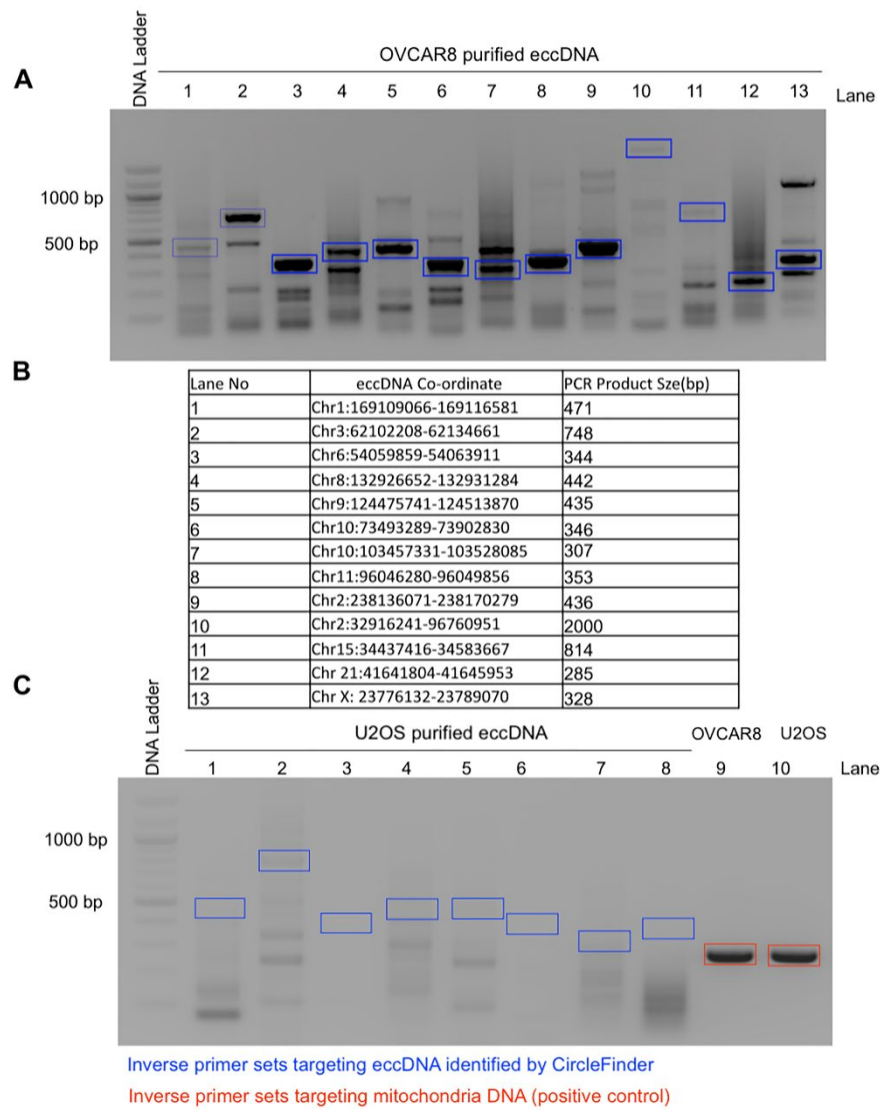


Figure 4. Representative eccDNA identified from the ATAC-seq library and validated by inverse PCR in OVCAR8 cells.

A. EccDNAs were amplified using inverse PCR primers (shown in blue boxes), gel purified, and validated for the presence of junctional sequences by Sanger sequencing. Example Sanger sequencing results can be found in Figure 3D of the original manuscript (Kumar *et al.*, 2020). B. The table represents the distribution of eccDNA on different chromosomes with coordinates and their expected PCR product size; the numbers represent the different lanes on the gel. C. As a negative control, the same inverse PCR primers were used on purified eccDNAs from U2OS cells (lanes 1-8). As a positive control, inverse PCR primers against mitochondrial DNA were used on eccDNAs (lanes 9-10).

- f. Centrifuge cells at 300 × g for 5 min and carefully aspirate most of the KCl solution, leaving about 300 µL. Resuspend cell pellet by gently tapping on the tube.

- g. Fix the resuspended cells by adding 5 mL ice-cold Carnoy's Fixative Solution dropwise using a 1,000 μ L pipette tip and invert the tube slowly to mix the cells.

Note: It is important to invert the tube slowly to avoid fragmentation of the mitotic chromosomes.

Note: At this stage, fixed cells can be stored at 4°C for several months.

- h. Centrifuge the cells at $300 \times g$ for 5 min and resuspend the pellet gently in 1-2 mL Carnoy's Fixative Solution.
- i. Humidify the glass slides, putting on a box at 55°C by slanting at a 45-degree angle, and add several drops of fixative cell suspension from 15-20 cm above the slides.

Note: It is very important to humidify the glass slides for proper disruption of the nuclear membrane and also to drop the fixative cell suspension from the above-mentioned height for proper spreading of the mitotic chromosomes.

- j. Dry the slides at room temperature away from light and stain with VectaShield Mounting Medium containing DAPI to view the mitotic chromosome spread under a microscope. The dry slides containing the mitotic spreads can be stored at 4°C for several months.

2. Denaturation of slides containing metaphase DNA

- a. Pre-warm 100 mL FISH Denaturation Buffer at 73°C for 5 min.
- b. Immerse the glass slides containing metaphase spread in a Coplin jar containing pre-warmed FISH Denaturation Buffer for 5 min.
- c. Immerse the slides in a Coplin jar containing 1× PBS, pH 7.4 for 5 min.
- d. Dehydrate the slides serially by immersing the slides in 70%, 85%, and 100% ethanol for 2 min each.
- e. Air dry the slides until all the ethanol has evaporated.

3. Probe denaturation and hybridization

Note: It is important to keep the FISH probe protected from light. Aluminium foil is used to cover the slides or hybridization chamber.

- a. Denature the FISH probe in Hybridization Buffer (19 μ L Hybridization Buffer + 1 μ L labeled probe) at 73°C for 5 min and immediately chill on ice.

- b. Apply the probe mixture onto the previously prepared, air-dried metaphase spread slide and cover with a coverslip. Seal the coverslip with rubber cement and place the slides in the humidified box and hybridize at 37°C in the hybridization chamber overnight. Parafilm is used to ensure sealing of the humidified box.

- c. After hybridization, immerse the slides in 1× PBS and remove the rubber cement and coverslip gently.

- d. Wash the slides in a Coplin jar with pre-warmed FISH Wash Buffer 1 at 73°C for 5 min.

- e. Wash the slides with FISH Wash Buffer 2 at room temperature for 5 min.

- f. Air dry the slides in the dark at room temperature, mount with VectorShield DAPI medium, and seal with nail polish.

4. Image and data analysis

Capture the images under a confocal microscope with a 63 \times oil-immersion objective. Set the laser power to output 40% and acquire the image with the full region of interest (512 \times 512) at 300 ms exposure times. For the detection of eccDNA, OVCAR8 (experimental cell line) and C4-2 (negative control cell line where we do not see any extrachromosomal signal) were probed against the eccDNA locus Chr2:238136071-238170279 or Chr10:103457331-103528085 (Figure 5). Potential eccDNA signals (indicated by the red arrows) are located off the main chromosomes, while the chromosomal signals overlap with the main chromosomes and usually appear as doublet signals (indicated by the yellow arrows).

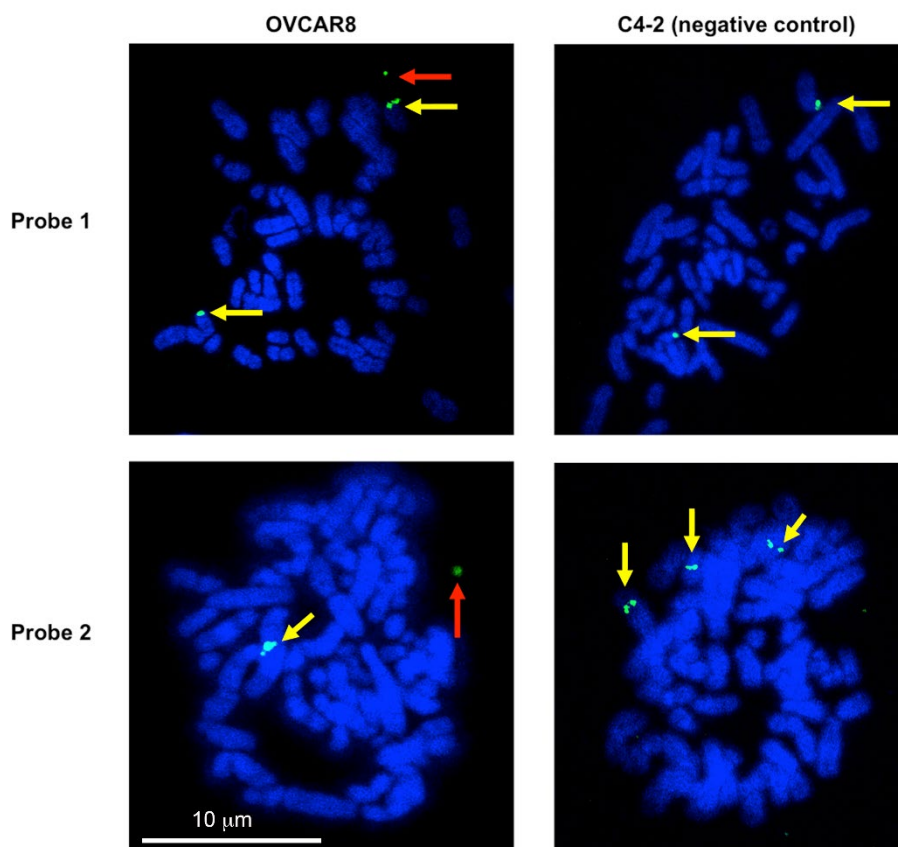


Figure 5. Validation of eccDNA in OVCAR8 cells by metaphase FISH.

Metaphase spread of the chromosomes was carried out and the eccDNAs were identified by FISH. A representative eccDNA locus Chr2:238136071-238170279 (top row – probe 1) or Chr10:103457331-103528085 (bottom row – probe 2) was identified from OVCAR8 ATAC-seq and used for specific BAC probe design. The metaphase spreads from C4-2B cells on the left show no extrachromosomal circular DNA (negative control), while the spreads from OVCAR8 cells on the right confirm the presence of an extrachromosomal eccDNA signal (green: BAC probe, blue: DAPI). The red arrow indicates the eccDNA signals (which can be a singlet or a doublet due to replication of the eccDNA). The yellow arrows mark chromosomal DNA signals (which is usually a doublet but can be a singlet because the signal is seen from only a single chromatid).

Data analysis

1. The OVCAR8 and C4-2B ATAC-seq data has been deposited in Gene Expression Omnibus (accession: GSE145409). Following the Circle-finder algorithm, the identified eccDNA coordinates output can be found in the Supplementary File under the same GEO accession. Hundreds of potential eccDNAs were identified from this dataset, including small circles of less than 1 kb and large circles of 400 kb encompassing several genes [refer to Figure 3 in the original manuscript (Kumar *et al.*, 2020)].
2. To validate the potential eccDNAs, PCR-based validation was used for 11 eccDNAs from OVCAR8 and 6 eccDNAs from C4-2B. The primer is designed based on the junctional sequence identified from ATAC-seq and will specifically amplify eccDNA but not the genomic DNA (unless tandem duplication). In total, 13 out of 17 eccDNAs were validated by this method [refer to Figure 3 in the original manuscript (Kumar *et al.*, 2020)].
3. FISH on metaphase spreads can be used to visually validate the presence of selective eccDNAs, but preferentially with large circles. Here, we were able to detect FISH signals off chromosomes corresponding to

34-kb and 71-kb eccDNAs in OVCAR8 cells (Figure 5). To understand the general distribution of eccDNA signals in a cell population, we counted eccDNA FISH signals in more than 20 cells and found a distribution between 0 and 4 eccDNA FISH signals in each cell examined [refer to Figure 4 in the original manuscript (Kumar *et al.*, 2020)].

Recipes

1. 1% (10 mg/mL) Digitonin

40 µL 20 mg/mL digitonin stock solution in DMSO
40 µL ddH₂O
Store at -20°C as aliquots, stable for 6 months

2. ATAC-Resuspension Buffer (ATAC-RSB) (50 mL)

500 µL 1 M Tris-HCl, pH 7.4 (10 mM final concentration)
100 µL 5 M NaCl (10 mM final concentration)
150 µL 1 M MgCl₂ (3 mM final concentration)
49.25 mL ddH₂O

3. ATAC-Lysis Buffer (ATAC-LB) (500 µL for 8 reactions)

5 µL 10% Nonidet P40 substitute (0.1% final concentration)
5 µL 10% Tween-20 (0.1% final concentration)
5 µL 1% digitonin (0.01% final concentration)
485 µL ATAC-RSB
Prepare fresh, keep on ice

4. ATAC-Wash Buffer (ATAC-WB) (10 mL for 8 reactions)

100 µL 10% Tween-20 (0.1% final concentration)
9.9 mL ATAC-RSB
Prepare fresh, keep on ice

5. ATAC-Reaction Mastermix (ATAC-RM) (450 µL for 8 reactions)

225 µL 2× TDB buffer (from Nextera kit, 25 µL per reaction)
22.5 µL TDE transposase (from Nextera kit, 2.5 µL per reaction)
148.5 µL DPBS
4.5 µL 1% Digitonin (0.01% final concentration)
4.5 µL 10% Tween-20 (0.1% final concentration)
45 µL H₂O
Prepare fresh, keep on ice

6. 100 mM Thymidine Solution

Dissolve 242 mg thymidine powder in 10 mL cell culture grade water and filter through a 0.2-µm filter

7. 75 mM KCl Hypotonic Solution

Dissolve 559 mg KCl in 100 mL cell culture grade water and filter through a 0.2-µm filter

8. Carnoy's Fixative Solution

Add 75 mL methanol to 25 mL glacial acetic acid (v/v) to make 100 mL fixative solution
Prepare under a chemical fume hood

9. 20× SSC Buffer

Mix 87.5 g NaCl and 44.1 g sodium citrate in 400 mL water and adjust the pH with a few drops of 12 N hydrochloric acid to pH 7.0
Adjust the volume with water to 500 mL and filter through a 0.2-μm filter

10. Hybridization Buffer

10 mL 20× SSC buffer pH 7.0
50 mL 100% formamide solution
10 g dextran sulfate
Adjust volume to 100 mL with water
Prepare under chemical fume hood

11. FISH Denaturation Buffer

70 mL 100% formamide solution
10 mL 20× SSC buffer
20 mL sterile water
Prepare under chemical fume hood

12. FISH Wash Buffer 1

2 mL 20× SSC buffer
3 mL 10% NP-40
95 mL water

13. FISH Wash Buffer 2

10 mL 20× SSC buffer
1 mL 10% NP-40
89 mL water

Acknowledgments

This work was supported by R01 CA060499 and P30 CA044579 to AD and Cancer Training Grant support from T32 CA009109 (PI: Amy Bouton) to TP. We thank all members of the Dutta Lab for many helpful discussions.

Competing interests

The authors declare no competing interests.

References

- Buenrostro, J. D., Giresi, P. G., Zaba, L. C., Chang, H. Y. and Greenleaf, W. J. (2013). [Transposition of native chromatin for fast and sensitive epigenomic profiling of open chromatin, DNA-binding proteins and nucleosome position](#). *Nat Methods* 10(12): 1213-1218.
- Buenrostro, J. D., Wu, B., Chang, H. Y. and Greenleaf, W. J. (2015). [ATAC-seq: A Method for Assaying Chromatin Accessibility Genome-Wide](#). *Curr Protoc Mol Biol* 109: 21 29 21-21 29 29.
- Corces, M. R., Mumbach, M. R., Greenleaf, W. J., Montine, T. J., Khavari, P. A., Kundaje, A., Risca, V. I., Orloff, L. A., Kasowski, M., Carter, A. C., Cho, S. W., Trevino, A. E., Kathiria, A., Wu, B., Montine, K. S., Rubin, A. J., Satpathy, A. T., Vesuna, S., Sinnott-Armstrong, N. A., Greenside, P. G., Hamilton, E. G. and Chang, H. Y.

- (2017). [Omni-ATAC-seq: Improved ATAC-seq protocol](#). *Protocol Exchange* 10.1038/protex.2017.096.
- Dillon, L. W., Kumar, P., Shibata, Y., Wang, Y. H., Willcox, S., Griffith, J. D., Pommier, Y., Takeda, S. and Dutta, A. (2015). [Production of Extrachromosomal MicroDNAs Is Linked to Mismatch Repair Pathways and Transcriptional Activity](#). *Cell Rep* 11(11): 1749-1759.
- Gresham, D., Usaite, R., Germann, S. M., Lisby, M., Botstein, D. and Regenberg, B. (2010). [Adaptation to diverse nitrogen-limited environments by deletion or extrachromosomal element formation of the GAP1 locus](#). *Proc Natl Acad Sci U S A* 107(43): 18551-18556.
- Hull, R. M., King, M., Pizza, G., Krueger, F., Vergara, X. and Houseley, J. (2019). [Transcription-induced formation of extrachromosomal DNA during yeast ageing](#). *PLoS Biol* 17(12): e3000471.
- Kim, H., Nguyen, N. P., Turner, K., Wu, S., Gujar, A. D., Luebeck, J., Liu, J., Deshpande, V., Rajkumar, U., Namburi, S., Amin, S. B., Yi, E., Menghi, F., Schulte, J. H., Henssen, A. G., Chang, H. Y., Beck, C. R., Mischel, P. S., Bafna, V. and Verhaak, R. G. W. (2020). [Extrachromosomal DNA is associated with oncogene amplification and poor outcome across multiple cancers](#). *Nat Genet* 52(9):891-897.
- Koche, R. P., Rodriguez-Fos, E., Helmsauer, K., Burkert, M., MacArthur, I. C., Maag, J., Chamorro, R., Munoz-Perez, N., Puiggros, M., Dorado Garcia, H., Bei, Y., Roefzaad, C., Bardinet, V., Szymansky, A., Winkler, A., Thole, T., Timme, N., Kasack, K., Fuchs, S., Klironomos, F., Thiessen, N., Blanc, E., Schmelz, K., Kunkele, A., Hundsorfer, P., Rosswog, C., Theissen, J., Beule, D., Deubzer, H., Sauer, S., Toedling, J., Fischer, M., Hertwig, F., Schwarz, R. F., Eggert, A., Torrents, D., Schulte, J. H. and Henssen, A. G. (2020). [Extrachromosomal circular DNA drives oncogenic genome remodeling in neuroblastoma](#). *Nat Genet* 52(1): 29-34.
- Koo, D. H., Molin, W. T., Saski, C. A., Jiang, J., Putta, K., Jugulam, M., Friebel, B. and Gill, B. S. (2018). [Extrachromosomal circular DNA-based amplification and transmission of herbicide resistance in crop weed Amaranthus palmeri](#). *Proc Natl Acad Sci U S A* 115(13): 3332-3337.
- Kumar, P., Dillon, L. W., Shibata, Y., Jazaeri, A. A., Jones, D. R. and Dutta, A. (2017). [Normal and Cancerous Tissues Release Extrachromosomal Circular DNA \(eccDNA\) into the Circulation](#). *Mol Cancer Res* 15(9): 1197-1205.
- Kumar, P., Kiran, S., Saha, S., Su, Z., Paulsen, T., Chatrath, A., Shibata, Y., Shibata, E. and Dutta, A. (2020). [ATAC-seq identifies thousands of extrachromosomal circular DNA in cancer and cell lines](#). *Sci Adv* 6(20): eaba2489.
- Li, H. (2013). [Aligning sequence reads, clone sequences and assembly contigs with BWA-MEM](#). arXiv:1303.3997.
- Martin, M. (2011). [Cutadapt removes adapter sequences from high-throughput sequencing reads](#). *EMBnet J* 17: 10-12.
- Møller, H. D., Larsen, C. E., Parsons, L., Hansen, A. J., Regenberg, B. and Mourier, T. (2016). [Formation of extrachromosomal circular DNA from long terminal repeats of retrotransposons in Saccharomyces cerevisiae](#). *G3 (Bethesda)* 6(2): 453-462.
- Møller, H. D., Parsons, L., Jorgensen, T. S., Botstein, D. and Regenberg, B. (2015). [Extrachromosomal circular DNA is common in yeast](#). *Proc Natl Acad Sci U S A* 112(24): E3114-E3122.
- Morton, A. R., Dogan-Artun, N., Faber, Z. J., MacLeod, G., Bartels, C. F., Piazza, M. S., Allan, K. C., Mack, S. C., Wang, X., Gimple, R. C., Wu, Q., Rubin, B. P., Shetty, S., Angers, S., Dirks, P. B., Sallari, R. C., Lupien, M., Rich, J. N. and Scacheri, P. C. (2019). [Functional enhancers shape extrachromosomal oncogene amplifications](#). *Cell* 179(6): 1330-1341 e13.
- Paulsen, T., Kumar, P., Koseoglu, M. M. and Dutta, A. (2018). [Discoveries of extrachromosomal circles of DNA in normal and tumor cells](#). *Trends Genet* 34(4): 270-278.
- Paulsen, T., Shibata, Y., Kumar, P., Dillon, L. and Dutta, A. (2019). [Small extrachromosomal circular DNAs, microDNA, produce short regulatory RNAs that suppress gene expression independent of canonical promoters](#). *Nucleic Acids Res* 47(9): 4586-4596.
- Shibata, Y., P. Kumar, R. Layer, S. Willcox, J. R. Gagan, J. D. Griffith and A. Dutta. (2012). [extrachromosomal microDNAs and chromosomal microdeletions in normal tissues](#). *Science* 336(6077): 82-86.
- Sin, S. T. K., Jiang, P., Deng, J., Ji, L., Cheng, S. H., Dutta, A., Leung, T. Y., Chan, K. C. A., Chiu, R. W. K. and Lo, Y. M. D. (2020). [Identification and characterization of extrachromosomal circular DNA in maternal plasma](#). *Proc Natl Acad Sci U S A* 117(3): 1658-1665.

Turner, K. M., Deshpande, V., Beyter, D., Koga, T., Rusert, J., Lee, C., Li, B., Arden, K., Ren, B., Nathanson, D. A., Kornblum, H. I., Taylor, M. D., Kaushal, S., Cavenee, W. K., Wechsler-Reya, R., Furnari, F. B., Vandenberg, S. R., Rao, P. N., Wahl, G. M., Bafna, V. and Mischel, P. S. (2017). [Extrachromosomal oncogene amplification drives tumour evolution and genetic heterogeneity](#). *Nature* 543(7643): 122-125.

Surface Engineering and Multimodal Imaging of Multistage Delivery Vectors in Metastatic Breast Cancer

Shreya Goel^{1,§, *}, Mauro Ferrari^{1,2, *} and Haifa Shen^{1, *}

¹Department of Nanomedicine, Houston Methodist Research Institute, Houston, Texas, USA

²Department of Pharmaceutics, School of Pharmacy, University of Washington, Seattle, Washington, USA

§Present address: Department of Cancer Systems Imaging, MD Anderson Cancer Center, Houston, Texas, USA

*For correspondence: hshen@houstonmethodist.org; shreya.goel.shreya@gmail.com; drmaurof@gmail.com

Abstract

The design of effective nanoformulations that target metastatic breast cancers is challenging due to a lack of competent imaging and image analysis protocols that can capture the interactions between the injected nanoparticles and metastatic lesions. Here, we describe the integration of *in vivo* whole-body PET-CT with high temporal resolution, *ex vivo* whole-organ optical imaging and high spatial resolution confocal microscopy to deconstruct the trafficking of injectable nanoparticle generators encapsulated with polymeric doxorubicin (iNPG-pDox) in pulmonary metastases of triple-negative breast cancer. We describe the details of image acquisition and analysis in a step-wise manner along with the development of a mouse model for metastatic breast cancer. The methods described herein can be easily adapted to any nanoparticle or disease model, allowing a standardized pipeline for *in vivo* preclinical studies that focus on delineating nanoparticle kinetics and interactions within metastases.

Keywords: *In vivo* imaging, Positron emission tomography, Optical imaging, Cancer, Metastasis, Mouse models

This protocol was validated in: SCIENCE ADVANCES (2020) DOI: 10.1126/sciadv.aba4498.

Background

Metastatic cancer accounts for >90% of mortality in cancer patients; yet, effective therapeutic strategies are missing due to the small size, heterogeneity, and dispersed nature of metastatic cancers (Bianchini *et al.*, 2016; Elia *et al.*, 2019). A series of biological barriers hinder the accumulation, and hence, the efficacy of conventional small molecule drugs and nanoparticle-based delivery systems in metastatic cancers (Blanco *et al.*, 2015). Our group has previously demonstrated the sequential and successful negotiation of most, if not all, biological barriers using iNPG-pDox composed of porous silicon microparticle-based injectable nanoparticle generators (iNPG) packaged with poly(lactic-co-glycolic acid) polymer-doxorubicin (pDox) conjugates (Xu *et al.*, 2016). pDox molecules self-assemble into nanoparticles after their release from iNPGs, and iNPG-pDox treatment significantly inhibited tumor metastasis, including a functional cure in 40-50% of mice with pulmonary metastatic breast cancer (Xu *et al.*, 2016). Visualization of the spatiotemporal kinetics of such nanomedicines that effectively target metastases can allow the directed development and rational improvement of other advanced therapies in the future (Goel, 2017).

Despite significant progress in the development of drug delivery systems, limited studies have evaluated the distribution and interactions of such systems in *in vivo* metastatic settings. Molecular imaging modalities can uncover a wealth of information across multiple length- and time-scales in disease settings; however, the application of rationally combined multiscale imaging methods to assess the biodistribution of complex drug delivery systems in metastatic tumors remains to be performed (Goel, 2017). Such knowledge, in conjunction with mathematical modeling approaches, can predict and evaluate therapeutic responses and efficacies of complex drug delivery systems, eventually being employed to guide the reverse engineering of advanced therapies (Michor, 2011). In this protocol, we provide a detailed guide to designing and implementing a multiscale and multimodal imaging toolkit for the systematic deconstruction of the trafficking and interactions of nanotherapeutics in a metastatic model of breast cancer, as described in our earlier work (Goel *et al.*, 2020).

We first designed a modular orthogonal surface engineering approach for the modification of iNPG-pDox to render them amenable to multimodal imaging (both nuclear and fluorescence imaging) and microscopy without affecting their intrinsic biophysical properties. Such an approach is independent of carrier type, cargo, formulation method, or delivery route, and can be adopted for any nano- or bioengineered platform and implemented in any disease model. Next, we designed and implemented a systematic imaging toolkit composed of: (1) positron emission tomography/computed tomography (PET/CT) for longitudinal *in vivo* whole-body imaging at a high spatiotemporal resolution; (2) multispectral optical imaging (OI) for *ex vivo* whole-organ imaging of metastatic lungs; and (3) multispectral confocal microscopy for intra-tissue imaging of iNPG-pDox distribution in metastatic lungs with high spatial resolution (Goel *et al.*, 2020). This protocol includes methods for each of the approaches described above.

Materials and Reagents

1. T-75 cell culture flasks
2. Serological pipettes (Thermo Fisher Scientific, catalog numbers: 13-676-10F and 13-676-10M)
3. FalconTM conical centrifuge tubes (Thermo Fisher Scientific, catalog number: 14-959-53A)
4. 1 cc Exel insulin syringes (28 G, 1 ml, Fisher, catalog number: 14-841-31)
5. BD 1 ml insulin syringe with slip tip (Fisher, catalog number: 22-253-260)
6. Sterile filter pipette tips
7. EppendorfTM tubes (various sizes)
8. Coverslips
9. 31 G disposable insulin syringes (BD, catalog number: 324921)
10. ParafilmTM M PM996 all-purpose laboratory film
11. MilliporeSigmaTM silica gel 60G TLC plates, glass-backed (MilliporeSigma, Catalog number: 1.00384.0001)
12. 26 G × ¾" mouse and rat tail vein Monoject IV catheter (Patterson Veterinary, catalog number: 07-836-8403)
13. BalB/c mice: Female, 4-6 weeks old (Invigo or The Jackson Laboratory) or another strain suitable for the selected cancer cell line

14. Murine triple-negative breast cancer cell line expressing luciferase: 4T1-GFP-Luc (ATCC) or another cancer cell line
15. Discoidal porous silicon particles (iNPG) and pDox nanoparticles (prepared in-house) or another amine-modified nanoparticle of choice (Xu *et al.*, 2016)
16. 2-S-(4-isothiocyanatobenzyl)-1,4,7-triazacyclononane-1,4,7-triacetic acid (p-SC-Bn-NOTA) (Macrocylics, Dallas, ID: B-605)
17. 0.9% sodium chloride injection USP, 100 ml fill in 150 ml PAB® (B. Braun, NDC number: 00264-1800-32)
18. Sterile de-ionized water
19. Phosphate-buffered saline (PBS) solution, pH 7.4 (Thermo Fisher Scientific, catalog number: 10010023)
20. 100 ml filter-sterilized 50 mM EDTA solution
21. N,N'-dimethylformamide (DMF; MiliporeSigma, catalog number: 227056-100ML)
22. Dimethyl sulfoxide (DMSO; MiliporeSigma, catalog number: 317275-100ML)
23. Diisopropylethylamine (MiliporeSigma, catalog number: 387649-100ML)
24. Isopropanol
25. 0.1 M sodium acetate solution
26. 0.1 M HCl solution
27. Copper-64 (⁶⁴Cu; Washington University St. Louis)
28. AlexaFluor™ 647 NHS ester (Thermo Fisher, catalog number: A20006)
29. Mouse serum (MiliporeSigma, catalog number: M5905-5ML)
30. OCT freezing compound (Tissue-Tek® O.C.T. Compound, Sakura® Finetek; VWR, catalog number: 25608-930)
31. Tissue-Tek® Cryomold® molds/adapters (Sakura® Finetek)
32. 4',6-diamidino-2-phenylindole (DAPI; Thermo Scientific, prepared according to vendor instructions; catalog number: 62247)
33. ProLong™ Gold Antifade Mountant (ProLong, catalog number: P36930)
34. RPMI-1640 medium (ATCC, catalog number: ATCC® 30-2001TM)
35. Fetal bovine serum (FBS) (GibcoTM, catalog number: 10-082-147)
36. Pencillin-streptomycin antibiotics (GibcoTM, catalog number: 15-640-055)
37. Isoflurane (MiliporeSigma, catalog number: Y0000858)
38. Aluminium stubs (PELCO® pin mount starter kit; PELCO, catalog number: 76250-10)
39. Recombinant Anti-CD31 antibody [EPR17260-263] (Abcam, catalog number: ab222783)
40. Goat anti-rabbit IgG H&L (FITC) (Abcam, catalog number: ab6717)
41. Complete culture medium (see Recipes)
42. 50 mM EDTA solution (see Recipes)

Equipment

1. Inveon™ PET/CT (Siemens Medical Inc., INVEON, catalog number: 138757)
2. IVIS® Spectrum *In vivo* Imaging System (PerkinElmer, catalog number: 124262)
3. Bioscan AR-2000 Radio-TLC Imaging Scanner (Eckert & Ziegler, Valencia, CA)
4. Scanning electron microscope (Nova NanoSEM 230, Thermo Fisher Scientific, USA)
5. Zetasizer Nano ZS (Malvern Instruments Ltd., Worcestershire, UK)
6. Ultraviolet-visible-NIR spectrophotometer (Synergy H4 Hybrid, BioTek, USA)
7. Wizard² 2-Detector Gamma Counter (PerkinElmer, catalog number: 2470-0020)
8. EVOS Auto FL System (Thermo Fisher Scientific, USA)
9. Nikon Eclipse Ti microscope
10. Centrifuge (Beckman Coulter, model: Avanti® J-26 XPI, catalog number: 393127)
11. Tissue culture incubator (Sanyo Scientific, catalog number: 133060)
12. Biological safety cabinet (The Baker company, SterilGARD, catalog number: 101951)
13. Fisherbrand™ Isotemp™ Hot Plate Stirrer, Ambient to 540°C, Ceramic (Fisherbrand, catalog number: SP88854200)

14. PCR thermal cycler (Bio-Rad Laboratories, model: T100TM, catalog number: 1861096)
15. Braintree Scientific Diversity Partner Mouse Tail Illuminator Restrainer (Fisher, catalog number: NC0772753)
16. SimportTM Scientific StainTrayTM Slide Staining System (Fisher, catalog number: 22-045-035)

Software

1. Inveon Research Workplace (INVEON, Siemens)
2. Living Image Software (PerkinElmer)
3. Nikon Elements software (Nikon)
4. FIJI (NIH)
5. Microsoft Office Suite
6. GraphPad Prism

Procedure

A. Animal models for pulmonary metastasis of triple-negative breast cancer

1. Grow and expand the cells according to the recommended conditions. Typically, 4T1-GFP-Luc cells are cultured in RPMI-1640 medium supplemented with 10% FBS and 1% Penicillin-streptomycin.
2. Harvest cells while in the exponential growth phase (approximately 80-90% confluence) using trypsin or an appropriate enzyme for the specific cell line. Resuspend cells in medium containing serum.
3. Count cells.
4. Centrifuge cells at 225 × g, 4°C for 5 min. Resuspend cells in 1× PBS to a concentration of 1 × 10⁵ cells/200 μL.
5. Place cells on ice and transport to the vivarium.
6. Restrain the mouse in a restrainer and position the tail such that the vein is facing upwards.
7. Draw 200 μL cells into a 28 G disposable insulin syringe and gently inject into the tail vein. The contents of the needle should inject easily without resistance.
8. Monitor tumor development regularly via bioluminescence imaging. Typically, 4T1-Luc cells take 10 days to develop lung metastases.

B. Surface modification of iNPG-pDox or other amine-modified nano/microparticles

1. For details of the structure of iNPG-pDox vectors and chemistry, readers are referred to the following references (Goel *et al.*, 2020; Xu *et al.*, 2016).
2. Dissolve 3 × 10⁹ amine-modified iNPG (or other nanoparticles of choice) in 0.5 ml DMF in a 1.5-ml EppendorfTM tube. Shake gently.
3. Dissolve 0.8 mg p-SCN-Bn-NOTA in 0.5 ml DMSO and add to the iNPG solution.
4. Sonicate the mixture until a homogenous solution is formed.
5. Add 20 μl diisopropylethylamine and incubate the reaction mixture at 25°C for 4 h under vigorous shaking at 700 rpm. This step can be performed on a hot plate stirrer or in a thermal cycler.
6. After the 4-h incubation, wash the iNPG-NOTA conjugates by centrifugation at 5,000 rpm for 5 min with DMSO as the solvent. Briefly, spin the conjugates down, carefully discard the supernatant and resuspend the pelleted nanoparticles in 0.5 ml DMSO by sonication. Repeat the wash step with DMSO (for a total of 2 times), followed by 0.5 ml isopropanol (one time) and 0.5 ml DI water (one time). The speed and time of the centrifugation can be adjusted according to the nanoparticles used.
7. After the final wash step, resuspend the iNPG-NOTA pellet in DI water and freeze at -80°C or freeze-dry (depending on the nanoparticle used) for further use (for up to 1 week).
8. Use the same process to obtain iNPG-AF647 by conjugating fluorescent dyes (*e.g.*, AlexaFluorTM 647

NHS ester) for optical imaging.

C. Radiolabeling of iNPG-NOTA

1. Resuspend iNPG-NOTA in 0.5 mL 0.1 M sodium acetate solution.
2. Adjust the pH of the solution to 5.5 using 0.1 M HCl.
3. Add 37 MBq $^{64}\text{CuCl}_2$ to the nanoparticle solution. All handling of radioisotopes and radiolabeled solutions should be performed behind a lead shield in a fume hood, in accordance with institutional radiosafety guidelines.
4. Carefully wrap parafilm around the cap and incubate the tube at 37°C for 1 h with gentle shaking. This step should be performed in a thermal cycler or on a hot plate stirrer behind a protective lead shield.
5. Remove the excess unchelated ^{64}Cu by centrifugation at $\sim 1,610 \times g$ for 5 min. Wash twice with DI water to obtain the final radiolabeled constructs ($[^{64}\text{Cu}]$ NOTA-iNPG). All radioactive waste should be appropriately discarded.
6. To calculate radiolabeling yield, radio thin-layer chromatography (radio TLC) is performed (Figure 1). Briefly, drop 2 μL $[^{64}\text{Cu}]$ NOTA-iNPG on one end (origin) of a silica gel TLC plate. Dip the strip vertically in 2 mL 50 mM EDTA solution in a 50-mL conical tube.

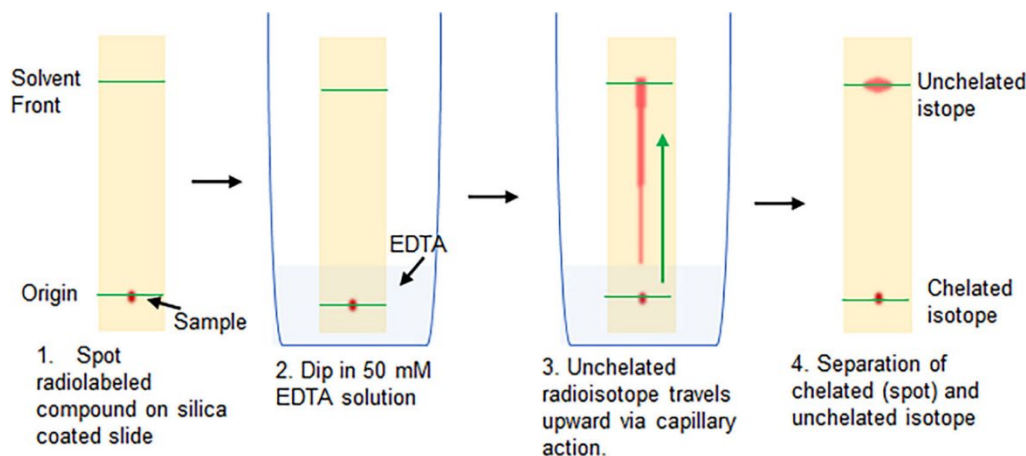


Figure 1. Schematic of the radio TLC procedure to calculate radiolabeling yield

7. The solution will slowly travel upward by capillary action. Once the solution has moved 2–4 cm upward (or 1 cm from the top of the strip; solvent front), remove the strip from the EDTA solution and allow to dry.
8. Scan the strip on a Bioscan AR-2000 RadiobTLC Imaging Scanner according to the vendor's instructions.
9. Typical radiolabeling yields using with this procedure range from 50% to 70%, with >99% radiochemical purity.

D. Loading pDox into $[^{64}\text{Cu}]$ NOTA-iNPG or iNPG-AF647

1. Suspend 3 mg polymeric pDox monomers in DMSO (70 mg/ml) and add the solution to the $[^{64}\text{Cu}]$ NOTA-iNPG or iNPG-AF647 conjugates.
2. Incubate the mixture for 3 h at room temperature with vigorous shaking. This step can be performed in a thermal cycler.
3. Remove unloaded pDox polymers by washing twice with DI water using centrifugation, as described in B above, to obtain the final constructs: $[^{64}\text{Cu}]$ NOTA-iNPG-pDox for PET/CT imaging and iNPG-AF647-pDox for optical imaging and confocal microscopy. Resuspend the final conjugates in 1 mL PBS.
4. Draw 200 μL $[^{64}\text{Cu}]$ NOTA-iNPG-pDox (~60-80 μCi per mouse) solution into a 1-mL syringe for

injections in the next step.

E. Small animal PET/CT imaging

1. Anesthetize 4T1 tumor-bearing mice under 2% isoflurane (in 100% O₂ gas).
2. Transfer each mouse to a mouse restrainer, carefully placing the nose cone to maintain anesthesia.
3. Insert the micro-catheter into the tail vein and flush with 50 µl PBS. Leave the syringe with PBS attached to the catheter.
4. Secure the mouse onto the microPET/CT scanner bed under 2% isoflurane anesthesia administered via the nose cone manifold. To minimize movement, the limbs can be secured to the side of the bed with tape.
5. Switch the PBS syringe in the catheter with the syringe containing [⁶⁴Cu]NOTA-iNPG-pDox.
6. Acquire a whole-body CT calibration image of the mouse.
7. The PET/CT acquisition protocol will depend on the particular experiment and the requirements of the researcher.
8. For dynamic PET scans, a 30-min dynamic PET mode, data are acquired using the 3D-OSEM iterative algorithm with a 256 × 256 × 256 voxel volume.
9. Immediately after the dynamic PET scan is started, slowly inject the radiolabeled nanoparticle solution as a single bolus dose over 30 s.
10. Continue the dynamic PET acquisition.
11. If PET images are required at more time points, data are acquired using the standard 3D PET acquisition protocol. To account for radioactive decay, longer scan times may be necessary.
12. Datasets are acquired as: standard static 3D PET reconstruction and dynamic 3D PET reconstruction with 6 × 300 s frames. CT attenuation correction is applied to all PET images.

F. Ex vivo gamma counting

1. When the PET/CT scans are at the final time point, euthanize the animal according to institutional protocols.
2. Harvest and weigh the major organs including the tumor-bearing lungs.
3. Radioactivity in the organs is measured using a gamma counter per the manufacturer's instructions.

G. Ex vivo whole-organ optical imaging

1. In a separate cohort of 4T1-tumor bearing mice, inject 200 µl iNPG-AF647-pDox prepared in section D via the tail vein (described in section A).
2. At the desired time point post-injection, euthanize the mouse according to institutional protocols.
3. Harvest the lungs and place on a black sheet in the IVIS Spectrum Scanner.
4. Acquire multiplexed *ex vivo* fluorescence images using the vendor's preset filter sets encompassing the excitation and emission spectra for GFP (tumor), doxorubicin (pDox), and AF647. For this combination of fluorophores, 18 filter sets are automatically selected when using the IVIS Spectrum system.
5. Set the field of view, acquisition time, and binning number. Data acquisition settings will vary from user to user but should be kept constant throughout the experimental study.
6. After image acquisition, rinse the tissues in PBS, preserve in OCT compound in cryomolds, and store at -80°C for sectioning.

H. Immunofluorescence microscopy

1. Cryo-section the frozen tissues into 6-µm-thick sections using a cryotome.
2. Incubate the sectioned tissues in cold acetone for 10 min. All steps for staining and incubation in this section should be performed in a staining tray or similarly fashioned light-blocking device.

3. Prepare the blocking solution as follows: Mix horse and goat serum at a 1:1 v/v ratio and add 0.1% (by volume) Triton X-100.
Note: The choice (species) of blocking serum depends on the host of the primary and secondary antibodies used for staining.
4. Add 100 µL blocking solution per tissue section. Incubate at 4°C for 1 h.
5. Prepare the solution of primary antibody for a total volume of 100 µL per tissue section. The anti-CD31 antibody can be used at a 1:200 dilution. For other primary antibodies, refer to the vendor's instructions for the suggested dilution.
6. After 1 h, gently tap the slide on its side to discard the blocking solution.
7. Add 100 µL primary antibody cocktail to each tissue section and incubate overnight at 4°C.
8. After overnight incubation, wash the tissue sections gently in PBS. For each wash, incubate the tissue section in PBS for 3 min, tap the slide on its side to drain the solution, and add fresh PBS. Repeat the wash step 3 times.
9. Prepare the secondary antibody in blocking solution at the vendor's recommended dilution. For the goat anti-rabbit-FITC secondary antibody, a 1:50 dilution is recommended.
10. Incubate the sections in secondary antibody solution for 1 h at 4°C.
11. Wash the secondary antibody with PBS as described in Step H8.
12. Add 50 µL DAPI solution to the tissue sections and incubate for 10 min.
13. Wash twice with PBS as outlined in Step H8.
14. Clean and dry the portions of the slide adjacent to the tissue, taking care not to disturb or dislodge the tissue.
15. Add a drop (or 5 µL) Gold Anti-fade Mounting Medium and gently place a coverslip on the tissue sections. Care must be taken to prevent the introduction of bubbles.
16. Dry the slide by tapping gently with Kimwipes and keep protected from light in a black box or slide cassette covered with aluminum foil. It is recommended to perform confocal microscopy within a day of staining.
17. Observe and photograph immunofluorescent slides by mounting on the stage of a confocal microscope according to the vendor's instructions, using the appropriate objectives. Typically, 10× and 40× objectives are sufficient for nanoparticle uptake studies. Take images of 5-10 fields of view per tissue section distributed over the entire section.
18. Prevent overexposure or stain bleaching of the samples. All images are acquired under identical conditions.
19. FITC and DAPI can be observed with their dedicated filter sets. To observe iNPG-AF647, use the cy5 common filter set. To observe fluorescence from pDox nanoparticles, the RFP common filter can be used.

Data analysis

A. MicroPET/CT analysis

1. PET/CT analysis varies by the user experimental system and institutional software and hardware set up. In this work, the following steps were followed:
2. Input the injected radioactivity dose, time of injection, name of isotope, and time of scan into the software.
3. Analyze the whole-body PET images of the mouse using the Inveon Workstation Software (Siemens Medical Inc.).
4. Manually draw the region-of-interest (ROI) centered around the organs of interest (e.g., lungs, liver, spleen, kidney, bone, muscle, and heart) on the co-registered PET/CT images (Figure 2). The decay-corrected radioactivity in each ROI is computed automatically by the software as the percentage of the injected dose per gram of organ (%ID/g).
5. Dynamic time-activity curves are plotted for each ROI using the dynamic 3D dataset.
6. To save images, select a coronal, axial, or sagittal view and export as .TIFF files. 3D maximum intensity

projection (MIP) reconstructions can be also obtained using the software.

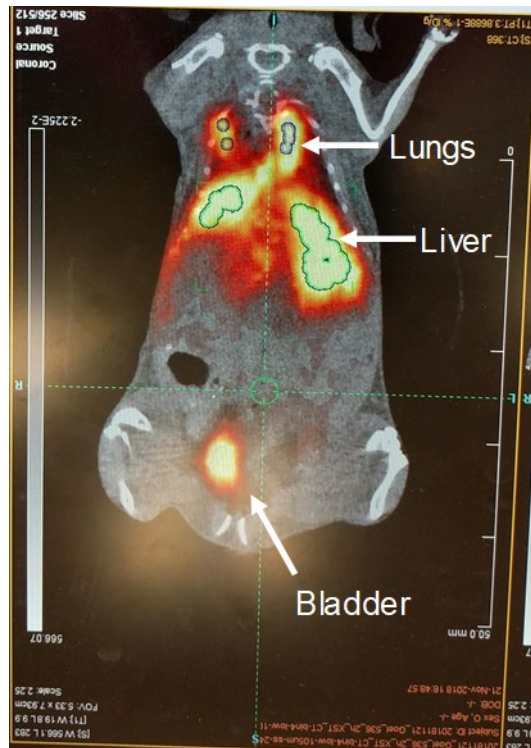


Figure 2. Example of PET image quantitation using the Inveon Workstation Software (Siemens Medical Inc.).

Coronal view of the whole-body distribution of $[^{64}\text{Cu}]$ NOTA-iNPG-pDox in a mouse bearing lung 4T1 lung metastases. White arrows depict the different organs, while ROI outlines are shown in green.

B. Optical imaging analysis

1. Analysis of multiplexed optical imaging will vary from user to user depending on the experimental and hardware/software setups. The following steps were used in this protocol.
2. Analyze the data using the LivingImageTM software (PerkinElmer).
3. Perform spectral unmixing using the automatic mode with four-component principal components analysis. Autofluorescence is subtracted from all images during analysis.
4. Draw volume- and area-matched ROIs on the spectrally unmixed images for each component (GFP for the tumor, AF647 for iNPG, and doxorubicin for pDox) (Figure 3).
5. ROIs are computed automatically and are presented as the average radiant efficiency [units: $(\text{p/s}/\text{cm}^2/\text{sr})/(\mu\text{W}/\text{cm}^2)$].
6. Pixelwise line analysis can also be performed using the software.
7. Export data as .TIFF files.

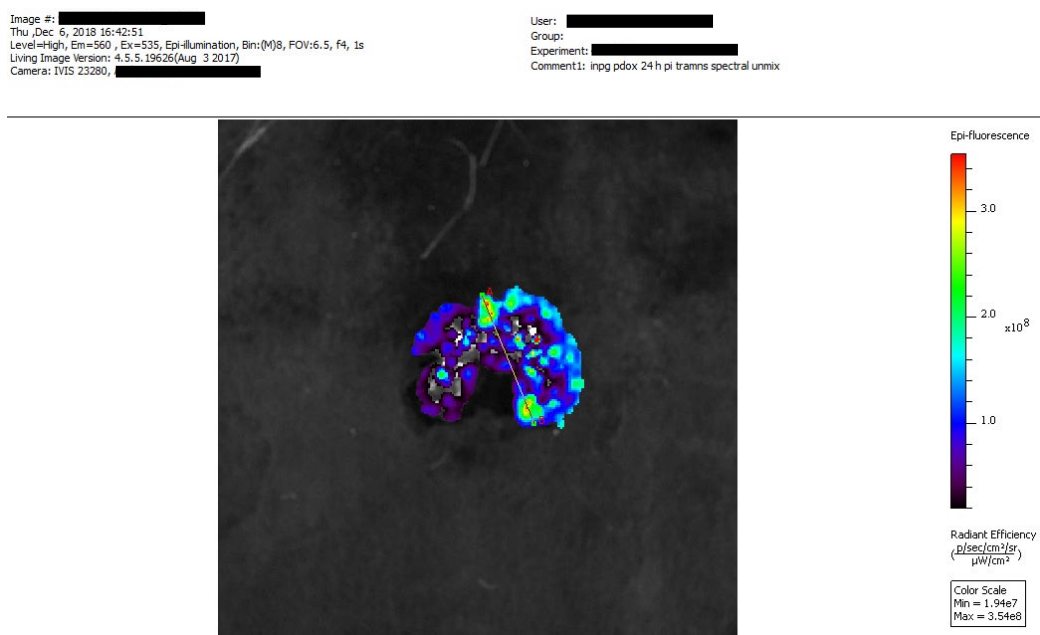


Figure 3. Example of *ex vivo* multiplexed optical imaging (IVIS® Imaging System) depicting the distribution of AF647-iNPG-pDox in 4T1 lung metastases using the PerkinElmer Living Image™ software.

Fluorescence signal from Dox (excitation: 535 nm, emission 560 nm) is shown.

C. Confocal microscopy analysis

1. In the present work, images were analyzed using the Nikon Elements (Figure 4) and FIJI software.

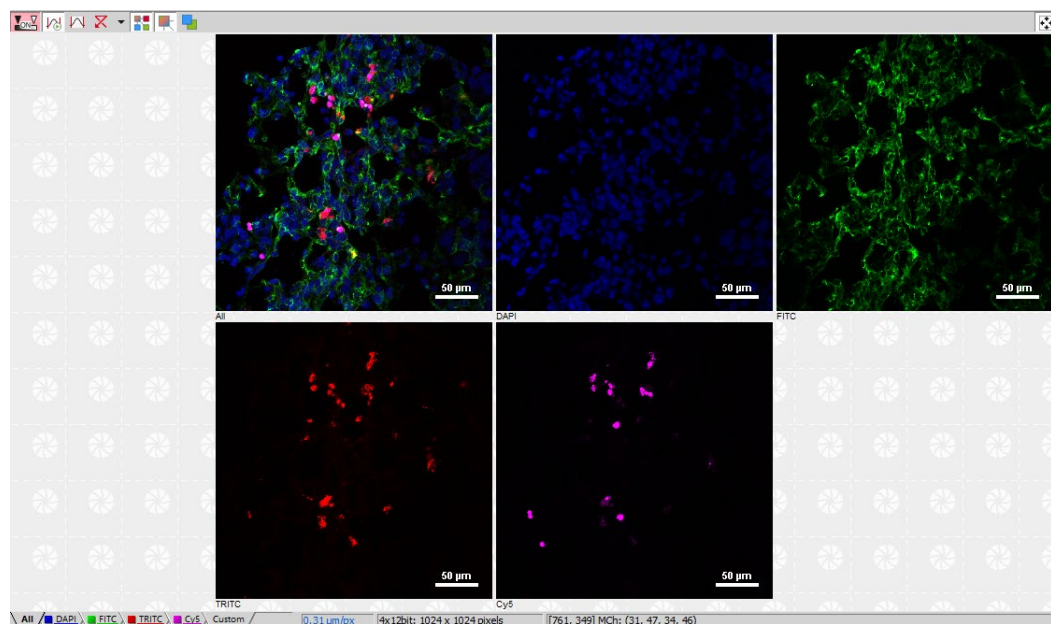


Figure 4. Example of multiplexed confocal microscopy immunofluorescence imaging analysis using the Nikon NIS-Elements™ software.

Merged (first panel) and single-channel images of DAPI (blue), blood vessels (CD31, green), AF647-

iNPG (magenta), and pDox (red) in 4T1 metastases-bearing lungs. Scale bars as shown.

2. Use constant settings for image analysis throughout the study.
3. Apply Gaussian blur and automatic thresholding to segment the images for quantitation.
4. Perform pixelwise quantitation of fluorescence intensity and area fraction coverage by drawing an ROI over the entire organ or individual tumor nodules.
5. Typically, quantitation is performed over 5 random fields of view per stain.

Recipes

1. Lysis buffer (Ingredients/1,000 mL)

500 mL RPMI 1640 Medium

50 mL 1:10 Gibco fetal bovine serum, Premium Plus

5.5 mL 1:100 Penicillin-Streptomycin (Pen/Strep) antibiotics

Notes:

- a. We recommend aliquoting FBS and Pen/Strep into 50 5.5-mL batches (sufficient to make one batch of 500 mL complete cell culture medium) to prevent repeated freezing/thawing of the components.
- b. The complete medium can be pre-prepared in advance and stored in 4°C for an extended period.
- c. We recommend warming the complete cell culture medium in a water bath at 37°C prior to use.

2. 1× neutral electrophoresis buffer 100 mL filter-sterilized 50 mM EDTA solution:

1.87 g EDTA (disodium ethylenediaminetetraacetate·2H₂O)

De-ionized water

- a. Add sterile de-ionized water to EDTA powder to a final volume of 100 mL
- b. Pass the solution through a 0.2-μm Nalgene bottle top sterile filter unit
- c. Store in 4°C for an extended period

Acknowledgments

The protocols described in this work are derived from the original research publication, Sci Adv. 2020 Jun 24;6(26):eaba4498 (Goel *et al.*, 2020). This work was partially supported by the NIH grants U54CA210181, R01CA193880, and R01CA222959, in addition to the U.S. Department of Defense grant W81XWH-17-1-0389.

Competing interests

Mauro Ferrari is the inventor of a U.S. patent from The University of Texas-Houston (patent no. US 8,920,625 B2, granted 30th December, 2014). Mauro Ferrari and Haifa Shen are inventors of a non-provisional patent application from the Houston Methodist Hospital (PCT/US 2014/0010879 A1). Both inventions are related to the scientific research described herein. More recently, Mauro Ferrari has formed a company (BrYet LLC) and has secured certain commercial rights on said patents. Though not an executive officer, he remains a majority shareholder, director, and scientific advisor of the company. All other authors declare that they have no competing interests.

Ethics

All animal studies were performed in accordance with the guidelines from the Institutional Animal Care and Use Committee (IACUC ID: IS00004452; Validity: 01/02/2018-01/01/2021) at the Houston Methodist Research

Institute.

References

- Bianchini, G., Balko, J. M., Mayer, I. A., Sanders, M. E. and Gianni, L. (2016). [Triple-negative breast cancer: challenges and opportunities of a heterogeneous disease](#). *Nat Rev Clin Oncol* 13(11): 674-690.
- Blanco, E., Shen, H. and Ferrari, M. (2015). [Principles of nanoparticle design for overcoming biological barriers to drug delivery](#). *Nat Biotechnol* 33(9): 941-951.
- Goel, S., England, C. G., Chen, F. and Cai, W. (2017). [Positron emission tomography and nanotechnology: A dynamic duo for cancer theranostics](#). *Advanced Drug Delivery Reviews* 113: 157-176.
- Goel, S., Zhang, G., Dogra, P., Nizzero, S., Cristimi, V., Wang, Z., Hu, Z., Li, Z., Liu, X., Shen, H. and Ferrari, M. (2020). [Sequential deconstruction of composite drug transport in metastatic breast cancer](#). *Science Advances* 6(26): eaba4498.
- Michor, F., Liphardt, J., Ferrari, M. and Widom, J. (2011). [What does physics have to do with cancer?](#) *Nat Rev Cancer* 11(9): 657-670.
- Elia, I., Rossi, M., Stegen, S., Broekaert, D., Doglioni, G., van Gorsel, M., Boon, R., Escalona-Noguero, C., Torrekens, S., Verfaillie, C., Verbeken, E., Carmeliet, G. and Fendt, S. M. (2019). [Breast cancer cells rely on environmental pyruvate to shape the metastatic niche](#). *Nature* 568(7750): 117-121.
- Xu, R., Zhang, G., Mai, J., Deng, X., Segura-Ibarra, V., Wu, S., Shen, J., Liu, H., Hu, Z., Chen, L., Huang, Y., Koay, E., Huang, Y., Liu, J., Ensor, J. E., Blanco, E., Liu, X., Ferrari, M. and Shen, H. (2016). [An injectable nanoparticle generator enhances delivery of cancer therapeutics](#). *Nat Biotechnol* 34(4): 414-418.

Analysis of the Effects of Hexokinase 2 Detachment From Mitochondria-Associated Membranes with the Highly Selective Peptide HK2pep

Francesco Ciscato^{1, #, *}, Federica Chiara^{2, #}, Riccardo Filadi^{1, 3} and Andrea Rasola^{1, *}

¹Department of Biomedical Sciences (DSB), University of Padova, Padova, Italy

²Department of Surgery, Oncology and Gastroenterology (DISCOG), University of Padova, Padova, Italy

³Neuroscience Institute, Italian National Research Council (CNR), Padova, Italy

*For correspondence: francesco.ciscato@gmail.com; andrea.rasola@unipd.it

#Contributed equally to this work

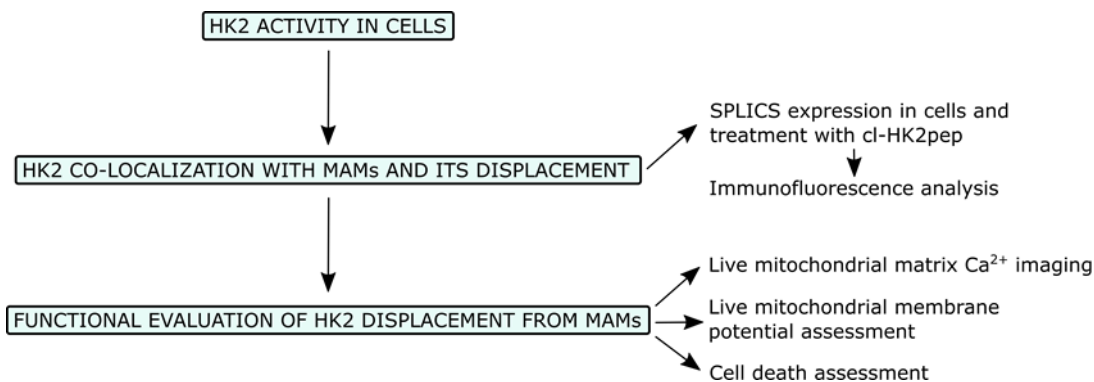
Abstract

The crucial role of hexokinase 2 (HK2) in the metabolic rewiring of tumors is now well established, which makes it a suitable target for the design of novel therapies. However, hexokinase activity is central to glucose utilization in all tissues; thus, enzymatic inhibition of HK2 can induce severe adverse effects. In an effort to find a selective anti-neoplastic strategy, we exploited an alternative approach based on HK2 detachment from its location on the outer mitochondrial membrane. We designed a HK2-targeting peptide named HK2pep, corresponding to the N-terminal hydrophobic domain of HK2 and armed with a metalloprotease cleavage sequence and a polycation stretch shielded by a polyanion sequence. In the tumor microenvironment, metalloproteases unleash polycations to allow selective plasma membrane permeation in neoplastic cells. HK2pep delivery induces the detachment of HK2 from mitochondria-associated membranes (MAMs) and mitochondrial Ca²⁺ overload caused by the opening of inositol-3-phosphate receptors on the endoplasmic reticulum (ER) and Ca²⁺ entry through the plasma membrane leading to Ca²⁺-mediated calpain activation and mitochondrial depolarization. As a result, HK2pep rapidly elicits death of diverse tumor cell types and dramatically reduces *in vivo* tumor mass. HK2pep does not affect hexokinase enzymatic activity, avoiding any noxious effect on non-transformed cells. Here, we make available a detailed protocol for the use of HK2pep and to investigate its biological effects, providing a comprehensive panel of assays to quantitate both HK2 enzymatic activity and changes in mitochondrial functions, Ca²⁺ flux, and cell viability elicited by HK2pep treatment of tumor cells.

Keywords: Hexokinase 2, Cell-penetrating peptide, Mitochondria-associated membranes, Ca²⁺, Anti-neoplastic strategy, Cancer, Mitochondria

This protocol was validated in: EMBO Rep. (2020) DOI: 10.15252/embr.201949117.

Graphical Abstract:



Flowchart for the analysis of the effects of HK2 detachment from MAMs.

Background

Metabolic rewiring in tumor cells (Boroughs and DeBerardinis, 2015; Vander Heiden and DeBerardinis, 2017) encompasses increased uptake and usage of glucose and decreased oxidative phosphorylation (OXPHOS) (Cannino *et al.*, 2018; Faubert *et al.*, 2020), conferring a selective advantage to neoplastic cells to survive and thrive under shortage of both nutrients and oxygen (Nakazawa *et al.*, 2016). Hence, targeting metabolic components offers promising therapeutic perspectives, and the selective inhibition of glucose utilization has been considered for clinical cancer therapy (Hay, 2016). Hexokinases convert glucose to glucose-6-phosphate and make it available for utilization in glycolysis, the pentose phosphate pathway, glycogenesis, and hexosamine biosynthesis (Wilson, 2003). The most active isozyme, hexokinase 2 (HK2), is overexpressed in numerous types of cancer and constitutes a promising target for the development of anti-neoplastic strategies (Roberts and Miyamoto, 2015). Indeed, HK2 plays a major role in the metabolic rewiring of tumors and is induced by oncogenic K-Ras activation (Patra *et al.*, 2013) or in response to hypoxia (Semenza, 2013). HK2 overexpression is related to stage progression, acquisition of invasive and metastatic capabilities, and poor prognosis (Mathupala *et al.*, 2010). In tumor cells, HK2 binds to the outer mitochondrial membrane following Akt-dependent phosphorylation (Miyamoto *et al.*, 2008), and mitochondrial binding of HK2 has been associated with the protection of cancer cells from noxious stimuli (Roberts and Miyamoto, 2015). The natural consequence of these observations was the development of therapeutic strategies aimed at inhibiting the activity of HKs; however, the clinical use of hexokinase inhibitors was hampered by the lack of specificity or the side effects (Akins *et al.*, 2018) elicited by the conserved nature of the active sites among the ubiquitously expressed hexokinase isozymes (Roberts and Miyamoto, 2015).

We have previously exploited an alternative approach to target HK2, based on detaching it from mitochondria with a peptide corresponding to the N-terminal hydrophobic domain of the enzyme. This treatment causes the opening of a mitochondrial channel, the permeability transition pore (PTP) (Rasola and Bernardi, 2011), and consequent cell death (Chiara *et al.*, 2008; Masgras *et al.*, 2012; Pantic *et al.*, 2013). Recently, we established that HK2 localizes to domains of interaction between the ER and mitochondria called mitochondria-associated membranes (MAMs), and its displacement elicits a massive Ca^{2+} flux from the ER and across the plasma membrane into mitochondria, inducing mitochondrial depolarization and death in a variety of cancer models, both *in vitro* and *in vivo*, in a calpain-dependent manner (Ciscato *et al.*, 2020). We have improved HK2 peptide efficacy and specificity by adding a polycation stretch required for plasma membrane permeation linked to a shielding polyanion sequence through a matrix metalloprotease 2 and 9 (MMP2/9) target sequence. This novel tool, called HK2pep, is specifically taken up by neoplastic cells when its polycation sequence is unmasked by removal of the polyanion stretch through MMP2/9 cleavage in the tumor microenvironment, where these proteases are highly induced (Figure 1). HK2pep has proven to be an excellent tool to dissect the precise localization of HK2 in MAMs and the cascade of events leading to tumor cell death, in addition to being effective in tumors allografted in mice, while leaving

hexokinase enzymatic activity unaffected, thus protecting healthy tissues from any off-target effects of the treatment (Ciscato *et al.*, 2020).

Taken together, our data disclose novel signaling pathways primed by HK2 displacement from MAMs and open possibilities for the development of effective anti-neoplastic strategies, alone or in combination with other chemotherapies.

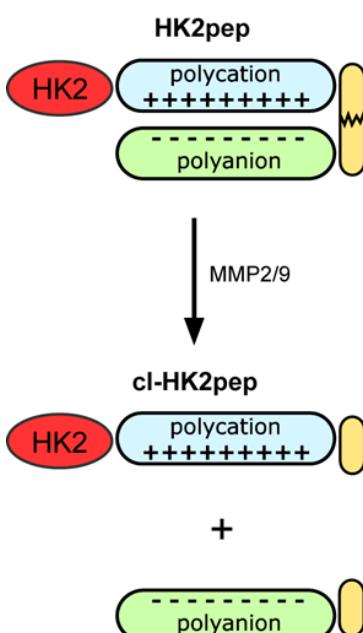


Figure 1. Modified from Ciscato *et al.*, 2020. Functional unit composition of HK2pep.

The HK2-targeting sequence is in red; the polycation and polyanion stretches are in light blue and light green, respectively; the MMP2/9 target sequence is in yellow. Cl-HK2pep is the active peptide after MMP2/9 cleavage.

Materials and Reagents

1. Flasks, 25 cm² (Falcon, catalog number: 353108)
2. 6-well plates (Falcon, catalog number: 353046)
3. 12-well plates (Falcon, catalog number: 353103)
4. 24-well plates (Falcon, catalog number: 353047)
5. 96-well plates (Falcon, catalog number: 353916)
6. 13-mm diameter coverslips (VWR, catalog number: 631-0149P)
7. 18-mm diameter coverslips (VWR, catalog number: 631-0153P)
8. 24-mm diameter coverslips (VWR, catalog number: 631-0161)
9. PBS (Sigma-Aldrich, catalog number: D8537, storage RT)
10. Trypsin-EDTA (GIBCO, catalog number: 25200-056, storage 4°C)
11. NaCl (Sigma-Aldrich, catalog number: S9888, storage RT)
12. Trizma® base (Sigma-Aldrich, catalog number: T6066, storage RT)
13. EDTA (Sigma-Aldrich, catalog number: E5134, storage RT)
14. Triton X-100 (Sigma, catalog number: 9002-93-1, storage RT)
15. Glycerol (Sigma-Aldrich, catalog number: G5516, storage RT)
16. Pierce™ BCA protein assay (Thermo Scientific™, catalog number: 23225, storage RT)
17. MgCl₂ (Sigma-Aldrich, catalog number: 63068, storage RT)
18. ATP (Sigma-Aldrich, catalog number: A2383, storage -20°C)
19. Glucose (Sigma-Aldrich, catalog number: G8270, storage RT)

20. Glucose 6-phosphate-dehydrogenase (Sigma-Aldrich, catalog number: SRP6505, storage -20°C)
21. NADP (Sigma-Aldrich, catalog number: 93205, storage -20°C)
22. SPLICSSs (split-GFP-based contact site sensor short) and SPLICSL (split-GFP-based contact site sensor long) plasmids (Cieri *et al.*, 2018, available from the authors) (storage -20°C)
23. OptiMEM (GIBCO, catalog number: 51985026, storage 4°C)
24. TransIT-LT1 (Mirus, catalog number: MIR 2304, storage 4°C)
25. KCl (Sigma-Aldrich, catalog number: P3911, storage RT)
26. KH₂PO₄ (Merck, catalog number: 1551139, storage RT)
27. CaCl₂ (Sigma-Aldrich, catalog number: 21097, storage RT)
28. HEPES (Sigma-Aldrich, catalog number: H3375, storage RT)
29. HK2pep (Chemical synthesis, seq. MIASHLLAYFFTELN-bA-RRRRRRRRR-PLLAG-Ahx-EEEEEEEEE, storage -20°C)
30. SCRpep (Chemical synthesis, seq. VGAHAGEYGAEALER-bA-RRRRRRRRR-PLLAG-Ahx-EEEEEEEEE, storage -20°C)
31. cl-HK2pep (Chemical synthesis, seq. MIASHLLAYFFTELN-βA-RRRRRRRRR-PLG, storage -20°C)
32. cl-SCRpep (Chemical synthesis, seq. VGAHAGEYGAEALER-βA-RRRRRRRRR-PLG storage -20°C). All peptides were synthesized by automatic solid-phase procedures (for details, see Ciscato *et al.*, 2020). Suggested purity ≥95% measured by analytical reversed-phase HPLC. Peptides are not commercially available but can be synthesized on demand by specialized companies.
33. PFA (Sigma-Aldrich, catalog number: P6148, storage 4°C)
34. NH₄Cl (Sigma-Aldrich, catalog number: A9434, storage RT)
35. BSA (Sigma-Aldrich, catalog number: AG4503, storage 4°C)
36. Goat serum (Sigma-Aldrich, catalog number: G6767, storage -20°C)
37. Gelatin (Sigma-Aldrich, catalog number: G2500, storage -20°C)
38. Rabbit monoclonal anti-HK2 antibody (Thermo Scientific, catalog number: H.738.7, storage -20°C)
39. AlexaFluor555 donkey anti-rabbit IgG (Thermo Fisher Scientific, catalog number: A-31572, storage -20°C)
40. Mowiol 4-88 (Sigma-Aldrich, catalog number: 81381, storage RT)
41. Plasmids encoding mitochondria-targeted GCAMP6f (Filadi *et al.*, 2018, available from the authors, storage -20°C)
42. Cyclosporin H (Vinci-Biochem, catalog number: AG-CN2-0447-M005, storage -20°C)
43. TetraMethyl-Rhodamine Methyl ester (TMRM) (Invitrogen, MitoProbeTM, catalog number: M20036, storage -20°C)
44. Annexin V-FITC - Annexin-V-FLUOS labeling reagent (Roche - now sold by MERCK, catalog number: 11828681001, storage -20°C)
45. 7-aminoactinomycin D (7-AAD; Sigma-Aldrich, catalog number: A9400, storage -20°C)

Equipment

1. Cell culture incubators (Thermo Scientific Forma™ Steri-Cycle™ CO₂ Incubator)
2. Equipped cell culture hoods (Angelantoni Industries, catalog number: VBH 48 C2)
3. Micropipettes (Gilson Pipetman Classic, P1,000, P200, P20, P10, P2)
4. Burker chamber (VWR, catalog number: HECH40443703)
5. Centrifuges from 200 to 2,000 × g, fixed bucket, no specific rotors needed (*e.g.*, MPW Med. Instruments, catalog number: MPW 251)
6. Thermo-shaker (Biosan, catalog number: TS-100)
7. Centrifuges from 200 to 16,000 × g, fixed bucket, no specific rotors needed (*e.g.*, Eppendorf, catalog number: 5417 R)
8. Plate-Reader Spectrophotometer (TECAN, model: Infinite M200 spectrophotometer)
9. Confocal microscope (Leica SP5-II equipped with a 100×/1.4 N.A. plan apochromat objective, a WLL laser to excite each specific dye, and a HyD detector for signal collection)
10. Inverted fluorescence microscope (Zeiss Axiovert 100, Fluar 40× oil objective, NA 1.30)

Cite as: Ciscato, F. et al., (2021). Analysis of the Effects of Hexokinase 2 Detachment From Mitochondria-Associated Membranes with the Highly Selective Peptide HK2pep. Bio-protocol 11(14): e4087. DOI: 10.21769/BioProtoc.4087.

11. Inverted fluorescence microscope (Leica, model: DMI6000 B)
12. Cytofluorimeter (BD FACSCantoTM II)

Software

1. i-controlTM (for TECAN, Infinite M200 spectrophotometer, https://lifesciences.tecan.com/plate_readers/infinite_200_pro?p=tab--3)
2. Excel data analysis software (Microsoft Office)
3. Leica Application Suite LAS-AF (for Leica SP5-II <https://www.leica-microsystems.com/products/confocal-microscopes/p/leica-tcs-sp5-ii>)
4. ImageJ (NIH, <https://imagej.nih.gov/ij/download.html>)
5. For the Zeiss microscope, synchronization of the cool camera with the excitation source is performed by a custom-made software package (Roboscope - developed by Catalin Dacian Ciubotaru at VIMM, Padova, Italy); alternatively, the specific manufacturer's microscope software is suitable for kinetic image acquisition
6. Leica Application Suite LAS-AF for the Leica fluorescence microscope (<https://www.leica-microsystems.com/products/microscope-software/p/leica-las-x-ls/>)
7. BD FACSDivaTM for the BD FACSCantoTM II cytofluorimeter (<https://www.bdbiosciences.com/en-us/instruments/research-instruments/research-software/flow-cytometry-acquisition/facsdiva-software>)

Procedure

A. HK2 activity in cells

Note: To carry out these measurements, we used mouse 4T1 breast carcinoma cells, mouse CT26 colorectal carcinoma cells, and human HeLa cervix carcinoma cells (Ciscato et al., 2020). It is possible to perform this protocol on both adherent and suspended cell lines and on primary cells.

1. Cell culture and sample collection
 - a. Plate 1-4 × 10⁶ cells (depending on the cell type; e.g., 2 × 10⁶ HeLa cells, 2 × 10⁶ 4T1 and CT26 cells) in 25 cm² flasks at least 24 h before harvesting/treatment.
 - b. Harvest the cells by washing the flask with PBS, detaching them with trypsin-EDTA, and blocking the reaction with fresh media (DMEM for HeLa and CT26 cells, RPMI for 4T1 cells) containing 10% FBS.
 - c. Pellet the cells (adjust the centrifugal force and time according to your cell lines to safely pellet them; e.g., 5 min, 400 × g for HeLa, 4T1, and CT26 cells).
 - d. Remove the supernatant.
 - e. Lyse cells in 100-200 µL Lysis Buffer.
 - f. Quantitate the protein content (PierceTM BCA protein assay kit).
 - g. Calculate the volume corresponding to 20 µg protein (this amount of protein can be modified according to the cell line under analysis), which is sufficient to detect hexokinase activity.
2. Sample preparation
 - a. Prepare 2 vials containing 20 µg protein for each experimental condition.
 - b. Incubate one vial at 4°C and the other at 46°C for 30 min. Heating 30 min at 46°C is sufficient to remove the catalytic activity of HK2, the only heat-sensitive hexokinase, preserving the activity of the other isozymes; HK2 is not degraded by this treatment.
 - c. After incubation, store the samples on ice.
3. Sample treatment with cl-HK2pep (and/or your compound of interest) and measurement of HKs/HK2 activity
 - a. Prepare fresh Reaction Buffer at room temperature.

- b. The final reaction volume is 100 μ L. Prepare the proper amount of buffer spotted in a 96-well plate and add 10 μ M cl-HK2pep (and/or your compound of interest - use cl-SCRpep as a control peptide).
 - c. Mix for 5 s using a plate mixer (generally, we shake using the plate reader, but any plate mixer is suitable).
 - d. Add 20-100 μ g cell extract (heated or not) and mix for 10 s.
 - e. Read the 96-well plate in kinetic mode (with a minimum 30 s interval) at 340 nm using a spectrophotometric plate reader (Infinite M200 spectrophotometer, TECAN) for 15 min at 37°C.
4. Data analysis
 - a. HK activities were calculated in nmol/min/mg: nmol per minute was obtained by calculating the slope (m) of the plotted absorbance at 340 nm during the first minute of recording and dividing it by the extinction coefficient of NADH ($\epsilon = 6.22$) and the cuvette path length ($l = 0.4$ cm for the 96-well plate). Then, values were normalized to total mg of protein added to the reaction (0.08 mg 4T1 total lysate).
 - b. To calculate HK2 activity, subtract the activity obtained in the samples pre-incubated at 46°C from that in the samples incubated at 4°C (Figure 2).
 - c. Apply the proper statistical analysis (e.g., Student's t-test to compare two groups or one-way ANOVA to compare more than two groups).

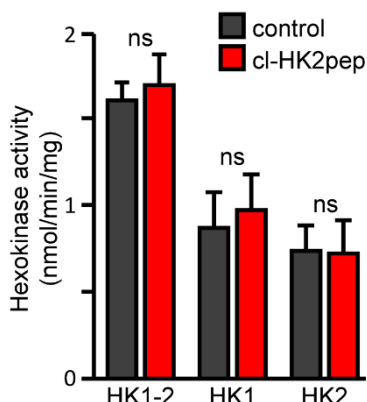


Figure 2. Modified from Ciscato *et al.*, 2020. Measurement of hexokinase enzymatic activities.
HK1+HK2, HK1, and HK2 enzymatic activity calculated after treatment with cl-HK2pep in 4T1 cell extract as described above. cl-SCRpep is used as a negative control.

B. HK2 co-localization with MAMS and its displacement by cl-HK2pep

1. Cell seeding and culture
 - a. Plate $0.5-1 \times 10^5$ cells in 24-well plates containing a 13-mm (diameter) coverslip and culture (37°C, 5% CO₂, humidified atmosphere) for at least 24 h. Cells can be grown for 48 h but must be at 60-70% confluence at the time of transfection (next step).
2. Cell transfection with SPLICS-encoding plasmids
 - a. Transfect cells with plasmids encoding the two subunits of SPLICSs (to evaluate ER-mitochondria contacts < 10 nm) or the SPLICS_L probe (for contacts < 40-50 nm) (Cieri *et al.*, 2018). Mix 0.5 μ g each plasmid/well in 100 μ L OptiMEM together with 2 μ L TransIT-LT1 (MIR 2304 - Mirus) and incubate for 15 min.
 - b. Add the transfection mix dropwise to the cells (leaving 0.5 mL culture medium) and incubate for 5 h.
 - c. Eliminate the medium containing the transfection mix and replace with 0.5 mL fresh medium.
 - d. Leave cells in the incubator overnight.
3. Cell treatment(s) with cl-HK2pep (and/or your compound of interest)

- a. Prepare a solution containing mKRB Buffer and 2 μ M cl-HK2pep (and/or your compound of interest; use cl-SCRpep as a control peptide). This amount of cl-HK2pep is able to detach part of HK2 from MAMs in less than 2 min, so please consider pre-incubating other compounds before using cl-HK2pep if they take longer to be effective in intact cells.
 - b. Substitute cell media with 500 μ L solution containing 1-2 μ M cl-HK2pep (and/or your compound of interest; use cl-SCRpep as a control peptide). Consider using different media according to experimental conditions; cl-HK2pep is effective in a broad range of physiological solutions.
 - c. Incubate at room temperature for 2 min. The 2 μ M cl-HK2pep treatment can lead to mitochondrial depolarization in a few minutes and apoptotic cell death in 15 min (Ciscato *et al.*, 2020). Consider not exceeding a 5-min treatment; otherwise, decrease the cl-HK2pep concentration. Depending on the cell type, different media can accelerate or delay the activity of cl-HK2pep.
 - d. Remove media and add 500 μ L PBS using a pipette to wash the cells.
 - e. Remove PBS and add 500 μ L 4% PFA (prepared in PBS) for 10 min to fix the cells for the immunofluorescence protocol.
 - f. Remove the PFA solution and wash the cells 3 \times 5 min with 0.5 ml PBS during gentle agitation (100-120 rpm on an orbital shaker).
 - g. Add 0.5 mL quenching solution for 20 min.
 - h. Remove the quenching solution and wash the cells 3 \times 5 min with 0.5 mL PBS during gentle agitation (100-120 rpm on an orbital shaker). Then proceed with immunofluorescence (step B4 below). Cells can be stored at 4°C in PBS for 1 week if it is not possible to proceed immediately with step B4.
4. HK2 immunofluorescence protocol and image acquisition
 - a. Remove the PBS and permeabilize the cells with 0.5 ml Triton X-100 for 3 min.
 - b. Remove the Triton X-100 and wash the cells with 0.5 mL PBS. The solutions must be added and removed using a pipette.
 - c. Incubate cells with 0.5 mL blocking solution for at least 30 min. Add the solution using a pipette. Protect from light.
 - d. Dilute the primary antibody (rabbit monoclonal anti-HK2 antibody, H.738.7, Thermo Scientific) 1:150 in blocking solution and incubate cells for 90 min at room temperature, protected from light.
 - e. Remove the antibody solution and wash the cells 3 \times 5 min with blocking solution during gentle agitation (100-120 rpm on an orbital shaker).
 - f. Dilute the secondary antibody (AlexaFluor555 donkey anti-rabbit IgG, A-31572 Thermo Fisher Scientific) 1:300 in blocking solution and centrifuge at 13,000 \times g for 10 min.
 - g. Incubate cells with this solution for 45 min at room temperature. Protect from light.
 - h. Remove the antibody solution and wash the cells 3 \times 5 min with blocking solution during gentle agitation (100-120 rpm on an orbital shaker). Perform an additional wash with PBS during gentle agitation (100-120 rpm on an orbital shaker).
 - i. Wash coverslips with H₂O and immediately mount with Mowiol (or a different mounting solution) on an object glass. Allow to dry overnight protected from light at room temperature, then store at 4°C until image acquisition.
 - j. Collect images using a confocal microscope (Leica SP5-II equipped with a 100 \times /1.4 N.A. plan apochromat objective, a WLL laser to excite each specific dye, and a HyD detector for signal collection). The power of the lasers should be set on the sample with the highest signal intensity to avoid signal saturation and kept the same for all samples/experimental conditions. Export images in TIFF format.
 5. Data analysis
 - a. Open TIFF images of the green (SPLICS probes) and red (HK2 staining) channels in ImageJ (version 1.47b or later, NIH).
 - b. Subtract the background. Trace a region of interest (ROI) in a background region; in Plugins, select ROI, BG subtraction from ROI, and press OK. Repeat for both channels.
 - c. Calculate the Pearson's co-localization coefficient in Plugins, Co-localization analysis, Manders coefficients, choose the appropriate combination of the red and green channels, select exclude zero-

- zero pixels, and press OK. The Mander's and Pearson's co-localization coefficients will be calculated by the software (Figure 3).
- Repeat for all images and apply the appropriate statistical tests. We recommend analyzing at least 10 different cells for each coverslip and repeating the experiment at least three times on three different days.

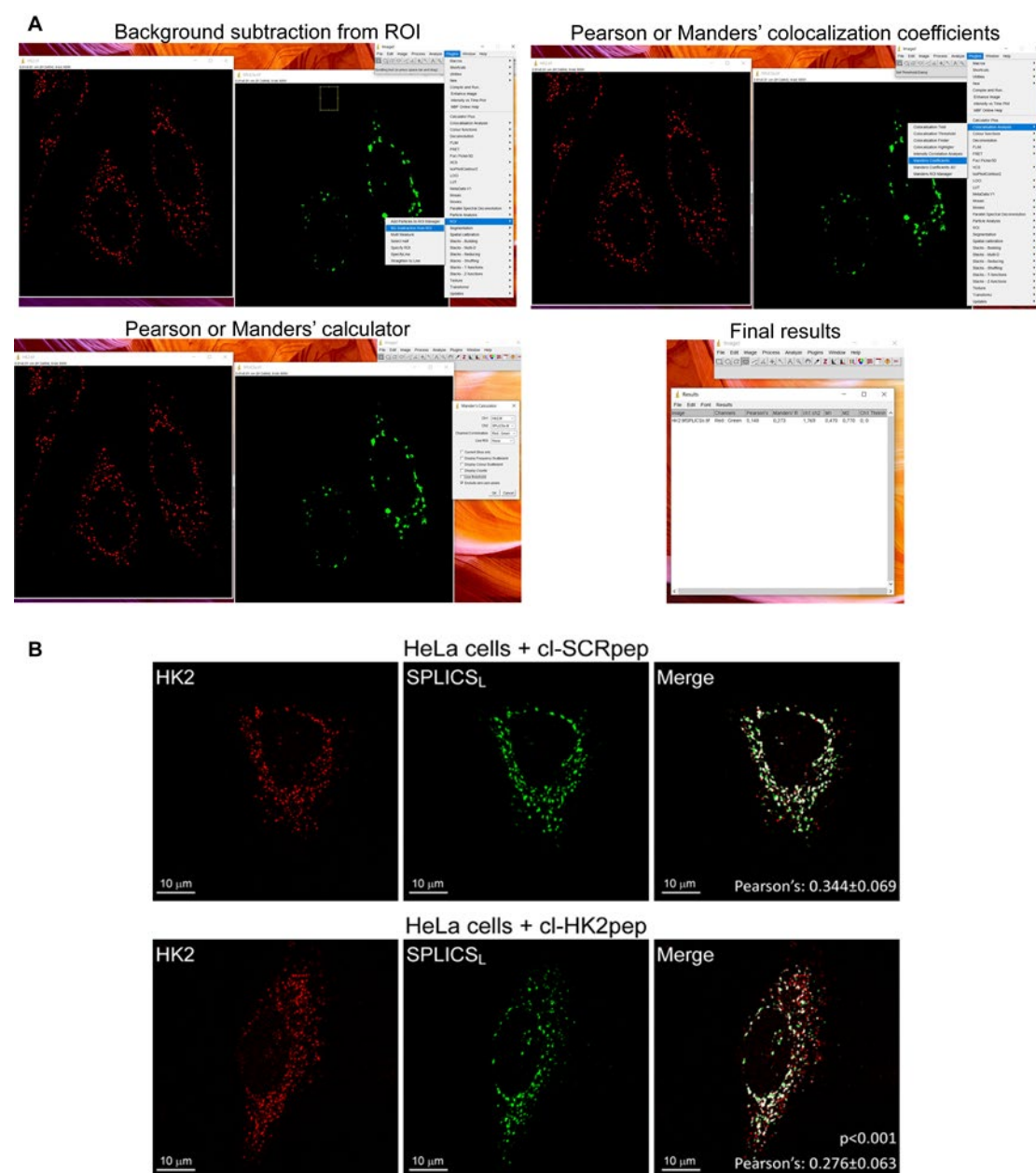


Figure 3. Pearson's co-localization coefficient calculation, modified from Ciscato *et al.* (2020).

(A) Step-by-step representative confocal image analysis in HeLa cells performed using ImageJ (version 1.47b or later, NIH). (B) Representative results from confocal image analysis: HK2 displacement from HeLa MAMs after treatment with cl-HK2pep is shown by the loss of the merged signal between HK2 (red) and the split-GFP-based probe for ER-mitochondria contacts (SPLICS_L, green); the merged signal is white. cl-SCRpep is used as a negative control, and Pearson's co-localization coefficient is indicated (cl-SCRpep n = 26 cells; cl-HK2pep n = 24 cells; P < 0.001 with a Student's t-test). Scale bar: 10 μ m.

C. Functional evaluation of HK2 displacement from MAMS by cl-HK2pep

1. Cell seeding and culture

Note: Consider adjusting the number of cells to be plated depending on the specific cell type under analysis. The following analyses must be performed on adherent cells.

- a. For live mitochondrial matrix Ca^{2+} imaging, plate 1×10^5 cells in 12-well plates containing 18-mm-diameter coverslips at least 24 h before transfection.
 - b. For live TMRM (tetramethylrhodamine methyl ester) imaging, plate 2.5×10^5 cells in 6-well plates containing 24-mm-diameter coverslips at least 24 h before the experiment.
 - c. For cell death assessment, plate 1.5×10^6 cells in 25 mm² flasks for each condition the day before the experiment.
2. Live mitochondrial matrix Ca^{2+} imaging and data analysis
 - a. Transfect cells with the plasmids encoding mitochondria-targeted GCAMP6f (see point B.2 for the transfection protocol; use 0.75 μg DNA for each coverslip and 1.5 μL TransIT-LT1 reagent).
 - b. 24 h after transfection, replace the medium with mKRB buffer supplemented with 1 μM cyclosporin H, and place the coverslip in a proper holder for live microscope imaging. Incubate for 10-20 min with 500 μL mKRB at room temperature. Specific drugs can be added and incubated for 30-60 min before the experiment.
 - c. Sequentially excite GCAMP6f at 475 nm (the Ca^{2+} -sensitive wavelength) and 410 nm (the isosbestic point) on an inverted fluorescence microscope (Zeiss Axiovert 100, Fluar 40 \times oil objective, NA 1.30), producing the excitation light from a monochromator (polychrome V; TILL Photonics) and filtering it with a 505 nm DRLP filter (Chroma Technologies). Collect the emitted fluorescence in the 500-530 nm range (using a band-pass filter, Chroma Technologies) and repeat this cycle every 5 s (Figure 4A). Imaging can be performed for up to 90 min.
 - d. Add 2 μM cl-HK2pep (and/or your compound of interest) 2-4 min after starting the recording. For a homogeneous distribution of added compounds, collect 100 μl solution on the holder, dissolve cl-HK2pep (and/or your compound of interest), and carefully add the already-made solution on top of the coverslip by mixing using a pipette. On a single experimental day, we recommend analyzing at least 3 different coverslips for each condition, with 4-10 cells in the acquired field. Repeat the experiment at least three times on three different days.
 - e. Export images in TIFF format and open in the ImageJ software.
 - f. Subtract the background (see above point B5.b), trace the appropriate ROIs including the mitochondrial network of each single cell, and measure the emitted fluorescence intensity for each frame upon excitation at 475 nm and 410 nm.
 - g. Calculate the ratio (R) between the generated emissions by exciting the cells at 475 and 410 nm. R is proportional to $[\text{Ca}^{2+}]$. The variation in R between conditions in which $[\text{Ca}^{2+}]$ in the mitochondrial matrix is relatively low (<100 nM, resting conditions) and those in which the probe is saturated (high $[\text{Ca}^{2+}]$, >10 μM) should be around 15-20 fold (Figure 4B).

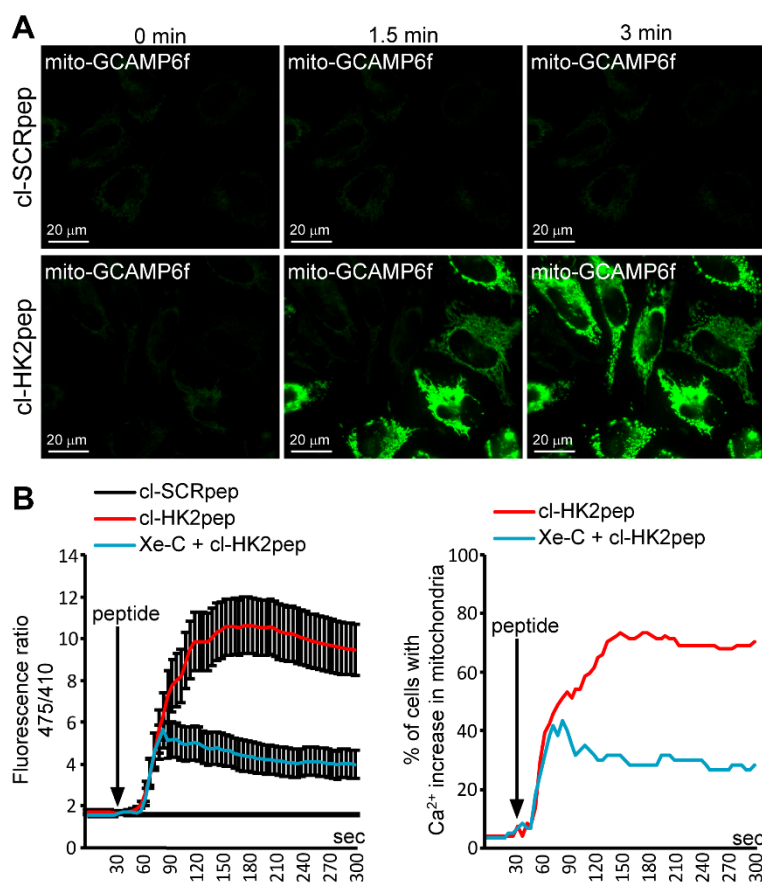


Figure 4. Modified from Ciscato *et al.*, 2020. Measurement of changes in mitochondrial Ca²⁺ levels. (A) Representative images of kinetic analysis of mitochondrial matrix Ca²⁺ variations (assessed with a mitochondria-targeted GCAMP6f probe) after cl-HK2pep treatment in HeLa cells. (B) Quantitation of mitochondria-targeted GCAMP6f signals as the mean \pm SEM of the 475/410 nm ratio (left panel) or the percentage of cells with increased Ca²⁺ in the mitochondria (right panel – threshold 475/410 ratio for positivity > 3 ; baseline mean ratio = 1.84 ± 0.54). cl-SCRpep is used as a negative control.

3. Live mitochondrial membrane potential assessment and data analysis
 - a. Prepare a solution containing mKRB (or the solution adapted to the cells/experimental conditions) plus 20 nM TMRM and 1 μM cyclosporin H (to inhibit probe extrusion through multidrug resistance pumps).
 - b. Wash the coverslip with PBS in another 6-well plate.
 - c. Place the coverslip in a proper holder for live microscope imaging (according to your microscope set up) and incubate for 20-40 min with 500 μL TMRM-containing solution at room temperature. The incubation time is dependent on cell type. TMRM accumulates in the mitochondrial matrix and takes time to equilibrate; at the beginning of the experiment, TMRM accumulation must be in the steady state (Figures 5 and 6).
 - d. After incubation, use an inverted fluorescence microscope (Leica DMI6000 B) to record TMRM fluorescence in kinetic mode every 30 s-3 min (depending on cell type). In some cell types, TMRM fluorescence can be phototoxic with consequent mitochondrial membrane depolarization. Therefore, before starting the experiments, monitor TMRM fluorescence in kinetic mode for 1 h: if the TMRM emission signal decreases, increase the lag time between acquisitions and/or decrease excitation intensity; experiments must be performed only under conditions in which cells display a stable signal during the entire hour of recording.
 - e. Add 2 μM cl-HK2pep (and/or your compound of interest; use cl-SCRpep as a control peptide) 2-4

min after starting the recording. For homogeneous distribution of added compounds, collect 100 μ L solution on the holder, dissolve cl-HK2pep (and/or your compound of interest), and carefully add the mix on top of the coverslip. On a single experimental day, we recommend analyzing at least 3 different coverslips for each condition, with 5-30 cells in the acquired field. Repeat the experiment at least three times on three different days.

- f. For image analysis: Open TIFF images in ImageJ (1.47b, NIH).
- g. Subtract the background (see above point B5.b), trace the appropriate ROIs including the mitochondrial network of each single cell, and measure the emitted fluorescence intensity in kinetic mode (Figure 5).
- h. Repeat for all kinetics and apply the appropriate statistical tests.

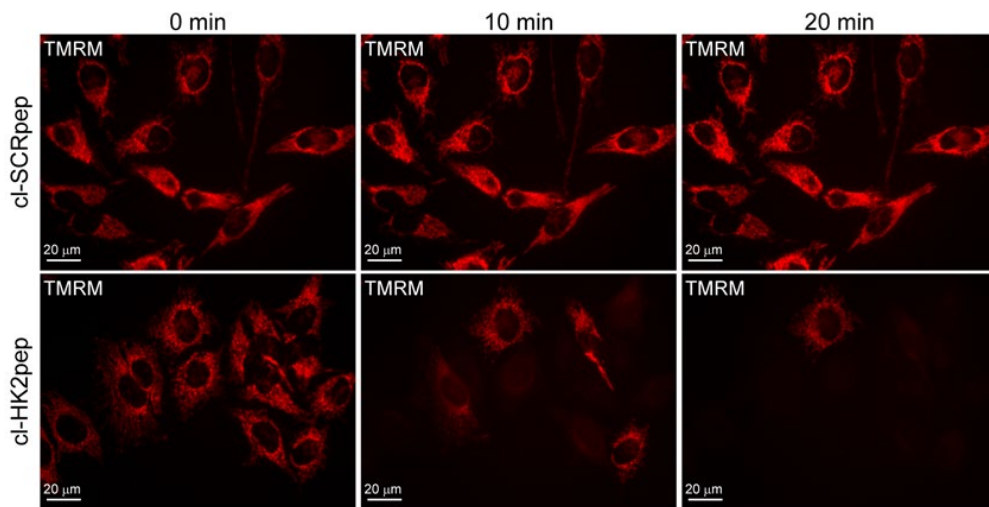


Figure 5. Modified from Ciscato *et al.*, 2020. Assessment of changes in mitochondrial membrane potential.

Effect of cl-HK2pep treatment on mitochondrial membrane potential assessed with the TMRM probe in HeLa cells.

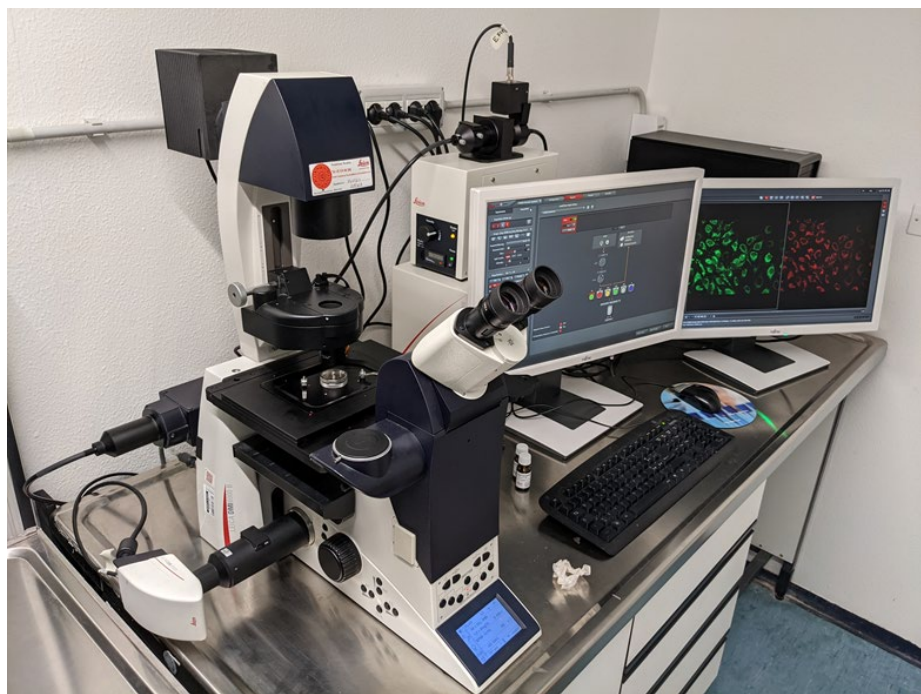


Figure 6. Representative set up with a coverslip chamber for live cell imaging

4. Cell death assessment and data analysis
 - a. Harvest cells by washing flasks one at a time with PBS, detaching cells with trypsin-EDTA, and blocking the reaction with 5 ml fresh medium containing 10% FBS. Collect the detached cells.
 - b. Count cells using a Burker chamber.
 - c. Collect 1.5×10^6 cells for each experimental condition and pellet them.
 - d. Prepare mKRB buffer containing 1:100 Annexin-V-FLUOS labeling reagent pre-made by Roche (alternatively, it is possible to use other Annexin V-FITC probes following the manufacturer's instructions) and 1 $\mu\text{g}/\text{ml}$ 7-aminoactinomycin D (7-AAD).

Note: It is possible to substitute mKRB buffer with other culture media if needed for the survival of some specific cell types (e.g., we used DMEM without phenol red and added 10 mM HEPES and 0.1% FBS (pH 7.4) for freshly isolated B cells or freshly isolated B-CLL cancer cells).

- e. Resuspend 1.5×10^6 cells in 900 μl mKRB buffer + Annexin V-FITC and 7-AAD and aliquot samples into three different cytofluorimeter-suitable tubes (300 μl sample containing 5×10^5 cells in each tube). These three tubes are technical replicates.
- f. To record staining under basal conditions in all tubes, analyze the green and far-red fluorescence using the cytofluorimeter set-up.
- g. Depending on the cell type, add 1-5 μM cl-HK2pep (and/or your compound of interest; use cl-SCRpep as a control peptide) and gently mix the sample after each addition. Cl-HK2pep is not efficient at killing the non-cancerous cell lines C2C12 or RAW.241, as described in (Ciscato *et al.*, 2020). However, since 5 μM cl-HK2pep can kill 75-96% of cancer cells in less than 15 min (Ciscato *et al.*, 2020), please consider pre-incubating other compounds before cl-HK2pep if they take longer to be effective in intact cells.
- h. Incubate for 15 min at room temperature and reanalyze all tubes in the same order.
- i. Repeat the cytofluorimeter recordings every 15-30 min to perform a kinetic analysis.
- j. Data analysis: Evaluate the percentage of live cells (double-negative for Annexin V-FITC and 7-AAD staining) at each time point and average the technical replicates. Apply the appropriate

statistical tests.

Data analysis

Methods of data analysis are specifically described for each technical approach.

Recipes

Note: Use freshly prepared solutions.

1. Lysis Buffer

150 mM NaCl
20 mM Tris
5 mM EDTA
1% Triton X-100
10% glycerol

2. Reaction Buffer

50 mM Tris
10 mM MgCl₂
4 mM ATP
2 mM glucose
0.1 U/mL glucose 6-phosphate-dehydrogenase (G6PDH)
1 mM NADP, pH 7.4

3. mKRB Buffer

135 mM NaCl
5 mM KCl
0.4 mM KH₂PO₄
1 mM MgCl₂
1 mM CaCl₂
20 mM HEPES
10 mM glucose, pH 7.4 at room temperature

4. Quenching Solution

0.24% NH₄Cl in PBS

5. Permeabilization Solution

0.1% Triton X-100 in PBS

6. Blocking Solution

2% BSA
10% goat serum
0.2% gelatin in PBS

Acknowledgments

This work was supported by grants from the University of Padova, Neurofibromatosis Therapeutic Acceleration

Cite as: Ciscato, F. et al., (2021). Analysis of the Effects of Hexokinase 2 Detachment From Mitochondria-Associated Membranes with the Highly Selective Peptide HK2pep. Bio-protocol 11(14): e4087. DOI: 10.21769/BioProtoc.4087.

Program, Associazione Italiana Ricerca Cancro (AIRC grant IG 2017/20749 to A.R.), Piano for Life Onlus, and Linfa OdV. Protocols were derived from Ciscato *et al.* (2020).

Competing interests

A patent application (Italian patent No. IT102019000002321, priority: 18/02/2019; PCT: PCT/IB2020/051329) has been filed by the University of Padova for the use of the HK2-targeting peptide described in this manuscript as an anti-neoplastic tool in *in vitro* and *in vivo* experiments.

References

- Akins, N. S., Nielson, T. C. and Le, H. V. (2018). [Inhibition of Glycolysis and Glutaminolysis: An Emerging Drug Discovery Approach to Combat Cancer](#). *Curr Top Med Chem* 18(6): 494-504.
- Boroughs, L. K. and DeBerardinis, R. J. (2015). [Metabolic pathways promoting cancer cell survival and growth](#). *Nat Cell Biol* 17(4): 351-359.
- Cannino, G., Ciscato, F., Masgras, I., Sanchez-Martin, C. and Rasola, A. (2018). [Metabolic Plasticity of Tumor Cell Mitochondria](#). *Front Oncol* 8: 333.
- Chiara, F., Castellaro, D., Marin, O., Petronilli, V., Brusilow, W. S., Juhaszova, M., Sollott, S. J., Forte, M., Bernardi, P. and Rasola, A. (2008). [Hexokinase II detachment from mitochondria triggers apoptosis through the permeability transition pore independent of voltage-dependent anion channels](#). *PloS One* 3(3): e1852.
- Cieri, D., Vicario, M., Giacomello, M., Vallese, F., Filadi, R., Wagner, T., Pozzan, T., Pizzo, P., Scorrano, L., Brini, M. and Cali, T. (2018). [SPLICS: a split green fluorescent protein-based contact site sensor for narrow and wide heterotypic organelle juxtaposition](#). *Cell Death Differ* 25(6): 1131-1145.
- Ciscato, F., Filadi, R., Masgras, I., Pizzi, M., Marin, O., Damiano, N., Pizzo, P., Gori, A., Frezzato, F., Chiara, F., Trentin, L., Bernardi, P. and Rasola, A. (2020). [Hexokinase 2 displacement from mitochondria-associated membranes prompts Ca\(2+\) -dependent death of cancer cells](#). *EMBO Rep* 21(7): e49117.
- Faubert, B., Solmonson, A. and DeBerardinis, R. J. (2020). [Metabolic reprogramming and cancer progression](#). *Science* 368(6487): eaaw5473.
- Filadi, R., Leal, N. S., Schreiner, B., Rossi, A., Dentoni, G., Pinho, C. M., Wiehager, B., Cieri, D., Cali, T., Pizzo, P. and Ankarcrona, M. (2018). [TOM70 Sustains Cell Bioenergetics by Promoting IP3R3-Mediated ER to Mitochondria Ca\(2+\) Transfer](#). *Curr Biol* 28(3): 369-382 e366.
- Hay, N. (2016). [Reprogramming glucose metabolism in cancer: can it be exploited for cancer therapy?](#) *Nat Rev Cancer* 16(10): 635-649.
- Masgras, I., Rasola, A. and Bernardi, P. (2012). [Induction of the permeability transition pore in cells depleted of mitochondrial DNA](#). *Biochim Biophys Acta* 1817: 1860-1866.
- Mathupala, S. P., Ko, Y. H. and Pedersen, P. L. (2010). [The pivotal roles of mitochondria in cancer: Warburg and beyond and encouraging prospects for effective therapies](#). *Biochim Biophys Acta* 1797(6-7): 1225-1230.
- Miyamoto, S., Murphy, A. N. and Brown, J. H. (2008). [Akt mediates mitochondrial protection in cardiomyocytes through phosphorylation of mitochondrial hexokinase-II](#). *Cell Death Differ* 15(3): 521-529.
- Nakazawa, M. S., Keith, B. and Simon, M. C. (2016). [Oxygen availability and metabolic adaptations](#). *Nat Rev Cancer* 16(10): 663-673.
- Pantic, B., Trevisan, E., Citta, A., Rigobello, M. P., Marin, O., Bernardi, P., Salvatori, S., and Rasola, A. (2013). [Myotonic dystrophy protein kinase \(DMPK\) prevents ROS-induced cell death by assembling a hexokinase II-Src complex on the mitochondrial surface](#). *Cell Death Dis* 4: e858.
- Patra, K. C., Wang, Q., Bhaskar, P. T., Miller, L., Wang, Z., Wheaton, W., Chandel, N., Laakso, M., Muller, W. J., Allen, E. L., Jha, A. K., Smolen, G. A., Clasquin, M. F., Robey, B. and Hay, N. (2013). [Hexokinase 2 is required for tumor initiation and maintenance and its systemic deletion is therapeutic in mouse models of cancer](#). *Cancer Cell* 24(2): 213-228.

- Rasola, A. and Bernardi, P. (2011). [Mitochondrial permeability transition in Ca\(2+\)-dependent apoptosis and necrosis](#). *Cell Calcium* 50: 222-233.
- Roberts, D.J. and Miyamoto, S. (2015). [Hexokinase II integrates energy metabolism and cellular protection: Akting on mitochondria and TORCing to autophagy](#). *Cell Death Differ* 22(2): 248-257.
- Semenza, G. L. (2013). [HIF-1 mediates metabolic responses to intratumoral hypoxia and oncogenic mutations](#). *J Clin Invest* 123(9): 3664-3671.
- Vander Heiden, M. G. and DeBerardinis, R. J. (2017). [Understanding the Intersections between Metabolism and Cancer Biology](#). *Cell* 168(4): 657-669.
- Wilson, J. E. (2003). [Isozymes of mammalian hexokinase: structure, subcellular localization and metabolic function](#). *J Exp Biol* 206(Pt 12): 2049-2057.

Antisense Oligo Pulldown of Circular RNA for Downstream Analysis

Debojyoti Das^{1, 2, #}, Aniruddha Das^{1, 2, #} and Amaresh C. Panda^{1, *}

¹Institute of Life Sciences, Nalco Square, Bhubaneswar, Odisha, India; ²School of Biotechnology, KIIT University, Bhubaneswar, India

*For correspondence: amaresh.panda@ils.res.in

#Contributed equally to this work

Abstract

Circular RNAs (circRNAs) are a large family of noncoding RNA molecules that have emerged as novel regulators of gene expression by sequestering microRNAs (miRNAs) and RNA-binding proteins (RBPs). Several computational tools have been developed to predict circRNA interaction with target miRNAs and RBPs with a view to studying their potential effect on downstream target genes and cellular physiology. Biochemical assays, including reporter assays, AGO2 pulldown, ribonucleoprotein pulldown, and biotin-labeled RNA pulldown, are used to capture the association of miRNAs and RBPs with circRNAs. Only a few studies have used circRNA pulldown assays to capture the associated miRNAs and RBPs under physiological conditions. In this detailed protocol, the circRNA of interest (e.g., *circHipk2*) was captured using a biotin-labeled antisense oligo (ASO) targeting the *circHipk2* backsplice junction sequence followed by pulldown with streptavidin-conjugated magnetic beads. The specific enrichment of circRNA was analyzed using reverse transcription quantitative PCR (RT-qPCR). Furthermore, the ASO pulldown assay can be coupled to miRNA RT-qPCR and western blotting analysis to confirm the association of miRNAs and RBPs predicted to interact with the target circRNA. In summary, the specific pulldown of circRNA using this quick and easy method makes it a useful tool for identifying and validating circRNA interaction with specific miRNAs and RBPs.

Keywords: CircRNAs, CircRNA pulldown, Antisense oligo, Biotin pulldown, RT-qPCR, miRNA, RNA-binding proteins

This protocol was validated in: Nucleic Acids Res. (2017), DOI: 10.1093/nar/gkw1201

Background

The RNA family can be broadly classified into coding (mRNAs) and noncoding RNAs. Interestingly, the vast majority of cellular RNAs are noncoding RNAs, including rRNA, lincRNA, miRNA, snRNA, snoRNA, tRNA, piRNA, and poorly characterized circular (circ) RNAs (Palazzo and Lee, 2015). The use of next-generation RNA sequencing and bioinformatics tools has uncovered more than a hundred thousand circRNAs in humans (Vromman *et al.*, 2020). CircRNAs are generated from pre-mRNAs by head-to-tail splicing of specific exons by a process called backsplicing, which is regulated by transcription speed, RBPs, and inverted repeat sequences. Their length can vary from less than 100 nucleotides to a few thousand nucleotides. Depending on the sequence of circRNA origin from the parent gene, circRNAs have been classified into exonic circular RNA (circRNA), lariat-derived circular intronic RNA (ci-RNA), stable intronic sequence RNA (sisRNA), and exonic-intronic circular RNA (EIcircRNA) (Guria *et al.*, 2019). Although a vast number of circRNAs have been identified in different cellular systems and disease models, only a fraction of circRNAs has been functionally characterized (Vromman *et al.*, 2020). Recent evidence suggests that circRNAs play a critical role in regulating cellular events by interacting with miRNAs and RBPs (Guria *et al.*, 2019). The majority of studies use computational tools to predict the association of circRNAs with cellular miRNAs and proteins that could regulate the expression of downstream target genes (Dudekula *et al.*, 2016). Several biochemical techniques are currently used to analyze the circRNA-miRNA interaction, including luciferase reporter assays, AGO2 pulldown, and fluorescence *in situ* hybridization (FISH). Similarly, ribonucleoprotein pulldown assays using an antibody against the predicted RBP and biotin-labeled RNA pulldown assays to capture the target RBPs are used to validate the interaction of circRNA with specific RBPs. However, some of these methods are indirect assays to conclude whether the circRNA is associated with target miRNAs or RBPs. Our previous studies have successfully used circRNA pulldown assays with biotin-labeled antisense oligos targeting the circRNA backsplice junction sequence. Furthermore, circRNA-pulldown followed by RT-qPCR and western blotting analysis identified the miRNA or RBP associated with the circRNA of interest (Abdelmohsen *et al.*, 2017; Panda *et al.*, 2017; Pandey *et al.*, 2020). Here, we adapted the published method to successfully pull down *circHipk2* in BT26 cells. The detailed protocol for the pulldown of circRNA to analyze the associated miRNA or RBP is described here.

Materials and Reagents

1. Nuclease-free 1.5-mL microcentrifuge tubes (Tarson, catalog number: 500010)
2. Nuclease-free 2-mL microcentrifuge tubes (Tarson, catalog number: 500020)
3. 10 µL, 20 µL, 200 µL, and 1 mL tips (Tarson, catalog numbers: 524053, 528101, 528104, 528106)
4. 96-well PCR plates (Thermo Fisher Scientific, catalog number: 4483485)
5. Nuclease-free water (Thermo Fisher Scientific, catalog number: 10977023)
6. 0.25% Trypsin (Thermo Fisher Scientific, catalog number: 25200056)
7. Phosphate-buffered saline (PBS) (Sigma, catalog number: P4417-50TAB)
8. 1 M Tris-HCl, pH 7.5 (Thermo Fisher Scientific, catalog number: 15567027)
9. 1 M Tris-HCl, pH 8.0 (Thermo Fisher Scientific, catalog number: 15568025)
10. 2 M Potassium chloride (Thermo Fisher Scientific, catalog number: AM9640G)
11. 1 M Magnesium chloride (Thermo Fisher Scientific, catalog number: AM9530G)
12. 5 M Sodium chloride (Thermo Fisher Scientific, catalog number: AM9759)
13. Nonidet P-40 (Amresco, catalog number: M158-100ML)
14. 0.5 M EDTA, pH 8.0 (Amresco, catalog number: E177-100ML)
15. Triton X-100 (SRL, catalog number: 64518)
16. Murine RNase inhibitor (NEB, catalog number: M0314S, 40 U/µL)
17. 20× Protease inhibitor (Sigma, catalog number: S8830)
18. Streptavidin Dynabeads (NEB, catalog number: S1420S)
19. TRIzol (Thermo Fisher Scientific, catalog number: 15596018)
20. Ethanol (HiMedia, catalog number: MB228)

21. Chloroform (SRL, catalog number: 96764)
22. Isopropanol (SRL, catalog number: 38445)
23. GlycoBlue™ Coprecipitant (15 mg/mL) (Thermo Fisher Scientific, catalog number: AM9515)
24. Maxima reverse transcriptase (Thermo Fisher Scientific, catalog number: EP0743)
25. dNTP set, 100 mM solutions (Thermo Fisher Scientific, catalog number: R0181)
26. Random primers (Thermo Fisher Scientific, catalog number: 48190011)
27. PowerUp SYBR Green master mix (Thermo Fisher Scientific, catalog number: A25778)
28. MicroAmp optical adhesive film (Thermo Fisher Scientific, catalog number: 4311971)
29. Divergent DNA oligo primers synthesized by SIGMA for PCR amplification of circHipk2 (circHipk2-F: 5'-TCCAGACAACCGTACCGAGT-3' and circHipk2-R: 5'-GGCACTTGATTGAAGGGTGT-3')
30. Custom antisense oligos labeled with biotin-TEG synthesized by SIGMA for control (Ctrl-ASO: 5'-TGCCTAACGAACGACGAATCGTCGCAGATC-3'[BtnTg]) and circHipk2 (circHipk2-ASO: 5'-CATGTGAGGCCATACCGTAGTATCTGGAT-3'[BtnTg])
31. 3× SDS loading dye (NEB, catalog number: B7703S)
32. Polysome extraction buffer (PEB) (see Recipes)
33. 2× Tris, EDTA, NaCl, Triton (TENT) buffer (see Recipes)
34. 1× TENT (see Recipes)

Equipment

1. Manual pipette set, 2 µL, 20 µL, 200 µL, and 1 mL (various manufacturers)
2. Vortex mixer (Tarson, catalog number: 3001)
3. Magnetic stand (Tarson, catalog number: S1509S)
4. Tube rotator (Tarson, catalog number: 3071)
5. Refrigerated centrifuge (Eppendorf, model: 5810R)
6. Benchtop microfuge (Tarson, catalog number: 1010)
7. Thermomixer (Eppendorf, catalog number: 5384000012)
8. PCR machine (various manufacturers)
9. QuantStudio 3 real-time PCR system (Thermo Fisher Scientific, catalog number: A28567)

Software

1. UCSC genome browser (<https://genome.ucsc.edu/>)
2. Primer3 webtool (<https://bioinfo.ut.ee/primer3/>)
3. GeneRunner (<http://www.generunner.net/>)
4. QuantStudio 3 and 5 system software
5. Circinteractome website (<https://circinteractome.nia.nih.gov/>)

Procedure

A. Oligo design

1. Obtain the mature sequence of the circRNA of interest from the RNA sequencing data or the UCSC genome browser using the genome coordinates of backsplice sites. Here, we retrieved the sequence of mouse circHipk2 (chr6|38818229|38819313|-) from the mouse mm10 UCSC genome browser (Figure 1).

Note: The mature splice sequence of multiexonic circRNA can be obtained by combining all the exon

sequences between the genomic coordinates of the backsplice site.

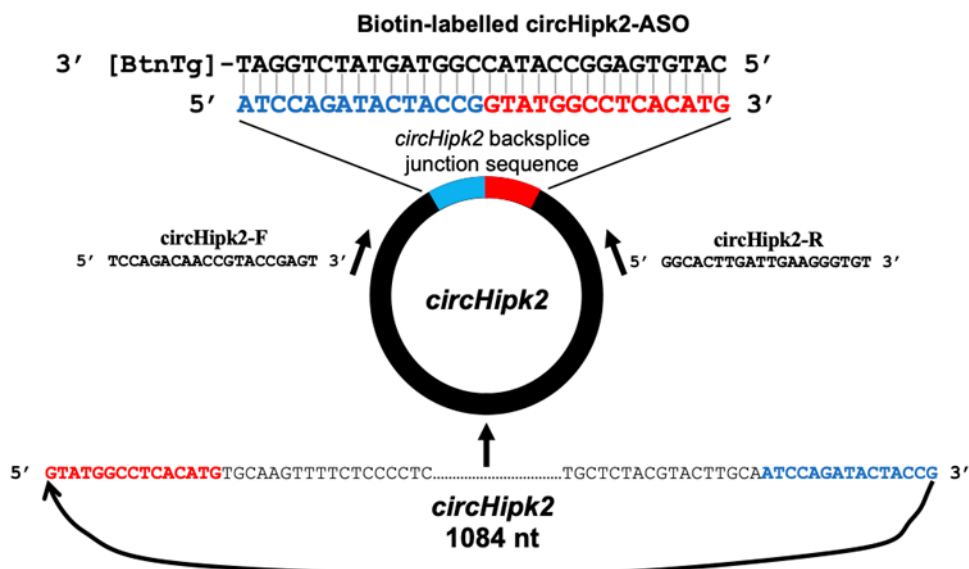


Figure 1. Design of the divergent primers and biotin-labeled antisense oligo targeting *circHipk2*

- As shown in Figure 1, join the last 15 nucleotides of the circRNA sequence to the upstream of the first 15 nucleotides to obtain the 30-nucleotide sequence spanning the circRNA backsplice junction.
- To design ASO, generate the reverse complement sequence of the 30-nucleotide junction sequence using GeneRunner. Have this sequence synthesized with biotin-TEG added to the 3' end by the preferred vendor.
- Design primers for the target housekeeping gene mRNAs or rRNAs using the Primer 3 web tool.
- Design the divergent primer for the target circRNA as described previously (Panda and Gorospe, 2018) or using the circinteractome website for human circRNAs (Dudekula *et al.*, 2016).

B. Cell lysis

- Take one 100-mm dish of ~70% confluent βTC6 cells and discard the culture media.

Note: A minimum of 5 million cells should be used for the pulldown assay. A higher amount of cells may help to obtain better pulldown of rare or low copy number circRNAs.

- Wash the cells three times with 5-10 mL ice-cold 1× PBS.
- Harvest the cells by trypsinization or scraping with a cell scraper.
- Pellet the cells by centrifuging at 1,000 × g for 2 min at 4°C and discard the supernatant.
- Resuspend the cell pellet in 1 ml ice-cold polysome extraction buffer (PEB).

Note: Lysis with PEB releases the cytoplasmic fraction, not the nuclear fraction.

- Immediately add 5 μL RNase inhibitor and 50 μL 20× protease inhibitor.
- Mix well by pipetting ten times and keep on ice for 15 min, pipetting or vortexing for a few seconds every 4-5 min until the cells are lysed.
- Centrifuge the lysate at 12,000 × g for 10 min at 4°C.
- Collect 900 μL supernatant and proceed to the hybridization step (Figure 2).

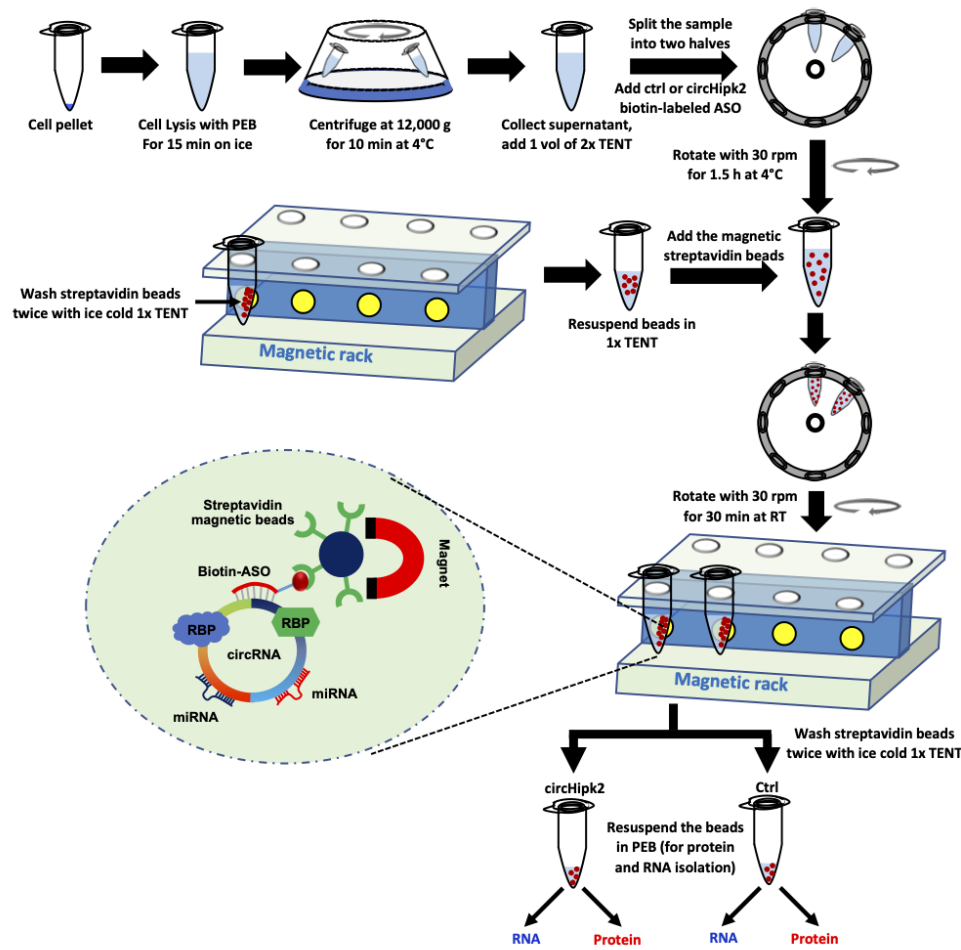


Figure 2. Schematic of the pulldown of circRNA using biotinylated-ASO targeting *circHipk2*

C. Antisense oligo hybridization

1. Add an equal volume (900 µL) of ice-cold 2× Tris, EDTA, NaCl, Triton (TENT) buffer to the supernatant collected in the above step in a 2-mL microcentrifuge tube.
2. Divide the mixture into two tubes (one for the control-ASO pulldown and the other for the circRNA-ASO pulldown).
3. Add 1 µL 100 µM (100 pmol) ctrl-ASO and circRNA-ASO to the control and circRNA pulldown tube, respectively.

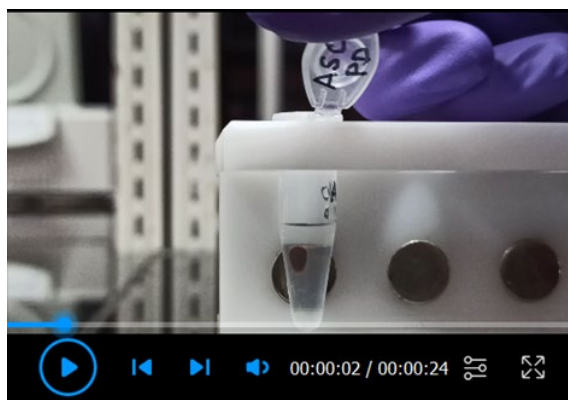
Note: The manufacturer's datasheet gives the streptavidin bead binding capacity. The ASO amount should be less than the streptavidin bead binding capacity for the pulldown in the next step. A higher amount of ASO may reduce the pulldown efficiency.

4. Incubate the reactions on a rotor at 30 rpm for 90 min at 4°C.

Note: The ASO hybridization reaction can be performed at room temperature or at 37°C to facilitate ASO binding to target circRNA; however, this may affect RNA integrity in samples with high levels of endogenous RNase.

D. Streptavidin bead preparation

1. Start the streptavidin bead preparation 15 min before the ASO hybridization step is completed.
2. Mix well and place 100 μ L magnetic streptavidin beads (50 μ L for each reaction) into a new tube.
3. Place the magnetic beads on a magnetic stand for 30 s and discard the supernatant.
4. Resuspend the magnetic beads in 500 μ L ice-cold 1 \times TENT buffer and place the tube on the magnetic stand for 30 s.
5. Rotate the tubes 180° on the magnetic rack twice to wash the beads (Video 1).



Video 1. Magnetic beads washing

6. Discard the supernatant.
7. Repeat the washing steps (Steps D4-D6) twice.
8. Resuspend the magnetic streptavidin beads in 100 μ L ice-cold 1 \times TENT buffer.

E. Circular RNA pulldown

1. Add 50 μ L washed magnetic streptavidin beads into each hybridization reaction tube (mentioned in Step C4) after completing the 90-minute hybridization step.
2. Add 1 μ L RNase inhibitor and 5 μ L 20 \times protease inhibitor to the tubes and mix well by pipetting.
3. Rotate both the control and circRNA ASO tubes at room temperature for 30 min on a tube rotator at 30 rpm.
4. Centrifuge the tubes briefly to bring all the liquid samples to the bottom of the tube without pelleting the beads.

Note: High-speed centrifugation may pellet the beads, which may affect the washing steps.

5. Place the tubes on a magnetic rack for 30 s and discard the supernatant.
6. Resuspend the magnetic beads in 500 μ L ice-cold 1 \times TENT buffer and place the tube on the magnetic stand for 30 s.
7. Rotate the tube twice on the magnetic stand to wash the beads (Video 1).
8. Allow the beads to settle toward the magnet and discard the buffer.
9. Repeat the washing steps (steps 6-8) twice.

Note: The number of washes may be decided depending on the fold enrichment of the target circRNA. We found that two to three washes are suitable to enrich circHipk2 in our pulldown assays.

10. After the last wash, centrifuge the tube for a few seconds to settle the beads at the bottom.

11. Place the tube on the magnetic stand for 30 s and discard the remaining supernatant.
12. Resuspend the beads in 30 μ L ice-cold PEB.
13. Take 15 μ L beads to a fresh tube for RNA isolation and RT-qPCR to analyze the pulldown efficiency of circRNA using the ASO and to detect the circRNA-associated miRNAs.
14. Add 7 μ L 3 \times SDS loading dye to the remaining 15 μ L beads and mix by pipetting, then heat at 95°C for 5 min. This sample can be immediately used for western blotting to identify interacting RBPs or stored at -20°C.

F. RNA and cDNA preparation from the pulldown sample

1. Add 250 μ L TRIzol reagent to the 15 μ L beads for RNA isolation and mix well by pipetting.

Note: Any similar RNA isolation reagent such as TriSure, RNazol, TRI reagent, or TriPure can be used to prepare RNA. Column-based RNA isolation kits should be avoided since miRNAs are not purified well using the standard RNA isolation kits. Otherwise, use a kit that can isolate both long RNAs and miRNAs together.

2. Add 50 μ L chloroform and vortex for 15 s.
3. Centrifuge at 12,000 \times g for 15 min at 4°C, then collect 100 μ L aqueous layer into a new tube.
4. Add 100 μ L isopropanol and 0.5 μ L glycoblu as a co-precipitant.
5. Mix well and keep at room temperature for 10 min, then centrifuge at 12,000 \times g for 10 min at 4°C.
6. Discard the supernatant, add 500 μ L 75% ethanol to the RNA pellet, and vortex the tube for a few seconds.
7. Centrifuge at 12,000 \times g for 5 min at room temperature.
8. Discard the supernatant and air-dry the RNA pellet for 3-5 min with the lid open.

Note: Excessive drying of the RNA pellet or residual ethanol may inhibit the solubility of the pellet.

9. Dissolve the pellet in 20 μ L nuclease-free water. The RNA can be stored at -20°C for future use or used immediately for cDNA synthesis.
10. Prepare a 20- μ L cDNA synthesis reaction containing 13 μ L prepared RNA, 0.5 μ L Maxima reverse transcriptase, 0.5 μ L RNase inhibitor, 1 μ L 10 mM dNTP mix, 1 μ L random primers, and 4 μ L 5 \times RT buffer.

Note: The cDNA can be prepared using any standard reverse transcription kit and random primers.

11. Mix the reaction gently and incubate for 10 min at room temperature followed by 1 h at 50°C.
12. Incubate the reaction at 85°C for 5 min to inactivate the reverse transcriptase.
13. Dilute the cDNA with 250 μ L nuclease-free water. This can be stored at -20°C or used immediately for PCR analysis.

G. circRNA enrichment analysis by RT-Qpcr

1. Mix 10 μ L 100 μ M forward and reverse primer stock with 980 μ L nuclease-free water to obtain a final concentration of 1 μ M primer mix.
2. Prepare 20- μ L reactions in a 96-well plate containing 5 μ L cDNA, 5 μ L primer mix, and 10 μ L 2 \times SYBR Green mix. Three technical replicates should be prepared.
3. Seal the plate with an optical adhesive cover and vortex for a few seconds.
4. Centrifuge the plate for a few seconds to bring the reactions to the bottom of the wells.
5. Perform quantitative PCR on a QuantStudio 3 Real-Time PCR System with the following reaction setup: initial cycle for 2 min at 95°C followed by 40 cycles of 5 s at 95°C and 20 s at 60°C.
6. Obtain the average Ct value of the technical replicates for each target in the control and circRNA

- pulldown samples.
- Calculate the percentage (%) enrichment of the target circRNA in the pulldown sample as compared with the control pulldown sample using the delta-CT method (Figure 3) (Livak and Schmittgen, 2001).

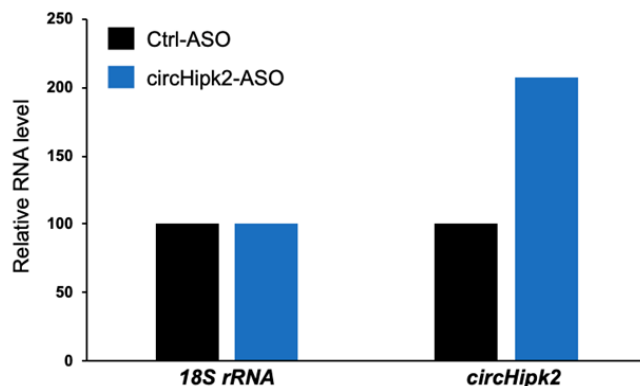


Figure 3. Example data showing the percentage enrichment of *circHipk2* in the circRNA-ASO pulldown sample relative to the control ASO pulldown sample

H. Detection of interacting miRNAs and RBPs

- After confirming the enrichment of target circRNA in the circRNA ASO pulldown sample, associated miRNAs and RBPs can be analyzed.
- The miRNAs associated with the target circRNA can be analyzed by RT-qPCR. The RNA prepared in the above step can be used to produce miRNA cDNA followed by qPCR analysis to study their specific enrichment in the circRNA pulldown samples.
- Perform standard western blotting to detect circRNA-associated RBPs. Briefly, subject the input, control ASO, and circRNA ASO pulldown samples mixed with SDS dye to SDS-PAGE, and transfer the proteins to nitrocellulose membrane. Incubate the membrane with primary antibody against the predicted RBP followed by the appropriate secondary antibody and detect the chemiluminescence signals.

Data analysis

This method describes circular RNA pulldown using an antisense oligo specifically targeting the backsplice junction sequence of the target circRNA. However, the success of this pulldown assay depends on the availability of the circRNA junction sequence, which may be inaccessible due to secondary structures or junction-interacting RBPs, preventing the ASO from binding. Moreover, the PEB used for cell lysis is good for releasing the cytoplasmic fraction, while lysis of the nucleus for the pulldown of nuclear-localized circRNAs remains to be standardized. Since most circRNAs are cytoplasmic in nature (Jeck *et al.*, 2013), we used PEB for the cell lysis and pulldown assay. Use the delta-Ct method to analyze the enrichment of target circRNA in the circRNA ASO pulldown sample compared with the control pulldown using a loading control such as *18S rRNA* or *Gapdh* mRNA (Livak and Schmittgen, 2001). As shown in Figure 3, the *circHipk2* levels are more than 2-fold higher in the *circHipk2* ASO pulldown than in the control ASO pulldown. Alternatively, the efficiency of circRNA pulldown can be measured by comparing the pulldown samples with the flow through or input. After checking the enrichment of circRNA in the pulldown samples, the remaining RNA can be subjected to miRNA RT-qPCR analysis to check for the specific enrichment of miRNAs predicted to interact with the circRNA of interest. Furthermore, the other half of the pulldown sample may be used for western blotting analysis to evaluate the RBPs associated with the target circRNA. This is a promising method to pulldown the circular RNA of interest and study the circRNA-associated miRNAs.

and RBPs, which are critical factors for circRNA-mediated gene regulation.

Recipes

1. Lysis buffer

Reagent	Stock	Vol required for 250 mL
20 mM Tris-HCl, pH 7.5	1 M	5 ml
100 mM KCl	2 M	12.5 ml
5 mM MgCl ₂	1 M	1.25 ml
0.5% Nonidet P-40	10%	12.5 ml

Adjust the volume to 250 mL with nuclease-free water

2. 2× Tris, EDTA, NaCl, Triton (TENT) buffer

Reagent	Stock	Vol required for 250 mL
20 mM Tris-HCl pH 8.0	1 M	2 ml
2 mM EDTA pH 8.0	0.5 M	0.4 ml
500 mM NaCl	5 M	10 ml
1% v/v Triton X-100	20%	5 ml

Adjust the volume to 100 mL with nuclease-free water

3. 1× TENT

Mix equal volumes of PEB/water and 2× TENT

Acknowledgments

This research was supported by intramural funding from the Institute of Life Sciences and the Wellcome Trust/DBT India Alliance Intermediate Fellowship (IA/I/18/2/504017) provided to ACP. DD and AD were supported by Junior Research Fellowships from the University Grant Commission, India. This protocol was adapted from previously published papers (Abdelmohsen *et al.*, 2017 and Panda *et al.*, 2017). The authors thank our colleagues at the Institute of Life Sciences, Bhubaneswar, for proofreading the article.

Competing interests

The authors declare no conflict of interest.

References

- Abdelmohsen, K., Panda, A. C., Munk, R., Grammatikakis, I., Dudekula, D. B., De, S., Kim, J., Noh, J. H., Kim, K. M., Martindale, J. L. and Gorospe, M. (2017). [Identification of HuR target circular RNAs uncovers suppression of PABPN1 translation by CircPABPN1](#). *RNA Biol* 14(3): 361-369.

- Dudekula, D. B., Panda, A. C., Grammatikakis, I., De, S., Abdelmohsen, K. and Gorospe, M. (2016). [CircInteractome: A web tool for exploring circular RNAs and their interacting proteins and microRNAs](#). *RNA Biol* 13(1): 34-42.
- Guria, A., Sharma, P., Natesan, S. and Pandi, G. (2019). [Circular RNAs-The Road Less Traveled](#). *Front Mol Biosci* 6: 146.
- Jeck, W. R., Sorrentino, J. A., Wang, K., Slevin, M. K., Burd, C. E., Liu, J., Marzluff, W. F. and Sharpless, N. E. (2013). [Circular RNAs are abundant, conserved, and associated with ALU repeats](#). *RNA* 19(2): 141-157.
- Livak, K. J. and Schmittgen, T. D. (2001). [Analysis of relative gene expression data using real-time quantitative PCR and the 2-ΔΔCT Method](#). *Methods* 25(4): 402-408.
- Palazzo, A. F. and Lee, E. S. (2015). [Non-coding RNA: what is functional and what is junk?](#) *Front Genet* 6: 2.
- Panda, A. C. and Gorospe, M. (2018). [Detection and Analysis of Circular RNAs by RT-PCR](#). *Bio Protoc* 8(6): e3241.
- Panda, A. C., Grammatikakis, I., Kim, K. M., De, S., Martindale, J. L., Munk, R., Yang, X., Abdelmohsen, K. and Gorospe, M. (2017). [Identification of senescence-associated circular RNAs \(SAC-RNAs\) reveals senescence suppressor CircPVT1](#). *Nucleic Acids Res* 45(7): 4021-4035.
- Pandey, P. R., Yang, J. H., Tsitsipatis, D., Panda, A. C., Noh, J. H., Kim, K. M., Munk, R., Nicholson, T., Hanniford, D., Argibay, D., Yang, X., Martindale, J. L., Chang, M. W., Jones, S. W., Hernando, E., Sen, P., De, S., Abdelmohsen, K. and Gorospe, M. (2020). [circSamd4 represses myogenic transcriptional activity of PUR proteins](#). *Nucleic Acids Res* 48(7): 3789-3805.
- Vromman, M., Vandesompele, J. and Volders, P. J. (2021). [Closing the circle: current state and perspectives of circular RNA databases](#). *Brief Bioinform* 22(1): 288-297.

Modeling the Nonlinear Dynamics of Intracellular Signaling Networks

Oleksii S. Rukhlenko¹ and Boris N. Kholodenko^{1, 2, 3, *}

¹Systems Biology Ireland, School of Medicine and Medical Science, University College Dublin, Belfield, Dublin 4, Ireland;

²Conway Institute of Biomolecular & Biomedical Research, University College Dublin, Belfield, Dublin 4, Ireland;

³Department of Pharmacology, Yale University School of Medicine, New Haven, USA

*For correspondence: boris.kholodenko@ucd.ie

Abstract

This protocol illustrates a pipeline for modeling the nonlinear behavior of intracellular signaling pathways. At fixed spatial points, nonlinear signaling dynamics are described by ordinary differential equations (ODEs). At constant parameters, these ODEs may have multiple attractors, such as multiple steady states or limit cycles. Standard optimization procedures fine-tune the parameters for the system trajectories localized within the basin of attraction of only one attractor, usually a stable steady state. The suggested protocol samples the parameter space and captures the overall dynamic behavior by analyzing the number and stability of steady states and the shapes of the assembly of nullclines, which are determined as projections of quasi-steady-state trajectories into different 2D spaces of system variables. Our pipeline allows identifying main qualitative features of the model behavior, perform bifurcation analysis, and determine the borders separating the different dynamical regimes within the assembly of 2D parametric planes. Partial differential equation (PDE) systems describing the nonlinear spatiotemporal behavior are derived by coupling fixed point dynamics with species diffusion.

Keywords: Cell signaling, Nonlinear dynamics, Multistability, Oscillations, Bifurcations, Ordinary and partial differential equations

This protocol was validated in: eLife (2020), DOI: 10.7554/eLife.58165

Background

Here, we present a protocol for computational analysis of the nonlinear dynamic behavior of signaling networks and their transitions between different dynamic regimes. The dynamics of spatially homogenous biochemical systems are described by ordinary differential equations (ODE), whereas the spatiotemporal dynamics are described by partial differential equation (PDE) systems. Knowledge about ODE and PDE is needed as a prerequisite for understanding this protocol. Our computational protocol analyzes the systems' dynamics at fixed spatial points, and it considers the nonlinear spatiotemporal behavior by coupling fixed point dynamics with species diffusion (Tsyganov *et al.*, 2012; Bolado-Carrancio *et al.*, 2020). A variable x_i that is the concentration or activity of each network node i depends on the time (t) in an ODE system and on both the time and the spatial coordinates in a PDE system. The described protocol operates with the already established interaction topology of the signaling network under study; that is, for each node i it is known what nodes activate and/or inhibit it. Mathematically, the network topology is determined by the signed incidence matrix of the ODE system,

$$\frac{dx_i}{dt} = f_i(x_1, \dots, x_n), \quad i = 1, 2, \dots, n \quad (1).$$

If node j activates or inhibits node i ($\partial f_i / \partial x_j > 0$ or $\partial f_i / \partial x_j < 0$, respectively), the element (i, j) of the signed incidence matrix equals 1 or -1, respectively, and it equals zero if node j does not affect node i .

Traditional modeling pipelines for ODE systems use parameter optimization procedures, which rely on the fitting of simulated trajectories to experimental data points, and then study the behavior of a calibrated model (Glover *et al.*, 2000; Maiwald and Timmer, 2008; Kreutz and Timmer, 2009; Penas *et al.*, 2015; Thomas *et al.*, 2016; Degasperis *et al.*, 2017; Mitra *et al.*, 2018 and 2019). These pipelines produce satisfactory results when the system under study has a single stable steady state or when the system trajectories are within the basin of attraction of a stable steady state for bistable or multistable biochemical systems. Recently, parameter optimization procedures have been applied to calibrate oscillatory processes and to search for oscillatory and bistable mass-action networks (Pitt and Banga, 2019; Porubsky and Sauro, 2019). However, for biological systems with multiple attractors – such as steady-state focus nodes, limit cycles, or more complex chaotic structures, which can co-exist at the same parameter values – the use of standard parameter optimization pipelines that fit time-series data might be extremely challenging. Also, systems of higher than 2D dimensions can potentially exhibit chaotic dynamics, typically happening according to one of the following scenarios: (i) period-doubling bifurcations, (ii) a transition to chaos through intermittency, and (iii) chaotization of quasi-periodic dynamics (i.e., through the destruction of multidimensional tori) (Argyris *et al.*, 1993; Kuznetsov, 2012).

Key aspects of the behavior of 2D dynamic systems are determined by the shapes of the nullclines (Tsyganov *et al.*, 2012). Likewise, when a high-dimensional system does not exhibit the chaotic behavior, the assembly of nullclines that are projections of quasi-steady-state (QSS) trajectories into different 2D spaces help us understand the intricate system dynamics. To obtain the QSS trajectories, we change only one variable, whereas all other variables became implicit functions of that variable. Parameter optimization software packages developed for systems biology do not operate with nullclines. A critical feature of our computational pipeline is a combination of intensive sampling of the parameters space, identification of the number and stability of steady states, and the calculation and analysis of nullclines. Only when the key properties of nullclines are determined, the standard fitting software [e.g., BioNetFit (Thomas *et al.*, 2016; Mitra *et al.*, 2019) or PEPSSBI (Degasperis *et al.*, 2017)] is used for fine-tuning of the parameters. After the dynamic regimes of the reduced 2D systems are established, the behavior of the original, high-dimensional system is investigated in the vicinity of attractors found for reduced systems. This pipeline allows developing predictive models of such systems in a semi-automatic regime.

A schematic diagram highlighting the main steps of the proposed protocol is shown in Figure 1. The process consists of five successive stages:

1. Build an ODE model of the signaling network and constrain the parameter ranges using the available data on the protein abundances and kinetic constants.
2. Using a software package, e.g., the DYVIPAC package (Nguyen *et al.*, 2015), which uses the libroadrunner library (Somogyi *et al.*, 2015) for importing and solving ODE models, sample the parameter space, determine the number and stability of steady states for a given set of parameters, and analyze the shapes of nullclines by projecting the QSS trajectories into different 2D planes.
3. Scan 2D parametric planes and determine the types of bifurcations that occur in the system.

4. If for given dynamic regimes the system trajectories are measured, fine-tune the parameters to minimize deviations of simulated trajectories from the measured time series data using local search algorithms [e.g., simplex from BioNetFit package (Mitra *et al.*, 2019)].
5. Based on the established dynamic regimes that often differ in distinct spatial regions, formulate a PDE system and perform spatial calculations.

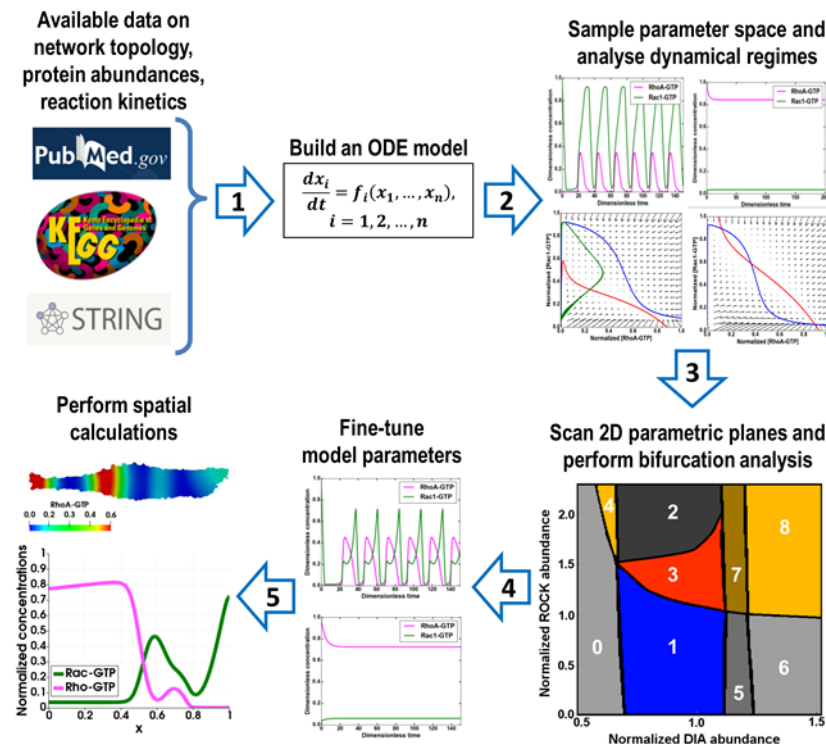


Figure 1. Protocol overview. Consecutive steps of the protocol are indicated by arrows.

Equipment

1. Laptop computer

Proposed protocols can be implemented on a laptop computer; however, parameter sampling procedure is time-consuming, and using a computational cluster is advantageous. For example, sampling parameter space of the model (Bolado-Carrancio *et al.*, 2020) to obtain a comprehensive list of different regimes took approximately 5 days at a workstation with 4-core Intel® Core™ i7 Processor. The high-quality scan of 2D parametric plane takes approximately 5 hours given the same computational power. Because the sampling procedures are very well parallelized, the computational time is inversely proportional to the number of available cores.

Since most computational clusters use Linux-based operating systems, we further refer to software packages mainly developed for Linux.

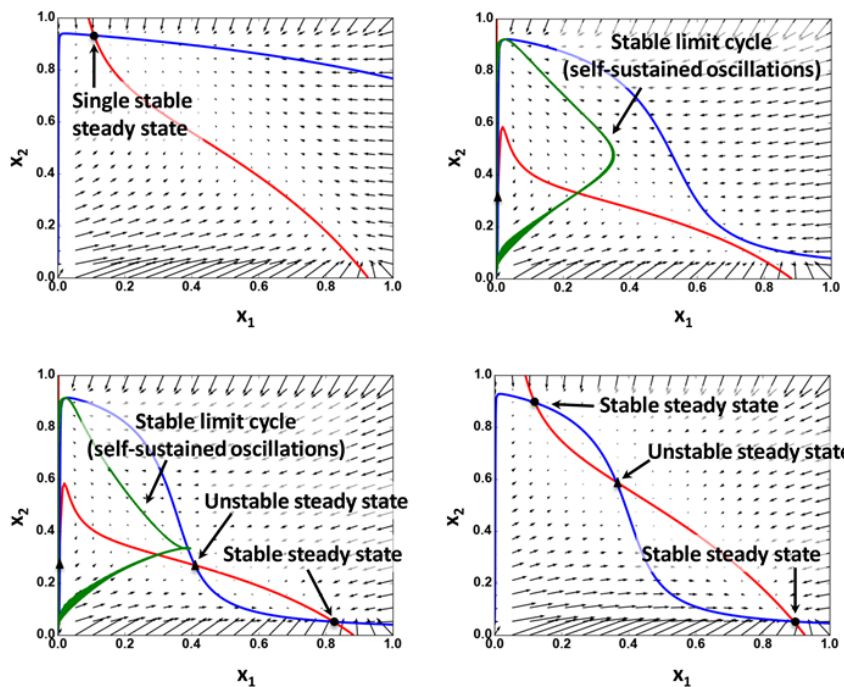
Software

1. Python and python libraries, including matplotlib (Hunter, 2007), NumPy (Harris *et al.*, 2020), and scipy (Virtanen *et al.*, 2020)
2. Python version of DYVIPAC software package (Nguyen *et al.*, 2015)

3. Software for parameter fitting of ODE systems, e.g., BioNetFit (Thomas *et al.*, 2016; Mitra *et al.*, 2019), PEPSSBI (Degasperis *et al.*, 2017), etc.
4. Software for performing spatiotemporal calculations of reaction-diffusion-convection models, e.g., FiPy (Guyer *et al.*, 2009), OpenFOAM (Jasak, 2009; OpenCFD, 2009) or Virtual Cell (Loew and Schaff, 2001)

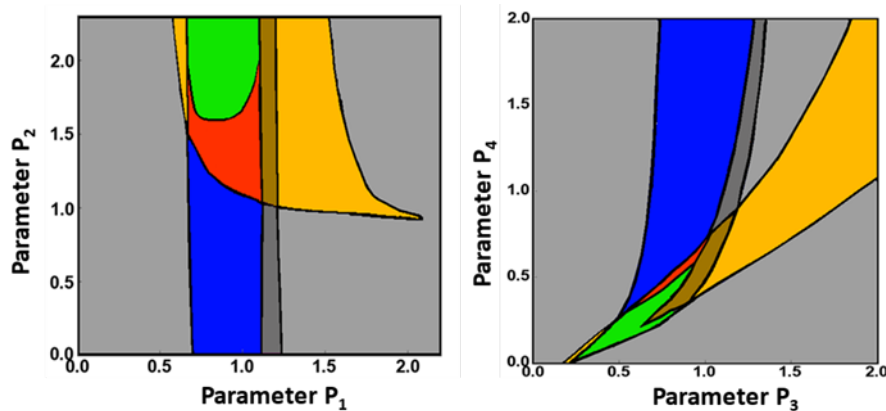
Procedure

1. Build an ODE model of the signaling network based on the available topology of interactions between nodes. Implement the model in a software package that supports export to the SBML format, such as COPASI (Hoops *et al.*, 2006) or BioNetGen (Blinov *et al.*, 2004; Harris *et al.*, 2016).
 - a. If the kinetics of interactions between two nodes is known, this network connection is modeled mechanistically.
 - b. For other connections, the interaction kinetics might not yet be exact mechanistically characterized, or these connections operate via intermediate species that are not included in the network under study. These connections are modeled using hyperbolic multipliers α_{ij} that specify the negative or positive influence of the activity (x_j) of node j on the activity (x_i) of node i (Tsyganov *et al.*, 2012; Bolado-Carrancio *et al.*, 2020),
$$\alpha_{ij} = \frac{1 + \gamma_{ij} \cdot x_j / K_j}{1 + x_j / K_j} \quad (2).$$
The coefficient $\gamma_{ij} > 1$ indicates activation; $\gamma_{ij} < 1$ inhibition; and $\gamma_{ij} = 1$ denotes the absence of regulatory interactions, in which case the modifying multiplier α_{ij} equals 1. K_{ij} is the activation or inhibition constant.
 - c. Specify the parameter ranges using the data on the protein abundances and kinetic constants and assign numerical values to model parameters.
 - d. Non-dimensionalize the model to reduce the number of parameters (Barenblatt, 2003).
 - e. Export the model to SBML format.
2. Determine dynamical regimes that can be observed in the system.
 - a. Import the sbml-file of the model into the DYVIPAC package. Sample parameter space of the model using the DYVIPAC package, which determines the number and stability of steady states for a given set of parameters.
 - b. Rank protein abundances in a model in descending order and pick two proteins (nodes) with the highest abundance. Using the QSS approximation for the other protein activities (Sauro and Kholodenko, 2004; Eilertsen and Schnell, 2020), derive a 2D model from the initial ODE model.
 - c. Based on the specification of the steady states and the analysis of the shapes of nullclines (Figure 2, for example), determine the dynamic regimes and validate these regimes by the integration of ODEs.

**Figure 2. Examples of the nullcline analysis.**

Nullclines and vector fields calculated for 2D ODE system are derived from a five-dimensional ODE system using a quasi-steady-state approximation. Circles show stable steady states; triangles represent unstable steady states. Red and blue curves are nullclines for variables x_1 and x_2 , respectively. Green line represents trajectories of limit cycles projected from the original five-dimensional system to 2D space of x_1 and x_2 [see Bolado-Carrancio *et al.* (2020) for details].

- d. If more than two proteins have high and comparable abundances, make a list of pairs of these proteins and apply the above point c) to the ODE system for each pair.
3. Scan 2D parametric planes and determine the types of bifurcations that can occur in the system.
 - a. Scan the parameter planes and determine the borders that separate different dynamic regimes (see Figure 3, for example). This step can predict the previously unobserved dynamic regimes, which must be validated in the experiments.

**Figure 3. Examples of 2D parametric scans.**

Different 2D parametric diagrams obtained using scanning of 2-parameter planes. Different colors indicate different dynamical regimes. Black lines represent borders between these regimes where bifurcations happen (see Bolado-Carrancio *et al.*, 2020 for details and Figure 2 there).

- b. The analysis of the changes in the number and stability of steady states can reveal local bifurcations, such as the Andronov-Hopf or saddle-node bifurcations (Kuznetsov, 2004). However, non-local bifurcations might exist in a 2D system where a limit cycle can appear or vanish (Nekorkin, 2015). Scan the parameters for dynamic regimes that contain focuses to determine the appearance or annihilation of limit cycles.
4. If there are time-series data, fine-tune model parameters to reproduce the system trajectories for a biologically relevant regime. This step uses standard software packages for parameter optimization (Glover *et al.*, 2000; Maiwald and Timmer, 2008; Kreutz and Timmer, 2009; Penas *et al.*, 2015; Thomas *et al.*, 2016; Degasperis *et al.*, 2017; Mitra *et al.*, 2018 and 2019).
5. Derive a PDE system by adding the terms describing mass transfer processes such as diffusion and convection to the ODE system studied (Tsyganov *et al.*, 2012; Bolado-Carrancio *et al.*, 2020). Perform spatiotemporal simulations using specific software packages, such as OpenFOAM, FiPy, or Virtual Cell.

A set of examples that illustrate the analysis of the dynamics of the RhoA-Rac1 signaling network model and python scripts can be found in “examples.zip” archive.

Acknowledgments

This protocol was adapted from Tsyganov *et al.* (2012) and Bolado-carrancio *et al.* (2020). This work was supported by NIH/NCI grant R01CA244660 and EU grant NanoCommons (grant no. 731032).

Competing interests

The authors declare no conflict of interest.

References

- Argyris, J., Faust, G., and Haase, M. (1993). [Routes to Chaos and Turbulence. A Computational Introduction](#). In: *Philosophical Transactions of the Royal Society of London. Series A: Physical and Engineering Sciences* 344: 207-234.
- Barenblatt, G. I. (2003). [Scaling](#). Cambridge University Press, Cambridge.
- Blinov, M. L., Faeder, J. R., Goldstein, B. and Hlavacek, W. S. (2004). [BioNetGen: software for rule-based modeling of signal transduction based on the interactions of molecular domains](#). *Bioinformatics* 20(17): 3289-3291.
- Bolado-Carrancio, A., Rukhlenko, O. S., Nikonova, E., Tsyganov, M. A., Wheeler, A., Garcia-Munoz, A., Kolch, W., von Kriegsheim, A. and Kholodenko, B. N. (2020). [Periodic propagating waves coordinate RhoGTPase network dynamics at the leading and trailing edges during cell migration](#). *Elife* 9: e58165.
- Degasperis, A., Fey, D. and Kholodenko, B. N. (2017). [Performance of objective functions and optimisation procedures for parameter estimation in system biology models](#). *NPJ Syst Biol Appl* 3: 20.
- Eilertsen, J. and Schnell, S. (2020). [The quasi-steady-state approximations revisited: Timescales, small parameters, singularities, and normal forms in enzyme kinetics](#). *Math Biosci* 325: 108339.
- Glover, F., Laguna, M. and Martí, R. (2000). [Fundamentals of scatter search and path relinking](#). *Control and Cybernetics* 29: 652-684.
- Guyer, J.E., Wheeler, D. and Warren, J. A. (2009). [FiPy: Partial Differential Equations with Python](#). *Comput Sci Eng* 11(3): 6-15.

- Harris, C. R., Millman, K. J., van der Walt, S. J., Gommers, R., Virtanen, P., Cournapeau, D., Wieser, E., Taylor, J., Berg, S., Smith, N. J., Kern, R., Picus, M., Hoyer, S., van Kerkwijk, M. H., Brett, M., Haldane, A., Del Rio, J. F., Wiebe, M., Peterson, P., Gerard-Marchant, P., Sheppard, K., Reddy, T., Weckesser, W., Abbasi, H., Gohlke, C. and Oliphant, T. E. (2020). [Array programming with NumPy](#). *Nature* 585(7825): 357-362.
- Harris, L. A., Hogg, J. S., Tapia, J. J., Sekar, J. A., Gupta, S., Korsunsky, I., Arora, A., Barua, D., Sheehan, R. P. and Faeder, J. R. (2016). [BioNetGen 2.2: advances in rule-based modeling](#). *Bioinformatics* 32(21): 3366-3368.
- Hoops, S., Sahle, S., Gauges, R., Lee, C., Pahle, J., Simus, N., Singhal, M., Xu, L., Mendes, P. and Kummer, U. (2006). [COPASI--a COmplex PATHway SIMulator](#). *Bioinformatics* 22(24): 3067-3074.
- Hunter, J. D. (2007). [Matplotlib: A 2D Graphics Environment](#). *Comput Sci Eng* 9(3): 90-95.
- Jasak, H. (2009). [OpenFOAM: Open source CFD in research and industry](#). *Int J Nav Archit Ocean Eng* 1(2): 89-94.
- Kreutz, C. and Timmer, J. (2009). [Systems biology: experimental design](#). *FEBS J* 276(4): 923-942.
- Kuznetsov, Y. A. (2004). [Elements of applied bifurcation theory](#). (3rd Edition). Springer.
- Kuznetsov, S. P. (2012). [Hyperbolic Chaos: A Physicist's View](#). Springer.
- Loew, L. M. and Schaff, J. C. (2001). [The Virtual Cell: a software environment for computational cell biology](#). *Trends Biotechnol* 19(10): 401-406.
- Maiwald, T. and Timmer, J. (2008). [Dynamical modeling and multi-experiment fitting with PottersWheel](#). *Bioinformatics* 24(18): 2037-2043.
- Mitra, E.D., Dias, R., Posner, R.G., and Hlavacek, W.S. (2018). [Using both qualitative and quantitative data in parameter identification for systems biology models](#). *Nat Commun* 9: 3901.
- Mitra, E. D., Suderman, R., Colvin, J., Ionkov, A., Hu, A., Sauro, H. M., Posner, R. G. and Hlavacek, W. S. (2019). [PyBioNetFit and the Biological Property Specification Language](#). *iScience* 19: 1012-1036.
- Nekorkin, V. I. (2015). [Chapter 9: Bifurcations of Limit Cycles. Saddle Homoclinic Bifurcation](#). In: *Introduction to Nonlinear Oscillations*. 113-122. John Wiley & Sons, Inc.
- Nguyen, L. K., Degasperis, A., Cotter, P. and Kholodenko, B. N. (2015). [DYVIPAC: an integrated analysis and visualisation framework to probe multi-dimensional biological networks](#). *Sci Rep* 5: 12569.
- OpenCFD. (2009). [OpenFOAM. The Open Source CFD Toolbox. User Guide](#). OpenCFD Limited.
- Penas, D. R., Banga, J. R., González, P. and Doallo, R. (2015). [Enhanced parallel Differential Evolution algorithm for problems in computational systems biology](#). *Appl Soft Comput* 33: 86-99.
- Pitt, J. A. and Banga, J. R. (2019). [Parameter estimation in models of biological oscillators: an automated regularised estimation approach](#). *BMC Bioinformatics* 20(1): 82.
- Porubsky, V. L., and Sauro, H. M. (2019). [Application of parameter optimization to search for oscillatory mass-action networks using python](#). *Processes* 7(163): 163.
- Sauro, H. M. and Kholodenko, B. N. (2004). [Quantitative analysis of signaling networks](#). *Prog Biophys Mol Biol* 86(1): 5-43.
- Somogyi, E. T., Bouteiller, J. M., Glazier, J. A., Konig, M., Medley, J. K., Swat, M. H. and Sauro, H. M. (2015). [libRoadRunner: a high performance SBML simulation and analysis library](#). *Bioinformatics* 31(20): 3315-3321.
- Thomas, B. R., Chylek, L. A., Colvin, J., Sirimulla, S., Clayton, A. H., Hlavacek, W. S. and Posner, R. G. (2016). [BioNetFit: a fitting tool compatible with BioNetGen, NFsim and distributed computing environments](#). *Bioinformatics* 32(5): 798-800.
- Tsyganov, M. A., Kolch, W. and Kholodenko, B. N. (2012). [The topology design principles that determine the spatiotemporal dynamics of G-protein cascades](#). *Mol Biosyst* 8(3): 730-743.
- Virtanen, P., Gommers, R., Oliphant, T. E., Haberland, M., Reddy, T., Cournapeau, D., Burovski, E., Peterson, P., Weckesser, W., Bright, J., van der Walt, S. J., Brett, M., Wilson, J., Millman, K. J., Mayorov, N., Nelson, A. R. J., Jones, E., Kern, R., Larson, E., Carey, C. J., Polat, I., Feng, Y., Moore, E. W., VanderPlas, J., Laxalde, D., Perktold, J., Cimrman, R., Henriksen, I., Quintero, E. A., Harris, C. R., Archibald, A. M., Ribeiro, A. H., Pedregosa, F., van Mulbregt, P. and SciPy, C. (2020). [SciPy 1.0: fundamental algorithms for scientific computing in Python](#). *Nat Methods* 17(3): 261-272.

Fe-NTA Microcolumn Purification of Phosphopeptides from Immunoprecipitation (IP) Eluates for Mass Spectrometry Analysis

Ethan J. Sanford and Marcus B. Smolka*

Department of Molecular Biology and Genetics, Weill Institute for Cell and Molecular Biology, Cornell University, Ithaca, NY 14853, USA

*For correspondence: mbs266@cornell.edu

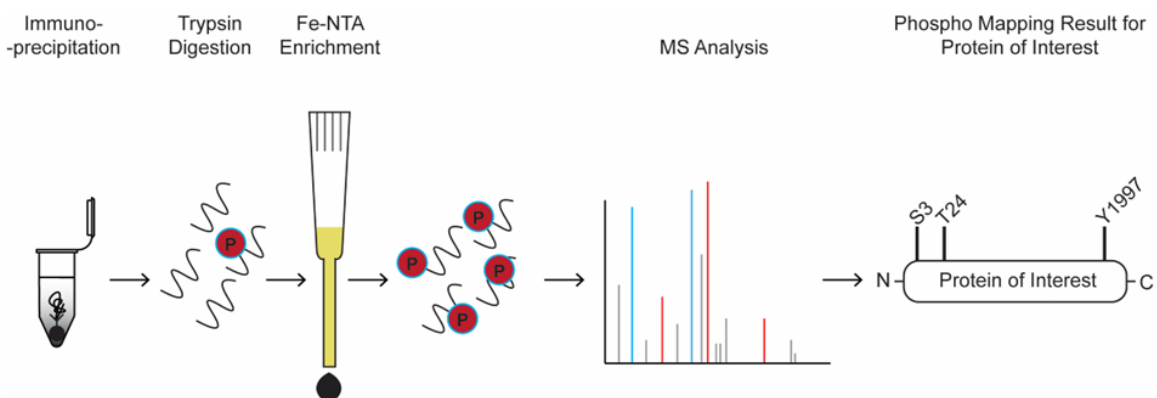
Abstract

Protein phosphorylation is a nearly universal signaling mechanism. To date, a number of proteomics tools have been developed to analyze phosphorylation. Phosphoproteome-wide analyses using whole cell extracts suffer from incomplete coverage, often missing phosphorylation events from low-abundance proteins. In order to increase coverage of phosphorylation sites on individual proteins of interest (“phospho-mapping”), immunoprecipitation (IP) followed by phosphoenrichment is necessary. Unfortunately, most commercially available phosphoenrichment kits are not readily scalable to the low-microgram quantities of protein present in IP eluates. Here, we describe a simple method specifically optimized for the enrichment of phosphopeptides from IP samples using an Fe-NTA based method. This method can be added downstream of any standard immunoprecipitation protocol and upstream of any MS analysis pipeline. The protocol described herein is cost effective, uses commonly available laboratory reagents, and can be used to obtain deep coverage of individual protein phosphorylation patterns, supplementary to phosphoproteomics data.

Keywords: Mass Spectrometry, Phosphorylation, Immunoprecipitation, Phosphoproteomics, Phosphopeptide

This protocol was validated in: Genes Dev (2018), DOI: 10.1101/gad.308148.117.

Graphical Abstract:



Phospho-mapping workflow for a hypothetical protein of interest

Background

Phosphorylation regulates key cellular processes such as transcription, translation, nutrient sensing, and the DNA damage response (Gingras *et al.*, 2001; Chapman *et al.*, 2007; Ohouo *et al.*, 2010; Kim *et al.*, 2011; Cussiol *et al.*, 2015). Given the ubiquity of protein phosphorylation, its importance in normal cellular function, and its potential for dysregulation in disease, a number of proteomics methods have been developed to identify and quantitate phosphorylation events (Dephoure *et al.*, 2013; Humphrey *et al.*, 2018; Li *et al.*, 2019; Faca *et al.*, 2020). Many of these methods for phosphopeptide purification and analysis are performed on the proteome-wide scale and may suffer from relatively low coverage of individual proteins, especially those with limited abundance. High coverage of phosphorylation sites in individual proteins is often necessary to comprehensively study a given protein and to increase the chances of generating mutations of phospho-acceptor residues that elicit a phenotype. One strategy of increasing coverage of individual proteins is to first conduct an immunoprecipitation (IP) of the protein of interest using either an antibody raised against the protein itself or a common recombinant tag such as FLAG, HA, or V5. Phosphopeptides can then be isolated from the IP eluate. Optionally, differences in phosphorylation patterns between mutants or treatments can be analyzed using quantitative mass spectrometry methods such as SILAC or TMT (Ong *et al.*, 2002; Zhang and Elias, 2017).

There are a number of commercially available kits for phosphopeptide enrichment, although these are difficult to scale down to the low-microgram quantities of protein yielded by immunopurification. There is a paucity of existing protocols for phosphopeptide enrichment following immunopurification, and those that do exist often require costly titanium dioxide (TiO_2) reagents, making it difficult to scale up to multiple IPs across a panel of bait proteins (Breitkopf and Asara, 2012). Iron-based phospho-enrichment takes advantage of the affinity of negatively charged phosphate groups toward Fe^{3+} cations and is a cheaper alternative to TiO_2 ; indeed, even where TiO_2 is feasible, iron-based resin can be used to collect additional phospho-site data since the two methods display different phosphopeptide specificities (Bodenmiller *et al.*, 2007).

The protocol described herein uses readily available Ni-NTA silica-based resin columns. The NTA-coupled resin is stripped of nickel, loaded with iron, and finally, the IP eluate is passed over the Fe-NTA resin to isolate phosphorylated peptides and remove unphosphorylated peptides. The procedure is performed using a home-made column (a gel-loading tip). The amount of resin generated from one Ni-NTA column is sufficient for 4-5 enrichments, making this protocol highly cost effective. Reproducibility is internally monitored via the inclusion of α/β casein phosphopeptides as controls for phosphopeptide enrichment. While this protocol has been primarily used for immunopurifications from yeast and mammalian cells, it is usable for any organism for which antibodies or

recombinant tagging are available.

Materials and Reagents

1. C18 Sep-Pak column (Waters, catalog number: WAT043395)
2. Capillary tubing, 125 µm inner diameter (Polymicro, catalog number: 1068151718)
3. Centrifuge tubes, 50 mL (VWR, catalog number: 21008-178 or similar)
4. Glass fiber (Corning, catalog number: UX-34552-01)
5. Gel-loading pipette tips 1-200 µL (Fisher, catalog number: 02-707-138)
6. Low-protein binding microcentrifuge tubes, 1.5 mL (Eppendorf, catalog number: 022431081)
7. Microcentrifuge tubes, 1.5 mL (Eppendorf, catalog number: 0030108442)
8. Micro-spin columns (Thermo, catalog number: 89879)
9. Kimwipes (Fisher, catalog number: 06-666-1A)
10. Parafilm (VWR, catalog number: 52858-076)
11. Qiagen Ni-NTA spin columns (Qiagen, catalog number: 31014)
12. Razor blades (VWR, catalog number: 55411-055)
13. Sample vials (Sun SRI, catalog number: 501-300)
14. Sample vial snap caps, 11 mm (Fisher, catalog number: 14-823-379)
15. Acetic acid (Fisher, catalog number: A38S-500)
16. Acetone (Fisher, catalog number: A11-1)
17. Acetonitrile (Fisher, catalog number: A998-1)
18. Alpha casein (Sigma, catalog number: C6780-250MG)
19. Ammonium hydroxide solution (Sigma, catalog number: 205840010)
20. Angiotensin II peptide (Sigma, catalog number: A9525-5MG)
21. Beta casein (Sigma, catalog number: C6905-250MG)
22. Dithiothreitol (Sigma, catalog number: 1019777001)
23. Ethanol (VWR, catalog number: 89125-186)
24. Ethylenediamine tetraacetic acid (VWR, catalog number: MK258012)
25. Formic acid (Sigma, catalog number: 33015-500ML)
26. Iodoacetamide (Sigma, catalog number: I1149-5G)
27. Iron (III) chloride hexahydrate (Honeywell, catalog number: 236489-500G)
28. NaCl (Promega, catalog number: PRH5273)
29. Sodium dodecyl sulfate (Sigma, catalog number: L3771-100G)
30. Target polypropylene conical insert (Thermo, catalog number: C4010-629P)
31. Trifluoroacetic acid (Thermo, catalog number: 28904)
32. Tris base (Fisher, catalog number: BP152-500)
33. Trypsin Gold, mass spectrometry grade (Promega, catalog number: V5280)
34. Urea (Fisher, catalog number: U15-500)
35. Urea/Tris solution (see Recipes)
36. α/β casein peptide digest (see Recipes)
37. 0.1 P solution (see Recipes)
38. Trypsin Gold solution (see Recipes)
39. C18 Buffer E (see Recipes)
40. C18 Buffer W1 (see Recipes)
41. C18 Buffer W2 (see Recipes)
42. C18 Buffer W3 (see Recipes)
43. FeCl₃ solution (see Recipes)
44. IMAC elution solution (see Recipes)
45. IMAC stripping solution (see Recipes)
46. IMAC wash I (see Recipes)
47. Iodoacetamide (IAc) solution (see Recipes)

48. IP elution buffer (see Recipes)
49. PPT solution (see Recipes)

Equipment

1. 1 ml BD syringes with slip-tip (BD, catalog number: 309659)
2. 2× water bath or heat block (Thermo, model: TSGP02 or similar)
3. Tweezers (VWR, catalog number: 89259-984)
4. Desktop centrifuge (Beckman, model: A99469 or similar)
5. Desktop microcentrifuge (Beckman, model: A46471 or similar)
6. Micropipettes (Gilson, catalog number: F167380 or similar kit with P2, P20, P200, P1000 types)

Note: One water bath/heat block should be set to 42°C and the other to 65°C.

7. Orbitrap mass spectrometer; for example, Q-Exactive HF (Thermo, IQLAAEGAAPFALGMBFZ)
8. Scissors (VWR, catalog number: 82027-596 or similar)
9. UHPLC system coupled to a mass spectrometer; for example, UltiMate 3000 (Thermo, model: IQLAAAGABHFAPBMBEX)
10. Vacuum concentrator centrifuge (Thermo, model: SPD131DDA)
11. Vacuum concentrator filter (Thermo, model: VPOF110)
12. Vacuum concentrator pump (Thermo, model: VLP120)
13. Vacuum concentrator vapor trap (Thermo, model: RVT5105)

Note: Items 9-12 are individual parts of what is referred to as a “speedvac” in the later steps of the protocol.

Software

1. XCalibur Qual Browser (Thermo Scientific, <https://www.thermofisher.com/order/catalog/product/OPTION-30965?SID=srch-srp-OPTION-30965#/OPTION-30965?SID=srch-srp-OPTION-30965>)
2. Comet (<http://comet-ms.sourceforge.net/>)

Note: Any other commonly available mass spectrometry analysis software can be used.

Procedure

A. Reduction, denaturation, alkylation, and trypsin digestion of IP eluate

1. Most standard IP protocols are adaptable to this procedure. It is recommended to immunoprecipitate bait protein from 2-10 mg protein extract for this procedure (the amount of protein present in the sample following immunoprecipitation will be in the low-microgram range). Following lysis, immunoprecipitation, and washes, add 3× resin volume of IP elution buffer (see Recipes section for info on bolded solutions) to the sample. Incubate at 65°C for 15 min.

Note: Resin volume refers to the quantity of beads used in the IP. For example, if 30 µL of a 50:50 agarose resin:buffer slurry is used, the resin volume is 15 µL, and the volume of elution buffer used would be 45 µL.

2. Spin down the sample at $1,000 \times g$ for 1 min. Take the supernatant (= volume of IP elution buffer used in the previous step) and transfer to a new tube.

Note: If the sample has been metabolically labeled for SILAC analysis, light and heavy IP eluates should be pooled prior to iodoacetamide treatment.

3. Add iodoacetamide (IAc) solution to a final concentration of 25 mM. Incubate in the dark at room temperature for 15 min.
4. Add 4 volumes PPT solution (see Recipes) to the sample. Vortex the tube for 10 s to wash the entire interior, and incubate on ice for 30 min-1 h. Longer incubation times may marginally improve the yield, but 30 min should be sufficient to precipitate most proteins. PPT contains flammable acetone and should be handled with care.
5. Spin the sample at max speed ($\sim 14,000 \times g$) in a benchtop centrifuge for 10 min.
6. Pour off PPT solution. You should see a small white pellet at the bottom of the tube. Alternatively, there may be small granules of protein spattered along the side of the tube.
7. Add 1 mL PPT solution to the tube and vortex to wash the top and sides. Spin down at max speed for 1 min. Pour off PPT.
8. Gently tap the open tube against a kimwipe to remove residual PPT, taking care not to dislodge the pellet at the bottom. Leave the tube open at room temperature for ~ 5 min, or until the acetone smell is nearly gone.
9. Add 20 μ L urea/tris solution to the tube. Vortex the sample 30 s, then add 60 μ L ddH₂O. Vortex again.
10. Add 1 μ L Trypsin Gold solution to the tube. Parafilm the top of the tube and nutate at 37°C overnight.

B. Desalting the sample

1. The next day, acidify the sample by adding formic acid (FA) at a final concentration of 0.25% and trifluoroacetic acid (TFA) at a final concentration of 0.25%. Additionally, add 2 μ L α/β casein peptide digest (see Recipes section for details on how to prepare this solution).

Note: It is recommended to make 10% working stocks of TFA and FA in water for use.

2. Prepare a micro-spin desalting column by adding 20 μ L 100 mg/mL C18 resin in acetonitrile.
 - a. First, remove the luer plug from the micro-spin column.
 - b. Obtain C18 resin by cutting open a Waters C18 Sep-Pak column of any size. Weigh out a small amount of C18 powder and resuspend in pure acetonitrile at a concentration of 100 mg/mL.
3. Spin at $1,500 \times g$ for 30 s. If C18 resin is not yet level at the bottom of the micro-spin column, add 40 μ L acetonitrile to the column and spin again.
4. Condition the column by adding 100 μ L C18 Buffer E and spin at $1,500 \times g$ for 30 s.
5. Equilibrate the column by adding 100 μ L C18 Buffer W1 and spin at $1,500 \times g$ for 30 s.
6. Load the acidified sample onto the column; approx. 100 μ L. Spin at $1,500 \times g$ for 30 s.
7. Wash the column by adding 100 μ L C18 Buffer W1 and spin at $1,500 \times g$ for 30 s.
8. Wash the column by adding 100 μ L C18 Buffer W2 and spin at $1,500 \times g$ for 30 s.
9. Wash the column by adding 100 μ L C18 Buffer W3 and spin at $1,500 \times g$ for 30 s.
10. Elute the sample into a low protein binding Eppendorf tube by adding 100 μ L C18 Buffer E and spin at $1,500 \times g$ for 30 s.
11. Place the sample in a speedvac until dry; approx. 40 min.

Note: It is important to ensure that the sample is completely dry. If some liquid persists after 40 min of drying, continue drying in the speedvac until all the liquid is gone.

12. Reconstitute the sample in 20 μ L 0.1% acetic acid in ddH₂O.

C. Preparation of Fe-NTA resin

1. Add 25 mL IMAC stripping solution to a 50-mL tube.
2. Remove a Qiagen Ni-NTA spin column from its package (Figure 1a) and associated collection tube. Make sure that the cap is open and hold the column over the open 50-ml tube containing 25 mL IMAC stripping solution (Figures 1b and 1c). With the tip of tweezers or similar thin, pointy object, poke the bottom aperture of the column to dislodge the two frits and the resin in between (Figure 1c). The frits and resin will fall into the 50-ml tube (Figure 1d). Nutate for 1 h to strip the nickel from the NTA resin.

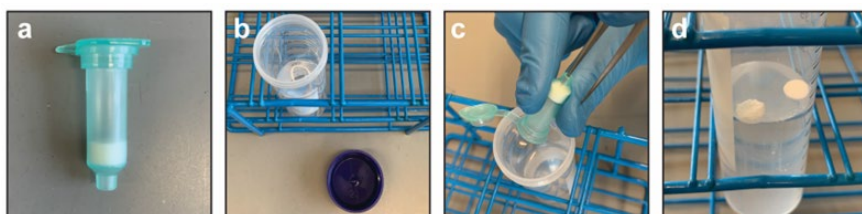


Figure 1. Harvesting Ni-NTA resin from spin column.

(a) Ni-NTA column removed from collection tube. (b) 25 mL IMAC stripping solution in 50-mL conical tube. (c) Tweezer method for poking frit and dry resin into IMAC stripping solution. (d) Frits from Ni-NTA column afloat in stripping solution. Resin will sink to the bottom. After a 50-min nutation in stripping solution, frits can be discarded.

3. Spin at $1,000 \times g$ for 1 min. Discard the supernatant. This first supernatant will include the two frits from the Ni-NTA column.
4. Wash once with 25 mL ddH₂O.
5. Wash once with 25 mL 0.6% acetic acid in ddH₂O.
6. Resuspend the resin in 18 mL 0.3% acetic acid in ddH₂O. Add 2 mL FeCl₃ solution. Nutate for 2-3 h to bind the iron to the NTA resin.
7. Spin at $1,000 \times g$ for 1 min. Discard the supernatant.
8. Wash once with 25 mL 0.6% acetic acid in ddH₂O.
9. Wash once with 25 mL IMAC wash I.

Note: For this step, nutate for 1 min before spinning down.

10. Wash once with 25 mL 0.1% acetic acid in ddH₂O.
11. Resuspend the resin in 0.1 mL 0.1% acetic acid in ddH₂O and transfer to a microcentrifuge tube. The Fe-NTA resin should be prepared fresh every time.

D. Preparation of gel-loader tip column.

1. Clean a small area of bench surface with ethanol. Have glass fiber (4), gel-loader tips (3), BD syringes with slip tip (2), and a small section of 125-μm capillary tubing ready (1) (see Figure 2a).
2. Fit the gel loader tip onto a micropipette. Take up 10 μL ddH₂O and make a mark at the 10 μL level with a permanent marker.
3. Remove the gel-loader tip from the pipette and cut the top of it with scissors so that it will fit snugly onto a 1-ml BD syringe.
4. Roll a tiny wisp of glass fiber between gloved fingers. Cut into a small 5-10 mm segment using a razor blade.
5. Insert the glass fiber segment into the top end of the gel-loader tip with the 10-μL mark (Figure 2b). Use the section of 125-μm capillary tubing to force the glass fiber segment into the tip of the gel-loader tip. Crimp the end of the gel loader tip with tweezers. Some glass fiber should be protruding from the end of

the gel-loader tip at this point (Figure 2b, note wisp at end of tip). Use a razor blade to cut off any protruding glass fiber (Figure 2c).

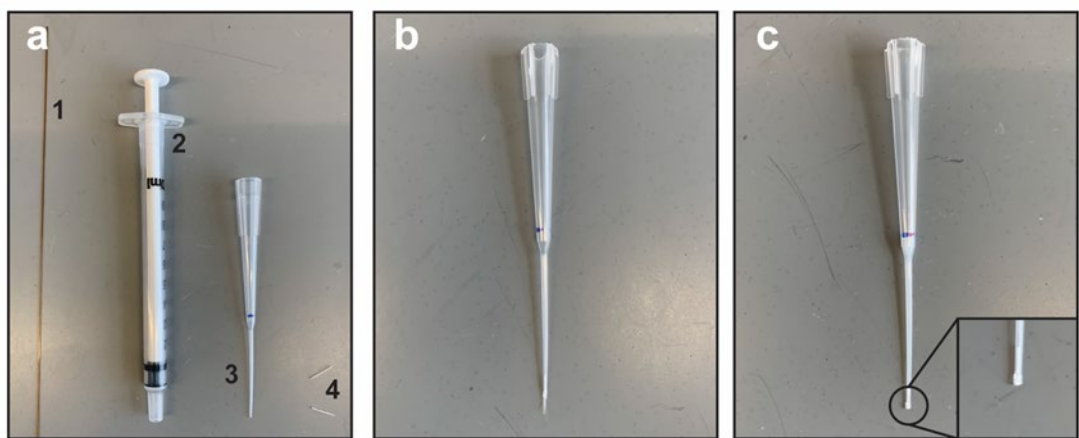


Figure 2. Preparation of gel-loader tip micro-column.

(a) Materials needed for column assembly: (1) 125- μ m capillary tubing; (2) 1-mL BD syringe with slip tip; (3) gel-loader tip; and (4) glass fiber, rolled and cut into small sections. (b) Gel-loader tip (note 10- μ L mark in blue ink) with top cut to adapt to BD syringe and glass fiber wisp protruding slightly from tip. (c) Final resin-filled gel-loader tip ready for phosphopeptide enrichment. Inset shows where end has been crimped and wisp removed to form a flat tip.

E. Phosphopeptide enrichment.

1. Prepare the column (see Figures 2 and 3 for column assembly) by adding 20 μ L 0.1% acetic acid:resin mixture from Step C11 to the gel-loader tip. Use the BD syringe to apply backpressure to the column, forcing the resin to settle. Keep the column vertical at all times to ensure that the resin bed is even and undisturbed. Keep adding 0.1% acetic acid:resin mixture until the resin level reaches the 10- μ L mark on the gel-loader tip. Once the settled resin has reached the 10- μ L mark, use the BD syringe to force the remaining 0.1% acetic acid solution through the column.

Note: It is critically important to not allow the column to dry out. This is challenging due to the small volumes being worked with. When initially preparing the column and when performing washes, allow the liquid to reach the very edge of the resin bed (meniscus should nearly disappear). At this point, the column must be quickly removed from the BD syringe to prevent drying. In between washes, place the resin-filled gel-loader tip upright in a 1.5-mL microcentrifuge tube.

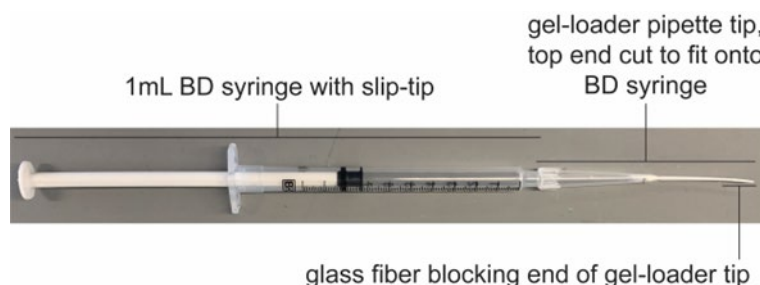


Figure 3. BD syringe with phosphopeptide enrichment column.

Figure shows a completed, assembled phosphopeptide enrichment column.

2. Once the phosphopeptide enrichment column has been assembled, wash once with 25 μ L IMAC wash II to equilibrate the column.

Note: When passing solutions over the column, great care must be taken not to disturb the resin bed. Pipette carefully!

3. Apply the acidified, trypsinized sample to the column (20 μ L reconstituted in 0.1% acetic acid, from protocol Step B12). Apply consistent pressure using the BD syringe and discard the flowthrough.

Note: Optionally, the flowthrough can be saved for a second attempt at phospho-enrichment if the first attempt fails.

4. Once the sample has been fully loaded onto the resin, pipette 100 μ L IMAC wash I onto the column, then remove 90 μ L, leaving 10 μ L. Push 10 μ L through the column using the BD syringe.
5. Pipette 100 μ L ddH₂O onto the column, then remove 90 μ L, leaving 10 μ L. Push 10 μ L through the column using the BD syringe. While the ddH₂O elutes, use a kimwipe to wipe the very tip of the gel-loader column. This will help to remove any residual contaminants.
6. Elute the phosphopeptides with 30 μ L IMAC elution solution into a target polypropylene conical insert tube inside a microcentrifuge tube labeled “90%”. Then transfer 3 μ L into another target polypropylene conical insert tube inside a microcentrifuge tube labeled “10%.”
7. Place both the samples in a speedvac until fully dry.
8. Resuspend both samples in 5 μ L 0.1 P solution.
9. Proceed to MS analysis. Due to the low abundance and hydrophobicity of phosphopeptides, it is recommended to avoid using a trapping column. First run 5% of the total sample. If the MS chromatogram is relatively free of polymers and other contaminants, load increasing amounts of sample (for example: 10%, 20%, and 50%). Proceed to the “Data analysis” section.

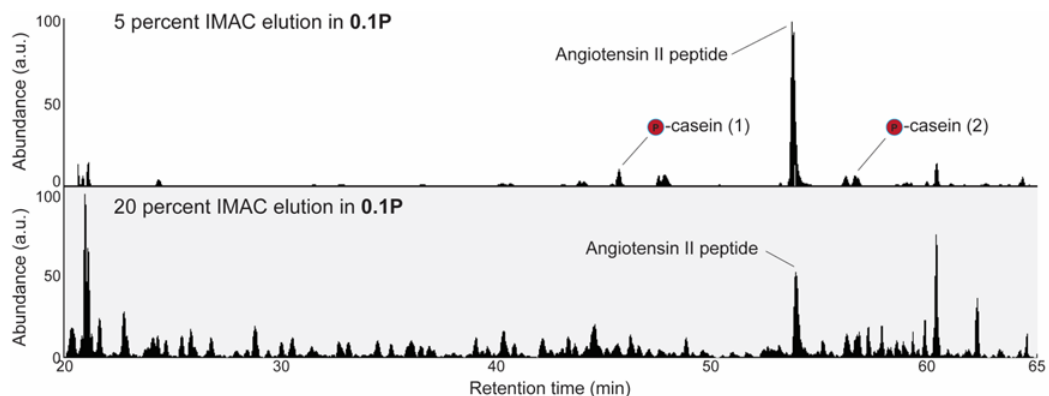


Figure 4. Representative IP-IMAC chromatogram.

Representative chromatogram from 5% sample in 0.1P solution (top panel). Proceed to an injection of 20% sample (bottom panel) if chromatography from the 5% sample shows symmetric peaks with few contaminants. Contaminants are identifiable as any +1 charge state ions present in the sample. The same quantity of angiotensin II peptide is present in both samples (~200 fmoles). Casein peptides are also indicated. Casein peptide (1): β casein, m/z 1031.41, FQSphosEEQQQTEDELQDK; casein peptide (2): α casein, m/z 830.90, VPQLEIVPNSphosAEER.

Data analysis

1. Internal control for phosphopeptide recovery (monitoring α/β casein phosphopeptides)

Cite as: Sanford, E. J. and Smolka, M. B. (2021). Fe-NTA Microcolumn Purification of Phosphopeptides from Immunoprecipitation (IP) Eluates for Mass Spectrometry Analysis. Bio-protocol 11(15): e4113. DOI: [10.21769/BioProtoc.4113](https://doi.org/10.21769/BioProtoc.4113).

Trypsinized α/β casein should be spiked into the sample prior to desalting as an internal control to verify that the phospho-enrichment portion of the protocol worked properly. Once 5% of the sample has been run on a mass spectrometer, add the following MS1 *m/z* ranges in Qual Browser (Thermo Scientific): 830.5-831.5; 1030.5-1031.5. Retention times may vary between users depending on the HPLC gradient profile that is used. These ranges encompass two diagnostic α/β casein phosphopeptides (see Figure 4 legend for details). The spectral intensity of the phosphorylated casein peptides should be greater than 1.00E6 in the 5% sample. Lower intensities indicate that phospho-enrichment troubleshooting is needed. Often, inefficient phospho-enrichment is due to excessive agitation of the Fe-NTA resin or column drying between washes.

2. Mass spectrometry data analysis

- a. Mass spectrometry data can be analyzed using any existing software such as MaxQuant, Sorcerer, Comet, or Proteome Discoverer. Parameters for the identification of phosphorylated peptides by mass spectrometry have been exhaustively described elsewhere (Mann and Jensen, 2003; Mueller *et al.*, 2008; Deutsch *et al.*, 2010; Bastos de Oliveira *et al.*, 2018; Faca *et al.*, 2020). Typical mass spectrometry data analysis parameters will include a semi-tryptic requirement, a precursor mass tolerance of 10-20 ppm, a differential mass modification of 79.966331 Da for the phosphorylation of serine, threonine, or tyrosine residues, and a static mass modification of 57.021465 for carbamidomethylcysteine.
- b. There are several ways to display the data generated from an IP phosphoenrichment experiment. Phosphopeptides with 2 or more peptide-spectral matches (PSMs) may be displayed in the absence of quantitative information along with a stick model of the protein of interest. In the presence of quantitative MS information, such as that obtained from SILAC or TMT analysis, scatterplots or histograms can be generated that indicate quantitative differences in bait protein phosphorylation between two genetic or pharmacological conditions. For example, we refer to the following work containing IMAC data generated in our lab (Lanz *et al.*, 2018; Baile *et al.*, 2019).

Recipes

1. 0.1 P solution

1 pmol/ μ L angiotensin II peptide, 0.1% trifluoroacetic acid in ddH₂O
Store at -20°C in 500- μ L aliquots

2. C18 Buffer E

80% acetonitrile, 0.1% acetic acid in ddH₂O
Store at room temperature

3. C18 Buffer W1

0.1% trifluoroacetic acid in ddH₂O
Store at room temperature

4. C18 Buffer W2

3% acetonitrile, 0.1% formic acid in ddH₂O
Store at room temperature

5. C18 Buffer W3

0.1% acetic acid in ddH₂O
Store at room temperature

6. DTT solution (for IP elution buffer)

Cite as: Sanford, E. J. and Smolka, M. B. (2021). Fe-NTA Microcolumn Purification of Phosphopeptides from Immunoprecipitation (IP) Eluates for Mass Spectrometry Analysis. Bio-protocol 11(15): e4113. DOI: [10.21769/BioProtoc.4113](https://doi.org/10.21769/BioProtoc.4113).

1 M DTT in ddH₂O

Freeze in small aliquots and minimize freeze-thaw cycles

7. FeCl₃ solution

1 M FeCl₃, 0.3% acetic acid in ddH₂O

Store at room temperature. Prepare a few days in advance of the experiment and do not agitate. Stable for several years at room temp.

8. IMAC elution solution

12% ammonium hydroxide, 10% acetonitrile in ddH₂O

Store at room temperature. Keep tightly capped to prevent evaporation of ammonium hydroxide.

9. IMAC stripping solution

50 mM EDTA, 1 M NaCl in ddH₂O

Store at room temperature

10. IMAC wash I

25% acetonitrile, 100 mM NaCl, 0.1% acetic acid in ddH₂O

Store at room temperature. Make sure that this solution is tightly capped to prevent evaporation of acetonitrile.

11. IMAC wash II

1% acetic acid in ddH₂O

Store at room temperature

12. Iodoacetamide (IAc) solution

500 mM iodoacetamide, 1 M Tris pH 8.0 in ddH₂O

Prepare fresh

13. IP elution buffer

1% sodium dodecyl sulfate, 100 mM Tris pH 8.0 in ddH₂O, 10 mM dithiothreitol (DTT).

IP elution buffer minus DTT may be stored long-term at room temperature; 10 mM DTT should be added fresh every time.

14. PPT solution

50% acetone

49.9% ethanol

0.1% acetic acid

Store at room temperature. Make sure that this solution is tightly capped to prevent evaporation of acetone and ethanol.

15. Trypsin Gold solution

1 μg/μL Trypsin Gold, 0.3% acetic acid in ddH₂O

Store at -80°C in 1-μl aliquots

16. Urea/Tris solution

8 M urea, 50 mM Tris pH 8.0 in ddH₂O

Prepare fresh

17. α/β casein peptide digest

5 pmol/ μ L trypsin-digested α -casein, 5 pmol/ μ L trypsin-digested β -casein, 1% acetic acid in ddH₂O
Store at -20°C in 500- μ L aliquots

Acknowledgments

The authors thank members of the Smolka Lab for valuable insights related to this work – particularly William Comstock for his careful testing of this protocol. We thank Beatriz S.V. Almeida for technical support. This work was supported by grants from the National Institutes of Health to M.B.S. (R35GM141159, R01GM097272, R01GM123018, and R01HD095296; Equipment Supplement R01GM097272-07S1). The protocol was derived from experiments appearing in Lanz *et al.* (2018) and Sanford *et al.* (2021).

Competing interests

The authors declare no competing interests.

Ethics

No human or animal ethics are relevant to this protocol.

References

- Baile, M. G., Guiney, E. L., Sanford, E. J., MacGurn, J. A., Smolka, M. B. and Emr, S. D. (2019). [Activity of a ubiquitin ligase adaptor is regulated by disordered insertions in its arrestin domain](#). *Mol Biol Cell* 30(25): 3057-3072.
- Bastos de Oliveira, F. M., Kim, D., Lanz, M. and Smolka, M. B. (2018). [Quantitative Analysis of DNA Damage Signaling Responses to Chemical and Genetic Perturbations](#). *Methods Mol Biol* 1672: 645-660.
- Bodenmiller, B., Mueller, L. N., Mueller, M., Domon, B. and Aebersold, R. (2007). [Reproducible isolation of distinct, overlapping segments of the phosphoproteome](#). *Nat Methods* 4(3): 231-237.
- Breitkopf, S. B. and Asara, J. M. (2012). [Determining *in vivo* phosphorylation sites using mass spectrometry](#). *Curr Protoc Mol Biol Chapter 18*: Unit18 19 11-27.
- Chapman, R. D., Heidemann, M., Albert, T. K., Mailhammer, R., Flatley, A., Meisterernst, M., Kremmer, E. and Eick, D. (2007). [Transcribing RNA polymerase II is phosphorylated at CTD residue serine-7](#). *Science* 318(5857): 1780-1782.
- Cussiol, J. R., Jablonowski, C. M., Yimit, A., Brown, G. W. and Smolka, M. B. (2015). [Dampening DNA damage checkpoint signalling via coordinated BRCT domain interactions](#). *EMBO J* 34(12): 1704-1717.
- Dephoure, N., Gould, K. L., Gygi, S. P. and Kellogg, D. R. (2013). [Mapping and analysis of phosphorylation sites: a quick guide for cell biologists](#). *Mol Biol Cell* 24(5): 535-542.
- Deutsch, E. W., Mendoza, L., Shteynberg, D., Farrah, T., Lam, H., Tasman, N., Sun, Z., Nilsson, E., Pratt, B., Prazen, B., Eng, J. K., Martin, D. B., Nesvizhskii, A. I. and Aebersold, R. (2010). [A guided tour of the Trans-Proteomic Pipeline](#). *Proteomics* 10(6): 1150-1159.
- Faca, V. M., Sanford, E.J., Tieu, J., Comstock, W., Gupta, S., Marshall, S., Yu, H., and Smolka, M.B. (2020). [Maximized quantitative phosphoproteomics allows high confidence dissection of the DNA damage signaling network](#). *Scientific Reports*: 10
- Gingras, A. C., Raught, B., Gygi, S. P., Niedzwiecka, A., Miron, M., Burley, S. K., Polakiewicz, R. D., Wyslouch-Cieszynska, A., Aebersold, R. and Sonenberg, N. (2001). [Hierarchical phosphorylation of the translation](#)

- [inhibitor 4E-BP1](#). *Genes Dev* 15(21): 2852-2864.
- Humphrey, S. J., Karayel, O., James, D. E. and Mann, M. (2018). [High-throughput and high-sensitivity phosphoproteomics with the EasyPhos platform](#). *Nat Protoc* 13(9): 1897-1916.
- Kim, J., Kundu, M., Viollet, B. and Guan, K. L. (2011). [AMPK and mTOR regulate autophagy through direct phosphorylation of Ulk1](#). *Nat Cell Biol* 13(2): 132-141.
- Lanz, M. C., Oberly, S., Sanford, E. J., Sharma, S., Chabes, A. and Smolka, M. B. (2018). [Separable roles for Mec1/ATR in genome maintenance, DNA replication, and checkpoint signaling](#). *Genes Dev* 32(11-12): 822-835.
- Li, J., Paulo, J. A., Nusinow, D. P., Huttlin, E. L. and Gygi, S. P. (2019). [Investigation of Proteomic and Phosphoproteomic Responses to Signaling Network Perturbations Reveals Functional Pathway Organizations in Yeast](#). *Cell Rep* 29(7): 2092-2104 e2094.
- Mann, M. and Jensen, O. N. (2003). [Proteomic analysis of post-translational modifications](#). *Nat Biotechnol* 21(3): 255-261.
- Mueller, L. N., Brusniak, M. Y., Mani, D. R. and Aebersold, R. (2008). [An assessment of software solutions for the analysis of mass spectrometry based quantitative proteomics data](#). *J Proteome Res* 7(1): 51-61.
- Ohouo, P. Y., Bastos de Oliveira, F. M., Almeida, B. S. and Smolka, M. B. (2010). [DNA damage signaling recruits the Rtt107-Slx4 scaffolds via Dpb11 to mediate replication stress response](#). *Mol Cell* 39(2): 300-306.
- Ong, S. E., Blagoev, B., Kratchmarova, I., Kristensen, D. B., Steen, H., Pandey, A. and Mann, M. (2002). [Stable isotope labeling by amino acids in cell culture, SILAC, as a simple and accurate approach to expression proteomics](#). *Mol Cell Proteomics* 1(5): 376-386.
- Sanford, E. J., Comstock, W.J., Faça, V. M., Vega, S. C., Gnugge, R., Symington, L.S., and Smolka, M. B. (2021) [Phosphoproteomics reveals a distinctive Mec1/ATR signaling response upon DNA end hyper-resection](#). *EMBO J* 40(10):e104566. doi: 10.15252/embj.2020104566.
- Zhang, L. and Elias, J. E. (2017). [Relative Protein Quantification Using Tandem Mass Tag Mass Spectrometry](#). *Methods Mol Biol* 1550: 185-198.

A Genetically Engineered Mouse Model of Venous Anomaly and Retinal Angioma-like Vascular Malformation

Xudong Cao[#], Beibei Xu[#], Xiao Li[#], Taotao Li and Yulong He^{*}

Cyrus Tang Hematology Center, Collaborative Innovation Center of Hematology, National Clinical Research Center for Hematologic Diseases, State Key Laboratory of Radiation Medicine and Protection, Cam-Su Genomic Resources Center, Soochow University, Suzhou 215123, China

*For correspondence: heyulong@suda.edu.cn

[#]Contributed equally to this work

Abstract

Characterization of key regulators in vein development will advance our understanding of mechanisms underlying venous anomalies and provide therapeutic targets for the treatment of vascular malformations. Here, we provide a detailed protocol for the generation of genetically engineered mouse models targeting the *Tek* gene for the analysis of vein formation and vein-associated vascular diseases at the embryonic and postnatal stages. It includes steps involved in the whole-mount processing of mouse skin, mesentery, and retina for the examination of vascular malformation during embryonic and postnatal development.

Keywords: TIE2, Vein development, Venous anomaly, Angioma-like, Retinal vascular tuft, Disease model

This protocol was validated in: eLife (2016), DOI: 10.7554/eLife.21032

Background

During embryogenesis in mammals, the blood vascular system is one of the first organs to develop from mesoderm-derived hemangioblasts. The developmental process includes the initial fusion of blood islands to form the primitive vascular plexus, followed by vascular specification to form a network comprised of arteries, veins, and capillaries. Characterization of the mechanisms underlying arteriovenous specification will advance our understanding of venous anomalies and provide therapeutic targets for the treatment of vascular diseases. Among the characterized regulators and pathways, the VEGF-A/VEGFR-2 pathway mediates the activation of RAF1 and ERK1/2 kinases to induce the expression of genes required for arterial development (Lanahan *et al.*, 2013; Deng *et al.*, 2013), including Delta-like 4 (Dll4)-mediated activation of NOTCH signaling (Lawson *et al.*, 2001; Duarte *et al.*, 2004; Wythe *et al.*, 2013). Chicken ovalbumin upstream promoter-transcription factor II (COUP-TFII, also known as Nr2f2) is a key regulator of venous identity via the inhibition of NOTCH-mediated signals (You *et al.*, 2005). Akt activation inhibits Raf1-ERK1/2 signaling in endothelial cells (ECs) to favor venous specification (Ren *et al.*, 2010); however, the upstream regulators of vein development are poorly characterized. TIE2 is a receptor tyrosine kinase that mediates angiopoietin signaling for EC survival and vascular remodeling and integrity (Augustin *et al.*, 2009). Patients with venous malformations possess *Tie2* missense point mutations (Vikkula *et al.*, 1996). TIE2 deficiency leads to embryonic lethality (Dumont *et al.*, 1994; Sato *et al.*, 1995). We have recently demonstrated that TIE2 is essential for the specification of venous EC identity via the Akt-mediated regulation of COUP-TFII protein stability (Chu *et al.*, 2016).

Here, we aim to describe a detailed protocol for analyzing the process of vein development and vein-associated vascular diseases in skin, mesentery, and retina, employing a genetically modified mouse model targeting the Tek gene (Chu *et al.*, 2016)

Materials and Reagents

1. Plastic pipette (disposable, 5 mL, cut the tip for tissue manipulation)
2. Needle (ENTO SPHINX s.r.o., 03.15-Minutens white, 03.20-Minutens white)
3. Insulin syringe (BD, Ultra-Fine®, catalog number: 328421)
4. Coverslips
5. 4% paraformaldehyde (PFA) (Sigma-Aldrich, catalog number: 158127)
6. Skimmed milk powder (Valio)
7. Triton X-100 (Sigma-Aldrich, catalog number: V900502-100ML)
8. Glycerol (Sigma-Aldrich, catalog number: G5516-500ml)
9. Rat anti-mouse PECAM-1 (BD Pharmingen, catalog number: 553370)
10. Goat anti-mouse/rat TIE2 (R&D, catalog number: AF762)
11. Goat anti-mouse EphB4 (R&D, catalog number: AF446)
12. Cy3-conjugated anti-mouse αSMA (Sigma-Aldrich, catalog number: C6198)
13. Alexa Fluor 488-conjugated secondary antibody (Invitrogen, catalog number: A-21208)
14. Cy3-conjugated secondary antibody (Jackson, catalog number: 705-165-147)
15. Cy5-conjugated secondary antibody (Jackson, catalog number: 705-175-147)
16. Tamoxifen (Sigma-Aldrich, catalog number: T5648-5G)
17. Silicone rubber (SYLGARD™ 184 Silicone Elastomer Kit)
18. Phosphate-buffered saline (PBS), pH 7.4 (see Recipes)
19. PBS-TX (see Recipes)
20. 50% glycerol (see Recipes)

Equipment

1. Confocal laser scanning microscope (Olympus, model: FluoView)

2. Fluorescence stereomicroscope (Olympus, model: SZX16)
3. Dissecting scissors (Medical scissors; 66 Vision-Tech Co., catalog number: 54002, straight tip, 100 mm; Vannas capsulotomy scissors: Suzhou Mingren Medical Apparatus and Instruments Co., catalog number: MR-S302A, pointed tips, 16 mm blades)
4. Stereomicroscope (Motic, catalog number: SMZ168 Series, magnification range: 7.5-50×)
5. Micro-forceps (Shanghai Medical Instruments Group Ltd., catalog number: WA3040, 14 cm straight, head width 0.3 mm)

Software

1. FV-ASW Viewer 3.0 or 4.2a

Procedure

A. Generation of Tek-targeted mouse models for vein analysis in skin and mesentery at the embryonic stage. This protocol is based on the paper by Chu *et al.* (2016).

1. Prepare mouse embryos. Place one male mouse (*Tek*^{+/−}; *UBC-CreERT2*, ≥ 2 months old) and two female mice (*Tek*^{Flox/Flox}, ≥ 2 months old) into a cage for mating in the late afternoon around 18:00. Check females for vaginal plugs in the early morning of the following day (around 8:00). If the female mouse is pregnant, the embryonic stages are estimated considering midday of the day on which the vaginal plug is present as embryonic day 0.5 (E0.5).
2. Induce gene deletion. Use sunflower seed oil (COFCO Fortune) as the diluent for the preparation of tamoxifen (tamoxifen free base, 10 mg/mL). Perform intraperitoneal injection of tamoxifen solution (100 μL, 10 mg/mL) from E12.5 to E14.5 (Figure 1A).
3. Euthanize the pregnant female by cervical dislocation at E17.5 (embryonic day 17.5) and place the mouse on its back on a dissecting board. Use pins to attach the feet of the mouse to the board, and adequately soak the fur with 75% ethanol.
4. Make a cut in the skin and the abdominal wall with scissors to expose the abdominal cavity and dissect the uterus with scissors.
5. Separate embryos in ice-cold PBS by removing the uterine muscle layers, pulling the extra-embryonic membranes off with fine forceps, and removing the placenta under a dissecting microscope.
6. Cut the tip off the tail of the embryos for genotyping.
7. Peel back the skin with ophthalmic scissors and fix the skin tissues to the 6-well plate containing silicone rubber using fine needles (Figure 1B).
8. Open the abdomen of the embryo. Cut a fragment of the small intestine long enough to form a ring to keep the mesentery intact for vascular visualization. Fix the intestine to the 6-well plate containing silicone rubber with fine needles (Figure 2A).
9. Fix the tissues with 4% paraformaldehyde (PFA) at 4°C or on ice for 2 h. Wash 3 times with PBS solution for 5 min each.
10. Block the tissues with PBS-TX solution containing 3% skimmed milk powder at 4°C for 6-8 h with gentle agitation on an orbital shaker.
11. Remove the blocking solution and incubate the tissues with primary antibodies (PECAM-1, αSMA, TIE2; dilution according to the manufacturer's recommendation) in blocking solution (total volume: 1 ml) with gentle agitation on an orbital shaker overnight at 4°C.
12. Wash the tissues 5 times with PBS-TX for 20 min each.
13. Incubate the tissues with secondary antibodies (Alexa Fluor 488, Cy5-conjugated secondary antibodies) in PBS-TX solution (dilution 1:500) with gentle agitation on an orbital shaker overnight at 4°C.
14. Cut off the excess tissues. Transfer the trimmed skin onto a glass slide, add a drop of 50% glycerol, place

- a coverslip and seal with nail polish at the edges. For the analysis of intestines, transfer the trimmed intestine directly onto a coverslip and keep the mesentery fully stretched under a dissecting microscope. Avoid drying of tissues by adding drops of 50% glycerol.
15. Analyze blood vessels under a confocal laser scanning microscope (Olympus Fluoview) and acquire and process images with the FV-ASW Viewer 3.0 /4.2a software (Figures 1C and Figure 2B).

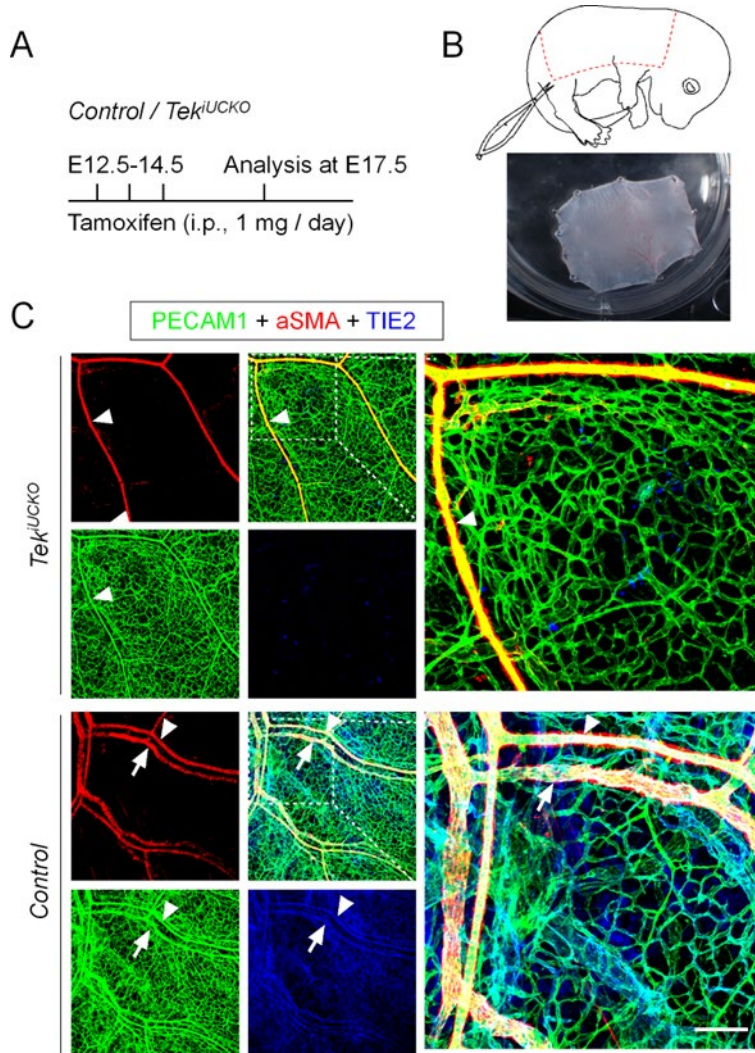


Figure 1. Disruption of cutaneous vein development following *Tek* deletion.

(A) Tamoxifen intraperitoneal administration and analysis scheme. (B) Diagram showing the area of dorsal skin of the embryos dissected for analysis (dotted line). (C) Analysis of dorsal skin blood vessels by whole-mount immunostaining of PECAM-1 (green), α SMA (red), and TIE2 (blue) in *Tek*^{-iUCKO} (*Tek*^{Flx/-}; *UBC-CreERT2*, *Tek*^{iUCKO}) and control (*Tek*^{Flx/+}; *UBC-CreERT2*) mice. Note that *Tek* deletion was confirmed by immunostaining analysis in *Tek*^{iUCKO} mice. Arrowheads indicate arteries, and arrows indicate veins. Scale bar: 100 μ m in C.

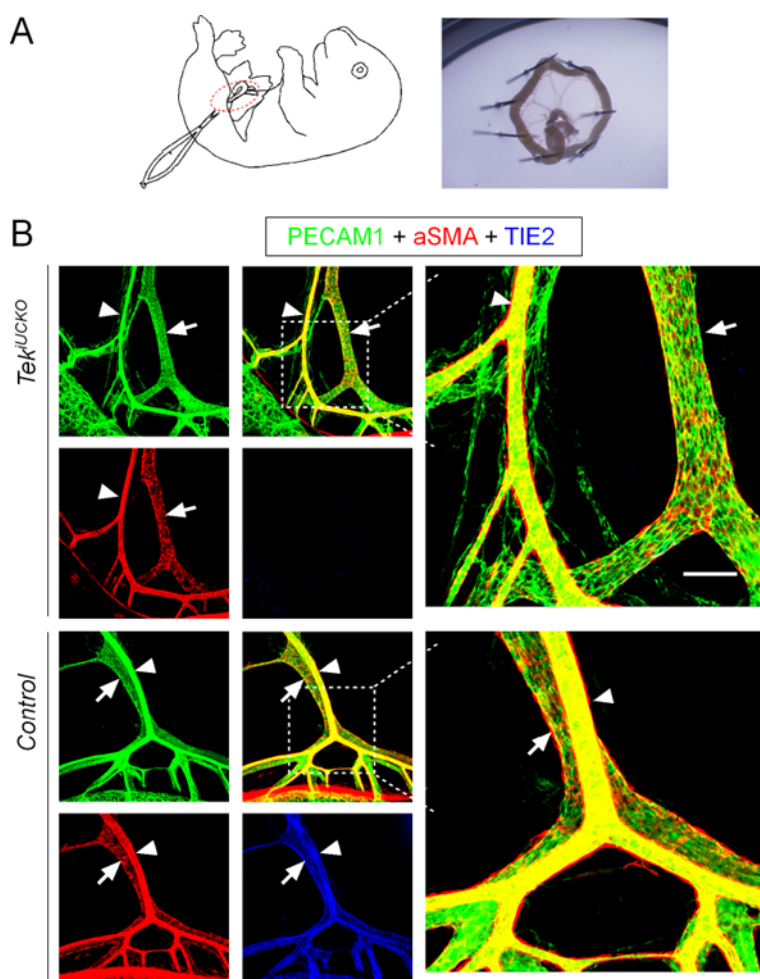


Figure 2. Misalignment of arteries and veins in the mesentery of *Tek* knockout mice.

(A) The tamoxifen administration and analysis scheme is described in Figure 1A. Diagram showing the dissection of intestines and preparation for further analysis by fixing in a 6-well plate containing silicone rubber using fine needles. (B) Analysis of mesenteric blood vessels by whole-mount immunostaining of PECAM-1 (green), α SMA (red), and TIE2 (blue) in *Tek^{iUCKO}* and control mice. Arrowheads indicate arteries, and arrows indicate veins. Scale bar: 100 μ m in B.

B. Generation of a Tek-targeted mouse model for retinal vein analysis at the neonatal stage

Note: Dissection of the retina was performed according to the protocol described by Pitulescu et al. (2010).

1. Administration of 30-50 μ L tamoxifen solution (tamoxifen free base, 2 mg/mL in seed oil) by intragastric injection (Insulin syringe, BD Ultra-Fine[®]) to neonatal mice daily from postnatal day 1 to 4 (P1-4) (Figure 3A).
2. Euthanize the mice by cervical dislocation at P21.
3. Dissect the eyeballs from the mice into a 2-mL tube, and fix eyeballs in 4% PFA on ice for 2 h.
4. Prepare the retina by removing the cornea, sclera, choroid, pigment layer, and lens from the eye in cold PBS under a dissecting microscope.
5. Make four radial incisions to divide the retina into four quadrants after detaching the hyaloid vessels (Figure 3B).
6. Transfer the retina into a 1.5-mL tube and wash 3 times with PBS for 15 min each.
7. Remove PBS completely and block the retina with 3% skimmed milk powder in PBS-TX solution with

- gentle agitation on an orbital shaker at 4°C overnight.
8. Remove the blocking solution and incubate the retina with primary (PECAM-1, EphB4) and secondary antibodies at the appropriate concentrations for 12-16 h at 4°C with gentle agitation on an orbital shaker.

Note: There is a wash step between the primary and secondary antibody incubation.

9. Wash the retina 5 times with PBS-TX for 20 min each.
10. Transfer the retina onto a glass slide with a few drops of 50% glycerol and cover with a coverslip.
11. Analyze the retinal blood vessels under a confocal laser scanning microscope (Olympus Fluoview) and acquire and process the images as described above (Figure 3C).

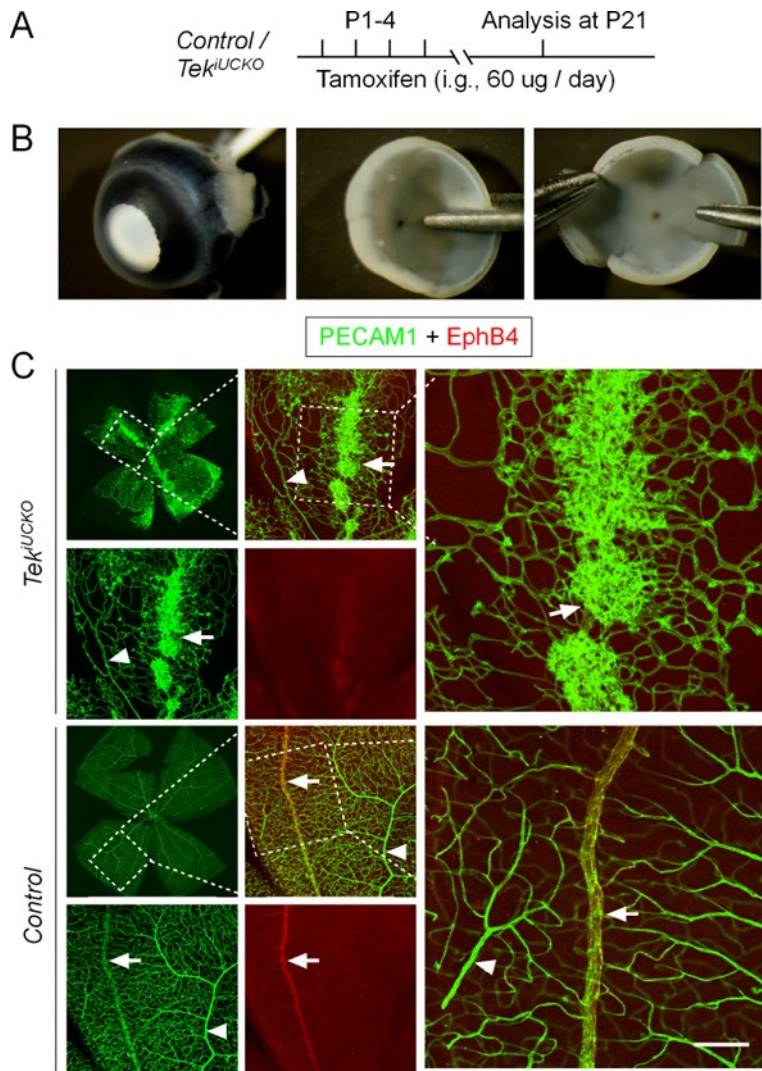


Figure 3. Formation of retinal vein-associated vascular tufts following TIE2 attenuation.

(A) Tamoxifen intragastric administration and analysis scheme. (B) Mouse eyeballs were collected with the cornea, sclera, choroid, and pigment layer removed. Retinas were cut by four radial incisions for further immunohistochemical analysis. (C) Analysis of retinal blood vessels for PECAM-1 (green) and EphB4 (red) in *Tek*^{iUCKO} and control mice at P21. Note that TIE2 insufficiency leads to vascular tuft formation along retinal veins. Arrowheads indicate arteries, and arrows indicate veins. Scale bar: 100 µm in C.

Data analysis

In this protocol, samples were analyzed under a confocal laser scanning microscope (Olympus Fluoview), and images were acquired and processed using the FV-ASW Viewer 3.0 or 4.2a software. Quantification of the retinal vascularization area and blood vascular density, which is not included in this protocol, was performed using the Image-Pro Plus 6.0 software as described in the original paper (Chu *et al.*, 2016). We have noticed that the vascular phenotypes of *Tek* mutants vary depending on the Cre deleter used. For example, when VEcad-CreERT2 was used to induce *Tek* deletion in the postnatal studies (Okabe *et al.*, 2014), we found that most of the *Tek* knockout mice (*Tek*^{fl/fl}; *VEcad-CreERT2*, *Tek*^{iECKO}) died before P21 (postnatal day 21, data not shown). Although *Tie2* mRNA could still be detected in *Tek*^{iECKO} mice, this may be due to the expression of *TIE2* in other cells, including hematopoietic cells, whereas *TIE2* in ECs was almost undetectable (data not shown). However, almost all the *Tek*^{iUCKO} mice generated in this study survived even though their body weight was slightly lower than that of their littermates (Chu *et al.*, 2016). The remaining *Tie2* transcripts were analyzed by quantitative PCR. In this study, the level of *Tie2* mRNA was 0.14 ± 0.05 (P7, n = 7) in the lungs of *Tek*^{iUCKO} mice as compared with 1.0 ± 0.16 in those of control mice (P7, n = 3).

In addition, it is noteworthy that the timepoints for tamoxifen administration and tissue analysis should be defined depending on vascular phenotypes following induced gene deletion and the specific questions to be addressed. For example, the administration of tamoxifen to pregnant mice was performed by intraperitoneal injection from E12.5 to E14.5 in this protocol as the earlier induction of *Tek* deletion (*e.g.*, from E10.5) will lead to embryonic lethality at E17.5. Detailed information regarding the selection of timepoints is also described in Chu *et al.* (2016) (Figures 1 and 3).

Notes

1. Tamoxifen is light sensitive. Keep tamoxifen protected from light.
2. All the incubation steps should be carried out with gentle agitation on an orbital shaker.
3. Avoid muscle attachments when separating skin from embryos.
4. Keep the mesentery samples moist during confocal imaging.
5. Isolate eyeballs immediately after the mice have been euthanized. Avoid touching the retina with the tip of pipettes or other instruments during dissection to prevent tissue damage.

Recipes

1. Phosphate-buffered saline (PBS), pH 7.4

10 mM Na₂HPO₄
1.8 mM KH₂PO₄
137 mM NaCl
2.7 mM KCl

2. PBS-TX

0.3% Triton X-100; PBS, pH 7.4

3. 50% glycerol

50% glycerol; PBS, pH 7.4

Acknowledgments

We thank the staff in the Animal facility of Soochow University for technical assistance. This work was supported by grants from the Ministry of Science and Technology of China (YFA0801100), the Project of State Key Laboratory of Radiation Medicine and Protection (No. GZN120 20 02), the National Natural Science Foundation of China (31970768, 81770489, 91739304), the Key Program of Natural Science Foundation of Jiangsu Higher Education Institutions (18KJA180012), the Graduate Innovation Program (KYCX19_1979), and the Priority Academic Program Development of Jiangsu Higher Education Institutions. This protocol is based on the original paper published in *Elife* (Chu *et al.*, 2016).

Competing interests

The authors have no financial or non-financial competing interests to declare.

Ethics

All animal experiments were performed in accordance with the institutional guidelines of the Soochow University Animal Center (#IACUC-201611).

References

- Augustin, H. G., Koh, G. Y., Thurston, G. and Alitalo, K. (2009). [Control of vascular morphogenesis and homeostasis through the angiopoietin-Tie system](#). *Nat Rev Mol Cell Biol* 10(3): 165-177.
- Chu, M., Li, T., Shen, B., Cao, X., Zhong, H., Zhang, L., Zhou, F., Ma, W., Jiang, H., Xie, P., Liu, Z., Dong, N., Xu, Y., Zhao, Y., Xu, G., Lu, P., Luo, J., Wu, Q., Alitalo, K., Koh, G. Y., Adams, R. H. and He, Y. (2016). [Angiopoietin receptor Tie2 is required for vein specification and maintenance via regulating COUP-TFII](#). *Elife* 5: e21032.
- Deng, Y., Larrivee, B., Zhuang, Z. W., Atri, D., Moraes, F., Prahst, C., Eichmann, A. and Simons, M. (2013). [Endothelial RAF1/ERK activation regulates arterial morphogenesis](#). *Blood* 121(19): 3988-3996, S3981-3989.
- Duarte, A., Hirashima, M., Benedito, R., Trindade, A., Diniz, P., Bekman, E., Costa, L., Henrique, D. and Rossant, J. (2004). [Dosage-sensitive requirement for mouse Dll4 in artery development](#). *Genes Dev* 18(20): 2474-2478.
- Dumont, D. J., Gradwohl, G., Fong, G. H., Puri, M. C., Gertsenstein, M., Auerbach, A. and Breitman, M. L. (1994). [Dominant-negative and targeted null mutations in the endothelial receptor tyrosine kinase, tek, reveal a critical role in vasculogenesis of the embryo](#). *Genes Dev* 8(16): 1897-1909.
- Lanahan, A., Zhang, X., Fantin, A., Zhuang, Z., Rivera-Molina, F., Speichinger, K., Prahst, C., Zhang, J., Wang, Y., Davis, G., Toomre, D., Ruhrberg, C. and Simons, M. (2013). [The neuropilin 1 cytoplasmic domain is required for VEGF-A-dependent arteriogenesis](#). *Dev Cell* 25(2): 156-168.
- Lawson, N. D., Scheer, N., Pham, V. N., Kim, C. H., Chitnis, A. B., Campos-Ortega, J. A. and Weinstein, B. M. (2001). [Notch signaling is required for arterial-venous differentiation during embryonic vascular development](#). *Development* 128(19): 3675-83.
- Okabe, K., Kobayashi, S., Yamada, T., Kurihara, T., Tai-Nagara, I., Miyamoto, T., Mukouyama, Y. S., Sato, T. N., Suda, T., Ema, M. and Kubota, Y. (2014). [Neurons limit angiogenesis by titrating VEGF in retina](#). *Cell* 159(3): 584-596.
- Pitulescu, M. E., Schmidt, I., Benedito, R. and Adams, R. H. (2010). [Inducible gene targeting in the neonatal vasculature and analysis of retinal angiogenesis in mice](#). *Nat Protoc* 5(9): 1518-1534.
- Ren, B., Deng, Y., Mukhopadhyay, A., Lanahan, A. A., Zhuang, Z. W., Moodie, K. L., Mulligan-Kehoe, M. J., Byzova, T. V., Peterson, R. T. and Simons, M. (2010). [ERK1/2-Akt1 crosstalk regulates arteriogenesis in mice](#)

- [and zebrafish](#). *J Clin Invest* 120(4): 1217-1228.
- Sato, T. N., Tozawa, Y., Deutsch, U., Wolburg-Buchholz, K., Fujiwara, Y., Gendron-Maguire, M., Gridley, T., Wolburg, H., Risau, W. and Qin, Y. (1995). [Distinct roles of the receptor tyrosine kinases Tie-1 and Tie-2 in blood vessel formation](#). *Nature* 376(6535): 70-74.
- Vikkula, M., Boon, L. M., Carraway, K. L., 3rd, Calvert, J. T., Diamanti, A. J., Goumnerov, B., Pasyk, K. A., Marchuk, D. A., Warman, M. L., Cantley, L. C., Mulliken, J. B. and Olsen, B. R. (1996). [Vascular dysmorphogenesis caused by an activating mutation in the receptor tyrosine kinase TIE2](#). *Cell* 87(7): 1181-1190.
- Wythe, J. D., Dang, L. T., Devine, W. P., Boudreau, E., Artap, S. T., He, D., Schachterle, W., Stainier, D. Y., Oettgen, P., Black, B. L., Bruneau, B. G. and Fish, J. E. (2013). [ETS factors regulate Vegf-dependent arterial specification](#). *Dev Cell* 26(1): 45-58.
- You, L. R., Lin, F. J., Lee, C. T., DeMayo, F. J., Tsai, M. J. and Tsai, S. Y. (2005). [Suppression of Notch signalling by the COUP-TFII transcription factor regulates vein identity](#). *Nature* 435(7038): 98-104.

Measuring DNA Damage Using the Alkaline Comet Assay in Cultured Cells

Elena Clementi, Zuzana Garajova and Enni Markkanen*

Institute of Veterinary Pharmacology and Toxicology, Vetsuisse Faculty, University of Zürich, Zürich, Switzerland

*For correspondence: enni.markkanen@vetpharm.uzh.ch

Abstract

Maintenance of DNA integrity is of pivotal importance for cells to circumvent detrimental processes that can ultimately lead to the development of various diseases. In the face of a plethora of endogenous and exogenous DNA-damaging agents, cells have evolved a variety of DNA repair mechanisms that are responsible for safeguarding genetic integrity. Given the relevance of DNA damage and its repair in disease, measuring the amount of both aspects is of considerable interest. The comet assay is a widely used method that allows the measurement of both DNA damage and its repair in cells. For this, cells are treated with DNA-damaging agents and embedded into a thin layer of agarose on top of a microscope slide. Subsequent lysis removes all protein and lipid components to leave so-called ‘nucleoids’ consisting of naked DNA remaining in the agarose. These nucleoids are then subjected to electrophoresis, whereby the negatively charged DNA migrates toward the anode depending on its degree of fragmentation and creates shapes resembling comets, which can be subsequently visualized and analyzed by fluorescence microscopy. The comet assay can be adapted to assess a wide variety of genotoxins and repair kinetics, in addition to both DNA single-strand and double-strand breaks. In this protocol, we describe in detail how to perform the alkaline comet assay to assess single-strand breaks and their repair using cultured human cell lines. We describe the workflow for assessing the amount of DNA damage generated by agents such as hydrogen peroxide (H_2O_2) and methyl-methanesulfonate (MMS) or present endogenously in cells, and how to assess the repair kinetics after such an insult. The procedure described herein is easy to follow and allows the cost-effective assessment of single-strand breaks and their repair kinetics in cultured cells.

Keywords: DNA damage, DNA repair, DNA repair kinetics, Genotoxic agents, Oxidative stress, Reactive oxygen species

This protocol was validated in: BMC Biol (2020), DOI: 10.1186/s12915-020-00771-x

Background

Maintaining the integrity of DNA is a pivotal prerequisite for cells to ensure that all physiological processes function impeccably. Cells are constantly exposed to a plethora of exogenous and endogenous agents that can damage their DNA. Examples of exogenous noxious agents include ultraviolet light, ionizing radiation, and reactive chemical compounds, while endogenous damage can arise due to, *e.g.*, reactive oxygen- and nitrogen species derived from cellular metabolism (Van Loon *et al.*, 2010). If left unrepaired, damage to DNA can lead to mutations, which in turn can alter the functionality of the affected DNA. This can potentially result in altered protein abundance or activity and give rise to diseases such as cancer, neurodegeneration, and aging (Hoeijmakers, 2009; Markkanen, 2017). To counteract the deleterious effects of DNA damage, cells have evolved a series of intricate DNA repair mechanisms that detect and repair such insults (Jackson and Bartek, 2009; Ciccia and Elledge, 2010). Given the relevance of DNA damage in disease, it is of considerable interest to be able to measure levels of DNA damage that are induced by exposure of cells to particular agents or to assess whether the repair kinetics of such damage is altered through specific treatments or genetic backgrounds. Methods to measure DNA damage and repair range from PCR-based methods and enzyme-linked immunosorbent assays to more elaborate next-generation sequencing-based methods (Li and Sancar, 2020). Among this multitude of assays, the comet assay is a widely used method to measure both the amount of DNA damage and its repair in cells (Olive, 2009; Collins, 2014). For this, cells are treated with DNA-damaging agents and embedded into a thin layer of agarose on top of a microscope slide (Figure 1). Subsequent lysis removes all protein and lipid components to leave so-called ‘nucleoids’ consisting of naked DNA remaining in the agarose. These nucleoids are then subjected to electrophoresis, whereby the negatively charged DNA migrates toward the anode depending on its degree of fragmentation and creates shapes resembling comets, which can be subsequently visualized and analyzed by fluorescence microscopy. The comet assay can be adapted to assess a wide variety of genotoxins and repair kinetics, in addition to both DNA single-strand and double-strand breaks. In this protocol, we describe in detail how to perform the alkaline comet assay to assess single-strand breaks and their repair using cultured human cell lines. In addition to cultured human cell lines, the assay can be used for cells directly derived from tissues, provided that they can be dissociated into single-cell suspensions. This exact protocol was used in our recent publication (Clementi *et al.*, 2020). For a detailed description of the neutral comet assay that can be used to detect DNA double-strand breaks, please refer to the separate protocol published in *Bio-protocol*.

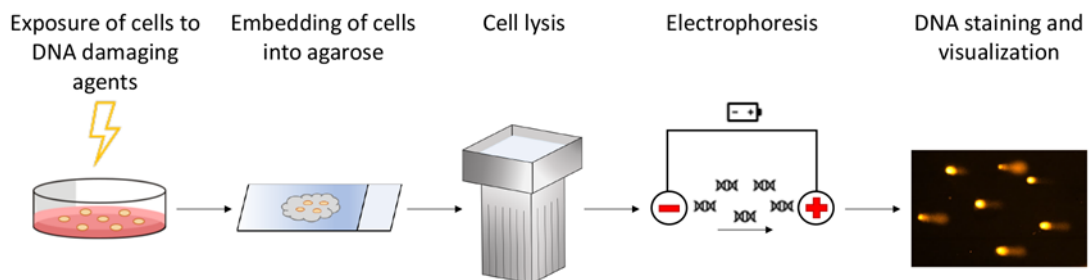


Figure 1. Flowchart of the comet assay.

Overview of the sequence of events as discussed in the text.

Materials and Reagents

1. Superfrost microscopy slides (ThermoScientific, Menzel-Gläser, Superfrost Plus, catalog number: J1800AMNZ), store at room temperature. The use of charged slides is necessary to ensure proper adhesion of agarose to the slides and to minimize sample loss during handling
2. Rectangular coverslips (Coverslips 22 × 50 mm; ThermoScientific, Menzel-Gläser, catalog number: MA062210), store at room temperature
3. 24-well cell culture plates (TPP, catalog number: 92024), store at room temperature

4. 15 mL Falcon tubes (Greiner, catalog number: 188271 Zentrifugenröhren 15 mL, Producer: Huberlab AG, catalog number: 7.188 271), store at room temperature
5. Trypsin 10× stock solution (Gibco, catalog number: 15090-046), store stock solution at -20°C. Dilute 1:10 in 1× PBS for a working solution; this is stable at 4°C for several weeks
6. Potassium chloride (KCl) (Merck, catalog number: 1.04936.1000), store at room temperature
7. Normal melting point agarose (Standard Agarose-Type LE; BioConcept, catalog number: 7-01P02-R), store at room temperature
8. Low melting point agarose (Low Melt Agarose 100 g; Bio & Sell, catalog number: BS20.47.100), store at room temperature
9. Na₂HPO₄·7H₂O (Sigma-Aldrich, catalog number: S9390-1Kg), store at room temperature
10. KH₂PO₄ (Sigma, catalog number: 602187), store at room temperature
11. NaCl (Sigma, catalog number: 71380-1KG), store at room temperature
12. EDTA disodium salt dihydrate (C₁₀H₁₄N₂Na₂O₈·2H₂O) (Sigma-Aldrich, catalog number: 03685-1KG), store at room temperature
13. Tris base (Sigma, Life science, catalog number: T1503-500G), store at room temperature
14. Sodium hydroxide pellets (NaOH) (Merck, catalog number: 1.06498.100), store at room temperature
15. DMSO (Sigma-Aldrich, catalog number: D5879-1L), store at room temperature
16. Triton X-100 (MP-biomedicals/LLC, catalog number: 807426), store at room temperature
17. SYBR Gold nucleic acid gel stain (Life Technologies, catalog number: S11494), aliquot and store at -20°C protected from light
18. 30% hydrogen peroxide (H₂O₂) (Roth, catalog number: 8070.2), store at 4°C
19. Methyl-methanesulfonate (MMS) (Sigma, catalog number: 129925), make 10 M solution in sterile dH₂O, aliquot, and store at -20°C
20. Lysis buffer for the alkaline comet assay (see Recipes)
21. Electrophoresis buffer for the alkaline comet assay (see Recipes)
22. Comet staining solution (see Recipes)
23. PBS (phosphate-buffered saline) (see Recipes)

Equipment

1. Trevigen CometAssay ESII apparatus (Trevigen, catalog number: 4250-050-ES)
2. Fluorescence microscope capable of excitation at 470-530 nm to image SYBR-Gold (excitation maximum around 495 nm, emission approx. 537 nm)
3. Water bath capable of maintaining a constant temperature of 37°C and large enough to hold a 250-mL glass bottle
4. Big styrofoam box or similar, large enough to hold a glass plate for 10-12 comet slides on ice
5. Small mechanic's level
6. Coplin jars capable of holding 5 or 10 slides
7. 'Humid chamber' consisting of a plastic box with a lid, large enough to hold 10-12 slides on a wet paper towel and be placed in an incubator at 37°C

Software

1. Fiji image processing package (<https://imagej.net/Fiji>)
2. OpenComet plugin for Fiji (<http://www.cometbio.org/>) (Gyori *et al.*, 2014)

Procedure

A. Preparation of agarose-coated slides (the day before the assay or earlier)

1. Completely dissolve 1 g normal melting point agarose in 100 ml dH₂O (1% solution) by heating in a glass bottle in the microwave. Make sure to place the lid only loosely on the bottle and be mindful of boiling retardation.
2. Pipet 1 mL agarose solution onto a superfrost slide, overlay with a coverslip to spread evenly across the slide, and allow the agarose to set at room temperature. The thickness of the agarose coating will be around 1 mm, and overlaying with the coverslip aids distribution of the agarose evenly across the slide.
3. When the agarose has set, gently remove the coverslip by sliding it toward the short end of the slide; air-dry the slides overnight.
4. When the slides have completely dried, they can be directly used or stored for several months in a dry cool space.

Note: Pre-coating the slides with normal melting point agarose increases the adhesion of the agarose layer containing the cells for comet analysis.

B. Culturing cells of interest

Make sure that your cells of interest are in culture and growing exponentially. Split cells 1-3 days before running the assay, according to your established cell culture procedure, in the medium of choice.

C. Preparation of material on the day of the assay

1. Prepare the appropriate amount of alkaline comet lysis buffer and cool to 4°C. Make sure to have enough cold dH₂O to freshly prepare cold electrophoresis buffer. The amount of lysis buffer required depends on the volume and the number of coplin jars that will be used. Typically, a medium-sized coplin jar can hold 10 slides and requires around 150 mL buffer. The amount of electrophoresis buffer needed depends on the apparatus used. For the CometAssay ESII apparatus used here, calculate approx. 850 mL. This amount does not depend on the number of slides since empty spaces for slides will be filled with dummy slides.
2. Place the comet electrophoresis apparatus (including the cooling pack) at 4°C to cool down.
3. Warm the water bath to 37°C.
4. Completely dissolve 0.5 g low melting point agarose (LMP) in 50 mL 1× PBS (1% solution; you will need 1 mL per sample plus some extra; increase the volume if more samples will be processed) by heating in a glass bottle in the microwave. Make sure to place the lid only loosely on the bottle and be mindful of the boiling retardation. Once completely dissolved, place the bottle in the 37°C water bath to equilibrate.

Note: Keeping the correct temperature of the water bath is essential – if too cold, the agarose will solidify; if too hot, this will cause additional damage to the cells.

5. Label the agarose-coated slides using a pencil. Make sure to prepare at least duplicate (or better, triplicate) slides for each assay condition (e.g., timepoint or amount of DNA-damaging agent).
6. Prepare your workplace (see Figure 2):

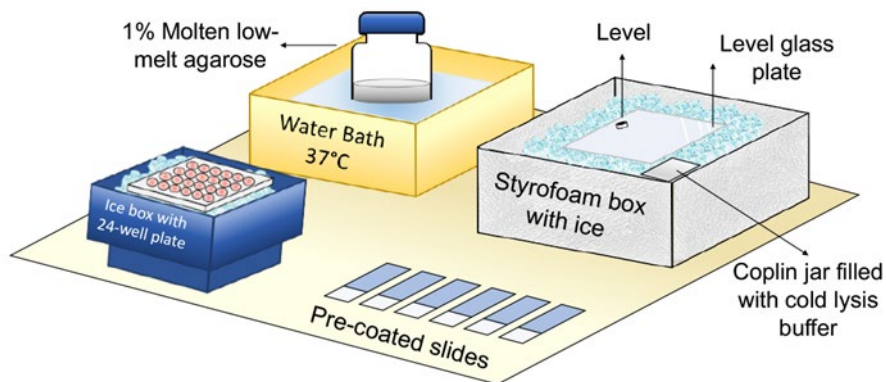


Figure 2. Proposed layout of a workplace to perform the comet assay.

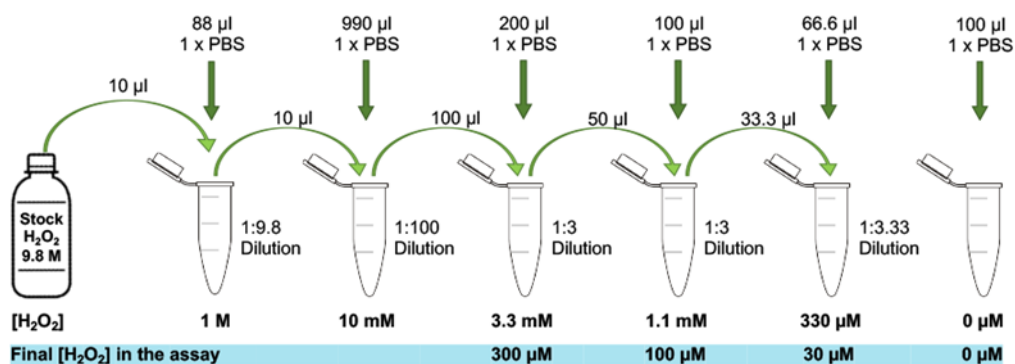
An optimal arrangement of the materials as discussed in the text.

7. Fill a large styrofoam bucket with ice, place a glass plate horizontally on top of the ice and check using a level to ensure that the cells in the agarose will be evenly spread across the entire slide.
8. Place a coplin jar filled with cold lysis buffer into the same bucket (or a different ice-containing bucket next to it).
9. Place an empty 24-well plate into a second ice bucket ready to receive the cell suspension.
10. Prepare the following materials to be close at hand next to the 37°C water bath: a P100 or P200 pipet plus tips, a P1000 pipet plus tips, molten low melting point agarose equilibrated at 37°C, labeled microscope slides, coverslips, and timer.

D. Treatment of cells and embedding in agarose

Depending on the research question, the alkaline comet assay can be used to assess the amount of DNA damage caused by a specific amount of a fast and direct-acting DNA-damaging agent, such as H₂O₂ (see Step D1), or by a DNA-damaging agent that requires longer incubation periods or metabolic activation in cells, such as MMS (see Step D2). Moreover, the comet assay can be exploited to assess the repair kinetics after exposure to a certain amount of a DNA-damaging agent (see Step D3) and also the levels of endogenous DNA damage present in cells (*e.g.*, due to a genetic ablation of the DNA repair pathway) (see Step D4).

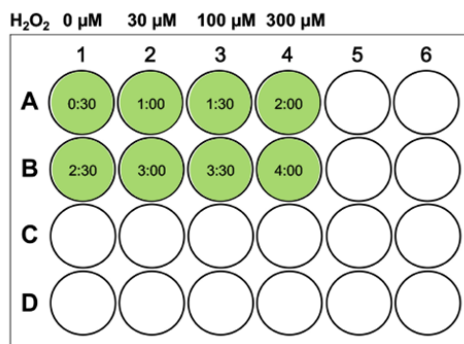
1. Treatment of cells with H₂O₂ as the DNA-damaging agent to determine the extent of DNA damage caused.
 - a. Trypsinize exponentially growing cells, neutralize the trypsin by the addition of complete medium, count cells, and dilute to 2×10^5 cells/ml in complete medium of choice in 15-mL Falcon tubes.
 - b. Place the Falcon tubes on ice for transfer from the cell culture lab to the work bench.
 - c. To ensure even suspension of the cells, carefully invert the Falcon tube a few times (avoid foam formation or vigorous shaking in order not to damage the cells) and then pipet 250 µl cell suspension into the wells of the 24-well plate (1 well per slide/sample) kept on ice.
 - d. Dilute your DNA-damaging agent of interest, *e.g.*, H₂O₂, to the desired concentrations using serial dilutions as follows: if you want to treat the cells with 30 µM H₂O₂, prepare an 11× treatment solution of 330 µM H₂O₂. 25 µL of this solution will be mixed with 250 µL of the cell suspension; hence, you need to prepare an 11× treatment solution to obtain 1× final concentration in the assay. For an example of a serial dilution to obtain treatment solutions of 3.3 mM, 1.1 mM, and 330 µM H₂O₂, which translate to 300 µM, 100 µM, and 30 µM final H₂O₂ in the assay, see Figure 3. Make sure to include a control treatment by adding PBS only to the cells.

**Figure 3. Example of a serial dilution.**

Follow the outlined dilution steps to obtain treatment solutions of 3.3 mM, 1.1 mM, and 330 μM H_2O_2 starting from a 9.8 M stock of H_2O_2 .

- Start the timer counting up; at 30 s, add 25 μl desired H_2O_2 treatment solution starting from the first well (e.g., top left) of the 24-well plate and swirl the plate gently for even distribution; repeat this with the rest of the wells adhering to the 30-s time intervals (1 well gets treated every 30 s), as outlined in Figure 4.

Note: The treatment intervals can be shortened to 20 or 15 s, but this requires a bit of practice by the experimenter. In our experience, 15 s is the shortest interval that can still be handled accurately. When adhering to such a short total incubation time as suggested here (5 min), the number of samples that can be processed in a single 'run' from the start of the treatment to lysis is limited by the chosen time interval. If samples need to be divided into different 'runs' performed directly after each other with the same cells and reagents, make sure to group one replicate of all treatment conditions into the same group (i.e., grouping control replicate 1, treatment A replicate 1, treatment B replicate 1, etc. together) rather than subdividing different treatment conditions into different groups in order to maintain equal conditions among the different treatment groups. While we have not observed strong batch effects between runs, we cannot exclude that there will be changes that make it inappropriate to directly compare samples from different runs without 'normalizing' to an inbuilt reference sample

**Figure 4. Example of sample organization in a 24-well plate for a H_2O_2 titration.**

After starting the timer, add 25 μl desired H_2O_2 treatment solutions to the wells every 30 s, as shown.

- After treatment of the last well, get the ice bucket ready with the glass plate and ensure it is still level; get the P1000 and the coverslips and open the low melting point agarose bottle (still in the 37°C water bath).

- g. After exactly 5 min (when the timer shows 05:30 min), stop the first H₂O₂ treatment by adding 1 mL LMP-agarose to the well, pipetting carefully to avoid strong bubble formation. Aspirate the mixture and transfer 1 ml cell-agarose mix onto the appropriate agarose-coated microscope slide. Immediately overlay with a coverslip and, paying attention to keep the slide as level as possible, transfer it onto the cold glass plate on ice for the agarose to settle. Repeat this for every well, adhering to the 30-s intervals, until all the cell samples have been transferred onto slides. This process can be visualized in Video 1.



Video 1. Embedding of cells into agarose

- h. When all samples have been transferred onto the slides and the agarose has set, gently remove each coverslip by sliding it along its longitudinal axis (starting with the first sample) and immerse the slides into lysis buffer in the coplin jar. Keep the samples in cold (on ice) lysis buffer for at least 1 h protected from light. This step can be prolonged to an overnight incubation provided that the samples are constantly kept at 4°C and protected from light.
2. Treatment of cells with MMS as a DNA-damaging agent to determine the extent of DNA damage.
 - a. Seed exponentially growing cells onto a 24-well plate to obtain approximately 2×10^5 cells/well 24 h later.
 - b. Twenty-four hours after seeding, dilute your DNA-damaging agent of interest, *e.g.*, MMS, to the desired concentrations in cold complete medium. You need 1 ml solution/well plus a bit extra.
 - c. To treat the cells, remove the normal medium by aspiration or inverting the plate and add 1 ml MMS solution to the respective wells. Make sure to include a control treatment of medium without MMS.
 - d. Incubate the plate at 37°C for the required time, *e.g.*, 60 min.
 - e. To harvest the cells, wash the wells with PBS, remove the PBS, and add 50 µL Trypsin solution to each well. Incubate the plate at 37°C, checking regularly whether the cells have detached. Once the cells have detached from the bottom, neutralize the Trypsin by adding 200 µL ice-cold complete medium and immediately place the plate on ice.
 - f. Embed the cells in agarose by adding 1 ml 37°C LMP-agarose to the well, pipetting carefully to avoid strong bubble formation. Aspirate the mixture and transfer 1 ml cell-agarose mix to the appropriate agarose-coated microscope slide. Immediately overlay with a coverslip and, paying attention to keep the slide as level as possible, transfer to the cold glass plate on ice for the agarose to settle. Repeat this for every well until all cell samples have been transferred onto slides.
 - g. When all samples have been transferred onto the slides, gently remove the coverslip by sliding it along its longitudinal axis (starting with the first sample) and immerse the slide into lysis buffer in the coplin jar. Keep the samples in cold lysis buffer (on ice) for at least 1 h protected from light. This step can be prolonged to an overnight incubation provided that the samples are constantly kept at a maximum of 4°C and protected from light.
3. Assessment of the repair kinetics after exposure to H₂O₂ as the DNA-damaging agent.
 - a. Make sure that the incubator is running and place the 'humid chamber' inside to equilibrate to 37°C.

- b. Prepare the cells as outlined in Steps D1a-D1d.
- c. Trypsinize exponentially growing cells, neutralize the trypsin by the addition of complete medium, count the cells, and dilute to 2×10^5 cells/ml in complete medium of your choice in 15-mL Falcon tubes.
- d. Place the Falcon tubes on ice for transfer from the cell culture lab to the work bench.
- e. To ensure an even suspension of cells, carefully invert the Falcon tube a few times (avoid foam formation or vigorous shaking in order not to damage the cells) and then pipet 250 μL cell suspension into the wells of the 24-well plate (1 well per slide/sample) kept on ice.
- f. Dilute your DNA-damaging agent of interest, e.g., H₂O₂, to the desired concentration as follows: if you want to treat the cells with 30 μM H₂O₂, prepare an 11 \times treatment solution of 330 μM H₂O₂; 25 μL solution will be mixed with 250 μL cell suspension. Hence, you need to prepare an 11 \times stock solution to obtain 1 \times final concentration. Consider the number of wells you will need to treat to obtain all timepoints for the kinetics when preparing the stock solution.

Note: To ensure that the amount of DNA damage generated by the treatment is within a physiological range and can be correctly repaired by the cells, choose a concentration of damaging agent that yields approximately 30-35% DNA in the tail as the mean value. For primary human fibroblasts, this is typically around 25-30 μM H₂O₂ when following the described procedure.

- g. Start the timer counting up; immediately (at 0 s) add 25 μL H₂O₂ treatment solution to the first well (e.g., top left) of the 24-well plate and swirl the plate gently for even distribution; repeat this with the rest of the wells adhering to the 30-s time intervals (1 well gets treated per 30 s), as outlined in Figure 5. Add only PBS to the last two wells as the control treatment.

Note: The treatment intervals can be shortened to 20 or 15 s, but this requires a bit of practice by the experimenter. In our experience, 15 s is the shortest interval that can still be handled accurately.

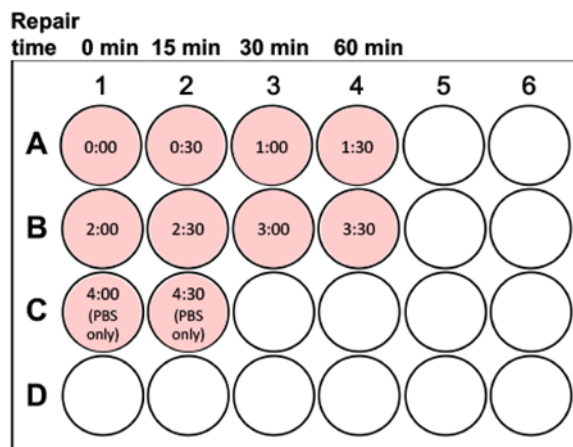


Figure 5. Example of sample organization in a 24-well plate when cells are treated with H₂O₂ to assess repair kinetics after exposure to a DNA-damaging agent.

After starting the timer, add 25 μL desired H₂O₂ treatment solution (e.g., 30 μM) to the wells every 30 s, as shown. Add only PBS to the last two wells as the control treatment. The repair time refers to the minutes that the samples will be incubated at 37°C for DNA repair to take place after their embedding in agarose on the slides.

- h. After treatment of the last well, get the ice bucket ready with the glass plate and ensure that it is still level. Get the P1000 and the coverslips and open the low melting point agarose bottle (still in the 37°C water bath).

- i. After exactly 5 min (when the timer shows 05:00 min), stop the first H₂O₂ treatment by adding 1 ml LMP-agarose to the well, pipetting carefully to avoid strong bubble formation. Aspirate the mixture and transfer 1 mL cell-agarose mix onto the appropriate agarose-coated microscope slide. Immediately overlay with a coverslip and, paying attention to keep the slide as level as possible, transfer the slide onto the cold glass plate on ice for the agarose to settle. Repeat this for every well, adhering to the 30-s intervals, until all cell samples have been transferred onto slides. Of note, the damaging agent is not removed in this setup but simply diluted using complete medium, which also serves to neutralize H₂O₂ very quickly and minimizes any additional damaging effects. If another type of damaging agent is used, which needs to be washed away, please adhere to the protocol used for MMS (Step D2) for the treatment/embedding into agarose.
- j. When all your samples are embedded in agarose on the slides, take on ice to the 37°C incubator. Move the 15 min, 30 min, and 60 min repair slides into the humid box in the incubator for DNA repair to take place. Restart the timer at 0, counting up.

Note: Typically, treatment of primary fibroblasts with 30 µM H₂O₂ for 5 min results in moderate levels of DNA damage (i.e., approximately 30% DNA in the tail), and repair of most of the damage is expected to occur rather quickly within the first 30-60 min (for an example, see Parsons et al., 2009).

- k. For the control and the 0 min timepoints, gently remove the coverslip from the slides by sliding it along its longitudinal axis and immerse them into the lysis buffer in coplin jars. Keep the samples in cold lysis buffer (on ice).
 - l. At 15 min, get the two slides for 15 min repair from the incubator, remove the coverslips, and immerse in lysis buffer protected from light. Repeat this for the 30 min and 60 min timepoints.
 - m. When all the slides are in lysis buffer, incubate the samples for at least 1 h before continuing with electrophoresis. This step can be prolonged to an overnight incubation provided that the samples are constantly kept at max. 4°C and protected from light.
4. Assessment of endogenous DNA damage in cultured cells.
 - a. Trypsinize exponentially growing cells (control versus, e.g., KO cells), neutralize the trypsin by the addition of complete medium, count the cells, and dilute to 2×10^5 cells/mL in complete medium of your choice in 15-mL Falcon tubes.
 - b. Place the Falcon tubes on ice for transfer from the cell culture lab to the work bench.
 - c. To ensure an even suspension of cells, carefully invert the Falcon tube a few times (avoid foam formation or vigorous shaking in order not to damage the cells) and then pipet 250 µL cell suspension into the wells of the 24-well plate (1 well per slide/sample) kept on ice.
 - d. Since there is no need to treat the cells with DNA-damaging agents, you can directly skip to embedding the cells in agarose as outlined in Step D1g.
 - e. Important: make sure to include samples with appropriate positive and negative controls (e.g., ionizing radiation and no-treatment control) to ensure that the assay has worked!
 - f. When all your samples are embedded in agarose on the slides, gently remove the coverslip from the slides by sliding it along its longitudinal axis and immerse them into the lysis buffer in coplin jars. Keep the samples in cold lysis buffer (on ice) for at least 1 h protected from light. This step can be prolonged to an overnight incubation provided that the samples are constantly kept at a maximum of 4°C and protected from light.

E. Electrophoresis and staining of comet slides

1. Prepare an appropriate amount of cold alkaline comet electrophoresis buffer and store at 4°C until required.
2. Slowly drain the lysis buffer from the coplin jars and replace with fresh cold electrophoresis buffer. Incubate for 30 min on ice, protected from light, to allow DNA unwinding.
3. Fill the comet buffer tank to the required level with electrophoresis buffer. Transfer the comet slides to

the comet assay apparatus, paying attention to the orientation of the slides. Make sure all slides are fully immersed in buffer and fill up the remaining space with dummy slides.

4. Close the lid of the comet apparatus and run at 21 V for 30 min.
5. Fill the coplin jar with dH₂O.
6. Remove the slides from the tank and transfer them to the coplin jar containing dH₂O.
7. Incubate for 5 min, then drain the dH₂O and carefully replace with fresh dH₂O. Repeat once more.
8. In the meantime, prepare sufficient comet staining solution (approximately 600 µL per slide plus a bit extra). Keep protected from light.

Note: It is possible to stain the comets directly in a coplin jar to ensure more even staining; however, this approach uses much more SYBR-Gold stain and is therefore much more expensive.

9. Transfer the slides to a tray lined with paper towels, paying attention to lay them down as level as possible.
10. Cover each slide with approximately 600 µL staining solution (ensure that the entire agarose part is covered with the solution), cover the tray with foil or a lid to protect from light, and incubate for 20 min at room temperature.
11. Decant the staining solution and briefly dip each slide into fresh dH₂O.
12. Allow the slides to air-dry overnight protected from light.

Note: In a well-ventilated area, slides are expected to dry overnight at room temperature. Slide drying can be expedited by exposing the slides to a warm air current (not hotter than 35°C to prevent the agarose from melting).

F. Imaging and analysis of comet slides

1. Image the slides on the fluorescence microscope, taking images at 10× or 20× magnification from different fields randomly picked across the entire slide. Make sure to use exposure and light intensities that allow the clear visualization of your comets from the background and try to focus as well as possible. Image an absolute minimum of 50 cells per condition, but preferentially more than 100. Keep separate image folders for every single slide, containing all separate images of the different fields. Save all the individual images of your comet slides as .tiff files in one folder per slide. As nucleoids situated very close to the edge of slides can sometimes show a different shape to the ones on the rest of the slide, try to avoid imaging areas located immediately at the border of slides.
2. Analyze the images using the OpenComet plugin available for FIJI as follows (Figure 6):

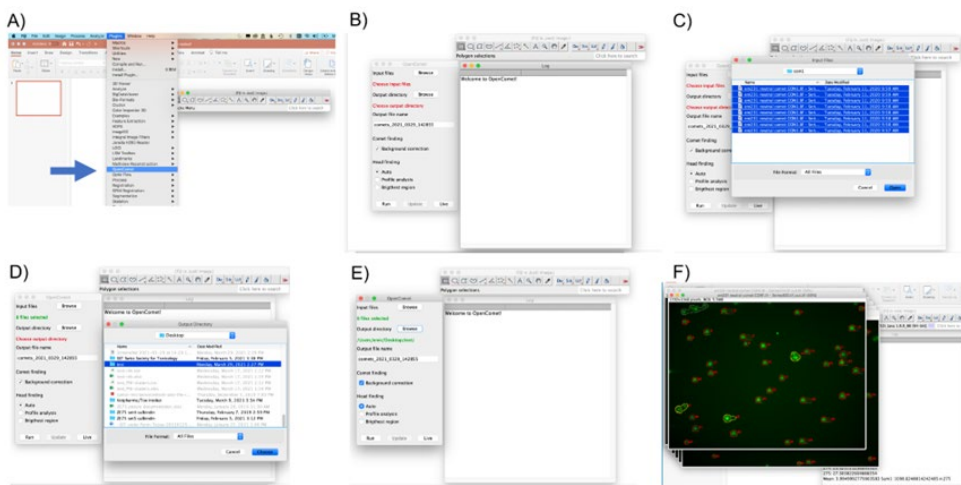


Figure 6. Analysis of images using OpenComet for FIJI.

A-F. Screenshots to illustrate the use of the plugin. A. In FIJI, choose the OpenComet plugin (see blue arrow). B. OpenComet plugin starting panel. C. Select as input files all. tiffs of a single condition/slide to analyze. D. Select Output directory. E. Click ‘RUN’ in the bottom left corner to start the analysis. F. Image files that have been analyzed using OpenComet, ready for review.

3. Open the OpenComet plugin.
4. Choose the input file folder (all images for one slide can be selected and analyzed at once) and an output file directory.
5. Using the ‘auto’ head finding mode, click run. Results of this analysis will be summarized in an Excel file that is saved in the output file directory that you chose.
6. Check that all the comets have been correctly detected, deselect the ones that clearly need to be excluded/are incorrect (*e.g.*, artifacts and debris that are not comets that have been scored, overlays of multiple nucleoids, comets in which the head has been wrongly defined, or similar) by clicking on them. OpenComet will outline every regularly detected comet in red (with a red circle around the head and a red line to delineate the tail; see Figure 7A). In addition, there will be a green line that shows you the intensity distribution of the signal detected as the head and a blue line for the signal detected as the tail. Sometimes, the software is unsure whether something is a correctly detected comet or not for a number of different reasons (*e.g.*, unusual head, or others). In that case, OpenComet will outline these ‘outliers’ in yellow (Figure 7B). However, it is also possible that shapes are incorrectly scored, as shown in Figure 7C. Here, the very low-intensity signal was incorrectly scored to have a minuscule head and most of the signal in the tail. The inclusion of such a shape would strongly influence the results, especially if this happens more than once or if only a few cells are assessed per condition. If OpenComet cannot analyze the shapes (*e.g.*, in the case that two or more comets are too close to each other or overlying, or other reasons), the shapes will be outlined in grey (Figure 7D). The same will happen to those comets that you have deselected/excluded by clicking on them. It is very important to visually double-check every comet, as incorrectly assessed ones can strongly influence the results!
7. After double-checking all comets on all slides, click ‘update.’ This will generate a second Excel sheet with the suffix ‘_update,’ which takes into account the comets that have been excluded, etc.
8. This Excel sheet will give you all the values for all comet images from the slide that was analyzed. In the last few rows, you will find values for the mean, median, standard deviation, and minimum and maximum for all detected comets, divided into either only all normal comets, or the normal + outlier comets. The choice of which of these values to use depends on whether you are fine with including the values of the outliers. Normally, both these values are very similar to one another.
9. There are two ways to plot your results. Firstly, you can calculate a mean value of the duplicates or triplicates that were analyzed as a % of DNA in the tail, tail moment, or olive moment, *e.g.*, using a bar graph (Figure 7E). (Repeat the entire assay at least 2 more times to obtain 3 or more independent values for each data point). Secondly, you can plot all the individual data points (*e.g.*, of the 50 cells that were quantitated) of at least 3 repeats of the entire assay (Figure 7F).

Note: The tail moment describes the product of multiplying the length of the comet tail with the % of DNA in the tail, while the olive moment is the product of the total % of DNA in the tail and the distance between the centers of the masses of both head and tail regions. The olive moment is particularly useful to describe heterogeneity within a cell population, as the olive moment picks up variations in how the DNA is distributed within the tail. Of the three options, the % of DNA in the tail is the measurement that seems the most intuitive to most researchers.

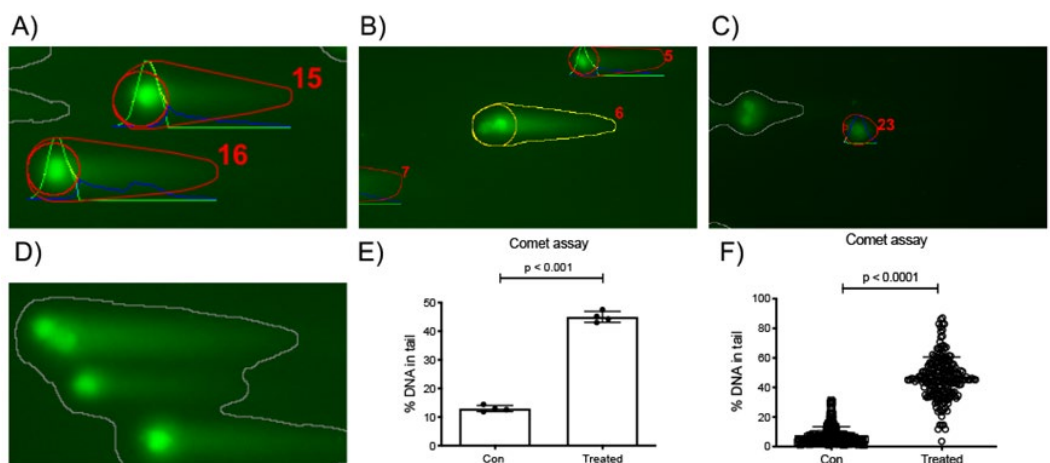


Figure 7. Example of comet slide images analyzed using the OpenComet plugin running the «auto» head finding mode and possible results plots.

A. Detection of regular comets by OpenComet. Red numbers serve to label the individual comets so they can be identified in the results sheet. B. Example of an ‘outlier’ comet. C. Example of an incorrect score of a comet shape. The very low-intensity signal was incorrectly scored to have a minuscule head and most of the signal in the tail. The inclusion of such a shape would strongly influence the results. D. A grey shape indicates the impossibility of OpenComet to score these comets. E-F. The results obtained in the Excel file can be plotted (E) as the mean value \pm standard deviation of the duplicates or triplicates analyzed as % of DNA in the tail, tail moment, or olive moment or (F) as individual data points (e.g., of the 50 cells that were quantitated) and the mean \pm standard deviation.

10. To test whether the groups differ significantly from each other, you can use the Student’s *t*-test when only 2 groups are being compared. When comparing 3 or more groups, use one-way ANOVA followed by, e.g., Bonferroni’s multiple comparison test.
11. When publishing comet assay data, we strongly advise adhering to the ‘minimum information for reporting on the comet assay (MIRCA)’ guidelines that were just recently published in an attempt to ensure better interpretation, verification, and reproducibility of results across laboratories (Møller *et al.*, 2020).

Recipes

1. Lysis buffer for the alkaline comet assay

- a. Prepare the ‘premix’ by dissolving 146.1 g NaCl (final: 2.5 M), 37.2 g EDTA disodium salt dihydrate ($C_{10}H_{14}N_2Na_2O_8 \cdot 2H_2O$) (final: 100 mM), 1.2 g Tris base (final: 10 mM), and 8 g solid NaOH in 800 mL dH₂O.

Note: It takes a while to dissolve all the solid ingredients. Use a magnetic stirrer and allow enough time for the preparation of this buffer.

- b. Once all the solids have dissolved, adjust the pH to 10.5 by the dropwise addition of 5 M NaOH. Adjust the volume to 1 L by adding dH₂O and store at 4°C.
- c. To prepare a ‘complete solution’ of lysis buffer immediately prior to use, add 1 mL DMSO and 1 mL Triton X-100 to 98 mL cold lysis buffer.

2. Electrophoresis buffer for the alkaline comet assay

- a. Prepare separate stock solutions: 5 M NaOH (100 g NaOH in 500 ml dH₂O), 200 mM EDTA disodium salt (C₁₀H₁₄N₂Na₂O₈·2H₂O; 14.89 g in 200 mL; no pH adjustment necessary).
- b. To prepare electrophoresis buffer (final composition: 300 mM NaOH, 1 mM EDTA, and 1% DMSO), add 60 ml 5 M NaOH, 5 ml 200 mM EDTA, and 10 mL DMSO to 925 mL cold dH₂O; check that the pH is >13 (using a pH strip) and store at 4°C until required.

3. Comet staining solution

Dilute SYBR Gold 1:10,000 in dH₂O immediately prior to use. Protect from light.

4. PBS (phosphate-buffered saline)

- a. To make a 10× PBS stock solution, dissolve 80 g NaCl, 2 g KCl, 26.8 g Na₂HPO₄·7H₂O, and 2.4 g KH₂PO₄ in 800 mL dH₂O. Adjust the pH to 7.4 using HCl, add dH₂O to 1 L, and autoclave to store.
- b. To make 1× PBS working solution, dilute 100 ml 10× PBS stock solution in 900 ml dH₂O. Tris base (mol. wt. = 121.14) – 60.57 g

Acknowledgments

The authors wish to thank the following funding bodies for supporting research in the group of EM: Swiss National Science Foundation, Promedica Stiftung Chur, the Sassella Stiftung, and the Kurt und Senta Herrmann Stiftung.

Competing interests

The authors declare no conflicts of interest.

References

- Ciccia, A. and Elledge, S. J. (2010). [The DNA damage response: making it safe to play with knives](#). *Mol Cell* 40(2): 179-204.
- Clementi, E., Inglin, L., Beebe, E., Gsell, C., Garajova, Z. and Markkanen, E. (2020). [Persistent DNA damage triggers activation of the integrated stress response to promote cell survival under nutrient restriction](#). *BMC Biol* 18(1): 36.
- Collins, A. R. (2014). [Measuring oxidative damage to DNA and its repair with the comet assay](#). *Biochim Biophys Acta* 1840(2): 794-800.
- Gyori, B. M., Venkatachalam, G., Thiagarajan, P. S., Hsu, D. and Clement, M. V. (2014). [OpenComet: an automated tool for comet assay image analysis](#). *Redox Biol* 2: 457-465.
- Hoeijmakers, J. H. (2009). [DNA damage, aging, and cancer](#). *N Engl J Med* 361(15): 1475-1485.
- Jackson, S. P. and Bartek, J. (2009). [The DNA-damage response in human biology and disease](#). *Nature* 461(7267): 1071-1078.
- Li, W. and Sancar, A. (2020). [Methodologies for detecting environmentally induced DNA damage and repair](#). *Environ Mol Mutagen* 61(7): 664-679.
- Markkanen, E. (2017). [Not breathing is not an option: How to deal with oxidative DNA damage](#). *DNA Repair (Amst)* 59: 82-105.
- Møller, P., Azqueta, A., Boutet-Robinet, E., Koppen, G., Bonassi, S., Milic, M., Gajski, G., Costa, S., Teixeira, J. P., Costa Pereira, C., Dusinska, M., Godschalk, R., Brunborg, G., Gutzkow, K. B., Giovannelli, L., Cooke, M. S., Richling, E., Laffon, B., Valdiglesias, V., Basaran, N., Del Bo, C., Zegura, B., Novak, M., Stopper, H., Vodicka, P., Vodenkova, S., de Andrade, V. M., Sramkova, M., Gabelova, A., Collins, A. and Langie, S. A. S. (2020).

- [Minimum Information for Reporting on the Comet Assay \(MIRCA\): recommendations for describing comet assay procedures and results.](#) *Nat Protoc* 15(12): 3817-3826.
- Olive, P. L. (2009). [Impact of the comet assay in radiobiology.](#) *Mutat Res* 681(1): 13-23.
- Van Loon, B., Markkanen, E. and Hübscher, U. (2010). [Oxygen as a friend and enemy: How to combat the mutational potential of 8-oxo-guanine.](#) *DNA Repair (Amst)* 9(6): 604-616.

Neutral Comet Assay to Detect and Quantitate DNA Double-Strand Breaks in Hematopoietic Stem Cells

Irene Mariam Roy[#], Pon Sowbhagya Nadar[#] and Satish Khurana*

School of Biology, Indian Institute of Science Education and Research Thiruvananthapuram, Kerala, 695 551, India

*For correspondence: satishkhurana@iisertvm.ac.in

[#]Contributed equally to this work

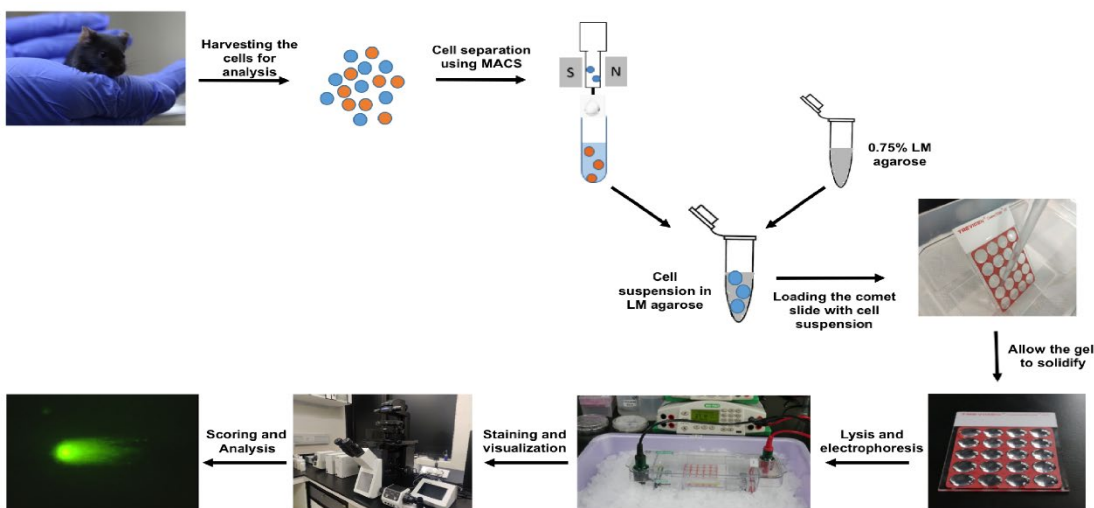
Abstract

In vertebrates, hematopoietic stem cells (HSCs) regulate the supply of blood cells throughout the lifetime and help to maintain homeostasis. Due to their long lifespan, genetic integrity is paramount for these cells, and accordingly, a number of stem cell-specific mechanisms are employed. However, HSCs tend to show more DNA damage with increasing age due to an imbalance between proliferation rates and DNA damage responses. The comet assay is the most common and reliable method to study DNA strand breaks at the single-cell level. This procedure is based on the electrophoresis of agarose-embedded lysed cells. Following the electrophoretic mobilization of DNA, it is stained with fluorescent DNA-binding dye. Broken DNA strands migrate based on fragment size and form a tail-like structure called “the comet,” whereas intact nuclear DNA remains a part of the head of the comet. Since the alkaline comet assay fails to differentiate between single and double-strand breaks (DSBs), we used a neutral comet assay to quantitate the DSBs in HSCs upon aging and other physiological stresses. The protocol presented here provides procedural details on this highly sensitive, rapid, and cost-effective assay, which can be used for rare populations of cells such as HSCs.

Keywords: Hematopoietic stem cells, DNA damage, Double-strand breaks, Neutral comet assay

This protocol was validated in: Stem Cell Reports. (2020) DOI: 10.1016/j.stemcr.2020.06.022.

Graphical Abstract:



The neutral comet assay is an extremely useful tool that allows the detection and quantitation of double-strand DNA breaks at the single-cell level.

The graphical abstract represents a flowchart for the neutral comet assay procedure.

Background

During every round of cell proliferation, the genomic content is faithfully replicated, albeit with some errors. These errors lead to changes or modifications in the structure and chemical nature of genomic DNA. The replication machinery is tightly associated with DNA damage repair (DDR) pathways, thereby recovering cells from such damage (Chatterjee and Walker, 2017). Alternatively, the DNA damage response pathways can induce apoptosis (Nowsheen and Yang, 2012); however, some DNA damage is undetected and unrepaired, accumulating over a period of time. Accumulation of this DNA damage during aging poses a serious challenge to the healthy functioning of a variety of tissues, including hematopoietic systems. Recent studies have indicated that accumulation of age-related physiological changes in the stem cell population leads to alterations in immune system function (Oh *et al.*, 2014). In addition, several age-associated malignancies have been linked to DNA damage accumulation in the stem cell compartment (Beerman, 2017). Hematopoietic stem cells have cytoprotective and genoprotective mechanisms to safeguard their long-lasting functional potential; however, it has been demonstrated that DNA damage accumulates in HSCs during the aging process. Several research groups have proposed that this accumulation is due to increased proliferation rates in old HSCs. In contrast, others show that long-term dormancy may prevent rare DNA damage from accumulating due to lack of replication-associated repair (Beerman *et al.*, 2014).

To understand the fundamental processes involved in DNA damage accumulation and repair, quantitation of DNA damage is vital (Lu *et al.*, 2017). In 1984, Ostling and Johanson demonstrated the electrophoretic mobility of DNA fragments from the core nuclei (Ostling and Johanson, 1984). When single cells embedded in low-melting-point agarose are electrophoresed, the DNA-damaged fragments move faster, giving rise to tail-like structures resembling a comet. The intact part of the DNA is called the head of the comet and the trail produced due to impaired DNA is known as the tail of the comet. This single-cell gel electrophoresis assay, also known as the comet assay, is one of the most reliable and commonly used methods for analyzing DNA damage in cells. It has been successfully applied to understand the processes involved in genotoxicity, molecular epidemiology, and human bio-monitoring, along with solving basic biology questions regarding DNA damage and repair (Collins, 2004). This technique was further modified by Singh *et al.*, who showed a substantial increase in reproducibility under alkaline conditions (Lu *et al.*, 2017). At alkaline pH, the sensitive sites are knocked down and the strands break due to distortion in their

conformation. Therefore, the alkaline comet assay is commonly used to analyze strand breaks, DNA-protein crosslinks, and alkali-labile sites; nevertheless, the specificity for double-strand breaks is compromised (Lu *et al.*, 2017). To overcome this issue, the neutral comet assay was further developed (Calini *et al.*, 2002); it protects the DNA double strands from distortion, thus aiding in the specific detection of double-strand DNA damage. These DNA strand breaks result in the lengthening of DNA loops in genomic DNA, which form a comet-like tail in an electrophoretic mobility assay (Cortes-Gutierrez *et al.*, 2012). Because double-strand DNA breaks lead to mutations and chromosomal abnormalities, it is important to detect and quantitate them. The neutral comet assay is of immense importance and is highly efficient for *in vivo* and *ex vivo* systems (Sharma *et al.*, 2011). The comets formed due to electrophoretic mobility can be visualized by fluorescence microscopy. The percentage of DNA damage can be estimated from the percentage of DNA present in the comet tail since they are directly proportional to one other. With advancements in technology such as fluorescent staining and automated comet scoring software, the comet assay has become popular for detecting DNA damage (Beedanagari, 2017). In the case of rare cell populations such as HSCs, the neutral comet assay has emerged as a promising technique to study DNA damage responses due to physiological, pathological, and age-associated stresses (Hazlehurst and Dalton, 2001; Milyavsky *et al.*, 2010). The present protocol describes the method to assess DNA damage in freshly sorted hematopoietic stem cells from mice bone marrow.

Materials and Reagents

1. Autoclaved lint-free tissue paper
2. 60-mm tissue culture plates (Eppendorf, catalog number: 0030701119)
3. 26 G needle (BD PrecisionGlide, BD Medical (S) Pvt Ltd, catalog number: 302806)
4. 1-mL syringe (BD Medical (S) Pvt Ltd, catalog number: 303060)
5. 40- μ m nylon strainer (Falcon, catalog number: 352340)
6. Bone marrow cells from mice
7. FACS tubes (Falcon, catalog number: 352054)
8. Comet slides (CometSlides™ 20 well, Trevigen, catalog number: 4252-02K-01)
9. MACS apparatus
 - a. MS column (MACS, Miltenyi Biotec, catalog number: 130-042-201)
 - b. MACS multistand (MACS, Miltenyi Biotec, catalog number: 002139)
 - c. MiniMACS™ separator (MACS, Miltenyi Biotec, catalog number: 130-042-102)
10. Antibodies
 - a. APC-conjugated lineage antibody cocktail [2:100 concentration] (BD Pharmingen™, BD Biosciences, catalog number: 51-9003632)
 - b. Anti-mouse c-kit PE [1:100 concentration] (Biolegend, catalog number: 105807)
 - c. Anti-mouse Sca-1 PerCP-Cy5.5 [1:100 concentration] (Biolegend, catalog number: 122524)
11. 1% agarose (Sigma-Aldrich, catalog number: A9539)
12. 0.75% low-melting-point agarose (LM agarose) (Sigma-Aldrich, catalog number: A9414)
13. 70% ethanol (Changshu Hongsheng Fine Chemical Co., Ltd, catalog number: 1170)
14. SYBR® Gold staining solution (ThermoFisher Scientific, Invitrogen, catalog number: S33102)
15. 10× RBC lysis buffer (Biolegend, catalog number: 420301)
16. Lysis buffer (see Recipes)
17. 1× neutral electrophoresis buffer (see Recipes)
18. DNA precipitation solution (see Recipes)
19. 1× phosphate-buffered saline (PBS) (see Recipes)

Equipment

1. Electrophoresis unit (Mini-Sub® Cell GT, Bio-Rad, catalog number: 329BR014542)

2. Epifluorescence microscope (Olympus IX2-ILL100, OLYMPUS CORPORATION, catalog number: 0M04213)
3. Brightfield microscope (Primovert, Ziess, catalog number: 3842010199)

Software

1. ImageJ – Open Comet (Benjamin M. Gyori and Gireedhar Venkatachalam, www.cometbio.org)
2. Excel 2016 (Microsoft Corporation)
3. GraphPad Prism (GraphPad Software, Inc., www.graphpad.com)

Procedure

A. Cell preparation

1. Euthanize a C57Bl6/J mouse, dissect out the hind limbs, and remove the extra tissue from the bones to separate the femur and tibia.
2. Flush the bone marrow cells into a 50-mL polypropylene tube using autoclaved 1× PBS and a 26 G needle with a 1-mL syringe until the bones are cleared inside.
3. Mix the cells to make a single cell suspension and strain through a 40-µm nylon strainer. Centrifuge at 600 × g for 5 min at 4°C.
4. Lyse the RBCs by adding 500 µL 1× RBC lysis buffer (diluted in 1× PBS) to the pellet and neutralize the reaction after 2 min by adding 2 mL 1× PBS. Centrifuge at 600 × g for 5 min at 4°C.
5. Resuspend the cell pellet in 1 mL 1× PBS and count the cells using a hemocytometer.
6. Incubate the cells with the required antibodies (2 µL/5 million cells for Lin APC and 1 µL/5 million cells for c-Kit PE and Sca-1 PerCP-Cy5.5) to stain hematopoietic progenitor cells (Lin APC cocktail, c-Kit PE, Sca-1 PerCP-Cy5.5) for 30 min.
7. Centrifuge at 600 × g for 5 min at 4°C. Wash the cells with 1× PBS and transfer to a 5-mL FACS tube for sorting.
8. Sort the pure LSK (Lineage– Sca-1+ ckit+) population into 1× PBS and store at 4°C until further use.

Note: Alternatively, MACS sorting can be used to isolate less pure HSC progenitor populations.

B. Slide preparation

1. Weigh 1 g agarose and dissolve in 100 mL 1× PBS using a microwave oven.
2. Place the comet slides inside a plastic container in a slanted position (Figure 1A). Pipette out 1 mL agarose and evenly coat the slides and, leave to solidify for 10–15 min at room temperature (Figure 1B).
3. Freshly prepare 0.75% low-melting (LM) agarose using 1× PBS in a 100-mL beaker. Dissolve using a microwave oven.

Note: Transfer the molten 0.75% LM agarose to a storage bottle for further use. Before use, re-melt in a beaker containing hot water.

4. Allow the hot LM agarose to cool for at least 20 min at 37°C.
5. Add 1×10^5 cells/mL to the molten LM agarose at a ratio of 1:10 (v/v).

Note: If you take 500 µL molten LM agarose, add 50 µL cells in 1× PBS (Ca^{2+} and Mg^{2+} free) at 1×10^5 cells/mL.

6. Immediately pipette 50 µL suspension onto the comet slide. Use the tip of the pipette to spread the

mixture uniformly over the surface area and allow to solidify (Figure 1C).

Note: If the sample mixture is not dispersing uniformly on the slide, heat up the LM agarose at 37°C before suspending the cells, and prepare the sample mixture again.

7. Keep the slides at 4°C for 10 min in the dark (e.g., place in a refrigerator).

Note: A clear 0.5 mm ring appears at the edge of the well (Figure 1D). To increase the adherence of the sample to the slide, the gelling time and humidity should be increased.

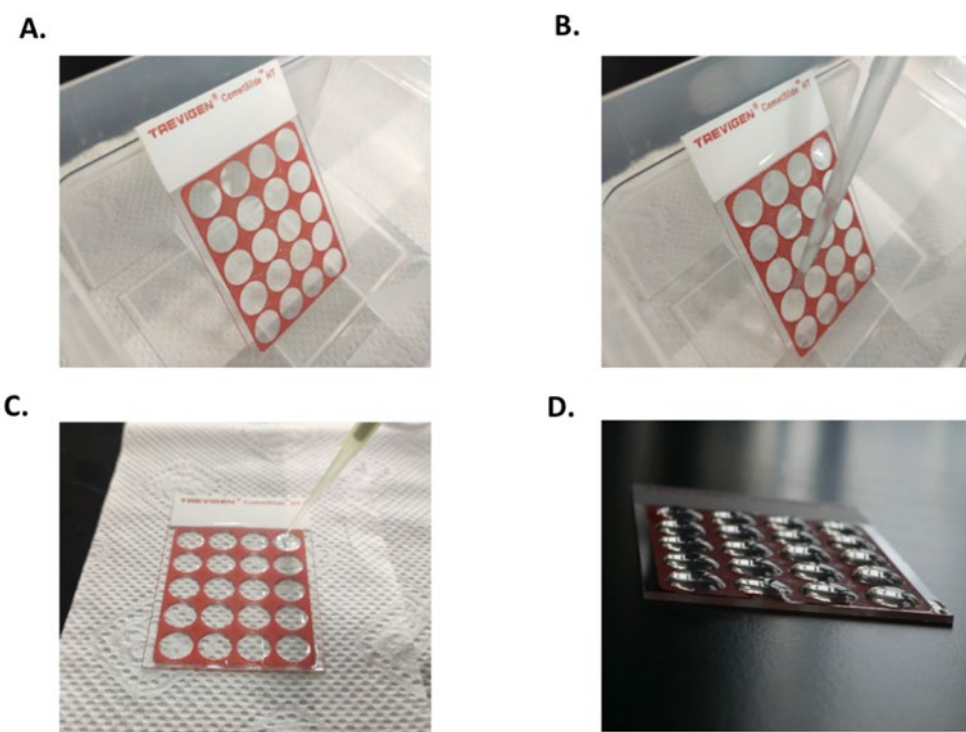


Figure 1. Preparation of a comet slide.

A. A clean Trevigen® CometSlide™ HT is placed inside a plastic container. B. The comet slide is pre-coated with molten 1% agarose. This ensures that cells adhere to the slide efficiently. After pre-coating with agarose, allow the gel to solidify. C. The 0.75% LM agarose containing the cells is added gradually to the slide. Allow the gel to solidify at 4°C. D. The comet slide after solidification of the gel.

C. Lysis and Electrophoresis

1. Prepare the lysis solution (see Recipes) and place on ice for at least 20 min before use.
2. Pour the required amount of pre-chilled lysis solution in a tray and immerse the slides. Place the tray on ice or at 4°C for 1 h.
3. Take the slides from the lysis solution and drain the excess.
4. Wash the slides by placing them in 50 mL pre-chilled 1× neutral electrophoresis buffer (see Recipes) at 4°C for 30 min.
5. Pour 950 mL pre-chilled 1× neutral electrophoresis buffer into the Comet Assay® ES tank. Place the slides in the electrophoresis slide tray and cover with the slide tray overlay (Figure 2A).
6. Set the power supply to 21 volts and perform electrophoresis for 1 h at 4°C.
7. For other electrophoresis units, align the slides equidistant from the electrodes, add 1× neutral

- electrophoresis buffer not exceeding 0.5 cm above the slide (Figure 2B), and apply voltage for 30 min at 1 volt per cm, measuring the distance between the two opposite electrodes of the electrophoresis tank (*e.g.*, If the distance is 21 cm then apply 21 V).
8. Run the electrophoresis unit either in a cold room or over an ice tray containing enough ice to partially cover the unit (Figure 2C).

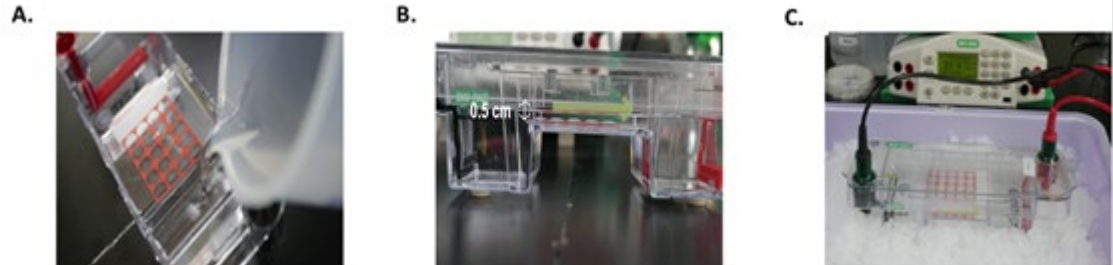


Figure 2. Electrophoresis under neutral conditions.

A. After lysis, the comet slide is placed in the electrophoretic unit and neutral electrophoresis buffer is added to the buffer tank. B. The neutral electrophoresis buffer should not exceed 0.5 cm above the slide. C. Perform electrophoresis at 21 volts for 1 h at 4°C.

D. Staining and visualization of slides

1. Drain the excess neutral electrophoresis buffer and immerse the slides in DNA precipitation solution for 30 min at room temperature (see Recipes).
2. Remove the slides and immerse them in 70% ethanol for 5 min at room temperature.
3. Allow the samples to dry for 10-15 min at room temperature.

Note: Drying the samples will allow the cells to settle in a single plane, making visualization, recording, and quantitation easier. Samples can be stored with desiccant at room temperature before scoring.

4. Add 100 µL diluted SYBR® Gold onto each sample and incubate for 30 min.

Note: Trevigen provides the CometAssay® Silver Staining Kit designed for comet staining. Silver staining helps in the visualization of comets on any transmission light microscope and permanently stains the samples for long-term storage. It is recommended that samples are dried before silver staining.

5. Tap the slides gently to remove excess SYBR® Gold solution. Allow the slide to dry completely at room temperature in the dark.
6. View the slides using epifluorescence microscopy and obtain unbiased images for every cell that could be visualized.

Note: The efficiency of the method can be tested using cells challenged with genotoxic stress as a positive control. Here, hematopoietic stem and progenitor cells from young adults (8 weeks old) (Figure 3A) were compared with cells from aged mice (2 years old) (Figure 3B). Comet tail formation in cells from aged mice is clearly visible. Comparison between the two cell types for the proportion of genomic DNA in the head versus the tail can be used as a reliable quantitation of the extent of DNA damage.

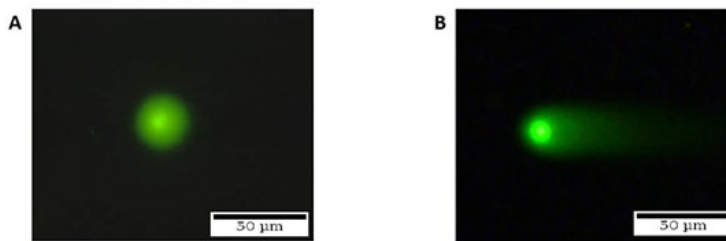


Figure 3. Staining and visualization of cells.

A. HSC from young mice; the nucleus in the cell is intact, indicating that there is no DNA damage. B. HSC from old mice; the nucleus in the cell is not intact and is forming a head and a comet tail, indicating that there is DNA damage.

E. Scoring and analysis of the cells

1. Scoring of the comet is performed in the ImageJ plugin – Open Comet. Launch the plugin in ImageJ (Figure 4A).
2. Input your image files to the Input files option by clicking on the Browse button (Figure 4B).
3. Choose an Output directory where the output files will be stored, along with the name of the file that it should be saved under (Figure 4C and 4D).

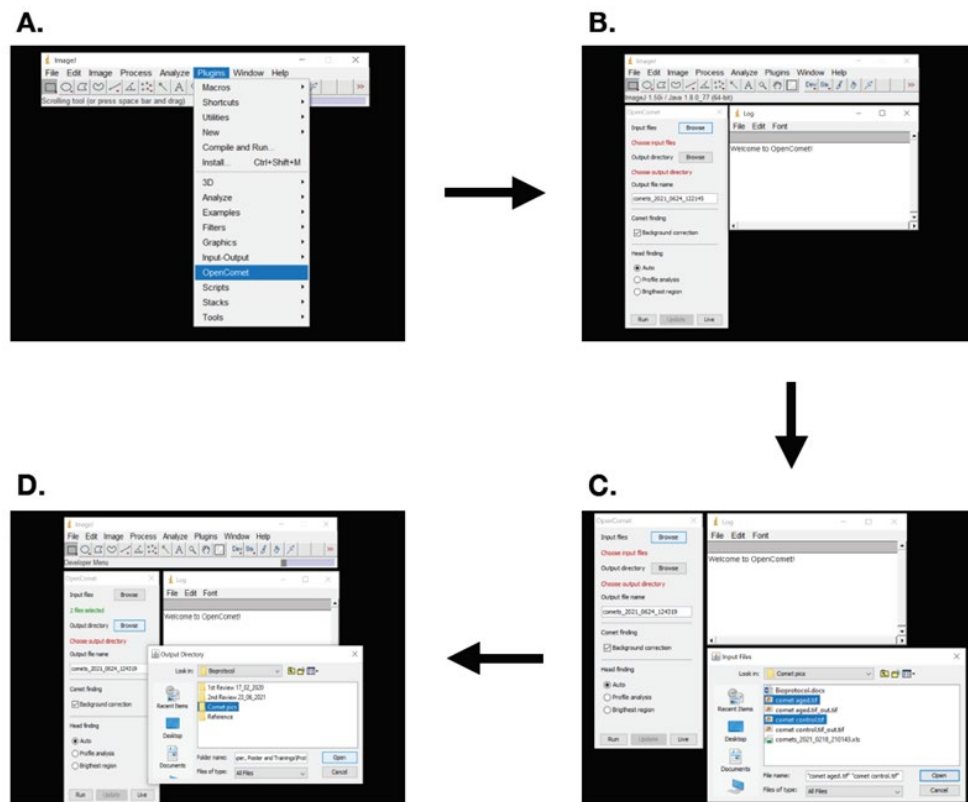


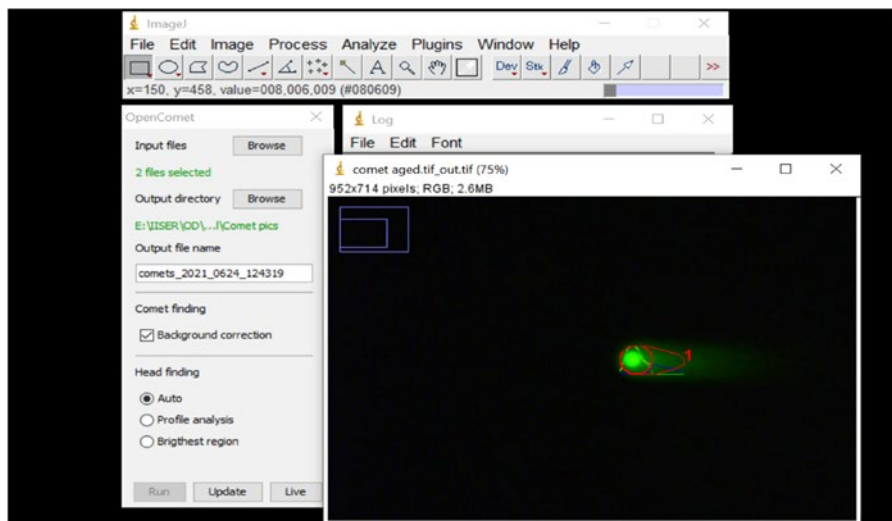
Figure 4. Comet scoring using ImageJ.

A. Open the ImageJ software and click on Plugins. Select OpenComet_src_v1.3.1 and click on

OpenComet. B. A dialogue box will open, where you need to browse the Input files and Output directory. C. Select the images for scoring the input file. D. Choose the Output directory.

4. Choose the default analysis option and Click RUN.
5. The analyzed output data will appear in the Output directory.
6. The Output file consists of an Output Image and an Output Spreadsheet. Review all the Output images for false analysis and outliers. Note the Number given specifically for each image (Figure 5A).
7. Open the Spreadsheet and manually delete the outlier numbers.
8. Obtain the values for Olive moment and Tail moment from the Spreadsheet and graphically represent the data using GraphPad PRISM (Figure 5B).

A.



B.

	A	B	C	D	E	F	G	H	I	J	K	L	M	N	O	P	Q	R	S
1	FileName	Num	Flag	CometArea	CometLen	CometDN	HeadArea	HeadLen	HeadDN	TailArea	TailLen	TailDN	TailLen/HeadArea	TailDN/HeadArea	TailDN/Pc	TailMoMe	OliveMoMe		
2	comet_aged	1	normal	3572	77.66019	80	199742	1243	114.173	40	141917	71.05015	1329	43.51016	40	57825	28.94985	11.57994	9.842947
3	Mean		normal	2572	77.66019	80	199742	1243	114.173	40	141917	71.05015	1329	43.51016	40	57825	28.94985	11.57994	9.842947
4	Median		normal	2572	77.66019	80	199742	1243	114.173	40	141917	71.05015	1329	43.51016	40	57825	28.94985	11.57994	9.842947
5	StdDev		normal	0	0	0	0	0	0	0	0	0	0	0	0	0	0	0	
6	Min		normal	2572	77.66019	80	199742	1243	114.173	40	141917	71.05015	1329	43.51016	40	57825	28.94985	11.57994	9.842947
7	Max		normal	2572	77.66019	80	199742	1243	114.173	40	141917	71.05015	1329	43.51016	40	57825	28.94985	11.57994	9.842947
8	Mean		normaleoI	2572	77.66019	80	199742	1243	114.173	40	141917	71.05015	1329	43.51016	40	57825	28.94985	11.57994	9.842947
9	Median		normaleoI	2572	77.66019	80	199742	1243	114.173	40	141917	71.05015	1329	43.51016	40	57825	28.94985	11.57994	9.842947
10	StdDev		normaleoI	0	0	0	0	0	0	0	0	0	0	0	0	0	0	0	
11	Min		normaleoI	2572	77.66019	80	199742	1243	114.173	40	141917	71.05015	1329	43.51016	40	57825	28.94985	11.57994	9.842947
12	Max		normaleoI	2572	77.66019	80	199742	1243	114.173	40	141917	71.05015	1329	43.51016	40	57825	28.94985	11.57994	9.842947
13																			
14																			
15																			
16																			
17																			
18																			
19																			
20																			
21																			
22																			
23																			

Figure 5. Results of comet scoring.

A. Identification of the comet head and tail. B. Excel spreadsheet containing the computed comet parameters.

Recipes

1. Lysis buffer (Ingredients/1,000 mL)

3.5 M NaCl – 146.1 g

100 mM EDTA – 37.2 g

100 mM Trizma Base – 1.2 g

Dissolve the ingredients in 700 mL dH₂O.

Add 8 g NaOH pellets and adjust the pH to 10.0 using HCl or NaOH (concentrated).

50 mL is required for each assay.

Add 1% Triton X-100 – 0.5 mL.

10% dimethyl sulphoxide (DMSO) – 5 mL

2. 1× neutral electrophoresis buffer

To prepare 10× neutral electrophoresis buffer:

Tris base (mol. wt. = 121.14) – 60.57 g

Sodium acetate (mol. wt. = 136.08) – 204.12 g

Dissolve in 450 mL dH₂O and adjust the pH to 9.0 using glacial acetic acid.

Adjust the volume to 500 mL and filter sterilize. Store at room temperature.

Dilute the 10× stock to 1× in dH₂O to prepare 1 L working strength buffer and pre-chill at 4°C.

3. DNA precipitation solution

Prepare a 10 ml stock solution of 7.5 M ammonium acetate: NH₄Ac (mol. wt. = 77.08) = 5.78 g

dH₂O (after NH₄Ac is dissolved) – 10 mL

For 50 mL DNA precipitation solution:

7.5 M NH₄Ac (mol. wt. = 77.08) – 6.7 mL

95% EtOH (reagent grade) – 43.3 mL

4. SYBR® Gold staining solution

From SYBR® Gold concentrate (10,000× in DMSO)

SYBR® Gold – 1 μL

Electrophoresis Buffer – 10 mL

Store at 4°C in the dark

5. 1× phosphate-buffered saline (PBS)

To prepare 10× PBS stock solution:

NaCl – 80 g

KCl – 2 g

Na₂HPO₄ – 14.4 g

KH₂PO₄ – 2.4 g

Take 800 mL Milli-Q water, dissolve the salts and adjust the pH to 7.4, and make up the volume to 1,000 mL

Dilute the 10× stock to 1× in dH₂O

Acknowledgments

This work was supported by the Wellcome Trust/DBT India Alliance Fellowship (IA/I/15/2/502061) awarded to SK and intramural funds from the Indian Institute of Science Education and Research Thiruvananthapuram (IISER TVM). The institutional animal facility is supported by funds from the Department of Science and Technology, Government of India (under FIST scheme; SR/FST/LS-II/2018/217). IMR is supported by a Senior Research

Fellowship from the University Grants Commission (UGC), India. This protocol was taken from the article by Biswas *et al.* (2020) “The Periostin/Integrin-av Axis Regulates the Size of Hematopoietic Stem Cell Pool in the Fetal Liver” and was modified from the protocol described in the Trevigen comet assay kit (Biswas *et al.*, 2020).

Competing interests

The authors have no competing financial or non-financial interests relevant to this study.

Ethics

The animals used to isolate the HSCs for DNA damage analysis (C57BL/6J-CD45.2) were bred and maintained in the animal facility at IISER Thiruvananthapuram. The animals were maintained as per the guidelines provided by the Committee for the Purpose of Control and Supervision of Experiments on Animals (CPCSEA), Ministry of Environment and Forests (MoEF), Government of India. During the experiments, mice were maintained in isolator cages and allowed access to autoclaved acidified water and irradiated food *ad libitum*. All animal experiments were approved by the Institutional Animal Ethics Committee (IAEC) of the institute.

References

- Beedanagari, S. (2017). [4.11-Genetic Toxicology](#). In: Chackalamannil, S., Rotella, D. and Ward, S. E. (Eds.). *Comprehensive Medicinal Chemistry III*. pp 195-203. Elsevier, Oxford.
- Beerman, I. (2017). [Accumulation of DNA damage in the aged hematopoietic stem cell compartment](#). *Semin Hematol* 54(1): 12-18.
- Beerman, I., Seita, J., Inlay, M. A., Weissman, I. L. and Rossi, D. J. (2014). [Quiescent hematopoietic stem cells accumulate DNA damage during aging that is repaired upon entry into cell cycle](#). *Cell Stem Cell* 15(1): 37-50.
- Biswas, A., Roy, I. M., Babu, P. C., Manesia, J., Schouteden, S., Vijayakurup, V., Anto, R. J., Huelsken, J., Lacy-Hulbert, A., Verfaillie, C. M. and Khurana, S. (2020). [The Periostin/Integrin-alphav Axis Regulates the Size of Hematopoietic Stem Cell Pool in the Fetal Liver](#). *Stem Cell Reports* 15(2): 340-357.
- Calini, V., Urani, C. and Camatini, M. (2002). [Comet assay evaluation of DNA single- and double-strand breaks induction and repair in C3H10T1/2 cells](#). *Cell Biol Toxicol* 18(6): 369-379.
- Chatterjee, N. and Walker, G. C. (2017). [Mechanisms of DNA damage, repair, and mutagenesis](#). *Environ Mol Mutagen* 58(5): 235-263.
- Collins, A. R. (2004). [The comet assay for DNA damage and repair: principles, applications, and limitations](#). *Mol Biotechnol* 26(3): 249-261.
- Cortes-Gutierrez, E. I., Hernandez-Garza, F., Garcia-Perez, J. O., Davila-Rodriguez, M. I., Aguado-Barrera, M. E. and Cerda-Flores, R. M. (2012). [Evaluation of DNA single and double strand breaks in women with cervical neoplasia based on alkaline and neutral comet assay techniques](#). *J Biomed Biotechnol* 2012: 385245.
- Hazlehurst, L. A. and Dalton, W. S. (2001). [Mechanisms associated with cell adhesion mediated drug resistance \(CAM-DR\) in hematopoietic malignancies](#). *Cancer Metastasis Rev* 20(1-2): 43-50.
- Lu, Y., Liu, Y. and Yang, C. (2017). [Evaluating In Vitro DNA Damage Using Comet Assay](#). *J Vis Exp*(128).
- Milyavsky, M., Gan, O. I., Trottier, M., Komosa, M., Tabach, O., Notta, F., Lechman, E., Hermans, K. G., Eppert, K., Konovalova, Z., Ornatsky, O., Domany, E., Meyn, M. S. and Dick, J. E. (2010). [A distinctive DNA damage response in human hematopoietic stem cells reveals an apoptosis-independent role for p53 in self-renewal](#). *Cell Stem Cell* 7(2): 186-197.
- Nowsheen, S. and Yang, E. S. (2012). [The intersection between DNA damage response and cell death pathways](#). *Exp Oncol* 34(3): 243-254.
- Oh, J., Lee, Y. D. and Wagers, A. J. (2014). [Stem cell aging: mechanisms, regulators and therapeutic opportunities](#). *Nat Med* 20(8): 870-880.

Ostling, O. and Johanson, K. J. (1984). [Microelectrophoretic study of radiation-induced DNA damages in individual mammalian cells](#). *Biochem Biophys Res Commun* 123(1): 291-298.

Sharma, A., Shukla, A. K., Mishra, M. and Chowdhuri, D. K. (2011). [Validation and application of Drosophila melanogaster as an in vivo model for the detection of double strand breaks by neutral Comet assay](#). *Mutat Res* 721(2): 142-146.

Comprehensive Identification of Translatable Circular RNAs Using Polysome Profiling

Yanwen Ye^{1,2}, Zefeng Wang^{1,2,*} and Yun Yang^{1,*}

¹Bio-med Big Data Center, CAS Key Laboratory of Computational Biology, CAS Center for Excellence in Molecular Cell Science, Shanghai Institute of Nutrition and Health, Chinese Academy of Sciences, China

²University of Chinese Academy of Sciences, Chinese Academy of Sciences, Shanghai 200031, China

*For corresponding: wangzefeng@picb.ac.cn; yangyun@picb.ac.cn

Abstract

Circular RNAs (circRNAs), a special type of RNAs without 5'- and 3'-ends, are widely present in eukaryotes and known to function as noncoding RNAs to regulate gene expression, including as miRNA sponges. Recent studies showed that many exonic circRNAs, generated by back-splicing of pre-mRNAs, can be translated in a cap-independent fashion through IRESs or m6A RNA methylation. However, the scope of the translatable circRNAs and the biological function of their translation products are still unclear in different cells and tissues. Ribosome footprinting and proteomic analysis were usually used to globally identify translatable circRNAs. However, both methods have low sensitivity due to the low efficiency in the discovery of circRNA specific reads or peptides (*i.e.*, the back-splicing junctions are difficult to recover by the short reads of ribosome footprinting and the limitation of proteomic analysis). Here, we described an alternative method to identify translatable circRNAs using polysome profiling and circRNA-seq. Generally, polysome-associated RNAs were separated with sucrose gradients. Then polysome-bound circRNAs were enriched by an RNase R treatment and identified through paired-end deep sequencing. Thus, this method is more sensitive than ribosome footprint and proteomic analyses for the identification of translatable circRNAs.

Keywords: Polysome profiling, circRNA translation, RNA-seq, back-splicing junction, RNase R

This protocol was validated in: Cell Res (2017), DOI: 10.1038/cr.2017.31.

Background

Circular RNAs (circRNAs) are a special type of RNA without 5'- and 3'-ends, which form a covalent close loop. They were first discovered in viroids four decades ago (Sanger *et al.*, 1976). Recently, many studies showed that circRNAs were widely present in eukaryotes and expressed in a tissue-specific manner (Rybäk-Wolf *et al.*, 2015; Chen, 2020). Several types of circRNAs are found in cells, including exonic circRNA, EIciRNA, and ciRNA (Kristensen *et al.*, 2019); however, the majority of them are exonic circRNAs that are generated through back-splicing of pre-mRNAs (Salzman *et al.*, 2012 and 2013; Memczak *et al.*, 2013; Ashwal-Fluss *et al.*, 2014; Zhang, X. O. *et al.*, 2014). Thus, most exonic circRNAs sequences are the same as those of linear mRNAs, and the back-splicing junctions are unique sequences for circRNA detection.

CircRNAs regulate biological processes through their activities as miRNA sponges, protein scaffolds, and transcription regulators (Kristensen *et al.*, 2019). However, the functions of most circRNAs are still unclear. Recently, several studies showed that many circRNAs can be translated through cap-independent translation from IRESs or m6A RNA modifications (Legnini *et al.*, 2017; Pamudurti *et al.*, 2017; Yang *et al.*, 2017). In addition, some circRNA encode peptides reported to influence cancer proliferation or lifespan in flies (Weigelt *et al.*, 2020; Yang *et al.*, 2018; Zhang, M. *et al.*, 2018), indicating that the translation products from circRNAs play important biological roles. However, the roles of translatable circRNAs are still unknown. Therefore, transcriptome-wide identification of translatable circRNAs is an important way to study their biological function.

Two different types of omics approaches are usually used to comprehensively measure the translation of mRNAs at RNA (translatome) and protein (proteome) levels. Ribosome footprinting is an emerging technique to globally measure mRNA translation via high-throughput sequencing of ribosome-protected mRNA fragments; however, it's difficult to capture the translating circRNAs. Since the ribosome-protected mRNA fragments are short (around 28–35nt), the back-splicing junctions are easy to be missed by this method. Proteomic analysis is a technique to directly determine the translation products of mRNAs through identification of enzymatically digested peptides. Similar to ribosome footprinting, the peptides coded by back-splicing junctions are difficult to identify through tandem mass spectrometry.

We developed a new method to identify translatable circRNAs using polysome profiling and circRNA-seq. The polysome-associated RNAs can be separated using sucrose gradients and then isolated from different fractions. The polysome-bound circRNAs are enriched by an RNase R treatment and used to generate the circRNA-seq libraries. The resulting libraries are pair-end sequenced, and the circRNAs are identified by the back-splicing junction reads. Therefore, our method is easier and more sensitive than ribosome footprint and proteomic analyses for identifying translatable circRNAs.

Materials and Reagents

1. 10 cm and 15 cm dish (Thermo Scientific™, Nunc™ EasYDish, catalog numbers: 150464, 150468)
2. 50 mL and 15 mL centrifuge tube (Thermo Scientific™, Thermo Scientific™ Nunc™, catalog numbers: 339650, 339652)
3. 1.5 mL and 2 mL Eppendorf tube (RNase free) (CORNING, Axygen, catalog numbers: MCT-150-C, MCT-200-C)
4. 10 mL and 25 mL serological pipette (Thermo Scientific™, Nunc™, catalog numbers: 170357N, 170356N)
5. 10 mL syringe (Sigma-Aldrich, catalog number: Z248029)
6. Pipetting needle (BioComp, belong to Gradient Master in Equipment)
7. 25 cm cell scraper (JET BIOFIL, catalog number: CSC011025)
8. Polypropylene centrifuge tube (Beckman coulter, catalog number: 331372)
9. Vacuum Filtration Systems (Corning, catalog number: 430758)
10. Cell line: HEK293T
11. Nuclease free water (Sigma-Aldrich, catalog number: W4502)
12. TRIzol™ reagent (Thermo Fisher, catalog number: 15596018)
13. Chloroform (Sinoreagent, catalog number: 10006818)

14. Isopropanol (Sinoreagent, catalog number: 80109218)
15. Ethanol (Sigma-Aldrich, catalog number: E7023)
16. Dulbecco's modified eagle medium (DMEM) (meilunbio, catalog number: MA0212)
17. Phosphate buffered saline (PBS) (Hyclone, catalog number: SH30256.01)
18. Ribonuclease inhibitor (Promega, catalog number: N2518)
19. RQ1 RNase-free DNase (Promega, catalog number: M6101)
20. RNase R (Lucigen, catalog number: RNR07250)
21. cCompleteTM EDTA-free Protease Inhibitor Cocktail (Roche, catalog number: 11873580001)
22. Cycloheximide (CHX) (Sigma, catalog number: C7698)
23. Dithiothreitol (DTT) (Sigma-Aldrich, catalog number: 43815)
24. TritonTM X-100 (Sigma-Aldrich, catalog number: T8787)
25. Bromophenol blue (Sigma-Aldrich, catalog number: B0126)
26. KAPA Stranded RNA-Seq Kit with RiboErase (HMR) (KAPA, catalog number: KK8483)
27. RNA clean and concentrator kit (ZYMO RESEARCH, catalog number: R1019)
28. 10× Polysome buffer (see Recipes)
29. Lysis buffer (see Recipes)
30. Wash buffer (see Recipes)
31. 70% sucrose solution (see Recipes)
32. 50% sucrose grading solution (see Recipes)
33. 10% sucrose grading solution (see Recipes)

Equipment

1. Ultracentrifuge (with rotor SW41) (Beckman, model: Optima XPN-100-IVD, catalog number: A99846)
2. Photo-spectrometer (Thermo Fisher, NanoDrop, catalog number: ND-1000)
3. Density gradient fractionation system (Complete system includes tube piercing system; syringe pump; UA-6 Detector with 254 and 280 nm filters, R1 Fraction Collector, Density Gradient Flow Cell, cables, and tubing) (BRANDEL, catalog number: BR-188)
4. Gradient Master (BioComp, catalog number: Biocomp 108)

Software

1. Peak chart (Data capture software for Density gradient fractionation system, www.brandel.com)
2. TopHat 2/ TopHat-Fusion (<https://ccb.jhu.edu/software/tophat/index.shtml>, https://ccb.jhu.edu/software/tophat/fusion_index.shtml)
3. CIRCExplorer2 (<https://circexplorer2.readthedocs.io/en/latest/>)

Procedure

A. Preparation of sucrose gradient (Figure 1)

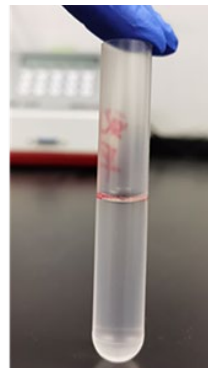
1. Prepare 500 mL of 10× polysome buffer in nuclease free water and 500 mL of 70% (w/v) sucrose solution in 1× polysome buffer (see Recipes). Filter solutions with Vacuum Filtration Systems.
2. Prepare 10% (w/v) and 50% (w/v) sucrose solution with 70% (w/v) sucrose solution (see Recipes).
3. Add the 10% and 50% sucrose solution, in that order, into a Beckman polypropylene centrifuge tube at room temperature.

Note: Add a half tube of 10% sucrose solution first and then the 50% sucrose solution to the bottom of the tube under the 10% solution using a needle.

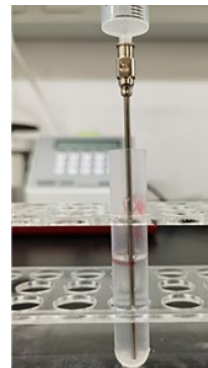
4. Load the centrifuge tube on the gradient master to make a 10-50% (w/v) sucrose gradient. Sucrose gradients can be used immediately or stored long-term at -80°C (no more than 2 weeks) (see Note 1).



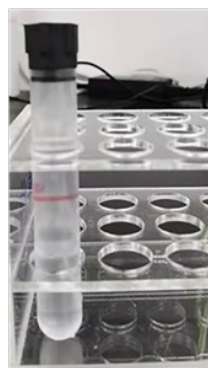
1. Label the tubes



2. Add 10% sucrose solution to the label



3. Add 50% sucrose solution from the bottom of tube



4. Cap the tubes



5. Load the centrifuge tube on the gradient master



6. Run 10-50% (w/v) sucrose gradient procedure

Figure 1. Protocol for Sucrose Gradient Preparation

B. Sample preparation

Note: Cool all the solutions and buffers before use. Keep the samples on ice all the time if possible.

1. Seed the cells in 10 cm or 15 cm dishes one day before the experiment (see Note 2 and Table 1).

Table 1. Recommend schedule of this protocol

Prepare 10× polysome buffer and 70% sucrose solution for long use.		
Day 1	1	Seed cells.
Day 2	1	Prepare lysis buffer and wash buffer.
	2	Harvest samples following the steps of Sample preparation in order.
	3	Prepare sucrose gradient according to step A of the Procedure.
	4	Run polysome profiling following step C of the Procedure.
	5	Store the fractionated samples at -80°C.

Day 3	1	Thaw the samples on ice.
	2	Extract RNA and prepare RNA-seq library following Procedure D.
Sequencing		
7-10 days	Run process for circRNAs identification	

- Add 100 µg/mL cycloheximide into the culture medium and incubate cells at 37°C for 10 min.
- Discard the medium and wash the cells with 10 mL ice-cold PBS containing 100 µg/mL cycloheximide twice.
- Add 10 mL ice-cold PBS to cells and harvest the cells with cell scraper.
- Transfer the cell suspension into 15 mL centrifuge tube and centrifuge at 1,000 × g for 3 min at 4°C.
- Remove the supernatant and add 250 µL lysis buffer to 15 mL centrifuge tube.
- Lyse the cells by gently pipetting and transfer the lysate into a 1.5 mL Eppendorf tube.
- Keep cell lysate on ice for 10 min and centrifuge the lysate at 14,000 × g for 10 min at 4°C to remove cell debris.
- Transfer the supernatant into a new 1.5 mL Eppendorf tube.
- Dilute 1 µL samples with 999 µL water, and measure the approximate RNA concentration using a NanoDrop photo-spectrometer (see Note 3).
- Keep the samples on ice for immediate use or freeze them in liquid nitrogen immediately and store at -80°C until use (no more than one month).

C. Polysome profiling

- Remove the same volume of solution as that of the loading sample from the top of the 10-50% sucrose gradient and then load the samples onto the sucrose gradient. The optimal loading volume is 200-500 µL (see Note 3). Keep 10% of lysates as an input.
- Centrifuge at 35,000 × g for 2.5 h at 4°C using the SW41 rotor in a Beckman Ultracentrifuge.
- Set up the density gradient fractionation system while the samples are centrifuging. Fill the syringe with chasing solution [70% (w/v) sucrose with bromophenol blue], flush the line, and calibrate the ultraviolet spectrophotometer following the equipment instructions.
- Gently remove tubes from the rotor and put them into the density gradient fractionation system. Alternatively, keep them at 4°C until use (no more than 4 h).
- Load the sample under the UA-6 Detector and puncture the bottom of the tube, communicating the syringe pump and detector system (see Figure 2).

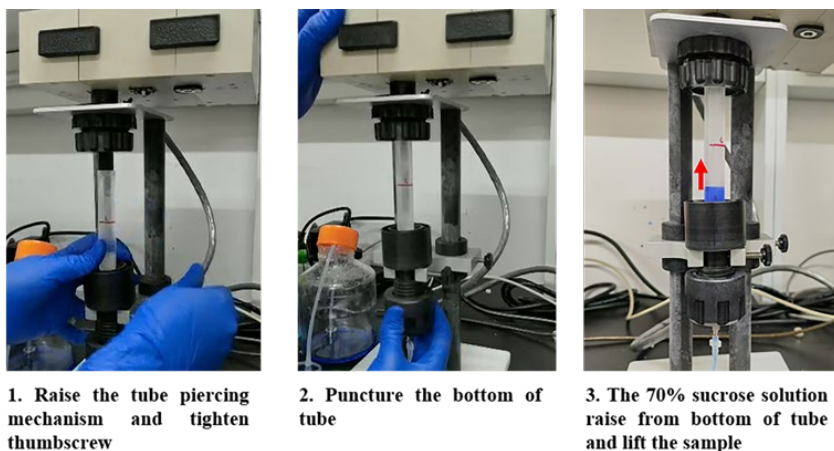


Figure 2. Protocol for Density Gradient Fractionation System Set-off

- Number the 2 mL Eppendorf tubes and place them onto the R1 Fraction Collector.

Note: About 750 µL of sample will be collected in each tube.

- Set syringe pump at 1.5 mL/min flow rate and switch on remote model. Set the fraction collector by time.
- Turn on density gradient fractionation system using Peak chart software. Record the data with Peak chart (see Figure 3) and collect the fractions with the fraction collector.
- Store the samples at -80°C until use (no more than one month).

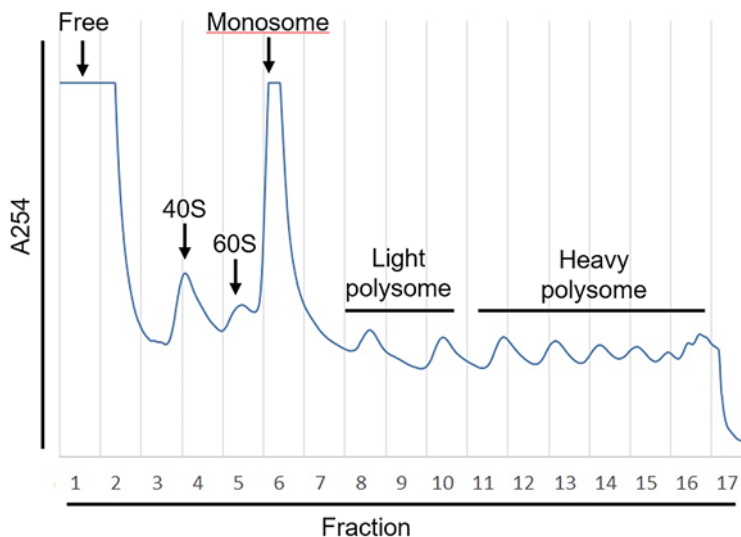


Figure 3. Example of Polysome Profiling.

The absorbance of OD₂₅₄ (A₂₅₄) that represents the abundance of RNA fragments was measured by UA-6 detector. The sucrose gradient was fractionated into 17 fractions with Density gradient fractionation system. The value of A₂₅₄ was recorded by Peak Chart and plotted as shown.

D. RNA-seq library preparation

- Add 750 µL of TRIzol into each tube, and extract the RNAs according to the manufacturer's instruction (use chloroform, isopropanol, and 70% ethanol to separate RNAs from samples and elute in about 30 µL water) or store at -80°C.
- Pool RNA samples in free, monosome, light polysome or heavy polysome fractions with equal volume, respectively (e.g., as shown in figure 3, fraction 1 was termed "free fraction," fraction 6-7 was termed "monosome fraction," fractions 8-10 were pooled with equal volumes and termed "light polysome fraction," and fractions 11-16 were pooled with equal volume and termed "heavy polysome fraction").
- Measure the RNA concentration of each RNA mixture with NanoDrop.
- Treat the RNAs with DNase I (RNase free) at 37°C for 15 min.
2 µg of RNA x µL
DNase I 1 µL
10× DNase I buffer 5 µL
Water 44-x µL
- Clean up the RNAs using the ZYMO RNA clean and concentrator kit according to the manufacturer's instructions.
- Treat the DNase I treated RNAs with RNase R at 37°C for 30 min (see Note 4).
1 µg of RNA x µL
RNase R 1 µL
10× RNase R buffer 5 µL

- | | |
|-------|---------|
| Water | 44-x µL |
|-------|---------|
7. Clean up the RNAs using the ZYMO RNA clean and concentrator kit according to the manufacturer's instruction (eluted RNAs in 20 µL water).
 8. Construct the RNA-seq libraries with the KAPA stranded RNA-seq kit with RiboErase according to the manufacturer's instruction.
 9. Sequence the libraries using a 150 bp paired-end approach with a 100 million read depth per sample.

Note: We recommend Illumina HiSeq® 3000/HiSeq 4000 Sequencing Systems for RNA-seq.

E. Identification of translatable circRNAs

1. Perform quality control on raw sequencing reads and trim the adaptor sequences. Discard the low-quality reads. Trim the adaptor sequences from the reads and map them to the genome.
2. Align the reads to the reference genome with TopHat2, and map the unmapped reads with TopHat-Fusion.
3. Annotate and assembly the circRNA transcripts using the CIRCexplorer2 pipeline (see details in GitHub: <https://circexplorer2.readthedocs.io/en/latest/>) (Zhang, X. O. et al., 2016).

Notes

1. If there is not Gradient Master for the gradient forming, we suggest an alternative method to make gradient through freezing and thawing. To make a 10-50% (w/v) sucrose gradient, prepare 50% (w/v), 40% (w/v), 30% (w/v), 20% (w/v), and 10% (w/v) sucrose solutions. Put 2 mL of 50% sucrose into a Beckman centrifuge tube and freeze on dry ice-ethanol, then put the 40% solution (2 mL) and also freeze, and repeat with the other solutions. The tubes can be frozen and stored at -80°C. One day before use, thaw the tubes in the refrigerator (4°C) overnight, and they are ready to use.
2. To keep the cells with active translation, it is better to harvest them at around 70-80% confluence. For example, for HEK293T, cells can be seeded in 10 cm (2.2×10^6 cells) or 15 cm (5.0×10^6 cells) dishes one day before the experiment and harvested at about 7.0×10^6 cells/10 cm dish or 16.0×10^6 cells/ 15cm dish. Since different types of cells have diverse translation activities at different cell confluence, we recommend testing the harvest conditions and loading amount before your experiment.
3. The optimal RNA amount in loading samples is 80-100 µg (sensitivity of 0.5). In cases where the RNA amount is lower than 80 µg, the sensitivity of the UV-Detector can be set to 0.2. We recommend using 200-600 µl of loading sample to get ideal and reproducible results.
4. RNase R can digest most linear RNAs; however, some RNAs with highly structured 3' ends are resistant to RNase R treatment. In that case, a modified RNase R treatment with an additional polyadenylation step and replacement of K⁺ with Li⁺ in the reaction buffer can be used to deplete the linear RNAs (please see Xiao and Wilusz, 2019). In addition, the activity of RNase R varies between different batches; thus, we recommend checking the amount of enzyme and the reaction time before your experiments (Zhang, Y. et al., 2016).

Recipes

1. 10× polysome buffer

1 M KCl
50 mM MgCl₂·6H₂O
0.1 M HEPES (pH 7.4)
Nuclease free water

2. Wash buffer

1× PBS
100 µg/mL CHX

3. Lysis buffer

1× polysome buffer
100 units/mL Ribonuclease inhibitor
25 units/mL DNase I
1× Protease Inhibitor cocktail (EDTA-free)
2 mM DTT
0.5% Sodium Deoxycholate
0.5% Triton X-100
100 µg/ml CHX

4. 70% (w/v) sucrose solution

70%(w/v) sucrose
1× polysome buffer
filtered with filter system

5. 50% (w/v) sucrose grading solution

71.4%(v/v) 70% sucrose solution
1× polysome buffer
100 units/mL Ribonuclease inhibitor
1× Protease Inhibitor cocktail (EDTA-free)
100 µg/mL CHX

6. 10% (w/v) sucrose grading solution

1.43% (v/v) 70% sucrose solution
1× polysome buffer
100 units/mL Ribonuclease inhibitor
1× Protease Inhibitor cocktail (EDTA-free)
100 µg/mL CHX

Acknowledgments

We want to thank all the members of Wang lab. This work was supported by the National Key Research and Development Program of China (MOST grant# 2018YFA0107602 to ZW), the National Natural Science Foundation of China (NSFC grant #31730110, #91940303, and #32030064 to ZW, #31870814 to YY), the Strategic Priority Research Program of Chinese Academy of Sciences(grant #XDB38040100 to ZW and YY) and the Science and Technology Commission of Shanghai Municipality (STCSM grant # 19QA1410500 to YY). The present protocol was developed and applied in Yang *et al.* (2017).

Competing interests

The authors declare no competing financial interests.

References

- Ashwal-Fluss, R., Meyer, M., Pamudurti, N. R., Ivanov, A., Bartok, O., Hanan, M., Evantal, N., Memczak, S., Rajewsky, N. and Kadener, S. (2014). [circRNA biogenesis competes with pre-mRNA splicing](#). *Mol Cell* 56(1): 55-66.
- Chen, L. L. (2020). [The expanding regulatory mechanisms and cellular functions of circular RNAs](#). *Nat Rev Mol Cell Biol* 21(8): 475-490.
- Kristensen, L. S., Andersen, M. S., Stagsted, L. V. W., Ebbesen, K. K., Hansen, T. B. and Kjems, J. (2019). [The biogenesis, biology and characterization of circular RNAs](#). *Nat Rev Genet* 20(11): 675-691.
- Legnini, I., Di Timoteo, G., Rossi, F., Morlando, M., Brigandt, F., Sthandler, O., Fatica, A., Santini, T., Andronache, A., Wade, M., et al. (2017). [Circ-ZNF609 Is a Circular RNA that Can Be Translated and Functions in Myogenesis](#). *Mol Cell* 66(1): 22-37 e29.
- Memczak, S., Jens, M., Elefsinioti, A., Torti, F., Krueger, J., Rybak, A., Maier, L., Mackowiak, S. D., Gregersen, L. H., Munschauer, M., et al. (2013). [Circular RNAs are a large class of animal RNAs with regulatory potency](#). *Nature* 495(7441): 333-338.
- Pamudurti, N. R., Bartok, O., Jens, M., Ashwal-Fluss, R., Stottmeister, C., Ruhe, L., Hanan, M., Wyler, E., Perez-Hernandez, D., Ramberger, E., et al. (2017). [Translation of CircRNAs](#). *Mol Cell* 66(1): 9-21 e27.
- Rybak-Wolf, A., Stottmeister, C., Glazar, P., Jens, M., Pino, N., Giusti, S., Hanan, M., Behm, M., Bartok, O., Ashwal-Fluss, R., et al. (2015). [Circular RNAs in the Mammalian Brain Are Highly Abundant, Conserved, and Dynamically Expressed](#). *Mol Cell* 58(5): 870-885.
- Salzman, J., Chen, R. E., Olsen, M. N., Wang, P. L. and Brown, P. O. (2013). [Cell-type specific features of circular RNA expression](#). *PLoS Genet* 9: e1003777.
- Salzman, J., Gawad, C., Wang, P. L., Lacayo, N. and Brown, P. O. (2012). [Circular RNAs are the predominant transcript isoform from hundreds of human genes in diverse cell types](#). *PLoS One* 7: e30733.
- Sanger, H. L., Klotz, G., Riesner, D., Gross, H. J. and Kleinschmidt, A. K. (1976). [Viroids are single-stranded covalently closed circular RNA molecules existing as highly base-paired rod-like structures](#). *Proc Natl Acad Sci U S A* 73(11): 3852-3856.
- Weigelt, C. M., Sehgal, R., Tain, L. S., Cheng, J., Esser, J., Pahl, A., Dieterich, C., Gronke, S., and Partridge, L. (2020). [An Insulin-Sensitive Circular RNA that Regulates Lifespan in Drosophila](#). *Mol Cell* 79(2): 268-279 e265.
- Xiao, M. S., and Wilusz, J. E. (2019). [An improved method for circular RNA purification using RNase R that efficiently removes linear RNAs containing G-quadruplexes or structured 3' ends](#). *Nucleic Acids Res* 47(16): 8755-8769.
- Yang, Y., Fan, X., Mao, M., Song, X., Wu, P., Zhang, Y., Jin, Y., Yang, Y., Chen, L.L., Wang, Y., et al. (2017). [Extensive translation of circular RNAs driven by N6-methyladenosine](#). *Cell Res* 27(5): 626-641.
- Yang, Y., Gao, X., Zhang, M., Yan, S., Sun, C., Xiao, F., Huang, N., Yang, X., Zhao, K., Zhou, H., et al. (2018). [Novel Role of FBXW7 Circular RNA in Repressing Glioma Tumorigenesis](#). *J Natl Cancer Inst* 110(3): 304-315.
- Zhang, M., Zhao, K., Xu, X., Yang, Y., Yan, S., Wei, P., Liu, H., Xu, J., Xiao, F., Zhou, H., et al. (2018). [A peptide encoded by circular form of LINC-PINT suppresses oncogenic transcriptional elongation in glioblastoma](#). *Nat Commun* 9(1): 4475.
- Zhang, X. O., Dong, R., Zhang, Y., Zhang, J. L., Luo, Z., Zhang, J., Chen, L. L., and Yang, L. (2016). [Diverse alternative back-splicing and alternative splicing landscape of circular RNAs](#). *Genome Res* 26(9): 1277-1287.
- Zhang, X. O., Wang, H. B., Zhang, Y., Lu, X., Chen, L. L. and Yang, L. (2014). [Complementary sequence-mediated exon circularization](#). *Cell* 159(1): 134-147.
- Zhang, Y., Yang, L. and Chen, L. L. (2016). [Characterization of Circular RNAs](#). *Methods Mol Biol* 1402: 215-227.

Analysis of Leukemia Cell Metabolism through Stable Isotope Tracing in Mice

Nick van Gastel^{1,2,*}, Jessica B. Spinelli^{3,4}, Marcia C. Haigis³ and David T. Scadden^{2,5}

¹de Duve Institute, Brussels, Belgium

²Department of Stem Cell and Regenerative Biology, Harvard Stem Cell Institute, Harvard University, Cambridge, MA, USA

³Department of Cell Biology, Blavatnik Institute, Harvard Medical School, Boston, MA, USA

⁴Whitehead Institute for Biomedical Research, Massachusetts Institute of Technology, Cambridge, MA, USA

⁵Center for Regenerative Medicine, Massachusetts General Hospital, Boston, MA, USA

*For correspondence: nick.vangastel@uclouvain.be

Abstract

Once thought to be a mere consequence of the state of a cell, intermediary metabolism is now recognized as a key regulator of mammalian cell fate and function. In addition, cell metabolism is often disturbed in malignancies such as cancer, and targeting metabolic pathways can provide new therapeutic options. Cell metabolism is mostly studied in cell cultures *in vitro*, using techniques such as metabolomics, stable isotope tracing, and biochemical assays. Increasing evidence however shows that the metabolic profile of cells is highly dependent on the microenvironment, and metabolic vulnerabilities identified *in vitro* do not always translate to *in vivo* settings. Here, we provide a detailed protocol on how to perform *in vivo* stable isotope tracing in leukemia cells in mice, focusing on glutamine metabolism in acute myeloid leukemia (AML) cells. This method allows studying the metabolic profile of leukemia cells in their native bone marrow niche.

Keywords: Cell metabolism, Metabolic tracing, Cancer biology, Mouse models, Leukemia, Glutamine

This protocol was validated in: Cell Metab (2020), DOI: 10.1016/j.cmet.2020.07.009

Background

Unraveling the molecular regulation of cancer cells is critical to understand their insurgence, functioning, and potential therapeutic vulnerabilities. A dysregulated cellular metabolism is now widely accepted as a hallmark of many cancers (DeBerardinis and Chandel, 2016). Cancer cells display considerably different metabolic requirements compared to most normal differentiated cells and reprogram pathways controlling nutrient acquisition and metabolism to meet their specific bioenergetic, biosynthetic, and redox demands. Emerging evidence, mostly from solid tumors, shows that several metabolic characteristics of cancer cells can also be linked to therapeutic resistance (Zhao *et al.*, 2013). Metabolic heterogeneity between cells, driven by genetic, cell state, or microenvironmental diversity, may further allow subpopulations of cells to escape therapy-related cell death (Martinez-Outschoorn *et al.*, 2016).

The importance of examining the metabolism of cells in their native environment is underscored by several studies that have shown that artificial *in vitro* conditions can create metabolic dependencies that do not exist *in vivo* (Davidson *et al.*, 2016; Cantor *et al.*, 2017; Muir *et al.*, 2017). However, studying metabolism in an *in vivo* setting brings several challenges. Gene or protein levels of metabolic enzymes may not always adequately reflect the metabolic state of a cell (Metallo and Vander Heiden, 2013). Measuring single metabolites in cells *in vivo* or on tissue sections is feasible, as is metabolic profiling of freshly-isolated cells through metabolomics analysis (Arnold *et al.*, 2015; Faubert and DeBerardinis, 2017). These approaches have proven extremely valuable, but they provide a snapshot of metabolite levels and no dynamic information or insight into the flow of metabolites. Metabolic tracer analysis is a complementary method that uses stable isotope-labeled metabolites, which are taken up and metabolized by the cells, after which the fate of the labeled atoms (usually carbon, nitrogen, or hydrogen) can be analyzed by mass spectrometry. In this way, the relative activity of one or more selected metabolic pathways can be studied. Metabolic tracer analysis, as well as metabolic flux analysis, which combines metabolic tracer analysis with tracer uptake data and computational modeling, has become a standard technique in the study of cancer cell metabolism, offering insights into the relations between cell biology and biochemistry (Antoniewicz, 2018). While metabolic tracing is mainly performed with cells in culture, it is also more and more used in *in vivo* settings, both in animal models and in humans (Faubert and DeBerardinis, 2017; Fernández -García *et al.*, 2020). Most *in vivo* metabolic tracing studies have focused on solid tumors, analyzing the tumor as a whole, without separating the cancer cells from other cells of the tumor microenvironment, such as immune cells, stromal cells, or blood vessel cells. The advantage of working with liquid tumors is that the cancer cells can be readily obtained from the bone marrow without the need for enzymatic tissue digestion and can be separated from the other cells by fluorescence-activated cell sorting (FACS), thus allowing specific analysis of cancer cell metabolism *in vivo*.

In our original study, we investigated the metabolic adaptations of acute myeloid leukemia (AML) cells *in vivo* during the course of induction chemotherapy treatment and identified transient changes in glutamine levels (van Gastel *et al.*, 2020). We performed *in vivo* stable isotope tracing, according to the protocol described here, to understand the metabolic fate of glutamine in control AML cells or cells persisting after chemotherapy. We used a transplant-based mouse model of human AML, driven by the MLL-AF9 fusion protein (Corral *et al.*, 1996). The AML cells also expressed GFP, which greatly facilitates cell sorting. The protocol described below should be compatible with any mouse leukemia model in which the leukemia cells express a fluorescent marker. It is also possible to perform metabolic tracing using our protocol in other hematopoietic cell populations, such as normal hematopoietic progenitor cells (Lineage-cKit⁺), as long as they can be readily isolated from bone marrow and separated from other cells by FACS.

Materials and Reagents

1. 5 mL round bottom polystyrene test tube with cell strainer snap cap (Corning, Falcon, catalog number: 352235)
2. 50 mL centrifuge tube, conical bottom (Corning, Falcon, catalog number: 352070)
3. 40 µm cell strainer (Corning, Falcon, catalog number: 352340)
4. 300 µL insulin syringe with 31 G needle (BD Biosciences, catalog number: 328440)
5. 1 mL syringe (VWR, catalog number: 612-0106)

6. Needle, 25 G × 5/8 (BD Biosciences, catalog number: 305122)
7. K2-EDTA Microtainer tubes (BD Biosciences, catalog number: 365974)
8. 1.7 mL Posi-Click microcentrifuge tubes (Denville, catalog number: C-2170)
9. Alcohol preparatory pads (Covidien, WEBCOL, catalog number: 89029-964)
10. LC/MS sample vials (ThermoFisher, catalog number: C4000-11)
11. LC/MS vial caps (ThermoFisher, catalog number: C5000-54B)
12. ZORBAX Extend-C18, 2.1 × 150 mm, 1.8 µm (Agilent, catalog number: 759700-902)
13. L-glutamine, ¹³C₅, 99% (Cambridge Isotope Laboratories, catalog number: CLM-1822-H)
14. L-glutamine, ¹⁵N₂, 98% (Cambridge Isotope Laboratories, catalog number: NLM-1328)
15. Sodium chloride (Sigma-Aldrich, catalog number: S5886)
16. Water for UHPLC, for mass spectrometry (Sigma-Aldrich, catalog number: 900682)
17. Methanol for UHPLC, for mass spectrometry (Sigma-Aldrich, catalog number: 900688)
18. Dulbecco's phosphate-buffered saline (PBS), without calcium and magnesium (Corning, catalog number: 21-031-CV)
19. Fetal bovine serum (FBS), USDA tested (Cytiva, HyClone, catalog number: SH3091003)
20. ACK lysing buffer (ThermoFisher, Gibco, catalog number: A1049201)
21. 7-AAD (BD Biosciences, BD Pharmingen, catalog number: 559925)
22. Tributylamine, for liquid chromatography (Fisher Scientific, catalog number: 60-046-943)
23. Glacial acetic acid, for liquid chromatography (Fisher Scientific, catalog number: A35-500)
24. Saline (see Recipes)
25. Flow buffer (see Recipes)
26. Cell lysis buffer (see Recipes)
27. Mobile Phase Buffer A (see Recipes)
28. Mobile Phase Buffer B (see Recipes)

Equipment

1. Mouse restraining device (Braintree Scientific Inc., Tailveiner Restrainer, catalog number: TV-150 STD)
2. Micro dissecting scissors (Roboz Surgical, catalog number: RS-5906SC)
3. Narrow pattern forceps (Fine Science Tools, catalog number: 11002-12)
4. Mortar (VWR, catalog number: 89038-144)
5. Pestle (VWR, catalog number: 89038-160)
6. Refrigerated swinging bucket centrifuge 5910R with S-4xUniversal rotor (Eppendorf, catalog number: 5942000315)
7. Refrigerated microcentrifuge 5430R with FA-45-30-11 rotor (Eppendorf, catalog number: 5428000010)
8. Analytical balance (Mettler Toledo, catalog number: ME54)
9. BD FACSAria II Cell Sorter (BD Biosciences)
10. SpeedVac Vacuum Concentrator (ThermoFisher, catalog number: RVT450)
11. LP Vortex Mixer (ThermoFisher, catalog number: 11676331)
12. 6470 Triple Quadrupole Mass Spectrometer (Agilent)

Software

1. BD FACSDiva Software, version 8.0.2 (BD Biosciences)
2. Excel (Microsoft)
3. Mass Hunter, version B.08.00 (Agilent)

Procedure

A schematic representation of the entire procedure is provided in Figure 1.

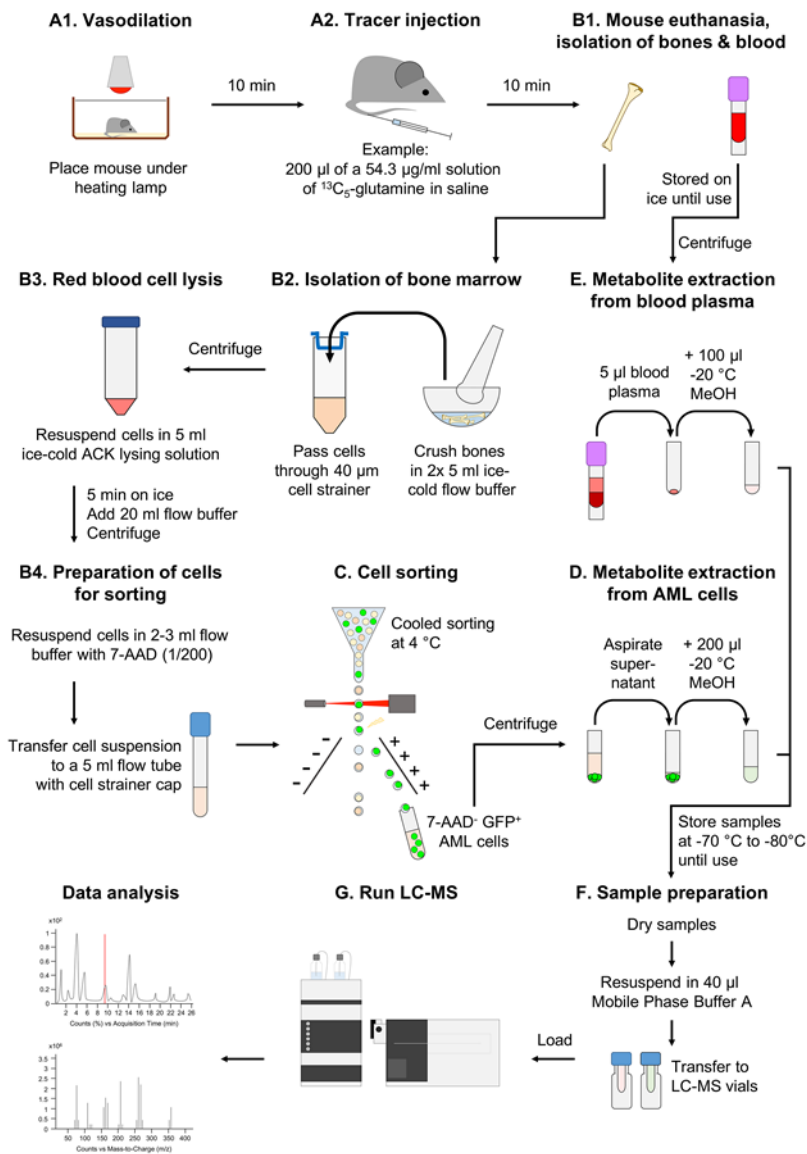


Figure 1. Schematic overview of the procedure

A. Metabolic tracer preparation and injection

1. Prepare the tracer by dissolving $^{13}\text{C}_5\text{-glutamine}$ or $^{15}\text{N}_2\text{-glutamine}$ powder in saline at a concentration of 54.3 mg/mL. Heat gently in a water bath at 37°C until dissolved. Per mouse, 200 μl of tracer solution is needed.
2. Place the mouse in a cage under a heating lamp for 5 to 10 min prior to injection (or use an alternative to cause vasodilation, such as a heating pad or by soaking the tail in warm water). Ensure the animal does not overheat.
3. Place the animal in the restraining device.
4. Swab the tail with an alcohol preparatory pad.

5. Aspirate 200 μ L of the tracer solution into a 300 μ L insulin syringe with 31 G needle.
6. Slowly inject the tracer solution in the lateral tail vein.
7. Start a timer set for 10 min.

B. Cell isolation and preparation

1. Exactly 10 min after tracer injection, euthanize the mouse.
2. Obtain peripheral blood by cardiac puncture using a 1 mL syringe with 25 G needle.
3. Transfer blood to a K2-EDTA tube and place on ice.
4. Isolate the femora and tibiae, clean them well to remove the muscle tissue, and place the bones in a pre-chilled mortar containing 5 mL of ice-cold flow buffer.

Note: The mortar should be pre-chilled by placing it in an ice bucket for 15 min before euthanizing the mouse.

5. Remove the mortar containing the bones from the ice bucket and crush the bones using a pestle by applying force in a vertical motion. Return the mortar to the ice bucket.

Note: Avoid grinding the bones as this will create small debris that can interfere with cell sorting.

6. Break up any visible cell clumps by pipetting the cell solution up and down several times using a 1 mL micropipette.
7. Transfer the cell suspension to a 50 mL conical tube with 40 μ m cell strainer, placed in an ice bucket.
8. Add another 5 mL of flow buffer to the mortar containing the bone fragments, crush again using a pestle until the bone fragments are completely white.
9. Break up any visible cell clumps by pipetting the cell solution up and down several times using a 1 mL micropipette.
10. Transfer the cell suspension to the 50 mL conical tube with 40 μ m cell strainer containing the cells from the first crush.
11. Centrifuge the cell suspension in a refrigerated swinging bucket centrifuge for 5 min at 350 $\times g$, 4°C.
12. Decant or aspirate the supernatant.
13. Resuspend the cell solution in 5 mL of ice-cold ACK lysing buffer (to remove red blood cells) and incubate on ice for 5 min.
14. Add 20 mL of flow buffer.
15. Centrifuge in a refrigerated swinging bucket centrifuge for 5 min at 350 $\times g$, 4°C.
16. Decant or aspirate the supernatant.
17. Resuspend the cells in 2-3 mL flow buffer containing 7-AAD at a 1/200 dilution, and transfer the cell solution to a 5 mL flow tube with cell strainer cap.

Note: In the original study (van Gastel et al., 2020), we only used GFP (marking the leukemia cells) and 7-AAD for cell sorting. It is possible to also stain the cells with fluorescently-labeled antibodies against cell surface markers. In that case, it is preferred to resuspend the cells first in a smaller volume (500 μ L) containing the antibodies, incubate them on ice in the dark for 10 min, and then add 1.5-2.5 mL of flow buffer containing 7-AAD. If an appropriate antibody dilution is used, it is usually not necessary to remove unbound antibody. It is recommended to perform pilot experiments to ensure adequate staining is achieved with a 10-min staining time and no washing.

18. Proceed immediately with cell sorting

C. Cell sorting

1. Ensure the sample input and sample collector of the cell sorter are cooled to 4°C and that laser voltage set up and compensation are performed prior to starting the experiment. This can be done before the tracer injection in the mice or by a different person during sample preparation.
2. Identify the target population (Figure 2), and sort at least 10,000 cells into a microcentrifuge tube containing 500 µL of ice-cold saline. Ideally, 50,000-200,000 cells are sorted. Limit sorting time to a maximum of 30 min. Be sure to write down the cell number obtained for each sample.
3. Place cells on ice immediately after sorting is completed.

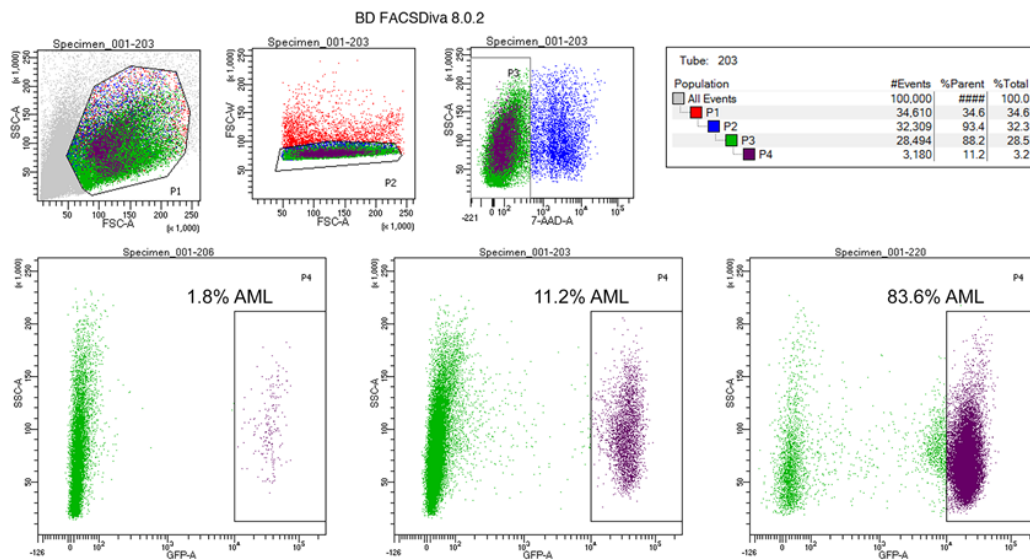


Figure 2. Representative FACS experiment.

Gating strategy for sorting viable AML cells (7-AAD-GFP^+) from the bone marrow of mice. Top graphs show the gating strategy for viable cells; bottom graphs show gating of AML cells in a mouse with low (left), medium (middle), or high (right) leukemic burden. P1 gate, leukocytes; P2 gate, single cells; P3 gate, viable cells; P4 gate, AML cells that are sorted.

D. Metabolite extraction from cells

1. Centrifuge cells in a refrigerated table-top microcentrifuge for 2 min at $500 \times g$, 4°C.
2. Gently aspirate the supernatant, leaving <20 µL behind. To avoid aspirating the cell pellet, which may be nearly invisible if the number of sorted cells is low, place the aspirator tip at the side of the tube that was nearest to the center of the centrifuge (thus farthest from the cell pellet).
3. Add 200 µL of cell lysis buffer, cooled to -20°C. Pipet up and down to mix well.
4. Store the samples at -70°C to -80°C.

E. Metabolite extraction from peripheral blood plasma

1. Centrifuge blood samples in a refrigerated table-top microcentrifuge for 5 min at $2,500 \times g$, 4°C.
2. Transfer supernatant to a microcentrifuge tube.
3. Transfer 5 µL of the plasma to a separate microcentrifuge tube (the rest of the plasma can be stored at -70°C to -80°C).
4. Add 100 µL of cell lysis buffer, cooled to -20°C. Pipet up and down to mix well.
5. Store the samples at -70°C to -80°C.

F. Sample preparation for liquid chromatography-mass spectrometry (LC-MS)

1. Prepare Mobile Phase Buffer A and Buffer B.
2. Remove samples from -70°C to -80°C storage and dry down in a SpeedVac Vacuum Concentrator set to 4°C.
3. Resuspend dried samples in 40 µL Mobile Phase Buffer A.
4. Vortex at 4°C for 10 min.
5. Centrifuge samples at 10,000 × g at 4°C for 10 min.
6. Move supernatant into LC-MS vials and load into the autosampler.

G. LC-MS analysis

1. Create a compound database on the Agilent MassHunter Acquisition software and include the compounds you wish to analyze, including information on the compound name, chemical formula, precursor ion mass, product ion mass, fragmentation energy, collision energy, and retention time. All this information can be found on the Agilent dMRM metabolomics database. For all new compounds, a standard must be run to optimize all of these parameters. When adding stable isotopes of metabolites to the list (such as ¹⁵N-UMP), use the same retention fragmentation energy, collision energy, and retention time as the light metabolite (¹⁴N-UMP).
2. Set up the liquid chromatography method as follows: Set up a ZORBAX Extend-C18, 2.1 × 150 mm, 1.8 µm column, and equilibrate the column for 15 min with Buffer A at 0.25 mL/min. Begin each run with a flow rate of Buffer A at 0.25 mL/min for 2.5 min, followed by a linear gradient from 100% Buffer A to 80% Buffer A: 20% Buffer B for 5 min. Follow with linear gradients of 80% Buffer A: 20% Buffer B to 55% Buffer A: 45% Buffer B for 5.5 min; 55% Buffer A: 45% Buffer B to 1% Buffer A: 99% Buffer B for 7 min; and 1% Buffer A: 99% Buffer B for 4 min. After the run is done, a backwash of 100% acetonitrile should be used to clean the column for 10 min followed by 8 min of re-equilibration with 100% Buffer A.
3. Ensure the instrument is cleaned and calibrated prior to use. Turn on the Agilent 6470 Triple Quadrupole mass spectrometer and let it warm up for at least 30 min prior to use. Set up the mass spectrometry method as follows: Agilent Jet Spray ionization; nebulizer, 45 psi; capillary voltage, 2,000 V; nozzle voltage, 500 V; sheath gas temperature, 325°C; and sheath gas flow, 12 L/min. Set the instrument to collect mass data for the duration of the first 24 min of the liquid chromatography method in which the metabolites are expected to elute.
4. Write a sequence applying the above compound database, liquid chromatography, and mass spectrometry protocols to each sample that will be run. Include in the sequence a 15 µL injection from the autosampler into the LC-MS for each sample and a subsequent needle wash to ensure that there is no cross contamination between samples.

Data analysis

1. Import the data into the Agilent Mass Hunter Software.
2. Click on each metabolite in each sample to ensure that the peak elutes at the correct retention time, has the appropriate parent and product ion masses, and that the peak is fully integrated.
3. Export the ion counts for each peak integrated.
4. Open the results in an Excel worksheet.
5. Calculate the fractional abundance of each isotopologue by dividing the ion count (IC) of each isotopologue by the sum of the ICs of all isotopologues for a particular metabolite. For example, for calculating the M+2 isotopologue fractional abundance of glutamine (where M denotes the mass of the unlabeled metabolite), use the following formula:

$$\frac{IC^{M+2}}{IC^{M+0} + IC^{M+1} + IC^{M+2} + IC^{M+3} + IC^{M+4} + IC^{M+5}}$$

An example of representative data obtained from a typical *in vivo* metabolic tracing experiment is given in Table 1.

6. The fractional abundance of M+5 glutamine (when using $^{13}\text{C}_5$ -glutamine) or M+2 glutamine (when using $^{15}\text{N}_2$ -glutamine) in the peripheral blood plasma is used to exclude samples with insufficient labeling. A successful experiment will show a fractional abundance of fully labeled glutamine in the plasma of 0.40-0.60. If the fractional abundance of fully labeled glutamine in the plasma is below 0.40 all samples of that mouse are excluded.

Table 1. Example of data obtained for an *in vivo* metabolic tracing experiment.

Mice were injected with $^{15}\text{N}_2$ -glutamine, and contribution of glutamine-derived nitrogen to the synthesis of other amino acids was investigated in peripheral blood and AML cells isolated from bone marrow. As starting material, 5 μL of peripheral blood plasma or 50,000 AML cells were used. Ion counts, obtained in MassHunter, were exported to Excel, where the fractional abundances of the isotopologues of interest, the averages, and standard deviations (STDEV) were calculated. Care should be taken when interpreting the isotopologue fractional abundances for low abundant metabolites (see the results for proline in the AML cells for example), which tend to give a large variability between samples.

		Peripheral blood plasma					AML cells								
		Mouse 1	Mouse 2	Mouse 3	Mouse 4	Mouse 5	Average	STDEV	Mouse 1	Mouse 2	Mouse 3	Mouse 4	Mouse 5	Average	STDEV
Glutamine	M+0	30830	25502	26762	27454	29612			20	25	86	36	22		
	M+1	7786	17595	14660	13673	5201			34	24	10	13	0		
	M+2	54684	34448	55789	50440	24197			39	56	114	90	31		
	M+4	411	126	351	318	211			48	20	45	67	22		
	M+5	39	22	12	13	20			10	3	7	3	6		
	M+2 (%)	58,3	44,3	57,2	54,9	40,8			25,5	43,7	43,5	43,1	38,5		
Glutamate	M+0	102826	117575	141882	103621	124702			43682	43570	61282	40755	47633		
	M+1	30579	37968	50749	36823	22678			6774	19726	24256	16268	5010		
	M+5	93	51	85	59	86			18	4	34	13	27		
	M+1 (%)	22,9	24,4	26,3	26,2	15,4			13,4	31,2	28,3	28,5	9,5		
	M+0	57401	60341	76049	45436	68752			48226	46951	64433	42069	50249		
	M+1	9363	12971	17571	9110	6558			5232	15293	18345	11843	3067		
Aspartate	M+4	13	13	2	6	12			2	1	8	7	2		
	M+1 (%)	14,0	17,7	18,8	16,7	8,7			9,8	24,6	22,2	22,0	5,8		
	M+0	514	488	445	578	335			30	11	17	35	8		
	M+1	25	61	43	57	43			14	3	19	8	15		
	M+5	5	5	1	4	1			0	1	1	5	2		
	M+1 (%)	4,5	11,0	8,8	8,9	11,4			31,4	17,9	50,9	16,4	59,9		
Proline	M+0	2646	1984	2284	2279	2471			63	137	41	261	239		
	M+1	183	208	218	223	187			4	3	13	19	3		
	M+2	119	104	186	327	134			39	615	254	611	332		
	M+1 (%)	6,2	9,1	8,1	7,9	6,7			3,5	0,4	4,2	2,2	0,6		
	M+2 (%)	4,0	4,5	6,9	11,5	4,8			36,5	81,4	82,4	68,5	57,8		
	M+0	2646	1984	2284	2279	2471			65,3	19,0					
Asparagine	M+1	183	208	218	223	187									
	M+2	119	104	186	327	134									
	M+1 (%)	6,2	9,1	8,1	7,9	6,7									
	M+2 (%)	4,0	4,5	6,9	11,5	4,8									
	M+0	2646	1984	2284	2279	2471									
	M+1	183	208	218	223	187									

Notes

- The number of biological replicates needed depends on the variability between samples. For mouse leukemia transplant-based models, the variability between individual mice is usually smaller than for more complex systems such as primary mouse leukemias or human PDX lines. In our studies, we start with 10 mice per group, split over 2-3 separate experiments. Depending on the skill of the person performing the tail vein injections, 10-40% of samples will need to be excluded due to insufficient tracer levels in the blood.
- This protocol requires three researchers to work together during Procedure A-E. We usually inject mice with tracer in a staggered fashion, injecting 1 mouse every 30 min. Person A injects the mouse, performs euthanasia, isolates the blood and bones, and crushes the bones (until Step B10). This sequence can be completed by a trained researcher in 30 min. Person B then takes over, centrifuges the cells, performs red blood cell lysis,

prepares the cells for FACS, and brings them to the cell sorter in an ice box (Steps B11 to B18; takes about 20 min), where they hand over the samples to person C, who oversees the cell sorting. Person B then takes the previous sample, which should be finished after 30 min of sorting, and performs metabolite extraction from the cells (Procedure D; takes less than 10 min). Metabolite extraction from the peripheral blood (Procedure E) is usually performed by person B while waiting during the centrifugation and incubation steps (Steps B11, B13, and B15), although this can also be performed by an additional person. If performing additional cell surface staining, the sequence is adapted depending on the required staining time, but normally can still be done by three people. A well-trained team will be able to isolate and process samples of 10 mice in an afternoon.

3. For some conditions, the number of cells that can be obtained from a single mouse may be too low for adequate analysis (for example, in some leukemic mice after chemotherapy). In that case, it is possible to lyse cells in a smaller adjusted volume of 80% methanol (Step D3) and pool samples of different mice before drying the samples.
4. Our protocol uses intravenous bolus delivery of labeled glutamine to study its metabolic fate in leukemia cells in mice, while other studies have used repeated bolus delivery or continuous infusion of tracers (Broekaert and Fendt, 2019; Muir *et al.*, 2017). Metabolite labeling in the leukemia cells will depend on several factors, including the enrichment of the precursor pool in the blood, metabolism of labeled glutamine in other organs complicating the ways in which the stable isotope can enter the leukemia cells, and the time required to establish complex labeling patterns (Faubert and DeBerardinis, 2017). The major advantages of administering a single bolus of tracer are the ease of delivery and the relatively small amount of tracer required, reducing the cost of the experiment. Also, if the leukemia is sampled soon after the bolus, the complicating effects of metabolism in other tissues may be minimized. In our original study, where we determined the optimal time point for leukemia cells isolation after tracer injection, we detected, for example, several other labeled metabolites in the peripheral blood of mice as soon as 15 min after tracer injection (van Gastel *et al.*, 2020).

Disadvantages of bolus injection include a lower degree of overall labeling and the absence of some specific labeling patterns that take longer to develop. Another concern is that bolus injection may increase the total precursor pool in the blood and that this by itself may alter the metabolism of the leukemia cells. While we found that total glutamine levels in peripheral blood indeed almost doubled with injection (50% unlabeled and 50% labeled), the levels of glutamine in AML cells in the bone marrow did not substantially change as a consequence of the bolus injection (see Figure 3). Glutamate, aspartate, and oxidized glutathione (GSSG) levels in AML cells also did not change.

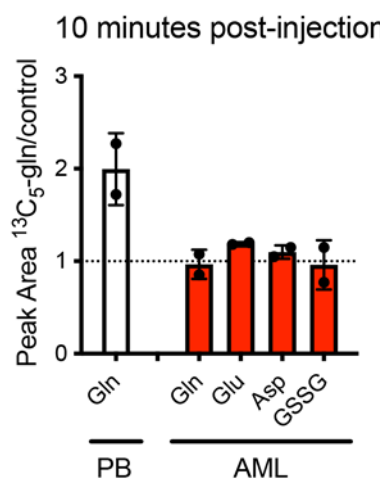


Figure 3. Effects of bolus injection of labeled glutamine on metabolite levels.

Metabolite levels in mouse peripheral blood (PB) plasma and bone marrow AML cells after bolus injection of $^{13}\text{C}_5$ -glutamine, compared to non-injected control mice. Gln, glutamine; Glu, glutamate; Asp, aspartate; GSSG, oxidized glutathione.

Recipes

1. Saline

0.9% NaCl in water (LC-MS grade)

2. Flow buffer

2% FBS in PBS

Note: EDTA can be added to the flow buffer at 2 mM to prevent cell-cell interactions and reduce doublet events in FACS.

3. Cell lysis buffer

80% methanol (LC-MS grade)

20% water (LC-MS grade)

4. A Mobile Phase Buffer A

97% water (LC-MS grade)

3% MeOH (LC-MS grade)

10 mM Tributylamine (LC-MS grade)

15 mM Glacial acetic acid (LC-MS grade)

pH 5.5

5. Mobile Phase Buffer B

MeOH (LC-MS grade)

10 mM Tributylamine (LC-MS grade)

15 mM Glacial Acetic Acid (LC-MS grade)

Acknowledgments

This protocol is based on our previously published study (van Gastel *et al.*, 2020). N.v.G. was supported by a grant from Alex's Lemonade Stand Foundation and Tap Cancer Out. J.B.S. was supported by the NCI F99/K00 Predoctoral to Postdoctoral Transition Fellowship (K00CA234839). D.T.S. was supported by the Harvard Stem Cell Institute and the Ludwig Center at Harvard, as well as the Gerald and Darlene Jordan Chair of Medicine at Harvard.

Competing interests

D.T.S. is a director and equity holder of Agios Pharmaceuticals, Magenta Therapeutics, Editas Medicines, Clear Creek Bio and LifeVaultBio; he is a founder of Fate Therapeutics and Magenta Therapeutics and a consultant to FOG Pharma, VCanBio, and Flagship Pioneering. N.v.G. and D.T.S. are inventors on patents related to this work.

Ethics

Mouse experiments were approved by the Institutional Animal Care and Use Committee (IACUC) of the Faculty of Arts and Sciences of Harvard University.

References

- Antoniewicz, M.R. (2018). [A guide to ¹³C metabolic flux analysis for the cancer biologist](#). *Exp Mol Med* 50(4): 19.
- Arnold, J.M., Choi, W.T., Sreekumar, A. and Maletić-Savatić, M. (2015). [Analytical strategies for studying stem cell metabolism](#). *Front Biol* 10(2): 141-153.
- Broekaert, D. and Fendt, S.M. (2019). [Measuring *in vivo* tissue metabolism using ¹³C glucose infusions in mice](#). *Methods Mol Biol* 1862: 67-82.
- Cantor, J. R., Abu-Remaileh, M., Kanarek, N., Freinkman, E., Gao, X., Louissaint, A. Jr., Lewis, C. A. and Sabatini, D. M. (2017). [Physiologic Medium Rewires Cellular Metabolism and Reveals Uric Acid as an Endogenous Inhibitor of UMP Synthase](#). *Cell* 169(2): 258-272.
- Corral, J., Lavenir, I., Impey, H., Warren, A. J., Forster, A., Larson, T. A., Bell, S., McKenzie, A. N., King, G. and Rabitts, T. H. (1996). [An MLL-AF9 fusion gene made by homologous recombination causes acute leukemia in chimeric mice: a method to create fusion oncogenes](#). *Cell* 85(6): 853-861.
- Davidson, S. M., Papagiannakopoulos, T., Olenchock, B. A., Heyman, J. E., Keibler, M. A., Luengo, A., Bauer, M. R., Jha, A. K., O'Brien, J. P., Pierce, K. A., et al. (2016). [Environment Impacts the Metabolic Dependencies of Ras-Driven Non-Small Cell Lung Cancer](#). *Cell Metab* 23(3): 517-528.
- DeBerardinis, R. J. and Chandel, N. S. (2016). [Fundamentals of cancer metabolism](#). *Sci Adv* 2(5): e1600200.
- Faubert, B. and DeBerardinis, R. J. (2017). [Analyzing Tumor Metabolism *In Vivo*](#). *Annu Rev Cancer Biol* 1: 99-117.
- Fernández-García, J., Altea-Manzano, P., Pranzini, E. and Fendt S.M. (2020). [Stable isotopes for tracing mammalian-cell metabolism *in vivo*](#). *Trends Biochem Sci* 45(3): 185-201.
- Martinez-Outschoorn, U.E., Peiris-Pagés, M., Pestell, R.G., Sotgia, F. and Lisanti, M.P. (2017). [Cancer metabolism: a therapeutic perspective](#). *Nat Rev Clin Oncol* 14(1): 11-31.
- Metallo, C.M. and Vander Heiden, M.G. (2013). [Understanding metabolic regulation and its influence on cell physiology](#). *Mol Cell* 49(3): 388-398.
- Muir, A., Danai, L.V., Gui, D.Y., Waingarten, C. Y., Lewis, C. A. and Vander Heiden, M. G. (2017). [Environmental cystine drives glutamine anaplerosis and sensitizes cancer cells to glutaminase inhibition](#). *Elife* 6: e27713.
- van Gastel, N., Spinelli, J. B., Sharda, A., Schajnovitz, A., Baryawno, N., Rhee, C., Oki, T., Grace, E., Soled, H. J., Milosevic, J., et al. (2020). [Induction of a Timed Metabolic Collapse to Overcome Cancer Chemoresistance](#). *Cell Metab* 32(3): 391-403.
- Zhao, Y., Butler, E. B. and Tan, M. (2013). [Targeting cellular metabolism to improve cancer therapeutics](#). *Cell Death Dis* 4(3): e532.

Measuring Real-time DNA/RNA Nuclease Activity through Fluorescence

Paulina Wyrzykowska¹, Sally Rogers² and Richard Chahwan^{1,*}

¹Institute of Experimental Immunology, University of Zurich, 8057 Zurich, Switzerland

²Living Systems Institute, University of Exeter, Exeter EX4 4QD, UK

*For correspondence: richard.chahwan@uzh.ch

Abstract

DNA and RNA nucleases are wide-ranging enzymes, taking part in broad cellular processes from DNA repair to immune response control. Growing interest in the mechanisms and activities of newly discovered nucleases inspired us to share the detailed protocol of our nuclease assay (Sheppard *et al.*, 2019). This easy and inexpensive method can provide data that enables understanding of the molecular mechanism for novel or tested nucleases, from substrate preference and cofactors involved to catalytic rate of reaction.

Keywords: Nuclease assay, RNA, DNA, Biochemistry, Catalytic activity

This protocol was validated in: Sci Rep (2021), DOI: 10.1038/s41598-019-45356-z

Background

Nucleases are enzymes that act on DNA and RNA by cleaving the phosphodiester bonds between nucleotides. In addition to their crucial role in the DNA repair machinery, they are involved in cell signalling pathways pertinent to DNA damage and immune responses, among others (Sheppard *et al.*, 2018). Their complex roles support several premature ageing-, immune-, and tumour-related processes. All of these can suffer from aberrations in the structural and/or catalytic functions of DNA and RNA nucleases (reviewed in Bartosova *et al.*, 2014; Rigby *et al.*, 2015). The growing interest in understanding the activities of numerous human DNA nucleases that remain contentious [*e.g.*, Mre11 (Paull and Deshpande, 2014) and CTIP (Mozaffari *et al.*, 2021)] and the presence of several uncharacterised proteins with predicted nuclease domains in mammalian genomes led us to design a real-time nuclease assay. The activity and kinetics of nucleases, DNA polymerases, nickases, RNA:DNA nucleases, or single-strand DNA nucleases can be studied in an uncomplicated and cost-effective manner. The fluorescence signal changes resulting from decreasing amount of intercalated DNA dye can be quickly and safely measured by most plate readers. A wide range of oligonucleotides mimicking the DNA substrate of the tested enzyme can be examined in each experiment simultaneously. We designed and tested an oligomer library of 80mers with different characteristics and substrate potential. The oligonucleotides described allow for the determination of the enzymatic direction of nuclease activity. For example, 3' or 5' activity can be tested and compared with oligonucleotides containing biotin-blocked or free 3'ends or 5'ends, in addition to overhangs, gaps, or nicks. This method can also illustrate the importance of cofactors or cations through simple comparison between reactions supplemented or not with the chemical/cation. Using the same principle, a modified protein (phosphorylation, dephosphorylation) or mutated/truncated forms can be easily tested for their nuclease activity. Importantly, the assay is sensitive enough to detect the kinetics of repair enzymes when confronted with DNA mismatches or DNA methylation sites.

Materials and Reagents

Prepare all buffers and solutions using ultrapure, nuclease free-water and analytical grade reagents. Filter with 0.2 µm filter at least once and store at 4°C or -20°C. Always use nuclease-free tubes and cotton-filter tips.

1. Black bottom plates [black bottom plate 96 well, polypropylene, flat bottom (Chimney well)] are necessary for the fluorescence assay to reduce background and crosstalk, and to absorb light (Greiner Bio-One, catalog number: 655209)

2. Streptavidin (Pierce, catalog number: PIER21122)

Streptavidin (SA) has a great affinity to biotin triethyleneglycol (BITEG). Oligonucleotides with this modification on 3', 5', or both ends are protected from nuclease activity after adding 2 µL (0.02 mg/mL) streptavidin to the reaction mix. Prepare 1 mg/ml in ultrapure water.

3. Oligonucleotides

Order lyophilised unmodified HPLC-purified oligonucleotide substrates and biotin or BITEG modified HPLC-purified oligonucleotides (Integrated DNA Technologies). Dilute them in 1× Annealing Buffer (Sigma-Aldrich) for DNA substrates (100 µM stock) and siMAX™ dilution buffer (Eurofins; 30 mM HEPES, 100 mM KCl, 1 mM MgCl₂, pH = 7.3) for all RNA substrates.

Note: Modified DNA or RNA bases can be ordered in the synthesised oligos. We have done so successfully in the past to measure the effect of base modifications on enzymatic functions.

Oligonucleotides from our library were designed and optimised against secondary structure formation using the ‘Predict a Secondary Structure Web Server’ (<https://rna.urmc.rochester.edu/RNAstructureWeb/Servers/Predict1/Predict1.html>).

The basic 80bp sequences are as follows:

Forward:

GATGGTTGTTGGTCTATTACTACTTGGAGCTTGTATGATTGAAACCTGGAGTACTTGCCTACTGGAGTGAACTTAG

Reverse:

CTAAGTTCACTCCAAGTAGGCAAGTACTCCAAGGTTCGAACATACAAGCTCCAAGTAGTAAT
AGACCAACAAACCATC

For designing all types of library oligomers, the basic oligonucleotide sequence can be shortened from both ends or split into two molecules to produce gaps or nicks in duplex DNA. Single nucleotides can be exchanged to add mismatches, substrate preferences, and so forth (Figures 1 and 2).

Oligomers set 1	Illustration	Oligomers set 2	Illustration
80bp		80bp-3B	
60bp		65bp-3B	 15
40bp		40bp-3B	
20bp		10bp-3B	
ssDNA			

Figure 1. For the calibration curve, two example sets are presented, with and without streptavidin blockade on ends.

These need to match the DNA substrates used in the experiment.

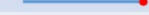
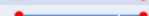
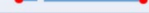
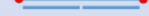
oligomer name	schematic representation
80mer-all4block	
80mer-3' block	
80mer-5' block	
80mer-all4block-1bpgap-5'	
80mer-all4block-1bpgap-3'	
80mer-all4block-3bpgap-5'	
80mer-all4block-3bpgap-3'	
80mer-top2block	
80mer-top2block-3bp-gap	
80mer-top2block-1bp-gap	
80mer-edge2block-5'-overhang	
80mer-edge2block-3'-overhang	
80mer-3block-3'-10bpoverhang	
80mer-3block-5'-10bpoverhang	
80mer-3block-3'-15bpoverhang	
80mer-3block-5'-15bpoverhang	

Figure 2. Set of 80-mer oligonucleotide substrates

4. Nucleases

Perform the calibration of the method using the commercial nucleases with known activity and preferably acting in a similar mechanism to the predicted activity of the enzyme to be tested. For example, to test the removal of 5' mononucleotides from duplex DNA, use Exonuclease T7 (T7, New England Biolabs, catalog number: M0263S). For nucleases acting 3' to 5', use Exonuclease III (ExoIII, Thermo Scientific, catalog number: EN0191) (Figure 3).

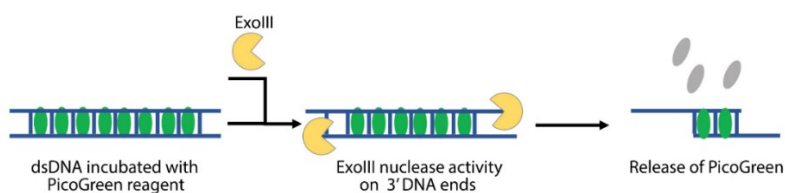


Figure 3. Scheme of PG release from dsDNA after nuclease treatment (ExoIII)

5. 1 M Tris, pH 7.5-8.0 (ThermoScientific, catalog number: 15567027)
6. 5 M NaCl, RNase-free (ThermoScientific, catalog number: AM9759)
7. 0.5 M EDTA pH 8.0 (ThermoScientific, catalog number: 15575020)
8. 10× Tango Buffer (ThermoScientific, catalog number: BY5)
9. CutSmart (New England Biolabs, catalog number: B7204S)
10. Glycerol (ThermoScientific, catalog number: 15514011)
11. Quant-iT™ PicoGreen™ dsDNA Assay Kit (Invitrogen, catalog number: P7589)
12. Quant-iT™ microRNA Assay Kit (Invitrogen, catalog number: Q33140)
13. Annealing Buffer Composition (1×) (see Recipes)
14. Storage buffers (see Recipes)
15. Reaction buffers (see Recipes)
16. Divalent cations (see Recipes)
17. PG buffer (see Recipes)
18. Nucleic acid dyes (see Recipes)

Equipment

1. Plate reader (Tecan or BMG)

Select the appropriate measurement parameters (temperature, wavelength, number of flashes, and settle time) for your assay.

Preheat the microplate reader to the optimal temperature for enzyme activity (commonly 37°C). To slow down the reaction, set to a lower temperature (*e.g.*, 20°C). Use the wavelength 483-15 nm for excitation (483 nm is the middle excitation peak with a bandwidth of 15 nm; *i.e.*, the excitation range is 475-490 nm) and 530-30 nm for emission (530 nm is the middle emission peak with a bandwidth of 30 nm; *i.e.*, the emission range is 515-545 nm). Increase the number of flashes per well until noise of BLANK wells does not improve further or until measurement time per well becomes unacceptable. Depending on the enzyme, read the samples every 45-60 s for 15 min to 2 h with a shake before each read.

Photobleaching occurring in the samples causes the fluorescence signal to decrease with time. Therefore, run a control curve run in every experiment simultaneously with samples to measure this effect. Longer readings can be inaccurate due to total photobleaching of PicoGreen to the level of the background.

We tested [Infinite M Plex](#) (TECAN) and [CLARIOstar](#) (BMG Labtech) plate readers. The nuclease assay can also be performed in the qPCR reader, but we found that the plate reader gives consistent results and offers more options, such as shaking the plate before a read.

While the best practices regarding reads per well vary with each enzyme, in general, an optimal duration of reads is approximately 1 h. If using a CLARIOstar, factor the whole time needed to read the entire plate, well by well, which for a full plate took approximately 48 s. So, each well could only be read every 50 s. If the plate reader permits it, try to use bidirectional reading row by row, and add the enzymes in the same order.

Procedure

A. Plate Preparation

Prepare the plate on ice and protect the samples from light. For every reaction, prepare the mix and run triplicates for the best accuracy. Use of multi-channel pipettes accelerates the set up of the reaction plate but can also lead to air bubbles in wells. Centrifuge the plate to remove them.

Always mark up the plate to aid with pipetting substrate and reaction mixtures and to blank off any empty wells. If using tape to label the rows and columns, peel this off before loading into the plate reader. Take time to plan out experiments and calculate volumes well ahead of time.

Reaction mix per well:

10 µL oligonucleotides 500 nM
10 µL reaction buffer
25 µL ddH₂O (or 23 µL if SA)
2 µL of streptavidin (for biotinylated oligos)
50 µL PG
5 µL enzyme

Note: For RNA reactions, a similar procedure could be followed by substituting PG with RNA dye.

1. Perform the annealing of complementary oligonucleotides in a thermocycler or heat block and use the molar ratio 1:1.
 - a. Mix equal volumes of the equimolar oligonucleotides (100 µM each) in a PCR tube.
 - b. Incubate for 5 min at 95°C.
 - c. Switch off the heat block leaving the samples in to cool down slowly or use the thermocycler (go down 1°C every 30 s).
 - d. Keep the annealed duplexes at -20°C for long-term storage.
 - e. Dilute the annealed oligos to 500 nM.
 - f. Use 10 µL (50 nM) per reaction/well.
 - g. For example, to anneal the oligonucleotide duplexes containing the gap, anneal three oligonucleotides using 2.5 µL each, and add 2.5 µL of annealing buffer. The concentration of the end product is 25 µM.

Notes:

- a. Use the reaction buffer appropriate for the enzyme. The wide range of activity buffers, like 10× CutSmart (New England Biolabs, B7204S) or 10× Tango (ThermoScientific, BY5), can facilitate the data analysis (no need for extra controls) and work well with many enzymes. Run a trial experiment to test the effectiveness of different reaction buffers to get the best results.
 - b. Use nuclease-free water.
2. Remember to add 2 µL of streptavidin for BIOTEG or biotinylated oligonucleotides. Incubate for 15 min on ice on a see-saw shaker to enhance binding.
 3. Add PicoGreen reagent (PG) to every well protecting the plate from light. Try to work quickly and cover the rows/columns already supplemented with PG with lid/aluminium foil.
 4. Add the denoted enzymes (or storage buffer as a negative control) to each well.
- Work at the bench at room temperature from now on to avoid the risk of enzyme precipitation. Prepare the desired amount of enzyme units/concentration in 5 µL. Take a full box of filter tips and use in the corresponding position in the tip box and plate to avoid pipetting mistakes. This way, if the position on the plate is lost, the tip box could orient the processing. Add 5 µL to each well, trying not to make any bubbles that could affect the fluorescence reads. The reaction starts now, so work quickly to be able to catch the first minutes of the reaction in the pre-heated plate reader. Remember to protect the plate from light.

Notes:

- a. Avoid using multi-channel pipettes as they tend to add bubbles to wells and are less consistent in adding the correct amount of enzyme.
- b. Centrifuge the plate briefly to remove air bubbles. For quick acting enzymes, this may not be advisable as the enzymatic reaction may have already started during that time.
- c. Attempt to titrate out the enzyme. If too much enzyme is present in the solution, the reaction is very fast, causing loss in data read in the early phase of the reaction.

B. Design of experiment

Plate with test experiment with T7 and ExoIII exonucleases. The samples were prepared in duplicate. The calibration control curve is also included, as illustrated in Figure 4.

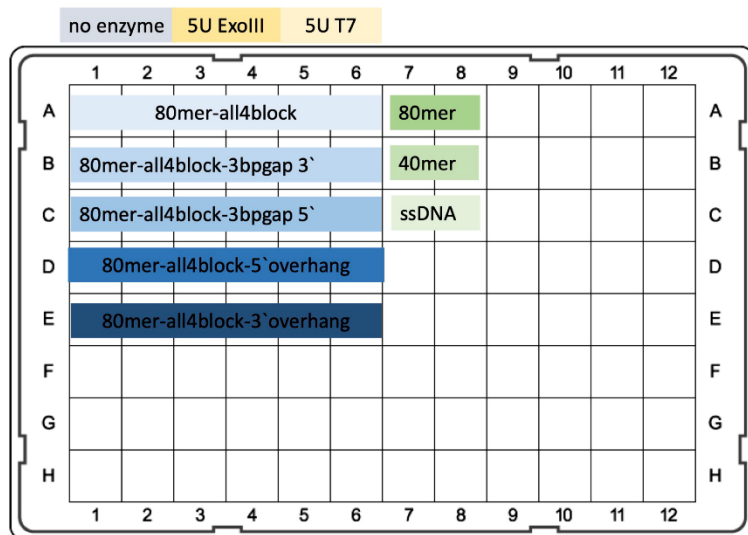


Figure 4. Scheme of the plate for test experiment.

A. Row A1-6 contains the negative control oligomer for both tested exonucleases. The correct binding between biotin-modified-oligonucleotides and streptavidin added to the mix protects both 3' and 5' ends from digestion. All4block signifies that all four ends on the oligos were blocked by biotin-streptavidin binding. B. Row B1-6 contains oligonucleotides with 3bp gap in proximity, 12bp to 3' end (which is the substrate for ExoIII acting in the 3' to 5' direction). T7 could only digest short 12bp fragments leading to the last nucleotide blocked by Biotin-Streptavidin. C. Row C1-6 contains oligonucleotides with 3bp gap in proximity, 12bp to 5' end (which is the substrate for T7 exonuclease acting in the 5' to 3' direction). ExoIII could only digest short 12bp fragments leading to the last nucleotide blocked by Biotin-Streptavidin. D. Row D1-6 contains oligonucleotides with 15bp overhang on 5'. E. Row E1-6 contains oligonucleotides with 15bp overhang on 3'. In Columns 1 and 2, storage buffer from ExoIII (or T7) was added to the samples. Columns 3 and 4: ExoIII 5U per well. Columns 5 and 6: T7 5U per well. A7 and A8: 80mer_3block (oligos that 80mers with both 3' ends blocked). B7 and B8: 40mer_3block (oligos that 40mers with both 3' ends blocked). C7 and C8: ssDNA, 80bp single strain DNA, as a control of totally digested duplex oligomer, minimum value of fluorescence for the experiment.

Data analysis

1. Create the calibration lines from the oligonucleotides with different nominal lengths: 80, 40, and 0 (single stranded). Obtain the reads from the oligonucleotides as a function of time, possibly two or three replicates per nominal length. Next, at each time point, calculate the linear relationship between the nominal lengths (80, 40, 0) and the raw fluorescence reads. As a result, a time evolution of slopes and intercepts that relate the control signal to the control nominal length is obtained.
2. Group the data reads of the same oligonucleotide in sets with appropriate negative control, which must be very similar to the tested sample. It could contain no enzyme, or optimally, the inactive form of the tested enzyme. DNA 80-oligomer, which is not the substrate for the enzyme, *i.e.*, 80 mer_all4block, can be the negative control too. At the zero-time point, the raw reads should be similar for all wells.
3. Correct for the effects of photobleaching and background reads by means of dividing the reads of the specimen by the average reads from the negative control well.
4. Using the slope and intercept from calibration lines, convert the corrected fluorescence units at each time point to length of duplex DNA. See Supplementary material ([Excel file with test experiment and calculations](#)) for a

template of data entry and calculations.

- The result should reflect the length of oligomers, where 80mer is the maximum size, and single ssDNA shows total dissolved duplex.

Both nucleases were tested on five different oligomers from the library.

The 80mer-all4block duplex is not the substrate for any of the tested nucleases (no nickase activity). Thus, we used the 80mer-all4block as a negative control in calculations. The duplex cannot be degraded during the assay because

changes in fluorescence occur only due to photobleaching of the PG reagent.

- ExoIII activity nuclease assay

ExoIII, with its 3' to 5' exodeoxyribonuclease activity, releases 5'-mononucleotides from the 3'-end. It acts effectively on 80 mer-3block-5'-15 bp_overhang and on 80mer-all4block-3bpgap-3'.

80mer-all4block-3bpgap-5' has a gap situated 12bp from the 5' end of the oligomer. The decrease in fluorescence signal reflects the ability of ExoIII to remove this few bp from the 3'-end starting in the gap. The lower 80mer_all4block control fluorescence signal compared to 80mer-3block-3'-15bp_overhang confirms that the PG reagent intercalates only with double stranded DNA and not with the ssDNA overhang that is part of the oligo and not a substrate for ExoIII.

The reaction with ExoIII starts quickly, and in this experiment, the substrate oligomers for ExoIII were registered at time point 0 as 60bp and 50bp fragments, respectively (Figure 5A).

- T7 activity nuclease assay

T7 exonuclease with its 5' to 3' activity, non-processively hydrolyses oligomers starting on free 5'-end on both 80mer-3block-3'-15bp and 80mer-all4block-3bpgap-5'. T7 can also remove few bp from the 5'-end of the gap in 80 mer-all4block-3bpgap-5' (Figure 5B).

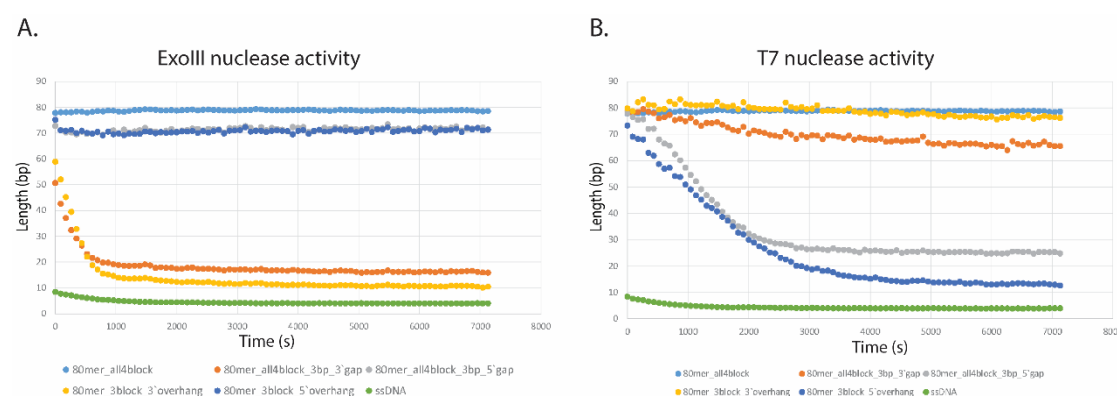


Figure 5. Sample of the nuclease activity results.

A. ExoIII nuclease activity, 5U per well. B. T7 nuclease activity, 5U per well. The graphs from the test experiment with ExoIII exonuclease and T7 exonuclease. The data is presented for each enzyme separately. The 80bp oligomer and ssDNA are shown on the graph. The x-axis denotes time in seconds. The y-axis denotes DNA oligo length in base pairs.

Summary: The nuclease assay summarised in this protocol is a powerful and easy toolkit for analysis of the activity of enzymes connected to DNA/RNA. Wide application, simplicity of test preparation, affordable reagents, and accessible equipment makes it a great method to implement in every molecular biology lab. We also postulate that this assay could be used in various variations to measure nucleic acid metabolism through non-nuclease activities.

Recipes

1. Annealing Buffer Composition (1×)

Make 100 μM stock of the oligonucleotides (ordered from IDT [idtdna.com])

Cite as: Wyrzykowska, P. et al. (2021). Measuring Real-time DNA/RNA Nuclease Activity through Fluorescence. Bio-protocol 11(21): e4206. DOI: [10.21769/BioProtoc.4206](https://doi.org/10.21769/BioProtoc.4206).

10 mM Tris, pH 7.5-8.0
50 mM NaCl
1 mM EDTA pH 8.0
Storage buffers

2. Prepare enzymes' specific storage buffers for both control wells (without any enzyme) and for diluting the enzyme. Do not add glycerol.

- For ExoIII enzyme: 50 mM Tris-HCl (pH 8.0), 50 mM KCl, 1 mM DTT (add fresh prior to use).
- For T7 enzyme: 10 mM Tris-HCl (pH 8.0), 0.1 mM EDTA, 10 mM DTT (add fresh prior to use).

Note: These storage buffers vary depending on the specific enzyme and the manufacturer producing it. They are usually provided by the manufacturer when purchasing specific enzymes.

3. Reaction buffers

Use recommend using reaction buffers delivered with nucleases. For unknown preference of tested nucleases, try wide range activity buffers, *i.e.*, 10× Tango Buffer and 10× CutSmart.

- 10× Reaction Buffer for ExoIII: 660 mM Tris-HCl (pH 8.0 at 30°C), 6.6 mM MgCl₂.
- 10× Reaction Buffer T7: 10× NEBuffer 4 (B7004S): 500 mM potassium acetate, 200 mM Tris acetate, 100 mM magnesium acetate, 10 mM DTT, pH 7.9 at 25°C.

Note: As reaction buffers can make a big difference, research the best one for each enzyme carefully and use the most appropriate one for the specific enzyme being tested.

4. Divalent cations

Supplement reaction buffer with MgCl₂ or MnCl₂ when needed. Use both in the first experiments; the information about preferred cation can be determined later.

5. PG buffer

TE buffer with v/v glycerol for diluting PG reagent
10 mM Tris-HCl
1 mM EDTA, pH 7.5
40% glycerol

6. Nucleic acid dyes

DNA dyes: The PicoGreen (PG) reagent from Quant-iT™ PicoGreen™ dsDNA Assay Kit was prepared immediately (producer recommendation) before use by making a 1:200 dilution of the PG in TE buffer with v/v glycerol.

Store the PG reagent long term at -20°C; while thawing, wipe off any moisture before opening the tube. Light and moisture both harm the PG reagent. We routinely keep the PG aliquoted and frozen, 5 µl per tube (1 ml of PG Buffer to be added prior to use), in a light proof box.

Note (RNA dyes): For the RNase assays, the dye from the Quant-iT™ microRNA Assay Kit was prepared by diluting the microRNA reagent A into buffer B in a 1/2,000 dilution, as detailed in the protocol.

Acknowledgments

The RC lab is funded by the BBSRC (BB/N017773/2), SNF (CRSK-3_190550), Rosetrees Trust Fund (M713), and UZH Research Priority Program (URPP—Translational Cancer Research). This protocol was adapted from the publication by Sheppard *et al.* (2019).

Competing interests

The authors declare no competing interests.

References

- Bartosova, Z. and Krejci, L. (2014). [Nucleases in homologous recombination as targets for cancer therapy](#). FEBS Lett 588(15): 2446-2456.
- Mozaffari, N. L., Pagliarulo, F. and Sartori, A. A. (2021). [Human CtIP: A 'double agent' in DNA repair and tumorigenesis](#). Semin Cell Dev Biol 113: 47-56.
- Paull, T. T. and Deshpande, R. A. (2014). [The Mre11/Rad50/Nbs1 complex: recent insights into catalytic activities and ATP-driven conformational changes](#). Exp Cell Res 329(1): 139-147.
- Rigby, R. E. and Rehwinkel, J. (2015). [RNA degradation in antiviral immunity and autoimmunity](#). Trends Immunol 36(3): 179-188.
- Sheppard, E. C., Morrish, R. B., Dillon, M. J., Leyland, R. and Chahwan, R. (2018). [Epigenomic modifications mediating antibody maturation](#). Front Immunol 9: 355.
- Sheppard, E. C., Rogers, S., Harmer, N. J. and Chahwan, R. (2019). [A universal fluorescence-based toolkit for real-time quantification of DNA and RNA nuclease activity](#). Sci Rep 9(1): 8853.

Measurement of DNA Damage Using the Neutral Comet Assay in Cultured Cells

Elena Clementi, Zuzana Garajova and Enni Markkanen*

Institute of Veterinary Pharmacology and Toxicology, Vetsuisse Faculty, University of Zürich, Zürich, Switzerland

*For correspondence: enni.markkanen@vetpharm.uzh.ch

Abstract

Maintenance of DNA integrity is of pivotal importance for cells to circumvent detrimental processes that can ultimately lead to the development of various diseases. In the face of a plethora of endogenous and exogenous DNA damaging agents, cells have evolved a variety of DNA repair mechanisms that are responsible for safeguarding genetic integrity. Given the relevance of DNA damage and its repair for disease pathogenesis, measuring them is of considerable interest, and the comet assay is a widely used method for this. Cells treated with DNA damaging agents are embedded into a thin layer of agarose on top of a microscope slide. Subsequent lysis removes all protein and lipid components to leave ‘nucleoids’ consisting of naked DNA remaining in the agarose. These nucleoids are then subjected to electrophoresis, whereby the negatively charged DNA migrates towards the anode depending on its degree of fragmentation, creating shapes resembling comets, which can be visualized and analysed by fluorescence microscopy. The comet assay can be adapted to assess a wide variety of genotoxins and repair kinetics, and both DNA single-strand and double-strand breaks. In this protocol, we describe in detail how to perform the neutral comet assay to assess double-strand breaks and their repair using cultured human cell lines. We describe the workflow for assessing the amount of DNA damage generated by ionizing radiation or present endogenously in the cells, and how to assess the repair kinetics after such an insult. The procedure described herein is easy to follow and cost-effective.

Keywords: DNA damage, DNA repair, DNA repair kinetics, Genotoxic agents, Oxidative stress, Reactive oxygen species

This protocol was validated in: BMC Biol (2020), DOI: 10.1186/s12915-020-00771-x

Background

Maintaining DNA integrity is a pivotal prerequisite for cells to ensure that all physiological processes function immaculately. Cells are constantly exposed to a plethora of exogenous and endogenous agents that can damage their DNA. Examples of exogenous noxious agents include ultraviolet light, ionizing radiation, and reactive chemical compounds, while endogenous damage can arise for example due to reactive oxygen- and nitrogen species derived from cellular metabolism (van Loon *et al.*, 2010). If left unrepaired, damage to DNA can lead to mutations, which can, in turn, alter the functionality of the affected DNA. This potentially results in altered protein abundance or activity, thereby giving rise to processes such as cancer, neurodegeneration, and ageing (Hoeijmakers, 2009; Markkanen, 2017). To counteract the deleterious effects of DNA damage, cells have evolved a series of intricate DNA repair mechanisms that detect and repair such insults (Ciccia and Elledge, 2010; Jackson and Bartek, 2009). Given the relevance of DNA damage for disease, it is of considerable interest to be able to measure levels of DNA damage that are induced by exposure of cells to particular agents, or to assess whether the repair kinetics of such damage is altered through specific treatments or genetic backgrounds. Methods to measure DNA damage and repair range from PCR-based methods and enzyme-linked immunosorbent assays, all the way to more elaborate next-generation sequencing based methods (Li and Sancar, 2020). Among this multitude of assays, the comet assay is a widely used method to measure both the amount of DNA damage as well as its repair in cells (Collins, 2014; Olive, 2009). For this, cells are treated with DNA damaging agents and embedded into a thin layer of agarose on top of a microscope slide. Subsequent lysis removes all protein and lipid components to leave the so-called ‘nucleoids,’ which consist of naked DNA remaining in the agarose. These nucleoids are then subjected to electrophoresis, whereby the negatively charged DNA migrates towards the anode. The migrating DNA, depending on its degree of fragmentation, creates shapes its degree of fragmentation and creates shapes resembling comets, which can subsequently be visualized and analysed by fluorescence microscopy. The comet assay can be adapted to assess a wide variety of genotoxins and repair kinetics, and both single-strand DNA breaks as well as double-strand breaks. In this protocol, we describe in detail how to perform the neutral comet assay to assess double-strand breaks and their repair in cultured human cell lines. This exact protocol was used in our recent publication (Clementi *et al.*, 2020). For a detailed description of the alkaline comet assay that can be used to detect single-strand DNA breaks, please refer to the separate protocol that is published in *Bio-protocol* (Clementi *et al.*, 2021).

Materials and Reagents

1. Superfrost microscopy slides (Superfrost Plus; ThermoScientific, Menzel-Gläser, catalog number: J1800AMNZ), store at room temperature
2. Square cover slips (Coverslips 22 × 50 mm; ThermoScientific, Menzel-Gläser, catalog number: MA062210), store at room temperature
3. 24-well cell culture plates (TPP, catalog number: 92024), store at room temperature
4. 15 mL Falcon tubes (Greiner ,188271 Zentrifugenrörchen 15 ml, Producer: Huberlab AG, 7.188 271), store at room temperature
5. Normal melting point agarose (Standard Agarose-Type LE; BioConcept, catalog number: 7-01P02-R), store at room temperature
6. Low melting point agarose (Low Melt Agarose 100 g; Bio & Sell, catalog number: BS20.47.100), store at room temperature
7. Trypsin 10× stock solution (Gibco, catalog number: 15090-046), store stock solution at -20°C. Dilute 1:10 in 1× PBS for working solution, which is stable at 4°C for several weeks.
8. Potassium chloride (KCl) (Merck, catalog number: 1.04936.1000), store at room temperature
9. Na₂HPO₄·7H₂O (Sigma-Aldrich, catalog number: S9390-1Kg), store at room temperature
10. KH₂PO₄ (Sigma, catalog number: 602187), store at room temperature
11. NaCl (Sigma, catalog number: 71380-1KG), store at room temperature
12. EDTA disodium salt dihydrate (C₁₀H₁₄N₂Na₂O₈·2H₂O) (Sigma-Aldrich, catalog number: 03685-1KG), store at room temperature

13. Tris base (Sigma, Life science, catalog number: T1503-500G), store at room temperature
14. Sodium hydroxide pellets (NaOH) (Merck, catalog number: 1.06498.100), store at room temperature
15. DMSO (Sigma-Aldrich, catalog number: D5879-1L), store at room temperature
16. Triton X-100 (MP-Biomedicals, catalog number: 807426), store at room temperature
17. SYBR Gold nucleic acid gel stain (Life Technologies, catalog number: S11494), aliquot and store at -20°C protected from light
18. N-Lauroylsarcosine (Sigma, catalog number: L5125), store at room temperature
19. Sodium acetate ($C_2H_3NaO_2$) (Fluka, Biochemika, catalog number: 71183), store at room temperature
20. Lysis buffer (see Recipes)
21. Electrophoresis buffer (see Recipes)
22. Comet staining solution (see Recipes)
23. PBS (phosphate buffered saline) (see Recipes)

Equipment

1. Trevigen CometAssay ESII apparatus (Trevigen, catalog number: 4250-050-ES)
2. Fluorescent microscope capable of excitation between 470 and 530 nm to image SYBR-Gold (excitation maximum around 495 nm, emission approx. 537 nm)
3. Water bath able to keep a constant temperature of 37°C and large enough to hold a 250 mL glass bottle
4. Big styrofoam box or similar, large enough to hold a glass plate for 10-12 comet slides on ice
5. Small mechanic's level
6. Coplin jars capable of holding 5 or 10 slides
7. Faxitron Cabinet X-ray system, Model RX-650 (faxitron.com)

Software

1. Fiji image processing package (<https://imagej.net/Fiji>)
2. OpenComet plugin for Fiji (<http://www.cometbio.org/>) (Gyori *et al.*, 2014)

Procedure

A. Preparation of agarose-coated slides (the day before the assay or earlier)

1. Completely dissolve 1 g of normal melting point agarose in 100 mL of dH₂O (1% solution) by heating in a glass bottle in the microwave. Be sure to place the lid on the bottle only loosely, and be mindful of boiling retardation.
2. Pipet 1 mL of the agarose solution onto a superfrost slide, overlay with a cover slip to spread it evenly across the slide, and let the agarose set at room temperature. The thickness of the agarose coating will be around 1 mm, and overlaying with the cover slip aids to distribute the agarose evenly across the slide and to ensure an even surface.
3. When the agarose has set, gently remove the coverslip by sliding it towards the short end of the slide and air-dry the slides overnight.
4. When the slides have dried completely, they can directly be used or stored for several months in a dry, cool space.

Note: Pre-coating the slides with normal melting point agarose increases the adhesion of the agarose layer containing the cells for comet analysis.

B. Culturing cells of interest

Ensure that your cells of interest are in culture and growing exponentially (i.e., approximately between 60% and 80% confluence at the time of the assay). Split your cells of interest 1-3 days before running the assay according to your established cell culture procedure in the medium of choice.

Note: The comet assay described here can be used to determine DNA damage in a wide variety of cultured cells, provided they can be brought into single cell solution. As the amount of DNA damage induced by a particular setting and the repair kinetics will depend on the cell line used, ideal settings for treatment and repair need to be experimentally determined.

C. Preparation of material on the day of the assay

1. Prepare appropriate amounts of neutral comet lysis buffer and cool to 4°C. Be sure to have enough cold DH₂O to freshly prepare the cold electrophoresis buffer. The amount of lysis buffer required depends on the volume and number of the coplin jars that will be used. Typically, a medium-sized coplin jar can hold 10 slides and requires around 150 mL of buffer. The amount of the electrophoresis buffer needed depends on the apparatus that is used. For the CometAssay ESII apparatus that is used here, calculate approximately 850 mL. This amount does not depend on the number of slides since empty spaces for slides will be filled up with dummy slides.
2. Place the comet electrophoresis apparatus (including cooling pack) at 4°C to cool down.
3. Warm the water bath to 37°C.
4. Completely dissolve 0.5 g of low melting point agarose (LMP) in 50 mL of 1× PBS (for this 1% solution, a volume of 1 mL per sample plus some extra will be required, so increase the volume if more samples will be processed) by heating in a glass bottle in the microwave. Be sure to place the lid on the bottle only loosely and mind the boiling retardation. Once completely dissolved, place the bottle in the 37°C water bath to equilibrate to 37°C.

Note: Keeping the correct temperature of the water bath is essential – if too cold, the agarose will solidify; if used too hot, this will cause additional damage to the cells.

5. Label the agarose-coated slides using a pencil. Be sure to prepare at least duplicates, or better, triplicate slides for each assay condition (e.g., time-point or amount of DNA damaging agent).
6. Prepare your workplace (see Figure 1):

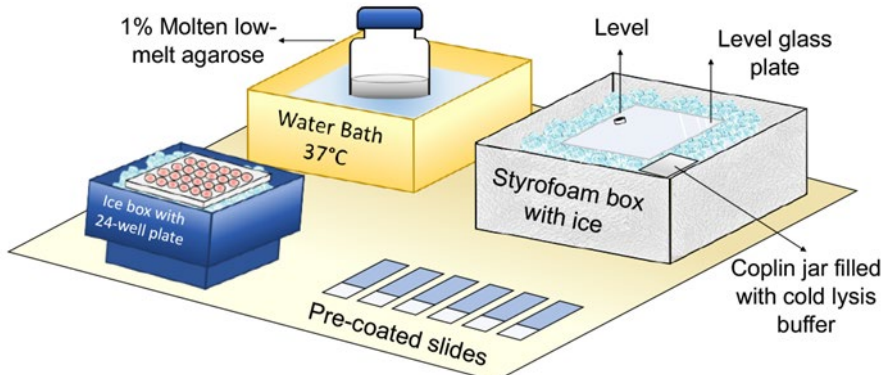


Figure 1. Proposed layout of a workplace to perform the comet assay.

An optimal arrangement of the materials as discussed in the text is shown.

7. Fill a large styrofoam bucket with ice, place a glass plate on top of the ice horizontally, and check using a level to ensure that cells in agarose will be evenly spread across the entire slide.
8. Place coplin jar filled with cold lysis buffer into the same bucket (or a different ice-containing bucket next to it).
9. Place an empty 24-well plate into a second ice bucket ready to receive the cell suspension.
10. Prepare the following materials to be ready and close at hand next to the 37°C water bath: a P100 or P200 pipet plus tips, a P1000 pipet plus tips, molten low-melting point agarose equilibrated at 37°C, labelled microscope slides, cover slips, and timer.

D. Treatment of cells and embedding into agarose

Depending on the research question, the neutral comet assay can be used to assess the amount of DNA damage caused by a specific amount of a fast and direct acting DNA damaging agent such as ionizing radiation (see D1). Moreover, the comet assay can be exploited to assess the repair kinetics after exposure to a certain amount of a DNA damaging agent (see D2) and also the levels of endogenous DNA damage present in cells (e.g., due to a genetic ablation of a DNA repair pathway) (see D3). Be sure to include appropriate positive and negative controls when running the assay.

D1) Assessment of DNA damage caused by treatment of cells with ionising radiation

1. Irradiate exponentially growing cells by placing the dish in the faxitron cabinet and following the manufacturer's detailed instructions to deliver the planned irradiation dose. As positive control, use a dose between 2 and 4 Gy.
2. Trypsinize cells, neutralize trypsin by addition of complete medium, and count cells and dilute to 2×10^5 cells/ml in cold complete medium of choice in 15 mL Falcon tubes.
3. Place Falcon tubes on ice to transfer them from the cell culture lab to the work bench.
4. To ensure an even suspension of cells, carefully invert the Falcon tube a few times (avoid foam formation or vigorous shaking to avoid damaging the cells); then, pipet 250 μ L of cell suspension into the wells of the 24-well plate (1 well per slide/sample) that is kept on ice.
5. Ready the ice bucket with the glass plate, ensure it is still level, get the P1000 and the cover slips, and open the low-melting point agarose bottle (still keeping it in the 37°C water bath).
6. Add 1 mL of LMP-Agarose into the well, pipetting carefully to avoid strong bubble formation, aspirate the mixture, and transfer 1 mL of the cell-agarose mix onto the appropriate agarose-coated microscopy slide. Immediately overlay with a cover slip and, paying attention to keep the slide as level as possible, transfer the slide onto the cold glass plate on ice for the agarose to gel. Repeat this for every well until all cell samples have been transferred onto slides. This procedure is visualised in Video 1.



Video 1. Transfer of cells in LMP-Agarose onto microscopy slide

- When all samples have been transferred onto the slides, gently remove the cover slips by sliding them along the longitudinal axis (starting with the first sample) and place the slides into the coplin jar to immerse them in the lysis buffer. Keep the samples in cold (on ice) lysis buffer protected from light for at least 1 h.

Note: This step can be prolonged to an overnight incubation provided that the samples are constantly kept at 4°C maximum and protected from light. Protection from light aims at reducing additional DNA damage that could be generated through, e.g., UV light or other sources.

D2) Assessment of the repair kinetics after ionising radiation

- Prepare one dish of exponentially growing cells per time-point.
- Irradiate exponentially growing cells (*i.e.*, approximately 60-80% confluence) by placing the dish in the faxitron cabinet and following the manufacturer's detailed instructions. As positive control use a dose between 2 and 4 Gy. The ideal dose of irradiation depends on your research question and the cell line used and should be experimentally determined.
- Start the timer to keep track of the post-irradiation time-points.
- Place the cell dishes that will be collected at later time-points back into the incubator.
- Trypsinize and embed the cells that are ready to be collected as outlined in section D, subsection D1, steps 2-7.
- Proceed with harvesting and embedding the cells of the remaining time-points accordingly.
- When all slides are in the lysis buffer, incubate the samples for at least 1 h before continuing with the electrophoresis.

Note: This step can be prolonged to an overnight incubation provided that the samples are constantly kept at 4°C maximum and protected from light. Protection from light aims at reducing additional DNA damage that could be generated through, e.g., UV light or other sources.

D3) Assessment of endogenous DNA damage in cultured cells

- Trypsinize exponentially growing cells (control versus, *e.g.*, KO cells), neutralize the trypsin by addition of complete medium, count cells and dilute them to 2×10^5 cells/ml in complete medium of choice in 15 mL Falcon tubes.
- To embed the cells, follow the procedure as outlined in section D, subsection D1, steps 2-7.

*Important note: Be sure to include samples with appropriate positive and negative controls (*e.g.*, ionizing radiation and no-treatment control) to ensure that the assay has worked!*

E. Electrophoresis and staining of comet slides

- Prepare an appropriate amount of cold neutral comet electrophoresis buffer and store at 4°C until required.
- Slowly drain the lysis buffer from the coplin jars and replace with fresh cold electrophoresis buffer. Then drain the electrophoresis buffer and replace with fresh electrophoresis buffer. Repeat once more. Finally, incubate the slides in electrophoresis buffer for 60 min on ice, protecting from light.
- Fill the comet buffer tank with fresh cold electrophoresis buffer to the required level. Transfer the comet slides to the comet assay apparatus, paying attention to the orientation of the slides. Ensure that all slides are fully immersed in buffer and fill up the remaining space with dummy slides.
- Close the lid of the comet apparatus and run at 21 V for 60 min (this will result in ca. 120 mA current).
- Fill the coplin jar with dH₂O.
- After electrophoresis, remove the slides from the tank and transfer them to the coplin jar containing dH₂O.
- Incubate for 5 min, then drain the dH₂O and carefully replace with fresh dH₂O. Repeat once.
- In the meantime, prepare sufficient comet staining solution (approximately 600 µL per slide plus a bit extra). Keep protected from light.
- Transfer the slides to a tray lined with paper towels, paying attention to lay them down as level as possible.
- Cover each slide with approximately 600 µL of staining solution (ensure that the entire agarose part is

covered with the solution), cover the tray with foil or a lid to protect from light, and incubate for 20 min at room temperature.

11. Decant the staining solution and shortly dip each slide into fresh dH₂O.
12. Let the slides air dry overnight, protected from light.

F. Imaging and analysis of comet slides

1. Image the slides on the fluorescent microscope, taking pictures at 10× or 20× magnification from different fields randomly picked across the entire slide. Be sure to use exposure and light intensities that allow clear visualization of your comets from the background, and try to focus as well as possible. Image an absolute minimum of 50 cells per condition, but preferentially at least 100 cells or more. Keep separate image folders for every single slide, containing all separate images of the different fields. Save all individual images as tiff files in one folder per slide.
2. Analyse the images using the OpenComet plugin available for FIJI as follows.
3. Open the OpenComet plugin.
4. Choose the input file folder (all images for one slide can be selected and analysed at once) and an output file directory.
5. Using the ‘auto’ head finding mode, click run. Results of this analysis will be summarized in an Excel file that is saved in the output file directory chosen previously.
6. Check that all the comets have been correctly detected and deselect the ones that clearly need to be excluded/are incorrect (*e.g.*, artefacts and debris that are not comets that have been scored, overlays of multiple nucleoids, comets in which the head has been wrongly defined, or similar) by clicking on them. OpenComet will outline every regularly detected comet in red (with a red circle around the head and a red line to delineate the tail, see Figure 2A and 2B). In addition to this, there is a green line that shows the intensity distribution of the signal detected as the head, and a blue line for the signal detected as the tail. Sometimes the software is unsure whether something is a correctly detected comet or not (*e.g.*, unusual head). In that case, OpenComet will outline these ‘outliers’ in yellow (Figure 2C and 2D). However, it is also possible that shapes are incorrectly scored, as in Figure 2E. Here, the very low intensity signal was incorrectly scored as having a minuscule head and most of the signal being in the tail. Inclusion of such a shape would strongly influence the result, especially if this happens more than once or if only a few cells are assessed per condition. If OpenComet can’t analyse the shapes (*e.g.*, if two or more comets are too close to each other or overlying), the shapes will be outlined in grey (Figure 2F). The same will happen to those comets that you have deselected/excluded by clicking on them. It is very important to visually double-check every comet, as incorrectly assessed ones can strongly influence the result.

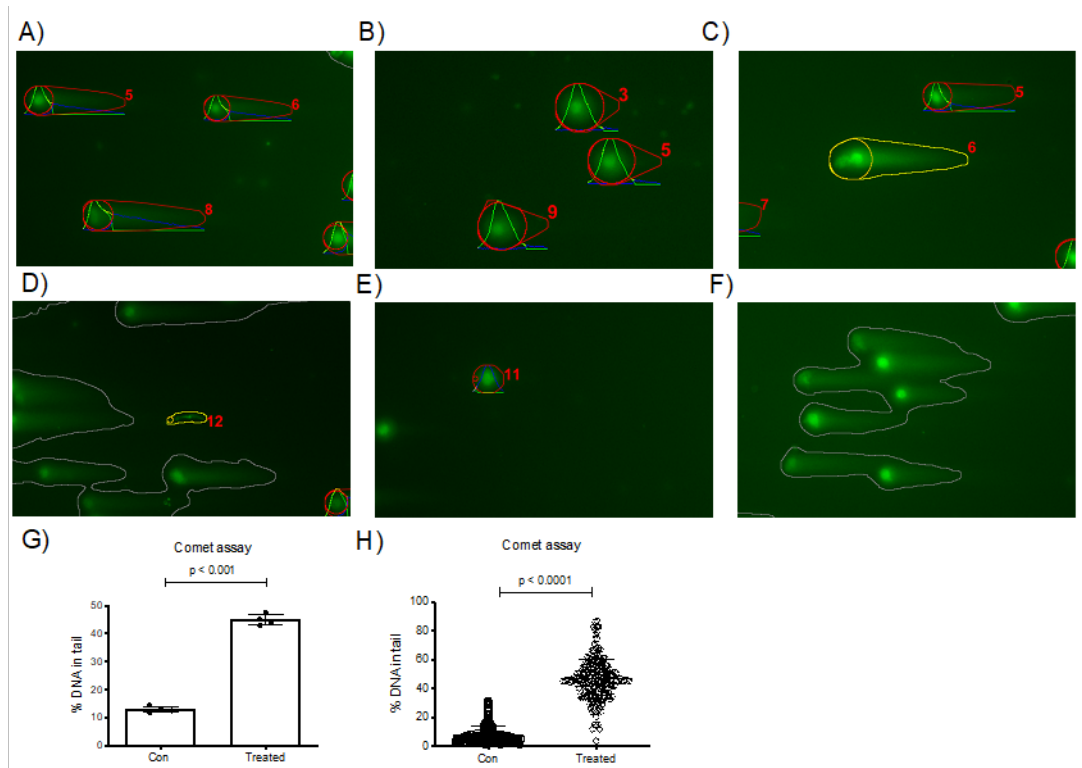


Figure 2. Example of images of comets analysed using the OpenComet plugin running the «auto» head finding mode and possible result plots.

These data were obtained using Tig-1 human primary fibroblasts after irradiation with 4 Gy. A) OpenComet outlines every regularly detected comet in red with a red circle around the head and a red line to delineate the tail. The green line shows the intensity distribution of the head signal, and the blue line shows the tail signal. Red numbers indicate the individual comets as listed in the quantification sheet. B) Representative picture showing control cells. Clearly, these cells show much less DNA in the tail than the cells in A), which were treated with ionizing radiation. C) and D) A yellow shape indicates that the software is unsure about the correct detection of comets. Be sure to visually inspect these comets and exclude/include as appropriate. E) Example of an incorrect score of a comet shape. The very low intensity signal was incorrectly scored to have a minuscule head and most of the signal in the tail. Inclusion of such a shape would strongly influence the result. F) A grey shape indicates that OpenComet is not able to outline comets, *e.g.*, because cells are too close together. G-H) The results obtained in the Excel file can be plotted (G) as a mean value of the duplicates or triplicates that were analysed as percentage of DNA in tail, tail moment, or olive moment or (H) as individual data points (*e.g.*, of 50 cells that were quantified).

7. After double-checking all comets on all slides, click ‘update’. This will generate a second Excel sheet with the suffix ‘_update’ that takes into account the comets that have been excluded.
8. This excel sheet contains all the values for all comet images of the slide that was analysed. In the last few rows are values for mean, median, standard deviation, minimum, and maximum for all detected comets, divided into either only all normal comets or the normal and outlier comets. The choice of which of these values to use depends on whether you are fine with including the values of the outliers or not. Normally, both these values are very similar to one another.
9. There are two ways to plot the results: first, you can calculate a mean value of the duplicates or triplicates that were analysed as percentage of DNA in tail, tail moment, or olive moment, *e.g.*, using a bar graph. Repeat the entire assay at least two more times to obtain three or more independent values for each data point (Figure 2G). Second, you can also plot all the individual data points (*e.g.*, of 50 cells that were quantified) of at least three repeats of the entire assay (Figure 2H).

Note: The tail moment describes the product of multiplying the length of the comet tail with the percentage of DNA in the tail, while the olive moment is the product of the total percentage of DNA in the tail and the distance between the centres of the masses of both head and tail regions. The olive moment is particularly useful to describe heterogeneity within a cell population, as the olive moment picks up variations in how the DNA is distributed in the tail. Of all the three options, the percentage of DNA in the tail is the measurement that seems the most intuitive to most researchers.

10. To test whether the groups differ significantly from each other, you can use the Student's *t*-test when only two groups are compared. When comparing three or more groups, use one-way ANOVA followed by, e.g., Bonferroni's multiple comparison test.
11. When publishing comet assay data, it's strongly advisable to adhere to the 'minimum information for reporting on the comet assay (MIRCA)' guidelines that were just recently published in an attempt to ensure better interpretation, verification and reproducibility of results across laboratories (Moller *et al.*, 2020).

Recipes

1. Lysis buffer for neutral comet assay

- a. Prepare 'premix' by dissolving 146.1 g of NaCl (final: 2.5 M), 37.2 g of EDTA disodium salt ($\text{C}_{10}\text{H}_{14}\text{N}_2\text{Na}_2\text{O}_8 \cdot 2\text{H}_2\text{O}$, final: 100 mM), 1.2 g of Tris base (final: 10 mM) and 10 g of N-Lauroylsarcosine (final: 1%) in 800 mL of dH₂O.
- b. Once all solids have dissolved, adjust pH to 9.5 by dropwise addition of 5 M of NaOH. Adjust volume to 1 L by adding dH₂O, store at 4°C.
- c. To prepare a 'complete solution' of lysis buffer just prior to use, add 1 mL of DMSO and 0.5 mL of Triton X-100 to 98.5 ml of cold lysis buffer.

2. Electrophoresis buffer for neutral comet assay

- a. Prepare separate stock solutions: 1 M Sodium-Acetate (82.03 g of $\text{C}_2\text{H}_3\text{NaO}_2$ in 1 L dH₂O), 1 M Tris-HCl pH 8.3 (121.14 g of Tris base in 1 L dH₂O; adjust pH dropwise using HCl to 8.3).
- b. To prepare electrophoresis buffer (final composition: 300 mM Sodium-Acetate ($\text{C}_2\text{H}_3\text{NaO}_2$), 100 mM Tris-HCl pH 8.3), add 300 ml of 1 M Na-Acetate and 100 mL of 1 M Tris-HCl pH 8.3 to 600 mL of cold dH₂O; store at 4°C until required.

3. Comet staining solution

Dilute SYBR Gold 1:10,000 in dH₂O just prior to use. Protect from light.

4. PBS (phosphate buffered saline)

- a. To make a 10× PBS stock solution, dissolve 80 g of NaCl, 2 g of KCl, 26.8 g of $\text{Na}_2\text{HPO}_4 \cdot 7\text{H}_2\text{O}$, and 2.4 g of KH_2PO_4 in 800 mL of dH₂O. Adjust pH to 7.4 using HCl, add dH₂O until 1 L, autoclave to store.
- b. To make 1× PBS working solution, dilute 100 ml of 10× PBS stock solution with 900 mL of dH₂O.

Acknowledgments

The authors wish to thank the following funding bodies for supporting research in the group of EM: Swiss National Science Foundation, Promedica Stiftung Chur, the Sassella Stiftung, and the Kurt und Senta Herrmann Stiftung.

Competing interests

The authors declare that they have no conflicts of interest.

References

- Ciccia, A. and Elledge, S. J. (2010). [The DNA damage response: making it safe to play with knives](#). *Mol Cell* 40(2): 179-204.
- Clementi, E., Garajova, Z. and Markkanen, E. (2021). [Measuring DNA Damage Using the Alkaline Comet Assay in Cultured Cells](#). *Bio-protocol* 11(16): e4119.
- Clementi, E., Inglin, L., Beebe, E., Gsell, C., Garajova, Z. and Markkanen, E. (2020). [Persistent DNA damage triggers activation of the integrated stress response to promote cell survival under nutrient restriction](#). *BMC Biol* 18(1): 36.
- Collins, A. R. (2014). [Measuring oxidative damage to DNA and its repair with the comet assay](#). *Biochim Biophys Acta* 1840(2): 794-800.
- Gyori, B. M., Venkatachalam, G., Thiagarajan, P. S., Hsu, D. and Clement, M. V. (2014). [OpenComet: an automated tool for comet assay image analysis](#). *Redox Biol* 2: 457-465.
- Hoeijmakers, J. H. (2009). [DNA damage, aging, and cancer](#). *N Engl J Med* 361(15): 1475-1485.
- Jackson, S. P. and Bartek, J. (2009). [The DNA-damage response in human biology and disease](#). *Nature* 461(7267): 1071-1078.
- Li, W. and Sancar, A. (2020). [Methodologies for detecting environmentally induced DNA damage and repair](#). *Environ Mol Mutagen* 61(7): 664-679.
- Markkanen, E. (2017). [Not breathing is not an option: How to deal with oxidative DNA damage](#). *DNA Repair (Amst)* 59: 82-105.
- Moller, P., Azqueta, A., Boutet-Robinet, E., Koppen, G., Bonassi, S., Milic, M., Gajski, G., Costa, S., Teixeira, J. P., Costa Pereira, C., et al. (2020). [Minimum Information for Reporting on the Comet Assay \(MIRCA\): recommendations for describing comet assay procedures and results](#). *Nat Protoc* 15(12): 3817-3826.
- Olive, P. L. (2009). [Impact of the comet assay in radiobiology](#). *Mutat Res* 681(1): 13-23.
- van Loon, B., Markkanen, E. and Hubscher, U. (2010). [Oxygen as a friend and enemy: How to combat the mutational potential of 8-oxo-guanine](#). *DNA Repair (Amst)* 9(6): 604-616.

Measurement of Bone Metastatic Tumor Growth by a Tibial Tumorigenesis Assay

Baotong Zhang^{1, 2, 3, *}, Xin Li^{4, 5}, Wei-Ping Qian^{3, 6}, Daqing Wu^{4, 5, *} and Jin-Tang Dong^{1, 2, 3, *}

¹Department of Human Cell Biology and Genetics, Southern University of Science and Technology School of Medicine, Shenzhen, China

²Department of Hematology and Medical Oncology, Emory University School of Medicine, Atlanta, GA, 30322, USA

³Winship Cancer Institute, Emory University, Atlanta, GA, 30322, USA

⁴Center for Cancer Research and Therapeutic Development and Department of Biological Sciences, Clark Atlanta University, Atlanta, GA, USA

⁵Department of Biochemistry and Molecular Biology, Georgia Cancer Center and Medical College of Georgia, Augusta University, Augusta, GA, 30912 USA

⁶Department of Surgery, Emory University School of Medicine, Atlanta, GA, 30322, USA

*For correspondence: zhangbt@sustech.edu.cn; dwu@cau.edu; dongjt@sustech.edu.cn

Abstract

Bone metastasis is a frequent and lethal complication of many cancer types (*i.e.*, prostate cancer, breast cancer, and multiple myeloma), and a cure for bone metastasis remains elusive. To recapitulate the process of bone metastasis and understand how cancer cells metastasize to bone, intracardiac injection and intracaudal arterial animal models were developed. The intratibial injection animal model was established to investigate the communication between cancer cells and the bone microenvironment and to mimic the setting of prostate cancer patients with bone metastasis. Given that detailed protocols of intratibial injection and its quantitative analysis are still insufficient, in this protocol, we provide hands-on procedures for how to prepare cells, perform the tibial injection, monitor tibial tumor growth, and quantitatively evaluate the tibial tumors in pathological samples. This manuscript provides a ready-to-use experimental protocol for investigating cancer cell behaviors in bone and developing novel therapeutic strategies for bone metastatic cancer patients.

Keywords: Bone metastasis, Mouse model, Tibial injection, Prostate cancer, Tumorigenesis, Osteolysis

This protocol was validated in: Nat Commun (2021), DOI: 10.1038/s41467-021-21976-w

Background

Bone metastasis is the most frequent metastasis for many cancer types, especially for those arising from prostate (90%), breast (70%), multiple myeloma (90%), lung (40%), and kidney (40%) (Coleman, 2006). The median survival of patients with bone metastasis ranges from approximately one year for lung cancer to 3-5 years for prostate cancer, breast cancer, and multiple myeloma (Campbell *et al.*, 2012). Bone metastases often require radiotherapy and lead to bone pain, hypercalcemia, pathologic fracture, and spinal cord or nerve root compression (Coleman, 2006). Bone metastases also develop resistance to chemotherapy, as docetaxel-treated prostate cancer patients with bone metastasis still have poor prognoses (Coleman *et al.*, 2020). Therefore, effective therapeutic strategies are still urgently needed for bone metastatic cancer patients.

Bone metastases can be classified as osteolytic or osteoclastic types according to their predominant characteristics in radiographic images. Although lysis or sclerosis may appear to predominate in some types of bone metastases, osteoclastic and osteoblastic activities are usually simultaneously involved in the formation of bone metastatic lesions. The outgrowth of cancer cells in the bone microenvironment is a process in which cancer cells communicate with osteoclasts and osteoblasts frequently via paracrine factors and receptors on their cell surfaces. Therefore, the behaviors of cancer cells in bone metastasis are distinct from those in primary tumors, thus potentially requiring different therapeutic methods.

Diverse *in vivo* animal models have been established to study bone metastasis. Intracardiac injection has been utilized as the gold standard to develop bone metastasis by injecting cancer cells into the left ventricle in mice, with a goal of recapitulating the bone metastasis process, including cancer cell survival in the bloodstream, extravasation, cancer cell arrest in bone, and bone metastatic tumor growth (James *et al.*, 2015). Similarly, intracaudal arterial injection was established to provide an easy-to-use model with higher efficiency of bone metastasis (Kuchimaru *et al.*, 2018). However, the intratibial injection model is used to mimic the scenario when cancer cells have metastasized to the bone, thus providing a better focus on the crosstalk between cancer cells and the bone microenvironment. Herein, we will focus on tibial tumorigenesis by using the intratibial injection model to mimic the setting of cancer patients who have developed bone metastasis.

In this protocol, we take the prostate cancer cell line PC-3 as an example, describe the hands-on procedures of cell preparation, intratibial injection, monitoring tibial tumor growth, and post tissue collection analyses, highlight the critical steps in cell preparation and intratibial injection, and detail how to quantitatively analyze the tibial tumors in histological samples.

Materials and Reagents

1. Nude mice (The Jackson Laboratory, catalog number: 002019)
2. NOD SCID mice (The Jackson Laboratory, catalog number: 001303)
3. Povidone Iodine Prep Pads (DYNAREX, catalog number: 1108)
4. Sterile Alcohol Prep Pads (DYNAREX, catalog number: 1116)
5. 27G $\frac{1}{2}$ " syringe (BD, catalog number: 305620)
6. 40 μ m Cell Strainer (Fisher Scientific, catalog number: 087711)
7. PC-3 cells (ATCC, catalog number: CRL-1435)
8. Ham's F-12K (Kaighn's) Medium (ThermoFisher, catalog number: 21127022)
9. FBS (Sigma, catalog number: F2442)
10. 0.05% trypsin-EDTA (ThermoFisher, catalog number: 25300054)
11. 0.4% trypan blue solution (Sigma, catalog number: T8145)
12. PBS (Sigma, catalog number: 806552-1L)
13. Isoflurane Inhalation Anesthetic (Southern Anesthesia & Surgical, catalog number: PIR001325)
14. Human Kallikrein 3/PSA Quantikine ELISA Kit (R&D system, catalog number: DKK300)
15. 14% EDTA (pH 7.4) (American Research Product, catalog number: BM-150A)
16. 10% neutral-buffered formalin (Sigma, catalog number: HT501128)
17. 100% Ethanol (KOPTEC, catalog number: 89426-252)
18. Hematoxylin (Electron Microscopy Sciences, catalog number: 26043-05)

19. Eosin Y-solution (Millipore Sigma, catalog number: 102439)
20. Permount (Fisher Scientific, catalog number: SP15100)
21. Xylene (Fisher Chemical, catalog number: X54)
22. Immu-Mount (Epredia, catalog number: 9990402)
23. Sodium acetate anhydrous (Sigma, catalog number: S-2889)
24. L-(+) tartaric acid (Sigma, catalog number: T-6521)
25. Fast Red Violet LB salt (Sigma, catalog number: F-3381)
26. Napthol AS-MX phosphate (Sigma, catalog number: N-4875)
27. Basic Staining Buffer for TRAP staining (see Recipes)
28. TRAP Staining Solution (see Recipes)
29. 10% EDTA (see Recipes)

Equipment

1. Refrigerated centrifuge (Eppendorf, model: 5810R)
2. Gas Anesthesia System (PerkinElmer, model: XGI-8)
3. Heating pad (Sunbeam Products, catalog number: 2139885)
4. IVIS® Spectrum Imaging System (PerkinElmer)
5. MX-20 X-ray system (Faxitron [Tucson, Arizona])
6. -80°C freezer (Fisher, catalog number: TSU600ARAK)
7. Embedding Center (Leica, catalog number: EG1160)
8. Rotary Microtome (Leica, catalog number: RM2135)
9. NanoZoomer Whole Slide Scanner (Olympus, Hamamatsu)

Software

1. NDP.view2 (HAMAMATSU, <https://www.hamamatsu.com/us/en/product/type/U12388-01/index.html>)
2. Living Image software (PerkinElmer, <https://www.perkinelmer.com.cn/product/li-software-for-lumina-1-seat-add-on-128110>)

Procedure

A. Collection of fresh cultured cancer cells

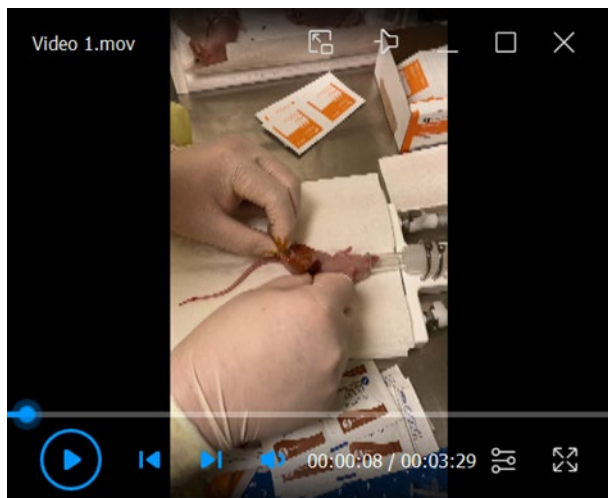
1. Seed prostate cancer PC-3 cells in F-12K medium with 10% FBS. For PC-3 cells, 0.5 million cells per 10 cm dish in 10 mL of media is ideal for cell culture. Culture cells at 37°C and 5% CO₂ in a cell culture incubator.
2. Passage the PC-3 cells every three days when cells reach 80-90% confluence. See below procedures for subculturing PC-3 cells:
 - a. Remove medium and wash the cells with 2 mL of sterile PBS.
 - b. Add detaching reagent 0.5% trypsin-EDTA and incubate the dishes at 37°C until the cells are fully detached from the dishes (approximately 2 min for PC-3 cells).
 - c. Add 2 mL of fresh media containing 10% FBS to inactivate the trypsin and collect the cells into 15 mL (or 50 mL) sterile centrifuge tubes.
 - d. Centrifuge at 1,200 × g for 3 min to pellet the cells. Remove the supernatant and resuspend the cells in 3 mL of fresh medium. Count the cells and perform the cell culture procedure described in Step A1.
3. Collect cultured PC-3 cells for tibial injection. For PC-3 cells, approximately 2-2.5 million cells will be

collected per dish when the cells are 80%-90% confluent in a 10 cm dish. Perform steps described in Steps A2a-A2c to collect the cells in sterile centrifuge tubes. Follow the procedures below to obtain a single cell suspension for tibial injection.

- a. Centrifuge at $1,200 \times g$ for 3 min to pellet the cells. Remove the supernatant and resuspend cells in 20 mL of sterile PBS. Centrifuge at $1,200 \times g$ for 3 min to pellet the cells again. Wash the cells with PBS by following this procedure twice.
- b. Resuspend the cells in 20 mL of sterile PBS, pipette thoroughly to obtain a single cell suspension. Filter the cells with a 40 μm Cell Strainer to guarantee a single cell suspension.
- c. Count the cells in 0.4% trypan blue solution to assess cell viability and calculate the total number of live cells.
- d. Centrifuge at $1,200 \times g$ for 3 min to pellet the cells and remove the supernatant. Approximately 300-500 μL of PBS will remain in the centrifuge tube. Use the pipette to measure the exact volume and then add the appropriate volume of PBS to obtain a cell suspension with a density of 5×10^7 cells/mL.
- e. Critical step: Prepare sufficient cells. Approximately 1.5 to 2-fold the required number of cells is ideal. For instance, if 10 million cells are needed for tibial injection, then prepare 15-20 million cells. Use fresh cells for tibial injection. Suspend the cells in PBS until tibial injection; for instance, proceed to Steps A3a-A3d within an hour before tibial injection.

B. Tibial injection

1. Mouse preparation for tibial injection. General requirements for the tibial injection procedure follow the standards of rodent survival surgery.
 - a. Sanitize the work surface and anesthetize nude mice by using 3% isoflurane.
 - b. Maintain the anesthesia with 2.5% isoflurane and check the toe reflex of muscle tone by pinching the toes. The animal is well anesthetized when no toe reflex is present.
 - c. If NOD SCID mice are used, remove the hairs from the ankle joint to expose the injection area before anesthesia.
 - d. Administer buprenorphine at 0.1 mg/kg by intraperitoneal injection.
 - e. Clean both legs of the mouse with 10% povidone/iodine swab/solution followed by 70% ethanol. Repeat three times.
2. Cell preparation for tibial injection. Mix the cells again to obtain a homogeneous cell suspension. Remove the plunger and pipette 20 μL of cells (1 million cells) into a 27G $\frac{1}{2}''$ syringe from the bottom. Install the plunger again and remove the air by slowly pushing the plunger inside. Hold the syringe vertically with the needle pointing up and gently tap the syringe to remove any bubbles. A drop of cell suspension will come out of the needle, ensuring no air remains in the syringe.
3. Tibial injection (see Video 1).
 - a. Using forefinger and thumb, gently grasp the lateral malleolus, medial malleolus, and lower half of the tibia, and bend the leg in a movement combining flexion and lateral rotation. The knee will be visible and accessible at this time.
 - b. While firmly grasping the ankle/leg of the mouse, insert a needle without cell suspension under the patella, through the middle of the patellar ligament, and into the anterior intercondylar area in the top of the tibia. We use a blank syringe first to avoid the blockage of the needle by bone tissues.
 - c. When inserting the needle into the tibia, guide the syringe through the growth plate using steady and firm pressure with a slight drilling action. Upon penetration of the tibial growth plate, the needle will encounter markedly less resistance.
 - d. Use a gentle and lateral movement of the needle to ensure the needle is in the tibia and through the growth plate. The movement will be limited because the needle is in the proper place within the tibia.
 - e. Remove the blank syringe and insert the syringe with the cell suspension following the same route. Gently move the needle to ensure the needle is in the tibia and through the growth plate. Inject a volume of 20 μL of cell solution very slowly. At this point, no resistance should be felt.

**Video 1. Procedures of tibial injection in a nude mouse.**

This video was made at Emory University according to guidelines from the Emory University on Animal Care and approved by the Animal Research Ethics Board of Emory University under protocol #PROTO201700737.

4. Place the mice on a heating pad during the recovery period. Monitor the mice every 12 h during the first 72 h.

C. Monitoring tumorigenesis in the tibia

1. Monitor bone lesions via X-ray/micro-computed tomography (CT).
 - a. Turn on the machine and wait until the “READY” green light is on.
 - b. Warm up the machine for 300 s under 20 KV.
 - c. Anesthetize the mice via intraperitoneal injection of ketamine (80 mg/kg)/xylazine (10 mg/kg) prior to surgery. Monitor anesthesia depth by pinching toes.
 - d. Open the door and place a film in the cassette at the bottom with the “+” laser guide in the center.
 - e. Place the mice on top of the tray with the proper enlargement, center it with the “+” laser guide, and close the door tightly.
 - f. Perform X-ray imaging under 25 KV for 60 s.
 - g. Following scanning, turn the machine off, develop and fix the films, and recover the mice in their cages.
2. Monitor tumorigenesis in tibia by IVIS once a week if the tumor cells are prelabeled with luciferase.
 - a. For the cancer cells prelabelled with firefly luciferase, administer D-luciferin at 150 mg/kg via intraperitoneal injection. Wait 15-20 min before imaging for maximum luciferase signal.
 - b. Anesthetize the mice with 3% isoflurane and maintain at 2% isoflurane. Monitor anesthesia depth by pinching toes.
 - c. Acquire bioluminescence images with a Xenogen IVIS Spectrum Imaging System (PerkinElmer) and measure the photon flux in the tibial area of mice by using Living Image software (PerkinElmer). Please follow the equipment instructions to complete this step.
 - d. Following scanning, recover the mice in their cages.
3. Monitor Prostate-Specific Antigen (PSA) levels in serum.
 - a. Some prostate cancer cell lines (*i.e.*, LNCaP, C4-2, C4-2B) and patient derived xenografts (*i.e.*, LuCaP 23.1) secrete PSA during tumorigenesis in bone (Li *et al.*, 2021). Determine the PSA levels in cell lines and patient derived xenografts by literature search or experiments.
 - b. Diverse methods can be used for blood collection from mice, and 150 µL of blood per mouse is sufficient for the measurement of PSA levels in serum. Herein, collect blood from the lateral tail vein

as below:

- i. Warm the animals on a heating pad at least 30 min before blood collection.
- ii. Restrain the animal using the mechanical restraint device of choice with the tail protruding.
- iii. Clean the collection site with 70% ethanol.
- iv. Align the needle parallel to the lateral tail vein with the beveled edge of the needle facing up.
- v. Insert the needle into the vein starting at the tip of the tail and gently aspirate to collect blood via the syringe. This step is easier if a butterfly needle and vacuum blood collection tube are used.
- vi. Apply gentle pressure with gauze until bleeding has stopped.
- c. After blood collection, allow the blood to clot by leaving it undisturbed at room temperature (RT) for 30 min. Remove the clot by centrifuging tubes at $2,000 \times g$ for 10 min. Carefully collect the supernatant in yellow, which is designated serum. Approximately 50 μL can be collected from 150 μL whole blood. Store the serum in a -80°C freezer until use.
- d. Measure the PSA levels in serum using PSA ELISA kits (*i.e.*, R&D System, #DKK300) following the manufacturer's instructions.

D. Collection of bone tissue and histological analysis

1. Bone tissue processing
 - a. Euthanize the animals. Dissect the tibia, the femur, and the joint together from both lateral limbs. At least some of the femur should remain to account for the possible migration of tumor cells from the tibia to the femur. Remove as much muscle tissue as possible. Store the bone tissues in 10% neutral-buffered formalin (10 mL/bone sample) at RT up to two weeks for optimal results.
 - b. Decalcify bone tissues with 10% EDTA (pH 7.4) at 4°C for 10 days. The fluid volume to tissue ratio is critical for the decalcification process. Use at least 40 volumes of EDTA to decalcify bone tissues. For instance, if the bone tissues occupy 0.5 mL, then use 20 mL EDTA. Shake intermittently to make sure the decalcification solution is flowing around the bone. Change the decalcification solution on day 5.
 - c. After decalcification, rinse the bone tissues with distilled water once and store them in 70% alcohol (10 mL/bone sample) for further standard tissue processing.
 - d. Section the tissues embedded in paraffin at 5 μm -thick to include the tibia, knee joint, and the distal femur.
2. Hematoxylin & eosin (H&E) staining
 - a. Deparaffinize the unstained slides in xylene and rehydrate them in an ethanol gradient as below:
 - 3 \times 3 min Xylene
 - 2 \times 3 min 100% ethanol
 - 1 \times 3 min 95% ethanol
 - 1 \times 3 min 80% ethanol
 - 1 \times 3' min 70% ethanol
 - 1 \times 3 min deionized water
 - b. Stain slides with hematoxylin for 10 min, rinse with deionized water twice, and incubate with PBS for 3 min. Rinse again with deionized water twice.
 - c. Stain slides with eosin for 30 s and then proceed to dehydration procedures as below:
 - 2 \times 3 min 95% ethanol
 - 2 \times 3 min 100% ethanol
 - 3 \times 10 min xylene
 - d. Coverslip slides using Permount. Place a drop of Permount on the slide using a glass rod, taking care to leave no bubbles. Dry overnight in the hood.
3. Tartrate-resistant acidic phosphatase (TRAP) staining
 - a. Prepare Basic Staining Buffer and TRAP Staining Solution (see Recipes) and prewarm to 37°C.
 - b. Deparaffinize the unstained slides in xylene and rehydrate them in an ethanol gradient as below:
 - 3 \times 3 min Xylene

- 2 × 3 min 100% ethanol
 - 1 × 3 min 95% ethanol
 - 1 × 3 min 80% ethanol
 - 1 × 3' min 70% ethanol
 - 1 × 3 min deionized water
- c. Incubate the unstained slides in the Basic Staining Buffer for 20 min in an oven at 37°C.
 - d. Stain the slides in TRAP Staining Solution for 30-45 min in an oven at 37°C. Monitor the color change every 15 min until the TRAP-positive area turns red.
 - e. Counterstain the slides with hematoxylin for 10 min, rinse with deionized water twice, and incubate with PBS for 2 min.
 - f. Coverslip slides with Immu-Mount for analysis. TRAP staining will be dissolved by ethanol. If Permount is desired, then incubate the slides directly in xylene for 10 min and repeat twice to remove water.

Data analysis

A. X-ray images

1. Review X-ray images of mouse tibia and determine tumor-induced osteolytic and osteoblastic lesions in a double blind manner.
2. Evaluate the degree of osteolysis as in Figure 1.

Note: X-ray is not a quantitative method, so there is no well-accepted scoring system for animal data.

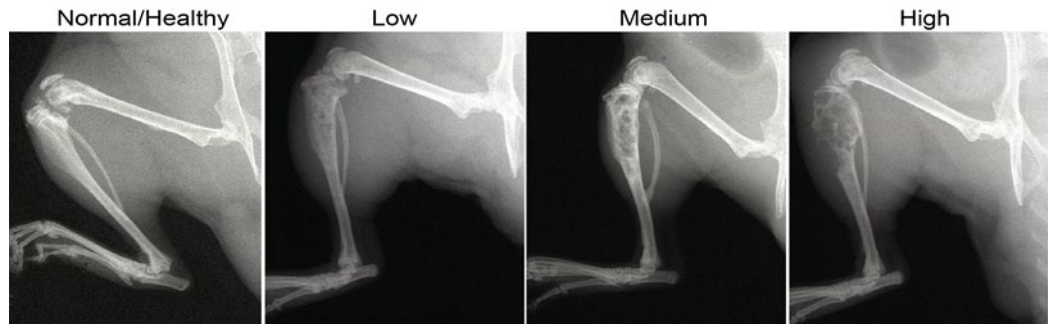


Figure 1. X-ray images of tibia bearing 5-week PC-3 tumors.

The degree of bone destruction is shown at the top of each image.

B. Analyze tumor area in H&E stained slides

1. Scan whole H&E stained tissue slides with an Olympus Hamamatsu NanoZoomer whole slide scanner at 40× magnification.
2. Use the Freehand Region tool in the NDP.view2 software to calculate total area (Figure 2B) and tumor area (Figure 2C) in tibial tumor samples. Typically, cancer cells have varied nuclei and more mitotic figures.
3. Calculate the ratio of tumor area to total area.
4. Show representative images with higher resolution as desired (Figure 2).

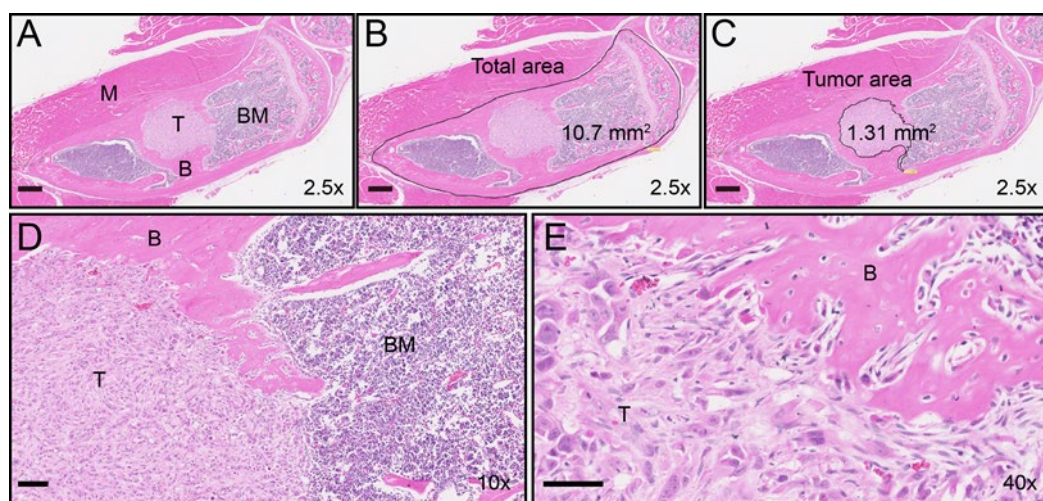


Figure 2. H&E staining in 5-week tibial tumors.

Shown are representative images of 2.5× (A-C), 10× (D), and 40× (E) magnifications of a PC-3 tibial tumor sample. Scale bars in A-C: 500 μm. Scale bar in D: 100 μm. Scale bar in E: 50 μm. T, tumor tissue. B, bone tissue. BM, bone marrow. M, muscle tissue.

C. Analyze osteoclast differentiation in TRAP stained slides

1. Scan whole TRAP stained tissue slides with an Olympus Hamamatsu NanoZoomer whole slide scanner at 40× magnification.
2. Use the Freehand Line tool in the NDP.view2 software to calculate the length of the interface between tumor and bone in tibial tumor samples. If multiple interfaces exist in the samples, calculate the sum of lengths.
3. Count the occurrence of TRAP positive cells at the tumor and bone interface.
4. Calculate the average occurrence of TRAP positive cells at the tumor and bone interface.
5. Show representative images with higher resolution as desired (Figure 3).

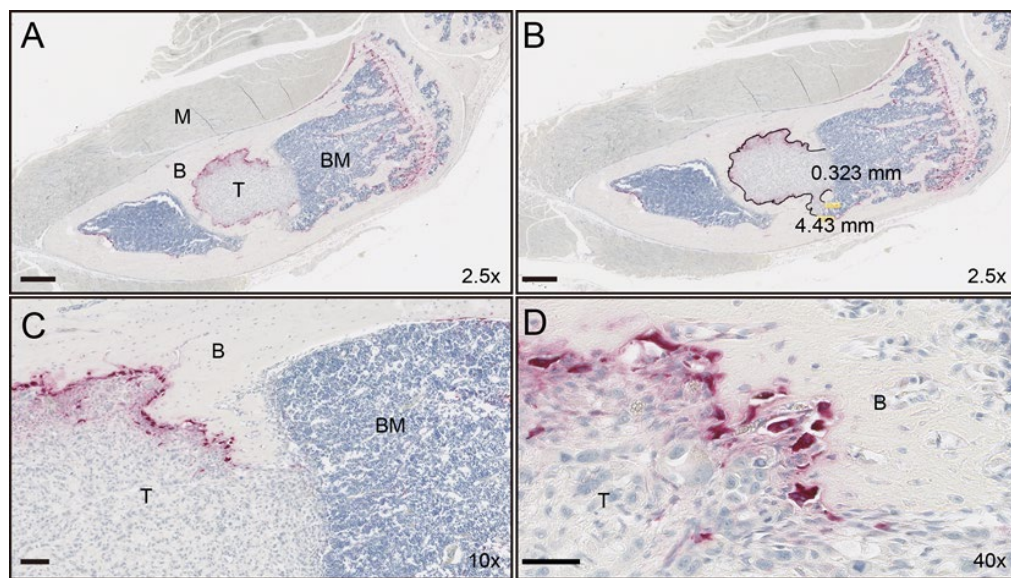


Figure 3. TRAP staining in 5-week tibial tumors.

Shown are representative images of 2.5× (A, B), 10× (C), and 40× (D) magnifications of a PC-3 tibial

tumor sample. Scale bars in A-B: 500 µm. Scale bar in C: 100 µm. Scale bar in D: 50 µm. T, tumor tissue. B, bone tissue. BM, bone marrow. M, muscle tissue. The lengths of tumor and bone interface were calculated in B using NDP.view2

Recipes

- 1. Basic Staining Buffer for TRAP staining (store at room temperature up to 6 months)**
 - a. Sodium acetate anhydrous 9.2 g
 - b. L-(+) tartaric acid 11.4 g
 - c. Adjust pH to 4.7-5.0 by adding acetic acid
 - d. Add deionized water to a total volume of 1 L
- 2. TRAP Staining Solution (make freshly before use)**
 - a. Basic staining buffer for TRAP staining: 200 mL
 - b. Fast Red Violet LB salt: 120 mg
 - c. Naphthol AS-MX phosphate: 20 mg (dissolved in 1 mL ethylene glycol monoethyl ether)
- 3. 10% EDTA**
Dilute 1,000 mL 14% EDTA by adding 400 ml deionized water.

Acknowledgments

We thank Dr. Anthea Hammond of Emory University for editing the manuscript. We thank Dr. Dezhi Wang at the Pathology Core Research Lab in the Department of Pathology of the University of Alabama at Birmingham for processing bone tissues. This work was supported by grant W81XWH-18-1-0526 from the Department of Defense Prostate Cancer Research Program. This protocol is a detailed version of our recent publications (Li *et al.*, 2021; Zhang *et al.*, 2021).

Competing interests

The authors declare no conflict of interest.

Ethics

The animal studies were approved by the Institutional Animal Care and Use Committee (IACUC) of Emory University with a protocol number of #PROTO201700737, which is validated from 7/12/2018 to 6/30/2024.

References

- Coleman, R. E. (2006). [Clinical features of metastatic bone disease and risk of skeletal morbidity](#). *Clin Cancer Res* 12(20 Pt 2): 6243s-6249.
- Campbell, J. P., Merkel, A. R., Masood-Campbell, S. K., Elefteriou, F. and Sterling, J. A. (2012). [Models of bone metastasis](#). *J Vis Exp*(67): e4260.
- Coleman, R. E., Croucher, P. I., Padhani, A. R., Clezardin, P., Chow, E., Fallon, M., Guise, T., Colangeli, S., Capanna,

- R. and Costa, L. (2020). [Bone metastases](#). *Nat Rev Dis Primers* 6(1): 83.
- James, N. D., Spears, M. R., Clarke, N. W., Dearnaley, D. P., De Bono, J. S., Gale, J., Hetherington, J., Hoskin, P. J., Jones, R. J., Laing, R., et al. (2015). [Survival with Newly Diagnosed Metastatic Prostate Cancer in the "Docetaxel Era": Data from 917 Patients in the Control Arm of the STAMPEDE Trial \(MRC PR08, CRUK/06/019\)](#). *Eur Urol* 67(6): 1028-1038.
- Kuchimaru, T., Kataoka, N., Nakagawa, K., Isozaki, T., Miyabara, H., Minegishi, M., Kadonosono, T. and Kizaka-Kondoh, S. (2018). [A reliable murine model of bone metastasis by injecting cancer cells through caudal arteries](#). *Nature communications* 9(1): 2981.
- Li, X., Gera, L., Zhang, S., Chen, Y., Lou, L., Wilson, L. M., Xie, Z. R., Sautto, G., Liu, D., Danaher, A., et al. (2021). [Pharmacological inhibition of noncanonical EED-EZH2 signaling overcomes chemoresistance in prostate cancer](#). *Theranostics* 11(14): 6873-6890.
- Zhang, B., Li, Y., Wu, Q., Xie, L., Barwick, B., Fu, C., Li, X., Wu, D., Xia, S., Chen, J., et al. (2021). [Acetylation of KLF5 maintains EMT and tumorigenicity to cause chemoresistant bone metastasis in prostate cancer](#). *Nat Commun* 12(1): 1714.

Reconstruction of Human AML Using Functionally and Immunophenotypically Defined Human Haematopoietic Stem and Progenitor Cells as Targeted Populations

Bernd B. Zeisig^{1,2}, Tsz Kan Fung^{1,2}, Estelle Troadec¹ and Chi Wai Eric So^{1,2,*}

¹Leukaemia and Stem Cell Biology Group, School of Cancer and Pharmaceutical Sciences, King's College London, London SE5 9NU, United Kingdom

²Department of Haematological Medicine, King's College Hospital, London SE5 9RS, United Kingdom

*For correspondence: eric.so@kcl.ac.uk

Abstract

Acute myeloid leukaemia (AML) is a highly heterogenous blood cancer, in which the expansion of aberrant myeloid blood cells interferes with the generation and function of normal blood cells. Although key driver mutations and their associated inhibitors have been identified in the last decade, they have not been fully translated into better survival rates for AML patients, which remain dismal. In addition to DNA mutation, studies in mouse models strongly suggest that the cell of origin, where the driver mutation (such as MLL fusions) occurs, emerges as an additional factor that determines the treatment outcome in AML. To investigate its functional relevance in human disease, we have recently reported that AML driven by MLL fusions can transform immunophenotypically and functionally distinctive human hematopoietic stem cells (HSCs) or myeloid progenitors resulting in immunophenotypically indistinguishable human AML. Intriguingly, these cells display differential treatment sensitivities to current treatments, attesting the cell of origin as an important determinant governing treatment outcome for AML. To further facilitate this line of investigation, here we describe a comprehensive disease modelling protocol using human primary haematopoietic cells, which covers all the key steps, from the isolation of immunophenotypically defined human primary haematopoietic stem and progenitor populations, to oncogene transfer via viral transduction, the in vitro liquid culture assay, and finally the xenotransplantation into immunocompromised mice.

Keywords: AML, MLL fusion, HSPC, CD34, Human disease modelling

This protocol was validated in: Sci Transl Med (2021), DOI: 10.1126/scitranslmed.abc4822

Background

Acute myeloid leukaemia (AML) is a highly heterogenous blood cancer driven by diverse mutations and distinctive cell populations, which is generally associated with poor prognosis in particular for older patients aged over 60. Recent research efforts have not only brought to light key AML driver mutations but also greatly enhanced our mechanistic understanding of how these mutations transform normal blood cells into leukaemia cells (Zeisig *et al.*, 2012). Despite this progress, the survival rates of most AML patients have only marginally improved and remain dismal (Shallis *et al.*, 2019).

Disease modelling is a powerful tool to study cancer biology, as it allows the researchers to readily access bona fide diseased cells for subsequent cellular and molecular studies. Mouse models have been particularly instrumental given the easy accessibility and well-established protocols for genetic manipulation, *in vitro*, and *in vivo* propagation of the cells. They have provided important insights into the biology of AML cells transformed by key driver mutations including MLL fusions and revealed promising novel therapeutic targets (Almosailakh and Schwaller, 2019; Zeisig and So, 2021). Murine disease models also led to the identification of candidate leukaemia cell of origins and their potential roles in influencing treatment responses (Krivtsov *et al.*, 2013; Stavropoulou *et al.*, 2016; Siriboonpiputtana *et al.*, 2017). While human and mouse cells share significant similarities, there are also clear differences including their contrasting transformation requirements, telomere lengths, and the non-coding regulatory genomes. As compared with mouse cell models, reconstruction of human AML using human primary cells has significantly lagged behind (Barabé *et al.*, 2007; Horton *et al.*, 2013; Wunderlich *et al.*, 2013). Until recently, it was not clear if human AML can also originate from multiple cells of origin, which may have different biology and treatment responses. Using immunophenotypically and functionally defined hematopoietic populations isolated from umbilical cord blood as the targeted cells to reconstruct MLL-AML, we have shown that human HSCs and common myeloid progenitors (CMPs) can be the cellular origins for MLL-AML, in which HSC-derived MLL-AML with a different transcriptional programme is more resistant to current chemo treatment than their myeloid progenitors-derived counterparts (Zeisig *et al.*, 2021). Here we describe in detail the experimental protocols for reconstruction of human MLL-AML using functionally and immunophenotypically defined hematopoietic cell populations as leukemia cells-of-origin.

Materials and Reagents

1. Antibodies (HSPC):
CD34 (clone: 581; APC-Cy7)
CD38 (clone: HB-7; FITC)
CD90 (clone: 5E10, PE)
CD123 (clone: 6H6; PE-Cy7)
CD45RA (clone: HI100, Pacific Blue)
2. Antibodies (Lineage) (all conjugated to the same fluochrome, *e.g.*, PE-Cy5):
CD2 (clone: RPA-2.10)
CD3 (clone: S4.1)
CD4 (clone: S3.5)
CD7 (clone: CD7-6B7)
CD8 (clone: 3B5)
CD10 (clone: MEM-78)
CD11b (clone: ICRF44)
CD14 (clone: HCD14)
CD19 (clone: HIB19)
CD20 (clone: 2H7)
CD56 (clone: B159)
CD235a (clone: GA-R2)
3. CD34 MicroBead Kit UltraPure (Miltenyi Biotec, catalog number: 130-100-453)

4. Cell Strainer 40 µm (Greiner Bio-One, catalog number: 542040)
5. Dulbecco's Modified Eagle Medium (DMEM) (Gibco, catalog number: 41966-029)
6. Fetal Bovine Serum (FBS) (Sigma, catalog number: F7524)
7. Ficoll-Paque Plus (GE Healthcare, catalog number: 17-1440-03)
8. Fresh cord blood or adult BM
9. Gag/pol plasmid (Addgene, plasmid number: 14887)
10. HEK293T cells (ATCC, catalog number: CRL-11268573)
11. Human cytokines:
Human IL-6, premium grade (Miltenyi Biotec, catalog number: 130-093-932);
Human IL-3 premium grade (Miltenyi Biotec, catalog number: 130-095-069);
Human SCF, premium grade (Miltenyi Biotec, catalog number: 130-096-695);
Human Flt3-Ligand, premium grade (Miltenyi Biotec, catalog number: 130-096-479);
Human TPO, premium grade (Miltenyi Biotec, catalog number: 130-108-339);
Prepare 10 µg/mL stock solutions in sterile filtered PBS + 0.1% FBS.
12. Isocove's Modified Dulbecco's Medium (IMDM) (Gibco, catalog number: 31980-022)
13. LS Columns (Miltenyi Biotec, catalog number: 130-042-401)
14. Minisart Filter unit 0.45 µm (Sartorius, catalog number: 16555-K)
15. MSCV plasmid (TaKaRa, catalog number: 634401)
16. Needles: 27G (BD, catalog number: 300635), 29G (BD, catalog number: 324824)
17. NSG mice (The Jackson Laboratory, catalog number: 05557)
18. OneComp eBeads Compensation beads (Thermo Scientific, catalog number: 01-1111-41)
19. Penicillin/Streptomycin (P/S) (Sigma, catalog number: P4333)
20. pMSCV-MLL-AF6, pMSCV-MLL-ENL (request to: eric.so@kcl.ac.uk)
21. Polybrene infection/transfection Reagent (10 mg/mL) (Merck, catalog number: TR-1003-G)
22. Polyethylenimine (PEI) 25kD linear ; Polysciences, catalog number: 23966-2)
23. Propidium iodide
24. Rely+On™ Virkon® tablets (VWR, catalog number: 115-0020)
25. Syringes: 1 mL (Terumo, catalog number: SS+01T1); 10 mL (Terumo, catalog number: SS+10ES1)
26. Tissue culture plastic:
10 cm dish (Thermo Scientific, catalog number: 150350)
96-well U-bottom plate (Falcon, catalog number: 353077)
48-well plate (Sarstedt, catalog number: 83.3923.500)
24-well plate (Greiner, catalog number: 662160)
12-well plate (Greiner, catalog number: 665180)
27. Tubes:
50 mL tubes (Greiner Bio-One, catalog number: 227261)
15 mL tubes (Greiner Bio-One, catalog number: 188261)
1.5 mL Eppendorf tubes (Starlab, catalog number: S1615-5550)
28. Ultracentrifuge tube (Thermo Scientific, catalog number: 3117-0380)
29. VSVG plasmid (Addgene, plasmid number: 14888)
30. Culture media (see Recipes)
31. D10 (see Recipes)
32. Expansion media (see Recipes)
33. FACS buffer (see Recipes)
34. MACS buffer (see Recipes)
35. Polyethyleneimine (PEI) (see Recipes)
36. Red cell lysis buffer (see Recipes)

Equipment

1. Pipettes

Cite as: Zeisig, B. B. et al. (2021). Reconstruction of Human AML Using Functionally and Immunophenotypically Defined Human Haematopoietic Stem and Progenitor Cells as Targeted Populations. *Bio-protocol* 11(24): e4262. DOI: [10.21769/BioProtoc.4262](https://doi.org/10.21769/BioProtoc.4262). ²²⁵

2. Aspirator
3. Cell counter (Hemocytometer)
4. Cell sorter (e.g., BD FACS Aria)
5. Centrifuge for 96-well plates
6. Freezer (-80°C)
7. Gamma-irradiation irradiator
8. Incubator (5% CO₂ 37°C)
9. Inverted microscope
10. Laminar flow cabinet
11. MACS MultiStand (Miltenyi Biotec, catalog number: 130-042-303)
12. MidiMACS Separator (Miltenyi Biotec, catalog number: 130-042-302)
13. Pipette aid
14. Swinging bucket rotor (Beckman Coulter, model: SW32 Ti)
15. Ultracentrifuge (Beckman Coulter, model: Optima L-100 XP)
16. Water bath

Software

1. Microsoft Excel

Procedure

Important information before you start: Carry out the procedures in a category II lab in line with local rules. Obtain all the necessary local Health and Safety and ethic approvals for viral work, primary human sample handling and manipulation as well as xenotransplantation studies. A schematic overview of the procedures described in this protocol is provided in Figure 1.

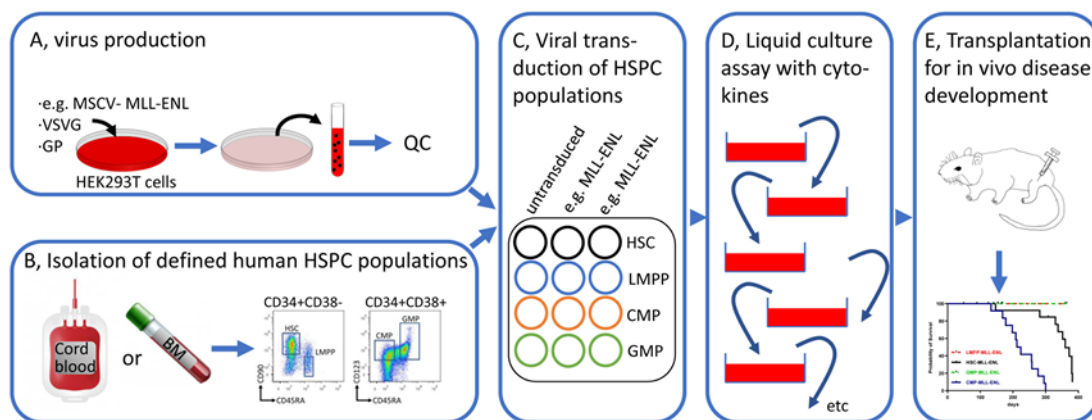


Figure 1. Schematic overview of the main steps to perform in vitro and in vivo transformation assay using highly purified human haematopoietic stem and progenitor cell populations as targeted populations.

A. Virus preparation

1. Generation of concentrated retrovirus carrying the oncogene of interest

- a. Plate 4 million HEK293T cells in 9 mL of D10 into each 10 cm plate. Prepare 3 plates for each viral construct to be tested in this protocol.
 - b. Put plates into a 37°C, 5% CO₂ incubator overnight.
 - c. The next day, bring all reagents to room temperature (RT), including IMDM, PEI, plasmids.
 - d. Change media. Aspirate media and replace with 8 mL of warm D10 media. Place the plates into a 37°C, 5% CO₂ incubator. For retrovirus production, pipette 3 mL of IMDM into a 15 mL Falcon tube. Add 7.5 µg Gag/Pol plasmid, 7.5 µg VSVG plasmid and 15 µg retroviral plasmid containing the gene of interest, e.g., MSCV-MLL-ENL-IRES-GFP. Mix by vortexing.
 - e. Add 90 µL (1 mg/mL) PEI to a 15 mL Falcon tube and vortex for 20 s. Incubate at RT for 15 min.
 - f. After incubation, briefly vortex the 15 mL Falcon tube. Label your plates accordingly and transfer 1 mL of this mixture into each of the three HEK293T plates. This is best done slowly in a drop-wise fashion covering most areas of the plates. Gently swirl the plates and return them to the 37°C, 5% CO₂ incubator overnight.
 - g. The next day, change media. Aspirate media and replace with 12 mL of warm D10 media.
 - h. Place the plates into 37°C, 5% CO₂ incubator overnight.
 - i. The following day, and at least 48 h after transduction, collect the supernatant of the transfected HEK293T plates using a 10 mL syringe. Attach a 0.45 µm filter to the syringe and pass the supernatant into a labelled ultracentrifuge tube. Repeat for other plates transfected with the same construct until all supernatant is collected in the same ultracentrifugation tube. Discard syringe and filter into freshly prepared 1% virkon solution.
 - j. Place the filled ultracentrifuge tube into the bucket and close lid. Prepare a balance if needed. Place all buckets onto the rotor and insert rotor following the manufacturer's instructions.
 - k. Spin at 25,000 rpm (>80,000 × g) for 3 h at 4°C.
 - l. After the spin, retrieve the labelled ultracentrifuge tube. Aspirate media, leaving ~3 mL in the tube. Vortex the remaining media (= concentrated retrovirus) gently and aliquot 220 µL each into pre-labelled Eppendorf tubes. Store virus at -80°C. Cells can be transformed by virus stored over 1 year at -80°C for this protocol.
2. Viral titration by FACS
 - a. Plate 50K HEK293T cells in 500 µL of D10 into each well of a 24-well plate. Prepare 7 wells.
 - b. Place plates into a 37°C, 5% CO₂ incubator overnight.
 - c. The next day, thaw one Eppendorf tube containing the concentrated virus and prepare several serial dilutions using D10, e.g., four 1:5 serial dilutions by mixing 30 µL of virus with 120 µL of D10.
 - d. For viral transduction of the HEK293T cells, add 0.25 µL of polybrene to each well of HEK293T cells. Label the wells 'untransduced', 'stock', and accordingly to your serial dilution, e.g., '1:5', '1:25', '1:125' and '1:725'. Add 100 µL of stock or the corresponding serially diluted virus to the labelled wells. Add 100 µL of D10 to the well labelled 'untransduced'.
 - e. Put the 24-well plate in a pre-warmed centrifuge and spin at 800 × g for 1 h at 33°C.
 - f. Put the 24-well plate into 37°C, 5% CO₂ incubator overnight.
 - g. The following day, and at least 24 h after adding the virus, aspirate the media. Resuspend the HEK293T cells in 400 µL of PBS, and transfer to a FACS tube. Analyse the GFP expression by FACS, using the untransduced cells as control to set the gate.
 - h. The virus titer in 100 µL of concentrated virus can be calculated by multiplying (number of plated cells) * (fraction of GFP⁺ cells) * (dilution factor)

B. Isolation of defined HSPC populations from human cord blood or adult bone marrow/mobilized peripheral blood

Note: In our experience, fresh cord blood or adult BM/PBMC gives much more robust transformation results compared to frozen ones.

1. Bring Ficoll-Paque Plus to RT.
2. Dilute fresh cord blood or adult BM/mobilized peripheral blood 1:1 in PBS, by transferring 15 mL of cord blood or adult BM into a 50 mL tube containing 15 mL PBS. Use multiple tubes to dilute all the original cord blood or adult BM/mobilized peripheral blood product if applicable.
3. Add 20 mL of Ficoll-plaque Plus to a separate 50 mL tube. Slowly overlay Ficoll with 30 mL of the diluted cord blood or adult BM/PB. Repeat for other tubes if applicable. Centrifuge RT for 30 min at $400 \times g$ with acceleration and deceleration set to 0.
4. Carefully aspirate around 2/3 of the top fraction containing the serum. Then collect the interphase containing the low-density mononuclear cells and transfer to a new 50 mL tube. This is best done by using a 10 mL pipette attached to a pipette aid. Repeat for the other tubes if applicable. Add PBS to make up 50 mL, to wash the mononuclear cells. Mix by inverting tubes several times and centrifuge at $700 \times g$ for 7 min with acceleration and deceleration set to maximum.
5. Aspirate most of the supernatant. If multiple tubes are used, leave around 3-5 mL in each tube. Resuspend cells in the remaining media and combine into a single 50 mL tube. Add PBS to make up 50 mL and centrifuge again at $700 \times g$ for 7 min.
6. Aspirate most of the supernatant. Resuspend the cell pellet (which should be red/ pink in color, due to the presence of residual red blood cells) in 5 mL of red cell lysis buffer, mix by pipetting and leave at RT for 10 min. After the incubation, add 45 mL of PBS and mix the tube by inverting. Filter cells through a 40 μm cell strainer into a new 50 mL tube. Count cells using a hemocytometer. Transfer 100K cells into one 1.5 mL Eppendorf tube labelled ‘MNC unstained’ and place at 4°C . Centrifuge the 50 mL tube with the remaining cells at $700 \times g$ for 7 min.
7. The cell pellet should appear white now (If still red, repeat Step B6 again). Aspirate supernatant and resuspend pellet in an appropriate volume of MACS buffer according to the manufacturer recommendation, *i.e.*, 300 μL for up to 10^8 cells. Add 100 μL of FcR blocking reagent for up to 10^8 cells and mix. Add 100 μL of CD34 microbeads for up to 10^8 cells, mix, and incubate for 30 min at 4°C protected from light. After the incubation, wash the cells by adding 45 mL of MACS buffer. Mix and centrifuge at $700 \times g$ for 7 min.
8. Put the MidiMACS separator onto the stand and insert a LS column. Place a 50 mL Falcon under the column and load 3 mL of MACS buffer to equilibrate the column. Buffer will flow through the column by gravity.
9. Aspirate supernatant from cells in Step B7 and resuspend in an appropriate volume of MACS buffer (500 μL MACS buffer per 10^8 cells) and load onto column. Wait until all volume passed through the column. Wash three times by loading 3 mL of MACS buffer each time onto column.
10. After the final wash, remove the column from the MidiMACS separator and place onto 15 mL Falcon tube. Add 5 mL of MACS buffer to column, insert, and slowly push the plunger. Count the eluted cells using a hemocytometer. Centrifuge Falcon tube at $700 \times g$ for 7 min. Aspirate supernatant.

Note: From a cord blood unit of 90 g, typically 100×10^6 - 200×10^6 MNC can be isolated. Around 0.3-1% of those are CD34 $^+$ cells, depending on the product. In our experience, very large cord blood units over 130 g yield higher numbers of MNC and CD34 $^+$ cells exceeding those obtained from pooling two smaller units of up to 90 g together.

11. Resuspend cells in 1 mL of MACS buffer and transfer into a 1.5 mL Eppendorf tube. Label this Eppendorf tube ‘CD34 stain’. Centrifuge at $2000 \times g$ for 2 min. Aspirate supernatant and resuspend pellet in 156 μL of MACS buffer. Add 4 μL (200 ng) of each HSPC antibody (working concentration 1 ng/ μL). Add 2 μL (100 ng) of each lineage antibody (working concentration 0.5 ng/ μL). Mix by pipetting and incubate at 4°C for 30 min.
12. After incubation, add 1 mL of MACS buffer to both Eppendorf tubes, labeled ‘MNC unstained’ and ‘CD34 stain’. Centrifuge at $2,000 \times g$ for 2 min, aspirate supernatant, and resuspend in 300 μL and 1 mL FACS buffer, respectively. Filter through 40 μm cell strainer into sterile FACS tubes.
13. Using a FACS sorter, *e.g.*, BD Aria or equivalent, sort hematopoietic progenitors such as HSC (lin^- CD34 $^+$ CD38 $^+$ CD90 $^+$ CD45RA $^-$), LMPP (lin^- CD34 $^+$ CD38 $^+$ CD90 $^-$ CD45RA $^+$), CMP (lin^- CD34 $^+$ CD38 $^+$ CD123 $^+$ CD45RA $^-$), GMP (lin^- CD34 $^+$ CD38 $^+$ CD123 $^+$ CD45RA $^+$). Compensation of different

fluorochromes must be performed before running the samples, according to the instruction of the corresponding FACS machine used. We routinely use compensation beads. We routinely sort directly into 1.5 mL Eppendorf tubes containing 500 μ L MACS buffer. The tube ‘MNC unstained’ can be used to define the negative unstained control population in all plots. An example of the gating strategy and expected frequencies is shown in Figure 2.

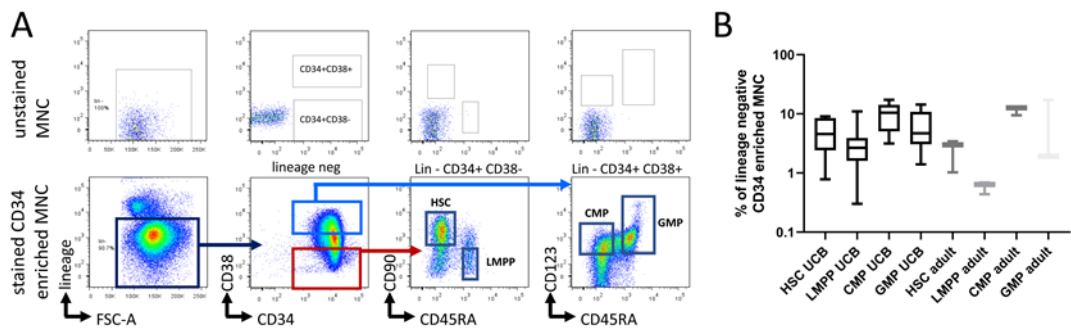


Figure 2. HSPC subpopulation gating strategy and frequencies.

A. The gating strategy for HSC, LMPP, CMP and GMP populations is shown. B. The frequencies of each population are shown as % of lineage negative CD34 enriched cells. UCB, umbilical cord blood (n = 12); adult, adult bone marrow or mobilized PBMC (n = 3).

Note: Different phenotypic definitions for human HSPC populations are described in the literature which may use different lineage marker cocktails and/or different HSPC markers to purify distinct populations (Edvardsson et al., 2006; Doulatov et al., 2012; Pellan et al., 2019).

14. Count sorted cells and use at least 300 cells to assess post-sort purity, which should be higher than 95%. To do so, transfer at least 300 cells into a new labelled FACS tube. Add FACS buffer to make up 150 μ L. Repeat for each sorted population. Assess post-sort purity by running the samples in the FACS sorter.
15. Centrifuge the Eppendorf tubes with the sorted populations at 2,000 \times g for 2 min. Aspirate supernatant and resuspend in expansion media with cell density of 2,000-20,000 per 100 μ L.
16. Transfer up to 200 μ L into one well of a U-bottom 96-well plate and mark the identity of the cell population on the cover plate. Repeat for all sorted cell populations. Add 250 μ L of MACS buffer to all outer wells of the 96-well plate to avoid evaporation of expansion media. Place in 37°C incubator with 5% CO₂ overnight.

C. Viral transduction of HSPC populations

1. Take out the 96-well plate with the sorted populations from the incubator.
2. Calculate the appropriate number of wells for each cell population depending on the number of oncogenes to be tested. Add an extra condition as your untransduced control. Resuspend cells in expansion media at concentrations of 1,000-10,000 cells/100 μ L and transfer 100 μ L into the desired number of wells of a new 96-well plate.

Note: As an example, if 2 oncogenes will be tested then prepare 2 wells for each population plus one extra well for each population for untransduced control (A total of 3 wells per sorted population).

3. For each prepared well, mix the following in a single 1.5 mL Eppendorf tube: 9.6 μ L of IMDM, 15% FBS, P/S, 0.12 μ L (1.2 ng) of each SCF, TPO, and FLT3L, 0.075 μ L (0.75 μ g) of Polybrene. Add 10 μ L of this mixture to each well containing cells (a master mix should be made for accurate pipetting).
4. The desired multiplicity of infection (MOI) for the viral transduction of HSPC populations is 5-10. Use the determined viral titer (see Step A2h) to calculate the required volume of virus for the prepared cell density (see Step C2) for each population.

5. First transduction: Thaw frozen virus in water bath at 37°C. Prepare the correct amount of virus for each transduction by pipetting the calculated virus volume into a new Eppendorf tube and add D10 media to make a total of 50 µL. Transfer 50 µL of the titrated concentrated virus to the cell populations in the 96-well plate. Add 50 µL warm D10 to the control cells. Now the total volume of cells/virus mix should be 150 µL. Mix cells and virus well by pipetting.
6. Place the 96-well plate in 37°C incubator with 5% CO₂ overnight.
7. The next day, take out the 96-well plate from incubator.
8. For each well, prepare the following mix in a single 1.5 mL Eppendorf tube: 9.8 µL IMDM, 15% FBS, 0.1 µL (1 ng) of each SCF, TPO, and FLT3L. Add 10 µL of this mixture to each well containing cells (a master mix should be made for accurate pipetting).
9. Second transduction: Thaw frozen virus. Prepare the correct amount of virus for each transduction by pipetting the calculated virus volume into a new Eppendorf tube and add D10 media to make a total of 50 µL (use the same calculation as in Step C4 and the virus volumes from Step C5). Transfer 50 µL of the concentrated virus to the cell populations as the day before. Add 50 µL of warm D10 to the control cells. Now the total volume of cells/ virus mix should be 200 µL. Mix cells and virus well by pipetting.

Note: If multiple different viruses are used, ensure that the same virus will be added to the wells as on the previous day.

10. Place the 96-well plate in 37°C incubator with 5% CO₂ overnight.

D. Liquid culture assay with cytokines

1. The next day, take out the 96-well plate from incubator and inspect the cells under the microscope using a 10× objective. A cell cluster should be visible in the centre of the well.
2. Aspirate 100 µL of supernatant from each well containing cells, without disturbing the cells. Add back 100 µL of IMDM, 15% FBS, 0.2 µL (2 ng) of each SCF, TPO, and FLT3L, and 0.4 µL (4 ng) of each IL-3, and IL-6. Mix well by pipetting.
3. Place the 96-well plate in 37°C incubator with 5% CO₂ overnight.
4. The next day, take out the 96-well plate from incubator and check under the microscope using a 10× magnification. If cells fill more than 2/3 of the field of view, then transfer cells to a 48-well plate, add 300 µL culture media and return to 37°C incubator with 5% CO₂ overnight. If not, then leave cells in 96-well plate, return to 37°C incubator with 5% CO₂ overnight and repeat step 4 the next day.
5. Once the cells are in the 48-well plate, monitor cell expansion under the microscope every other day. If the cells cover more than 70% of the surface of the well or if the color of media changes yellowish, add 500 µL fresh culture media once to a total volume of 1mL. Place the 48-well plate in 37°C incubator with 5% CO₂.
6. Once the cells are in a total volume of 1 mL and cover the whole well, transfer them to a 12-well plate and add 2 mL of culture media (now total volume is 3 mL). Place the 12-well plate in 37°C incubator with 5% CO₂.
7. Monitor the cells in the 12-well plate every other day and count the number of cells using a hemocytometer. Once the cell concentration is within 600K-1 million/mL transfer 400K cells resuspended in 2 mL fresh culture media (*i.e.*, 200K cells/mL) to a new well of a 12-well plate. Place the new 12-well plate in 37°C incubator with 5% CO₂.
8. Three days later, add another 2 mL of culture media to the new 12-well plate containing the cells (now total volume is 4 mL). Place the 12-well plate in 37°C incubator with 5% CO₂.
9. Another 4 days later (*i.e.*, 1 week after Step D7), count the cells, and transfer 400K cells resuspended in 2 mL of fresh culture media to a new well of a 12-well plate. Place the new 12-well plate in 37°C incubator with 5% CO₂.
10. Repeat Steps D8-D9 for up to 15 weeks to monitor the growth of the cells.

Notes:

- Control cells will usually cease to expand and fully differentiate between week 3-8, while transformed cells continue to proliferate in vitro (Figure 3A and 3B) and retain an immature myeloblast cell morphology (Figure 3C). The time to obtain fully differentiated control cultures varies from sample to sample. While sometimes untransduced HSCs may still show a proportion of immature cells at day 36, other cell populations may have fully differentiated long before day 36.*
- Once a difference in proliferation pattern between transduced and control cells from the same cell population is observed, make cytocentrifuge preparations (Figure 3C) and perform FACS (Figure 3D) to characterize these early transformed cells. Freeze cells (>1 million cells/vial).*
- Perform weekly characterisation of cell morphology and cell surface marker expression. Continue to freeze down cells bi-weekly to build up frozen stock of transformed cells which can be accessed in the future. As soon as the proliferation difference is observed between control and transduced cells, transduced cells can be used for other studies including transplantation into immunodeficient mice (protocol Procedure E).*

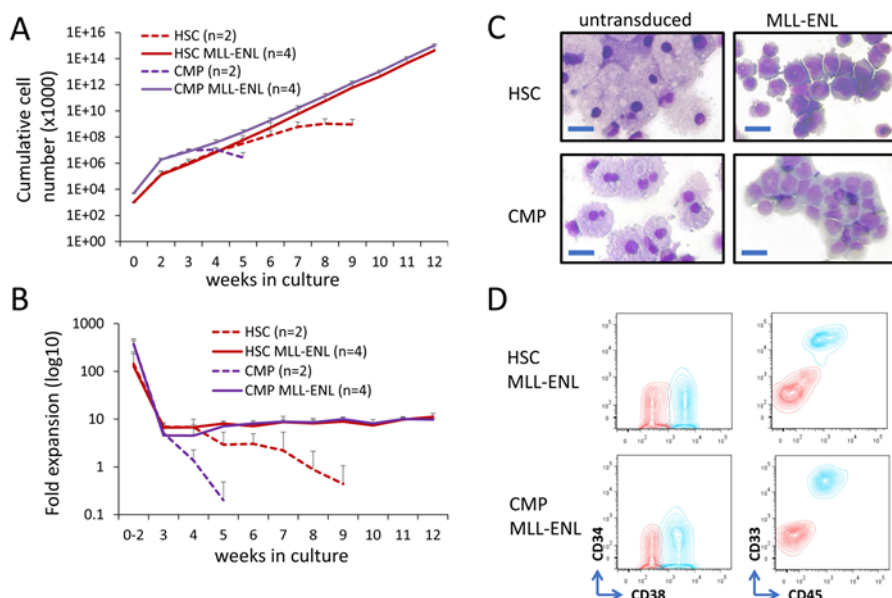


Figure 3. *In vitro* transformation of MLL-ENL transduced HSPC populations.

A-B. The cumulative cell number (A) and the fold expansion (B) of MLL-ENL transduced or untransduced HSC and CMP population are shown. C. May-Gruenwald Giemsa stained cell preparations show the typical cell morphology for the indicated cell types at day 36 in culture. D. Typical surface marker expression of transformed cells at day 36 in culture. Red profiles represent unstained cells and blue profiles are cells stained with the indicated surface marker.

E. Transplantation for *in vivo* disease development

Perform sublethal irradiation (200-250 cGy) of immunodeficient NSG mice no more than 24 h before transplantation. The mice should always be housed in independently ventilated cages (IVCs) and all procedures are always performed under the safety hood.

The mice are transplanted intravenously (i.v.) (Video 1) or intraosseously (i.o.) (Video 2) via a hind leg bone (femur is preferred over tibia, as it has a bigger bone marrow cavity). The transplantation route depends on the number of cells:

For i.v., a minimum of 500,000 and no more than 10 million cells should be transplanted.

For i.o., no minimum cell number is set but they should not exceed 1 million.



Video 1. Intravenous transplantation.

This video was made at King's College London. The experimental procedure shown in this video was approved by King's College London ethics committees and conform to the UK Home Office regulations.



Video 2. Intraosseous transplantation.

This video was made at King's College London. The experimental procedure shown in this video was approved by King's College London ethics committees and conform to the UK Home Office regulations.

1. Preparation of the cells for transplantation.

Cells should be resuspended in PBS or isotonic saline. The following volumes are injected into each mouse:
For i.v. injection, 150-200 μ L in a 29G 1 mL needle attached to an insulin syringe. For i.o. injection, a maximum 20 μ L in a 29G 1 mL needle attached to an insulin syringe. Cells should always be kept on ice and brought back to RT 5 min before transplantation.

Note: Matrigel can also be used as vehicle for i.o. injection. In this case, cells should always be kept on ice before injection.

2. Transplantation via i.v. injection.

- The mice are warmed in their IVCs with an infrared radiator (200-300 W) 15 cm apart for 10 min, or in a Mini-Thermacage set at 37°C for 10 min. The Mini-Thermacage is preferred as the warming is more homogeneous. Warming the mice prior to transplantation allows their tail veins to dilate and become more visible. The mice should be monitored regularly, and moved away from the heat source immediately if they show signs of heat exhaustion e.g., staying away from the heat source and breathing heavily.
- Place the mouse in a sterile animal holder and keep its tail outside the tube. There are four blood

vessels visible at the tail; the two veins are located at the tail's lateral sides. Only use veins for injection.

Note: Never inject via ventral and dorsal blood vessels of the tail; they are the arteries. It would cause severe bleeding!

- c. Carefully resuspend the cells by tipping the needle several times and ensure that there are no bubbles inside the syringe. Use a sterilizing wipe to clean the injection site. Insert the needle into the vein for about 5mm in the direction from tail to head, push the plunger gently, and inject all the volume slowly for 2-3 s. You should be able to push the plunger smoothly and see the tail vein temporarily turn white for 3-5 s, before turning red/pink again.

Note: If you feel resistance from pushing the plunger, and the area around the injection site turns white, then the injection failed, i.e., the needle is not inside the vein. Try injecting again, via the other lateral vein 5 to 10 min later, when the vein is visible again.

- d. When all the content in the syringe is injected, hold for 5 sec before withdrawing the needle (Removing the needle immediately after injection would flush some cells out from the injection site). If the injection is successful, there is mild bleeding once the needle is withdrawn. Clean the injection site again using a sterilizing wipe and stop the bleeding by gently pressing the injection site for around 10 s. Place the mouse back in the IVC.
3. Transplantation via i.o. injection into femur.

Note: All procedures should be performed under the safety hood.

- a. Keep cells on ice. Just before the injection, carefully resuspend the cells by tipping the needle several times and ensuring that there are no bubbles inside the syringe.

Note: When preparing the cell suspension, resuspend the cells in a volume of 22 µL per mouse, as there is about 1-2 µL dead volume in the insulin syringe. By doing so, you ensure injecting 20 µL of cells.

- b. The mouse is put under anesthesia in a sterile chamber by a light inhalational anesthesia agent such as 2-4% isoflurane by Plenum vaporizer (e.g., VetFloTM Vaporizer). Observe the breath of the mouse changing from “shallow but rapid” to “deep but slow”. When the mouse breaths deeply but slowly, it is in deep anesthesia, and can be transferred to a heat mat set at 37°C (or a prewarmed polystyrene board if heat mat is not available) and maintained under anesthesia by inhaling isoflurane. During the whole procedure, it is vital to keep monitoring the breath of the mouse, if it turns shallow but rapid again, you need to increase the dose of isoflurane. No invasive procedure should be performed when the mouse breaths shallow but rapid. If it turns shallow and slow, remove the mouse from anesthesia immediately, as the dose is too strong and the mouse can be killed.
- c. Place the mouse dorsal side up. Remove hairs around its knee by plucking. Clean the injection site using sterilizing wipe. Apply pain relief cream (e.g., EMLA cream) on the skin. Use the sharp bevel of a sterile 27G needle (NOT the needle for cell injection) to cut open the skin in a lateral direction (3-4 mm in length) at the knee region, and the patellar ligament (white in color) should now be exposed and visible. Use the same needle to drill a hole via the anterior end of the femur under the patellar ligament. Move the needle back and forth gently in all directions—you should feel scratching in the inner cavity of the bone in each movement.
- d. Withdraw the 27G needle gently and slowly, and remember the direction of the needle withdrawal. Insert the cell-containing 29G insulin needle into the same site with the same direction of the 27G needle withdrawn. You should feel no resistance when inserting the needle into the injection site. Adjust the direction of the needle going in slightly if you feel resistance. After the needle is inserted, scratch slightly in all directions to confirm the needle is in the bone marrow cavity. Inject all the

content in the syringe and withdraw the needle. Return the mice to the IVC warmed by infrared radiator, where they should recover from anesthesia within 3-5 min (if anesthetized by isoflurane).

- e. Monitor the mice transplanted via i.o. daily. Their injected legs should be slightly lame/dragged for at least 2 days but should recover to normal within one week. A pain relief agent can be administered to the mouse for 1 week according to the veterinarian's
4. Mouse monitoring
 - a. After transplantation, the health of the mice should be monitored daily. The engraftment of human cells can be tracked by blood sampling via the tail vein followed by FACS analysis, no more than once a week. Engrafted cells should be human CD45⁺. The engraftment of human primary *in vitro* transformed cells into NSG mice is highly variable for both tumor burden and time, and sometimes they even fail to engraft at all. From our experience, the human *in vitro* transformed cells could be detected as early as 2 weeks after transplantation.
 - b. When the transplanted mouse starts to show signs of moderate pain and distress (Burkholder *et al.*, 2012), or reaches humane endpoint (Burkholder *et al.*, 2012), the mouse needs to be culled by humane methods. Harvest blood, bone marrow, spleen, liver, thymus, and relevant organs to check for any human cell engraftment by FACS with appropriate cell surface markers (including but not limited to CD34, CD38, CD45, and CD33), and produce blood/ bone marrow smears to check the cell morphology. Spleen, liver, and/or thymus could be enlarged if leukemia cells infiltrated into those organs, so their weight and size should be recorded (Figure 4A), and their engraftment of human cells can be evaluated by FACS with appropriate cell surface markers (Figure 4B), and hematoxylin and eosin staining, after the tissue is fixed and sectioned (Figure 4C).

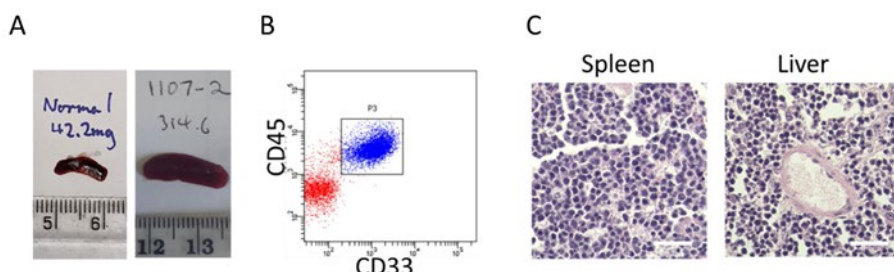


Figure 4. Analysis of human leukemia engrafted mice.

A. Photo of the spleen from the control mouse (weight = 42.2 mg) and the sick mouse (weight 314.6 mg), with ruler in cm. B. Representative FACS plot of engrafted human AML cells (blue), which are positive for both human CD45 and CD33. C. Hematoxylin and eosin staining of fixed spleen and liver of a sick mouse. The human AML cells are stained in dark blue, scale bar = 50 μ m.

Data analysis

It is recommended to perform the *in vitro* transformation assay at least 3 times using different cord blood or adult bone marrow samples, from which defined HSPC populations are sorted. Within each independent experiment, it is recommended to perform each condition at least in duplicates. Typical intra- and inter-assay variability of transformed cells for the weekly fold expansion are as follows:

Intra-assay variability early culture (week 2-4) HSC MLL-ENL (1%-85%), CMP MLL-ENL (3%-25%); mid-term culture (week 5-8): HSC MLL-ENL (1%-12%), CMP MLL-ENL (1%-21%); long term culture (week 8-12): HSC MLL-ENL (2%-10%), CMP MLL-ENL (3%-23%);

Inter-assay variability early culture (week 2-4) HSC MLL-ENL (18%-80%), CMP MLL-ENL (29%-50%); mid-term culture (week 5-8): HSC MLL-ENL (12%-32%), CMP MLL-ENL (6%-29%); long term culture (week 8-12): HSC MLL-ENL (7%-24%), CMP MLL-ENL (5%-21%). While the %CV is relatively high in the early phase of culture (week 2-4), reflecting the highly variable nature of the cord blood sample, the variation reduces over culture

time due to MLL-ENL mediated transformation.

Recipes

1. Culture media

IMDM, 15% FBS, P/S, 20 ng/ml of each SCF, TPO, FLT3L, IL-3, and IL-6

2. D10

DMEM, 10% FBS, P/S

3. Expansion media

IMDM, 15% FBS, P/S, 100 ng/ml of each SCF, TPO, FLT3L

4. FACS Buffer

PBS, 0.5% FBS, P/S, Propidium iodide

5. MACS buffer

PBS, 2 mM EDTA, 0.5% FBS, P/S

6. PEI (1 µg/µL)

- Dissolve PEI in endotoxin-free dH₂O that has been heated to ~80°C.
- Let cool to room temperature.
- Neutralize to pH 7.0, filter sterilize (0.22 µm), aliquot and store at -20°C; a working stock can be kept at 4°C.

7. Red cell lysis buffer

- 10 mM KHCO₃, 150 mM NH₄Cl, 0.1 mM EDTA
- Make up to 300 ml with endotoxin-free dH₂O, and filter sterilize (0.22 µm). Store at 4°C.

Acknowledgments

This study was supported by Cancer Research UK, Blood Cancer UK, Kay Kaydall Leukaemia Research Fund and TBRS RGC HK. This protocol is based on and used in a recent report (Zeisig *et al.*, 2021; DOI: 10.1126/scitranslmed.abc4822).

Competing interests

The authors declare no competing interests

Ethics

All experimental procedures were approved by King's College London ethics committees and conform to the UK Home Office regulations.

References

- Almosailleakh, M. and Schwaller, J. (2019). [Murine Models of Acute Myeloid Leukaemia](#). *Int J Mol Sci* 20(2).
- Barabé, F., Kennedy, J., Hope, K. and Dick, J. (2007). [Modeling the initiation and progression of human acute leukemia in mice](#). *Science (New York, NY)* 316(5824): 600-604.
- Burkholder, T., Foltz, C., Karlsson, E., Linton, C. G. and Smith, J. M. (2012). [Health Evaluation of Experimental Laboratory Mice](#). *Curr Protoc Mouse Biol* 2: 145-165.
- Doulatov, S., Notta, F., Laurenti, E. and Dick, J. E. (2012). [Hematopoiesis: a human perspective](#). *Cell Stem Cell* 10(2): 120-136.
- Edvardsson, L., Dykes, J. and Olofsson, T. (2006). [Isolation and characterization of human myeloid progenitor populations--TpoR as discriminator between common myeloid and megakaryocyte/erythroid progenitors](#). *Exp Hematol* 34(5): 599-609.
- Horton, S. J., Jaques, J., Woolthuis, C., van Dijk, J., Mesuraca, M., Huls, G., Morrone, G., Vellenga, E. and Schuringa, J. J. (2013). [MLL-AF9-mediated immortalization of human hematopoietic cells along different lineages changes during ontogeny](#). *Leukemia* 27(5): 1116-1126.
- Krivtsov, A. V., Figueroa, M. E., Sinha, A. U., Stubbs, M. C., Feng, Z., Valk, P. J., Delwel, R., Dohner, K., Bullinger, L., Kung, A. L., et al. (2013). [Cell of origin determines clinically relevant subtypes of MLL-rearranged AML](#). *Leukemia* 27(4): 852-860.
- Pellin, D., Loperfido, M., Baricordi, C., Wolock, S. L., Montepeloso, A., Weinberg, O. K., Biffi, A., Klein, A. M. and Biasco, L. (2019). [A comprehensive single cell transcriptional landscape of human hematopoietic progenitors](#). *Nat Commun* 10(1): 2395.
- Shallis, R. M., Wang, R., Davidoff, A., Ma, X. and Zeidan, A. M. (2019). [Epidemiology of acute myeloid leukemia: Recent progress and enduring challenges](#). *Blood Rev* 36: 70-87.
- Siriboonpiputtana, T., Zeisig, B. B., Zarowiecki, M., Fung, T. K., Mallardo, M., Tsai, C. T., Lau, P. N. I., Hoang, Q. C., Veiga, P., Barnes, J., et al. (2017). [Transcriptional memory of cells of origin overrides beta-catenin requirement of MLL cancer stem cells](#). *EMBO J* 36(21): 3139-3155.
- Stavropoulou, V., Kaspar, S., Brault, L., Sanders, M. A., Juge, S., Morettini, S., Tzankov, A., Iacovino, M., Lau, I. J., Milne, T. A., et al. (2016). [MLL-AF9 Expression in Hematopoietic Stem Cells Drives a Highly Invasive AML Expressing EMT-Related Genes Linked to Poor Outcome](#). *Cancer Cell* 30(1): 43-58.
- Wunderlich, M., Mizukawa, B., Chou, F. S., Sexton, C., Shrestha, M., Saunthararajah, Y. and Mulloy, J. C. (2013). [AML cells are differentially sensitive to chemotherapy treatment in a human xenograft model](#). *Blood* 121(12): e90-97.
- Zeisig, B. B., Fung, T. K., Zarowiecki, M., Tsai, C. T., Luo, H., Stanojevic, B., Lynn, C., Leung, A. Y. H., Zuna, J., Zaliova, M., et al. (2021). [Functional reconstruction of human AML reveals stem cell origin and vulnerability of treatment-resistant MLL-rearranged leukemia](#). *Sci Transl Med* 13(582).
- Zeisig, B. B., Kulasekararaj, A. G., Mufti, G. J. and So, C. W. (2012). [SnapShot: Acute myeloid leukemia](#). *Cancer Cell* 22(5): 698-698 e691.
- Zeisig, B. B. and So, C. W. E. (2021). [Therapeutic Opportunities of Targeting Canonical and Noncanonical PcG/TrxG Functions in Acute Myeloid Leukemia](#). *Annu Rev Genomics Hum Genet* 22.